December 2012

# Fundamental and Applied Studies of Metal Ion Extraction by Crown Ethers into Imidazolium-Based Room Temperature Ionic Liquids

Cory Hawkins
*University of Wisconsin-Milwaukee*

# FUNDAMENTAL AND APPLIED STUDIES OF METAL ION EXTRACTION BY CROWN ETHERS INTO IMIDAZOLIUM-BASED ROOM TEMPERATURE IONIC LIQUIDS

by

Cory Hawkins

A Dissertation Submitted in

Partial Fulfillment of the

Requirements for the Degree of

Doctor of Philosophy

in Chemistry

at

The University of Wisconsin-Milwaukee

December 2012

ABSTRACT
FUNDAMENTAL AND APPLIED STUDIES OF METAL ION EXTRACTION BY CROWN ETHERS INTO IMIDAZOLIUM-BASED ROOM TEMPERATURE IONIC LIQUIDS
by

Cory Hawkins

The University of Wisconsin-Milwaukee, 2012
Under the Supervision of Professor Mark Dietz, Ph.D.

Growing recognition of the extraordinary physicochemical properties and unique solvation environment afforded by ionic liquids (ILs) has drawn increasing attention to these solvents as media for chemical separations. Until recently, little was known about how ionic liquids behave as solvents in this application, particularly in the extraction of ionic solutes such as metal ions. In contrast to the single pathway observed using molecular diluents (*i.e.*, neutral complex extraction), metal ion extraction in these systems has been shown to proceed through as many as three competing pathways over a wide range of conditions. Despite this added complexity, the favorable physicochemical characteristics of the ionic liquids (*e.g.*, non-flammability and unprecedented structural tunability), along with the higher extraction efficiencies and selectivities sometimes observed with these solvents, suggest that they offer significant potential in various separations applications on both the industrial and analytical scale. This potential will not be fully realized, however, without an improved understanding of the fundamental aspects of metal ion partitioning between ionic liquids and aqueous solutions. The objective of this work, therefore, is to clarify the factors controlling the balance among

the various partitioning pathways observed when these solvents are employed in extraction.

To this end, a series of *N,N'*-dialkylimidazolium-based ionic liquids have been evaluated as substitutes for the conventional organic solvents (*i.e.*, *n*-alcohols) frequently employed in the extraction of alkali and alkaline earth cations from acidic aqueous phases by crown ethers. Insight into the fundamental aspects of metal ion extraction in these systems has been obtained by analysis of the acid and extractant dependencies of metal ion distribution ratios, measurements of the IL phase water content and of the solubility of the ionic liquids in the aqueous phase, determination of the partitioning of inorganic ions, and consideration of the relative hydrophobicities of the ionic liquids employed. To assess the potential practical utility of these ionic liquids as extraction solvents, these studies were aimed at obtaining information about the relationship between solvent structure and performance as solvents in the extraction of alkali and alkaline earth metal ions. The results obtained represent an important step in the development of guidelines for the rational design of ionic liquid-based metal ion separation systems.

# Table of Contents

# List of Figures

## List of Tables

# DEDICATION

For Jennifer, the love of my life…I am eternally grateful for your unwavering support throughout our journey. And for my parents, who nurtured my interest in the sciences.

ACKNOWLEDGEMENTS

I have many people to thank for their contributions over the years. First, I would like to extend my gratitude to my advisor, Professor Mark Dietz. His guidance and wisdom kept me engaged in this research. He has always been interested in the latest results and as curious as I about their implications. Without his decisive involvement through the milestones in this program and support for my professional development, I would not be at this point in my career. I believe that we have cultivated a working partnership that has surpassed my expectations for productivity.

My committee members have advised me well throughout this endeavor. I recognize that Professor Joseph Aldstadt has been an advocate for me since applying for this program. His interest in history and breadth of knowledge in the analytical sciences are exemplary. Professor Andrew Pacheco has always listened well and offered helpful suggestions when a bewildering or peculiar result has been obtained. Professor Mahmun Hossain has been a valuable resource for understanding organic synthesis as well as in my professional development. Dr. Michael Kaminski has demonstrated strong leadership and has been an essential collaborator and benefactor for our research program. Additionally, I would like to thank the Department of Chemistry & Biochemistry, its staff, and other faculty members who have assisted in making this effort possible.

My research group has been replete with friends and colleagues having contributed in various ways. I am pleased with the results of working with Ms. Anna Rud for the two years she was employed as a researcher in this group. Her diligent efforts in synthesizing and characterizing ionic liquids have been essential to these studies. Sarah Garvey's research has often dovetailed with my own, providing relevant data and perspectives to

understand the varied aspects of ionic liquids. Among several contributions to my program, Alan Pawlak helped me get to know the thermogravimetric instrumentation and assisted with materials synthesis. I have learned from each of my research group members and I thank you for your support.

"If the goal of synthetic chemistry is to produce new chemical entities, it is up to analytical chemists to determine how well the chemical compounds are characterized. In general, it is easier to synthesize a compound with a definite chemical structure than with a certain required property."

- Roman Kaliszan, *Analytical Chemistry*, **1992**, 64, 619A-631A

# CHAPTER 1:
# INTRODUCTION

## 1.1 Overview and Scope

The separation and preconcentration of strontium is of great importance, both on the analytical scale on an industrial scale. Although radioactive strontium isotopes, primarily $^{90}$Sr, comprise only 5% of the light products of uranium fission [1.1], these radionuclides, along with an equal part $^{137}$Cs, account for the majority of heat production in spent nuclear fuel (SNF). This poses a problem for the efficient storage of SNF, as the protocols involved require the dissipation of the large amounts of heat in order to avoid damage to the fuel or storage facilities. As of December 2011, more than 67,000 metric tons of SNF, in more than 174,000 assemblies, is stored at 77 sites (including 4 Department of Energy facilities) located throughout the United States [1.2]. With the accumulation of SNF set to grow at a rate of roughly 2,000 metric tons per year [1.2], the amount of medium-to-long lived radionuclides will be on the rise, and the capacities of storage sites will be strained. To provide for greater capacity in these repositories, the processing of fuel to remove the heat-generating nuclides is an obvious first step. (Of course, the full reprocessing of spent fuel in a closed-cycle is generally regarded as the wisest approach to these resources, but one that has faced substantial political opposition.) On an industrial scale, solvent extraction is the most commonly used technique, because it can be run in continuous mode (*e.g.*, countercurrent liquid-liquid extraction), imparting high selectivity factors without the use of high pressures. Current methods for the solvent extraction of $^{90}$Sr from SNF (*e.g.*, SREX) [1.3] rely on the placement of separate extraction stages downstream from the PUREX process [1.4]. One of the key requirements for the development of any advanced nuclear fuel cycle is

improved separations processes for the removal of SNF constituents that most contribute to the heat load and the overall waste volume. Consequently, the strontium removal process must be made as efficient as possible (*e.g.*, reduced number of stages and increased decontamination factors). Our exploration of the possibilities afforded by ionic liquids (ILs) originates from the notion that higher extraction efficiencies and greater selectivities for strontium versus alkali metal ions (present in high concentrations in SNL) could provide the needed improvements.

Interim facilities for the storage of SNF are scattered throughout the United States, and facilities internationally may be significantly less secure, posing a threat to society of the possible intentional or accidental release of stored materials. Bioassays that are currently implemented for the determination of internal exposure to radionuclides, such as $^{90}$Sr, are often cumbersome and involve time-consuming steps [1.5]. Accordingly, they would not be especially useful in the event of a radioactive material release involving significant numbers of potentially contaminated individuals. In analogy to the process-scale improvements described above, an increase in extraction efficiency and selectivity involved in the extraction of radiostrontium from aqueous media *via* liquid-liquid extraction could facilitate the preparation of extraction chromatographic materials for the rapid separation and preconcentration of radiostrontium in biological media.

The objective of the present studies is to explore the processes involved in metal ion extraction from aqueous solutions by crown ethers into imidazolium-based room temperature ionic liquids, and to eventually establish guidelines for the selection of an appropriate ionic liquid (IL) solvent for the selective extraction of strontium. In the interest of presenting a systematic study of the behavior of ILs as solvents for metal ion

extraction, the focus of this work is on a single family of hydrophobic 1,3-dialkylimidazolium room temperature ionic liquids. By affording a unique solvation environment, ILs such as these have, in some cases, shown promise to improve upon current metal ion extraction systems based on conventional solvents through greater extraction efficiencies and larger separation factors. Initial work has suggested that Groups 1 and 2 metal ion partitioning by crown ethers occurs via several distinct equilibria that remain, in some ways, inadequately understood. The range of possible physicochemical properties of ILs are as vast as the number of cation and anion combinations that may comprise an IL. In view of this diversity and the nature of their extraction behavior, the selection of an IL solvent for a particular process becomes challenging. That is to say, in the absence of guiding principles to make a well-informed choice, the selection method will rely largely on trial-and-error. Therefore, the work performed in this thesis is defined by the assessment of the major factors involved in partitioning processes employing ILs in the extraction of alkali and alkaline earth metal ions and the correlation of these factors with the structures and physicochemical properties of the ILs employed.

### 1.2 Ionic Liquids

Reviews of the field of ionic liquids span a range of subjects, but some of the more thorough examinations across disciplines are those by Welton [1.6], and Seddon [1.7], and Dietz [1.8] As the number of articles per year with the term “ionic liquid” in the title has reached into the thousands, it has become impossible to be comprehensive in describing the field. However, it is worth providing a brief history in this introduction to give the reader some sense of how the field has developed. Paul Walden, in 1914, was the

first to describe the low-melting (13-14°C) salt, ethylammonium nitrate, which was a product of the neutralization of ethylamine with concentrated nitric acid [1.9]. Although this observation is heralded as the beginning of the field of ionic liquids, his reports did not garner much interest at the time. There was some interest in the use of N-alkylpyridinium halide salts for the dissolution of cellulose for the production of raw materials in the 1930's [1.10] and the application of mixtures of these halide salts with aluminum(III) chloride for aluminum deposition in the years following World War II [1.11, 1.12]. Yet, it was not until the "rediscovery" of mixtures of aluminum(III) chloride with *N*-alkylpyridinium chloride in the mid-1970's by Osteryoung *et al*. [1.13], however, that interest began to develop more widely. The range of compositions that yielded room temperature liquids (*i.e*., 60 to 67 mol% $AlCl_3$) was found to be quite narrow and the cations were prone to reduction. In 1982, however, by evaluating an array of heterocyclic cations using molecular orbital calculations, Wilkes *et al*. [1.14] predicted a much wider electrolytic stability window for 1,3-dialkylimidazolium cations, and the resulting chloroaluminate salts provided a wider liquidus composition range (from 33 to 67 mol%). Still, the major drawback of these Lewis acid-based ILs was their moisture sensitivity, constraining all work with the materials to a dry box. It was not until 1992, when Wilkes and Zawarotko [1.15] reported air and water stable room temperature ILs with definite composition that the wide variety of ILs featuring the range of cations and anions known today became available. Figure 1.1 shows a few examples of the most common cations and anions that comprise modern ILs.

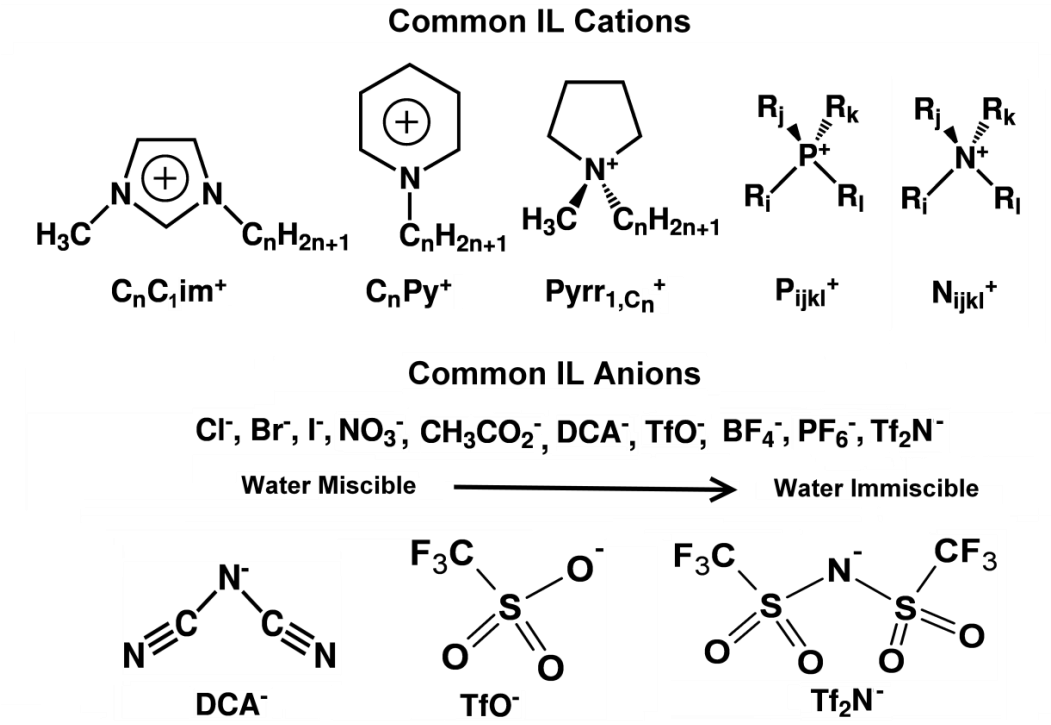


**Figure 1.1: Structures of common ionic liquid cations and anions.**

The currently accepted definition of an ionic liquid is a salt that melts below 100°C. From the cation and anion structures shown in Fig. 1.1 it is apparent that the cations tend to be bulky and often charge-delocalized organic moieties, whereas the anions range from water-miscible halides to the hydrophobic bis[(trifluoromethyl)sulfonyl]imide ($Tf_2N$) salts developed by Grätzel *et al*.[1.16]. The structure and physical properties of ILs are governed by short-range coulombic forces and long-range inductive forces mediated by the amphiphilic combination of the cationic polar head groups with hydrophobic tails. Such interactions lead to low lattice energies and the frustration of crystal formation. Charge ordering is less defined in systems composed of bulky, asymmetric, and flexible cations and anions as compared to metal halide salts [1.17]. The resulting properties of compounds with such ion combinations often include high decomposition temperatures

(≥ 200°C), low melting points or glass transitions (≥ -90°C), and negligible vapor pressures under ambient conditions (leading to nonflammability). Because their structures remain dominated by coulombic forces, however, ILs tend to exhibit high viscosities [1.18], which may render more difficult applications where solute transport is important (*e.g.*, use as solvents).

### 1.3 Solvent Extraction of Metal Ions into Conventional Organic Solvents

Solvent extraction is used frequently as an analytical technique, primarily in the form of a batch method with single contacts between two immiscible phases, which normally consist of aqueous and organic solvents. Solutes distributed between the two phases reach an equilibrium concentration according to the Nernst partition isotherm, where the distribution of solute X between the phases is a constant expressed by:

$$K = \frac{[X]_{org}}{[X]_{aq}} \qquad (1\text{-}1)$$

Although the thermodynamic partition coefficient is formally expressed using the activities and activity coefficients of the species, for many practical applications, the ratio of the total concentrations of a metal ion solute, M, in both phases is expressed as a distribution ratio, D (Eqn. 1-2), where all species present that contain the solute are combined.

$$D = \frac{[M]_{org}}{[M]_{aq}} = \frac{[X_1]_{org}+[X_2]_{org}+\cdots}{[X_1]_{aq}+[X_2]_{aq}+\cdots} \qquad (1\text{-}2)$$

The distribution ratio, therefore, is the parameter that best expresses the extent of extraction (*i.e.*, extraction efficiency, %E = D/(D+1) × 100% ), as a readily measureable quantity.

Because determining the concentration of a species in two immiscible liquids simultaneously is at times difficult, these measurements are often performed using radiolabeled solutes. For metal ions, radiotracers of the most common salt forms of the element are measured by the ratio of the count rates in each phase. Where the availability of a radionuclide is cost prohibitive or otherwise problematic, the concentration in the organic phase can be calculated by the depletion of the aqueous phase concentration of a non-radioactive form upon equilibrium, and measured by many means, including spectroscopy and chromatography. Generally, an extraction is qualified as being "good" when D values are larger than 10 (%E > 90.9%), but in some cases, distribution ratios can reach values larger than $10^4$ (E > 99.99%). An extraction process is deemed "inefficient" when D values are smaller than 1. D values on the order of up to $10^4$ are meaningful, owing to the very good detection limits of analytical techniques such as gamma spectroscopy, liquid scintillation counting, and ICP-MS.

Due to its charge, the metal ion will often have immeasurable distribution ratios in aqueous/organic biphasic systems. Therefore, a lipophilic ligand with a high formation constant for the metal ion of interest is often added to the organic phase to assist in its extraction. In the case where two metal ions that are to be separated, they will have a separation factor, $\alpha$, that is expressed by the ratio of their respective distribution ratios (Eq. 1-3).

$$\alpha = \frac{D_1}{D_2} \qquad (1\text{-}3)$$

When the separation factor approaches 1, their separation requires multiple stages. This technique, therefore, becomes quite cumbersome if it involves the arrangement of many separatory devices (*e.g.*, funnels) in series. An improved technique involves automating the process to provide a mode of continuous contact between phases.

### 1.4 Extraction Chromatographic Systems

Applying the typical organic phase in solvent extraction as the stationary phase in a column chromatographic platform provides the basis for extraction chromatography. This technique lends itself well to the analytical separation of metal ions by combining the selectivity of solvent extraction with the ease of operation provided by column chromatography. The setup has three components: an inert support, a stationary phase and a mobile phase. The inert support usually consists of beads of porous silica or a porous organic polymer on the order of 10 to 200 μm in average diameter. Extractants, either as pure compounds or as a solution in an appropriate solvent, are used as the stationary phase, which is impregnated in the macroporous solid support. Diluents are often used to facilitate dissolution of the extractant and to increase the hydrophobicity of the stationary phase. The mobile phase typically consists of a solution of a mineral acid (*e.g.*, $HNO_3$, HCl). The comparison of extraction chromatography to solvent extraction requires some background in chromatography.

Further development of solvent extraction has provided the means for multiple and continuous modes of extraction, including the countercurrent extraction ensembles used for industrial and process scale applications. Continuous countercurrent techniques are based on the theory of gas-liquid countercurrent distillation, where, in this case, the two phases are liquid, move in opposite directions, and are in constant contact. These methods are analogous to the technique of partition chromatography introduced by Martin and Synge [1.19], in which the solute(s) are distributed between two liquid phases of contrasting polarities, one of which is immobilized on a solid support, and the other that moves in a given direction. In contrast to the batch method, true equilibrium is never established in this mode. Using theory that has been applied to distillation columns, the chromatographic column is divided into equal cross-sectional lengths of the column termed the height equivalent of a theoretical plate (HETP), where the ratio between the average concentrations of the solute(s) egressing from the region is equivalent to the ratio achieved at true equilibrium [1.19]. The efficiency of a column is inversely proportional to the HETP. The migration of the solute through the column (*i.e.,* elution) is determined by the average distribution of that solute as it traverses the column length. Thus, a convenient parameter often used is the length divided by the HETP of the column, or the number of theoretical plates (N). Through the differentiation of expressions for the population distribution of the solute and the phase ratio, the effective retention volume (volume at the height of the Poisson curve generated by a normal distribution of the solute), $V_R$, can be expressed as a function of the volume of the mobile phase, $V_M$, the volume of the stationary phase, $V_S$, and the solute distribution coefficient, K.

$$V_R = V_M + K * V_S \qquad (1\text{-}4)$$

If it is assumed that D = K, from Eqn. 1-4, then the distribution coefficient is

$$D = \frac{V_R - V_M}{V_S} \qquad (1\text{-}5)$$

This treatment is ubiquitous in chromatography [1.20]. It follows that with the definition of the retention factor given by Eqn. 1-6, that the substitution of Eqn. 1-5 relates to the distribution ratio to the retention of the solute on the extraction chromatographic media through the phase ratio.

$$k' = \frac{V_R - V_M}{V_M} = D * \frac{V_S}{V_M} \qquad (1\text{-}6)$$

From these equations the retention of solute or selectivity factors may be predicted by D values obtained through solvent extraction [1.21].

The process to be considered in solvent extraction and in analogy, extraction chromatography, is that in which hydrated metal ions interact with reagents at the interface between the phases to form complexes, which are then extracted into the organic phase. The form of the complex will vary with the coordination numbers, the charge of the central atom, and the denticity and basicity of the reagent(s) [1.21]. However, when the complex formed is not fully coordinated by the reagent, its extraction will meet with difficulty because the coordination sites unoccupied by the reagent will be coordinated with water. The water molecules can either be displaced or can hydrogen bond with active extractants or ligands from the aqueous phase containing Lewis basic

moieties (e.g., $NO_3^-$, $Cl^-$). A distribution ratio must then cover all of the species present in each phase, and can be generically written as [1.21]:

$$D = \frac{mnalxhws[M_mA_n(HA)_aL_lX_x(OH)_h(H_2O)_wS_s]_{org}}{mnalxhws[M_mA_n(HA)_aL_lX_x(OH)_h(H_2O)_wS_s]_{aq}} \quad (1\text{-}7)$$

In this formula, HA represents acidic extractants, X is complexing agents, L is adduct-forming agents, and S is the organic solvent. Subscripts are assumed to be zero or integer values. While the extracted species as a whole is required to be electrically neutral.

To illustrate the concept of chelation extraction, one of the simplest systems describing the equilibrium is that which is simply dependent on the concentration of an acidic reagent in the aqueous phase, given by the process involving an acidic extractant, HA.

$$M_{aq}^{n+} + n\,HA_{org} \leftrightharpoons MA_{n,org} + n\,H_{aq}^{+} \quad (1\text{-}8)$$

The distribution ratio derived from Eqn. 1-8 is given by its relationship to the extraction constant, $K_{ex}$.

$$D = K_{ex}\frac{[HA]_{org}^{n}}{[H^+]_{aq}^{n}} \quad (1\text{-}9)$$

The logarithmic expression provides a practical approach to examining an extraction system.

$$\log D = n \log[HA]_{org} - n\, log[H^+]_{aq} + logK_{ex}$$

According to Eqn. 1-10, if the $[HA]_{org}$ or $[H^+]_{aq}$ is held constant, that is if the ionic strength of the aqueous phase is constant, then plots of log D *vs*. pH or log D *vs*. $\log[HA]_{org}$ should give lines with slopes equal to the charge of the metal ion. Similarly, when a neutral ligand is involved in complexing and extracting the metal, the bilogarithmic plots of the distribution ratio versus the extractant concentration (*i.e*., extractant dependency) should yield lines with slopes corresponding to the stoichiometry of the complex.

**1.5 Extraction of Metal Ions into Ionic Liquids**

Ionic liquids are considered a distinct class of fluids with the simple binary cation and anion combinations fitting the definition estimated to be $10^6$ possibilities [1.7]. This diversity, paired with the ease by which some of the basic common IL cation structures can be modified to change the physicochemical character, has led some to regard ILs as "designer solvents". As a result, there have been numerous studies demonstrating a remarkable ability to solubilize a wide range of organic substances [1.22-1.26], and inorganic species [1.27-1.35] can be readily extracted into them under suitable conditions. Considering the massive volume of data in the general area of metal ion extraction into ILs, a synopsis of the findings and a summary of the problems faced in these systems may be the best approach to the subject. However, before remarks are

made regarding the literature on the subject, it is important to note the metrics that determine if an IL system is considered "better" than its conventional solvent counterparts. First, a significant increase in $D_M$ would be considered an improvement. Next, an increase in the metal ion selectivity factor would also be of great interest. Lastly, systems providing efficient and facile recovery of extracted metal ions are of more practical use than those exhibiting only high extraction efficiencies.

Since the first publication proposing ILs as replacements for conventional solvents for metal ion extraction [1.27], many publications on various extraction systems have appeared. In this initial study to explore the possible utility of ionic liquids as solvents in the extraction of strontium, Dai *et al.* [1.27] reported extraordinarily efficient extraction of strontium from water by dicyclohexano-18-crown-6 in a series of 1,3-dialkylimidazolium-based ILs. As it happens, the extraction from water was radically enhanced by the participation of the IL in a cation exchange mechanism – a process that is obviously unsustainable for the recovery of both the IL solvent and the metal ions of interest [1.36]. This study was a harbinger of the results of many studies to come describing similarly high distribution ratios for various metals. For example, the extraction of $Ln^{3+}$ or $Y^{3+}$ from nitric acid by a diglycolamide extractant in an imidazolium-based IL was three-orders of magnitude greater than that observed for conventional solvents (*e.g.*, chloroform, 1,2-dichloroethane) [1.37]. A set of results for the separation of $Ce^{3+}$, $Y^{3+}$, or $Eu^{3+}$ from nitric acid using a phosphine oxide extractant (CMPO) in the same IL also resulted in extraordinarily high extraction efficiencies [1.38]. Their reports conclude that anion exchange [Turanov] and cation exchange [Nakashima] for the corresponding component of the IL is the primary mode of

extraction. As reported by Dietz, *et al*. [1.36], such systems are particularly deleterious to the recycling of the solvent. Moreover, in the pursuit of very high $D_M$, these systems would make it very expensive to recover the solutes of interest, by requiring the addition of complexing or salting-out agents in the aqueous phase. The solvent extraction adage, "What goes in must come out", is apropos in these circumstances.

In an interesting account of the extraction of uranium from nitric acid solutions into tetraalkylammonium-based ILs containing tri-n-butyl phosphate (as akin to the PUREX process) Bell and Ikeda [1.39] elucidated the U complexes by UV-VIS spectroscopy to conclude that for relatively hydrophilic ILs, a mixture of cation and anion exchange were at play, whereas for the most hydrophobic ILs, ion-pair extraction was to predominant mode of transport. As an example of a thorough study involving the effort to avoid ion exchange processes in the extraction of f-elements (uranyl ion and various trivalent lanthanides and actinides) by traditional dialkylphosphoric and dialkylphosphinic acids, Cocalia et al. [1.40] utilized traditional radiotracer measurements and UV-VIS spectroscopy, as well as EXAFS measurements, to demonstrate that the metal coordination environment in a hydrophobic imidazolium-based IL is the same as for the conventional *n*-dodecane diluent.

What is clear from many of the reports is that due to the ionic nature of ILs, their solvation of ligand-coordinated metal ion species can involve many different mechanisms resulting in a variety of possible extraction equilibria involving ion-pair extraction, ion exchange, and composites thereof, depending on the conditions [1.41, 1.42, 1.43, 1.44]. Managing the complex equilibria observed in IL-based metal ion extraction systems requires the systematic evaluation of the factors involved in the balance of those

pathways. The approaches to this may entail the use of a variety of techniques, some of them (*e.g.*, X-ray, neutron, and Raman spectroscopy) not available to all researchers, and others with which many laboratories are equipped (*e.g.*, UV-VIS, HPLC, IC, ESI-MS, ICP-MS, ICP-OES, gamma and scintillation counting equipment). Work in this laboratory has continued to attempt to clarify the factors responsible for determining the precise path followed in the extraction of a given metal ion into an IL by various extractants. In previous studies we have employed extraction by crown ethers as a test system for these factors. In continuing to explore this relatively well-behaved system, the current studies pertain to the extraction of strontium by substituted 18-crown-6 ethers, the details of which will be visited in depth in subsequent chapters.

### 1.6 Overview of the Chapters

Chapter 2 is a study that was conducted as part of a summer graduate appointment at Argonne National Laboratory exploring the innovative use of currently available sample preparation techniques and extraction chromatographic materials in order to improve upon the throughput of bioassays for radiostrontium. The results provide a context for the types of improvements to radioanalytical separations that may require novel materials.

Chapter 3 covers the investigations into the various pathways involved in the solvent extraction of alkali and alkaline earth metal ions *via* neutral crown ethers in ionic liquids. The results of these studies have provided the framework for a generalized model of the equilibria involved in these systems.

Chapter 4 describes the quest to determine the role of organic phase water content in the extraction of strontium into IL-based systems and to establish relationships between extraction efficiency and water content analogous to those discovered for similar systems

using molecular diluents. In summary, under conditions that provide extraction *via* a similarly coordinated crown ether complex, the water content of the IL phase can be used to control the extent extraction. A new set of 1,3-susbtituted imidazolium ILs incorporating an alcohol group are demonstrated to increase extraction efficiency, while maintaining the behavior becoming of the best 1,3-dialkylimidazolium-based ILs.

Chapter 5 provides the development of a high performance liquid chromatographic method for the rapid determination of IL cations (and thus ILs), and an investigation into the mechanisms involved in their retention.

Chapter 6 explores the behavior of the 1,3-dialkylimidazolium family of ILs with regards to their hydrophobicity. Specifically, the octanol-water distribution ratios of several representatives ILs are measured and correlations to their extraction behavior are presented in the critical context of the underlying principles of the partitioning processes involved. Furthermore, as the newly developed HPLC method (Chapter 5) was used for analysis, the retention factors for those ILs were explored as a means to provide more rapid estimates of extraction behavior.

In Chapter 7, a set of techniques have been combined to explore the relative contributions of various extraction pathways, heretofore unresolved. With the development of new analytical methods to determine the species that indicate the involvement of various modes of metal ion partitioning, a strategy is proposed to subtract the contribution of one pathway from another, under given conditions. Thus, a way to quantitatively determine the contributions from these pathways has been devised.

Chapter 8 considers the practical implications of using ILs as solvents for the selective extraction of strontium *via* neutral crown ethers. Explanations of the strategies

involved in preparing concentrated solutions of the extractants in ILs are given. The results of solvent extraction studies using the more hydrophobic di-*t*-butyl-substituted crown ethers are discussed in the context of system performance as an extraction chromatographic material. Additionally, a short section is provided entailing the unsuccessful attempts to apply magnetic ionic liquids to the same systems.

Chapter 9 offers a summary of the accomplishments in this work and recommendations for further research in this field.

## 1.8 References

[1.1] J. Rydberg, *Solvent Extraction Principles and Practice, Revised and Expanded*, CRC Press, New York, **2004**.

[1.2] J.D. Werner, U.S. Spent Nuclear Fuel Storage, Congressional Research Service, http://www.fas.org/sgp/crs/misc/R42513.pdf, accessed 10 October 2012.

[1.3] E.P. Horwitz, M.L. Dietz, D.E. Fisher, *Sol. Extr. Ion Exch*. **1991**, 9, 1-25.

[1.4] P.A. Baisden, G.R. Choppin, *RADIOCHEMISTRY AND NUCLEAR CHEMISTRY – Nuclear Waste Management and the Nuclear Fuel Cycle*, Ed. Sándor Nagy, in Encyclopedia of Life Support Systems (EOLSS), Developed under the Auspices of the UNESCO, Eolss Publishers, Oxford ,UK, **2007**, [http://www.eolss.net], accessed 10 October 2012.

[1.5] E.P. Horwitz, M.L. Dietz, D.E. Fisher, *Anal. Chem*. **1991**, 63, 522-525.

[1.6] J.P. Hallett, T. Welton, *Chem Rev*. **2011**, 111, 3508-3576.

[1.7] N.V. Plechkova, K.R. Seddon, *Chem. Soc. Rev*., **2008**, 37, 123–150.

[1.8] M.L. Dietz, *Sep. Sci. Technol*. **2006**, 41, 2047–2063.

[1.9] P. Walden, *Bull. Acad. Impér. Sci. St. Pétersbourg*, **1914**, 8, 405–422.

[1.10] C. Graenacher, *Cellulose solution*, US Pat., 1943176, **1934**.

[1.11] F. H. Hurley, *Electrodeposition of Aluminum*, US Pat., 4,446,331, **1948**.

[1.12] F. H. Hurley and T. P. Wier, *J. Electrochem. Soc*., **1951**, 98, 203–206.

[1.13] H. L. Chum, V. R. Koch, L. L. Miller, R. A. Osteryoung. *J. Am. Chem. Soc*. **1975**, 97, 3264–3267.

[1.14] J.S. Wilkes, J.A. Levisky, R.A. Wilson, C.L. Hussey, *Inorg. Chem*. **1982**, 21, 1263-1264.

[1.15] J.S. Wilkes, M.J. Zawarotko, *Chem. Commun*., 1992, 13, 965-967.

[1.16] P. Bonhote, A.P. Dias, N. Papageorgiou, K. Kalyanasundaram, M. Grätzel, *Inorg. Chem.* **1996**, 35, 1168-1178.

[1.17] C. Schröder, T. Rudas, G. Neumayr, W. Gansterer, and O. Steinhauser, *J. Chem. Phys.* 2007, 197, 044505.

[1.18] H. Tokuda, K. Hayamizu, K. Ishii, Md.A. Bin Hasan Susan, M. Watanabe, J. Phys. Chem. B 2005, 109, 6103-6110.

[1.19] A.J.P. Martin, R.L.M. Synge, *J. Biochem*. 1941, 35, 1358-1368.

[1.20] R. Consden, A.H. Gordon, A.J.P. Martin, *J. Biochem*. 1944, 38, 224-232.

[1.21] T.Braun and G. Ghersini, *Extraction Chromatography, Journal of Chromatography Library Vol. 2*, Elsevier, New York, **1975**.

[1.22] J.G. Huddleston, H.D. Willauer, R.P. Swatloski, A.E. Visser, R.D. Rogers *Chem. Commun*., **1998**, 1201-1202.

[1.23] S. Carda-Broch, A. Berthod, D.W. Armstrong, *Anal. Bioanal. Chem*. **2003**, 375, 191-199.

[1.24] J. McFarlane, W. B. Ridenour, H. Luo, R. D. Hunt, D. W. DePaoli, R.X. Ren, *Sep. Sci. Technol*. **2005**, 40, 1245-1265.

[1.25] R.P. Swatloski, S.K. Spear, J.B. Holbrey, R.D. Rogers, *J. Am. Chem. Soc*., **2002**, 124, 4974-4975.

[1.26] W. Li, N. Sun, B. Stoner, X. Jiang, X. Lu, R.D. Rogers, *Green Chem*. **2001**, 13, 2038-2047.

[1.27] S. Dai, Y.H. Ju, C.E. Barnes, *J. Chem. Soc., Dalton Trans.* **1999**, 1201-1202.

[1.28] A.E. Visser, R.P. Swatloski, W.M. Reichert, S.T. Griffin, R.D. Rogers, *Ind. Eng. Chem. Res*. **2000**, 39, 3596-3604.

[1.29] A.E. Visser, R.P. Swatloski, S.T. Griffin, D.H. Hartman, R.D. Rogers, *Sep. Sci. Technol*. **2001**, 36, 785-804.

[1.30] S. Chun, S.V. Dzyuba, R.A. Bartsch, *Anal. Chem*. **2001**, 73, 3737-3741.

[1.31] H. Luo, S. Dai, P.V. Bonnesen, *Anal.Chem*. **2004**, 76 2773-2779.

[1.32] J. Huang, A. Riiager, P. Wasserscheid, R. Fuhrmann, *Chem. Commun*., **2006**, 4027-4029.

[1.33] K. Binnemans, *Chem. Rev.*, **2007**, 107, 2592-2614.

[1.34] M.L. Dietz, D.C. Stepinski, *Talanta*, **2007**, 75, 598-603.

[1.35] D.C. Stepinski, G.F. Vandegrift, I.A. Shkrob, J.F. Wishart, K. Kerr, M.L. Dietz, D.T.D. Qadah, S.L. Garvey, *Ind. Eng. Chem. Res.* **2010**, 49 5863-5868.

[1.36] M.L. Dietz, J.A. Dzielawa, *Chem. Commun*. **2001**, 20, 2124-2125.

[1.37] A.N. Turanov, V.K. Karandashev, V.E. Baulen, *Sol. Extr. Ion Exch*. **2008**, 28, 367-387.

[1.38] K. Nakashima, F. Kubota, T. Maruyama, M. Goto, *Ind. Eng. Chem. Res*., **2005**, 44 , 4368-4372.

[1.39] T.J. Bell, Y. Ikeda, *Dalton Trans*. **2011**, 40, 10125.

[1.40] V.A. Cocalia, M.P. Jensen, J.D. Holbrey, S.K. Spear, M.C. Stepinski, R.D. Rogers, Dalton Trans., **2005**, 1957-1965.

[1.41] D.C. Stepinski, M.L. Dietz, *Green Chem.* **2005**, 7, 747-750.

[1.42] V.A. Cocalia, J.D. Holbrey, K.E. Gutowski, N.J. Bridges, R.D. Rogers, *Tsinghua Sci.*
*Technol.* **2006**, 11, 188.

[1.43] M.S. Murali, N. Bonville, G.R. Choppin, *Sol. Extr. Ion Exch*. **2010**, 28, 495-509.

[1.44] C.A. Hawkins, S.L. Garvey, M.L. Dietz, *Sep. Purif. Technol.* **2012**, 89, 31-38.888

# CHAPTER 2:

# DEVELOPMENT OF A NOVEL TANDEM METHOD FOR THE RAPID ISOLATION OF RADIOSTRONTIUM FROM HUMAN URINE

## 2.1 Introduction

The possibility of an accidental or intentional release of radioactive substances has increased demand for analytical methods capable of rapidly screening large numbers of individuals for possible internal exposure. Because of their decay characteristics, abundance in spent nuclear fuel, and occurrence in industrial and commercial products, certain radionuclides pose a particular health risk to humans. At approximately 6% of the total fission yield of uranium-235/238, strontium-90 is considered a medium-lived major fission product [2.2]. Strontium-90 decays with a half-life of 29 years, undergoing emission of a 0.55 MeV negatron to form yttrium-90, which in-turn decays with a half-life of 64 hours to stable zirconium-90 by emission of a 2.3 MeV negatron [2.3]. In its pure form, strontium-90 has several industrial uses, including as the primary heat source in radioisotope thermoelectric generators and as a radiation source in metal alloy thickness gauges [2.4], furnishing relatively low security sources of this material. Because of its close chemical resemblance to calcium, strontium follows the same biological pathways when ingested, and 20-30% of it accumulates internally, primarily in the bones and teeth [2.4], resulting in an effective (*i.e.*, biological) half-life of eighteen years [2.5]. It therefore poses a major risk to public health in the event of a nuclear or radiological emergency. The accident at the Chernobyl nuclear power plant in the former

Soviet Union, which represents the largest historical worldwide release of strontium-90 to date, has led to many cases of leukemia of other blood and bone diseases [2.4].

Accordingly, methods have been developed for the quantification of radiostrontium in a wide variety of sample types, including seawater [2.6], milk [2.7], urine [2.8-2.11], soil [2.12], and animal tissue [2.13]. Because of the relative ease of sampling and processing, urine is the most common sample matrix for radionuclide bioassays [2.10]. Urine analysis for the detection of internal radionuclide contamination is not without complications, however. Normal human urine contains organic molecules (*e.g.*, urea, uric acid, urobilin, bilirubin, creatinine, and smaller amounts of carbohydrates, proteins, fatty acids, hormones, pigments, mucins), and ions (*e.g.*, sodium, potassium, calcium) that can interfere with the isolation and detection of radionuclides. Widely used experimental protocols for monitoring radiation workers for potential exposure to actinides and fission products involve processing large volumes of urine by time-consuming precipitation, digestion, and ashing steps to preconcentrate the analytes and remove urine matrix components [2.8]. To improve urine sample throughput, methods have recently been developed in which the precipitation step is eliminated by applying smaller volumes (≤ 50 mL) of minimally-treated urine directly to extraction chromatographic (EXC) media for separation and preconcentration of the radioactive elements [2.9-2.11]. Although these methods eliminate the digestion and total precipitation steps; they also omit steps to remove high molecular mass organic constituents from raw urine that can lead to fouling of extraction chromatographic columns. Furthermore, the heme breakdown pigments (*i.e.*, bilirubin) in urine that pass through the column absorb the light emitted by secondary and ternary fluors during liquid scintillation counting, complicating accurate

measurements. As part of an effort to minimize sample pretreatment procedures, reduce costs, and decrease processing time in the determination of radiostrontium in urine, we have investigated the pretreatment of urine by organophilic adsorbents and the purification and preconcentration of strontium by a novel, tandem column arrangement employing a strong cation exchange resin (Diphonix®) in combination with a strontium-selective extraction chromatographic material (Sr resin). A simple retention model has been used to facilitate identification of the optimum chromatographic conditions.

## 2.2 Experimental

### 2.2.1 Materials

All reagents were ACS reagent grade or better. Strontium-85 and sodium-22 radiotracers were purchased as nominal solutions from Eckert and Ziegler Isotope Products, Inc. (Valencia, CA). Radiotracer measurements were performed on a spiked sample prior to treatment and on the equilibrated aqueous phase after treatment. Stock solutions used for ICP-OES determination were prepared from a stable strontium chloride salt purchased from Aldrich (St. Louis, MO). Deionized water of at least 18 $M\Omega \cdot cm^{-1}$ resistivity was used in the preparation of all solutions. Diphonix® resin (50-100 mesh) and Sr resin (50-100 μm particle size) were obtained from EiChroM Technologies, Inc. (Darien, IL). Activated charcoal was procured from Mallinckrodt Chemicals, Inc. (Phillipsburg, NJ). Amberlite XAD-7 (100-200 mesh) polymeric adsorbent and the sodium chloride and potassium chloride salts used to make the saline solution were obtained from Sigma-Aldrich (Milwaukee, WI). Frozen certified normal human urine was obtained from Innovative Research, Inc (Novi, MI, Lot IR100706), stored at < -10

°C, and thawed only once for use. In the discussion that follows, "raw urine" refers to that which has not been previously frozen. The strontium content of blank urine was not detectable.

### 2.2.2 Instruments

All UV spectra were measured against a water reference using a Perkin-Elmer Lambda 4B UV/VIS spectrophotometer with 1-cm pathlength quartz cuvettes. Elemental analysis of extraction chromatographic eluate was performed using a Perkin-Elmer Optima Model 3300 DV inductively-coupled plasma optical emission spectrometer (ICP-OES). Radiotracers were assayed using a Perkin-Elmer A5550 MINIMAXIγ Automatic Gamma Counter.

### 2.2.3 Methods

Weight distribution ratios ($D_w$) for strontium and sodium ions were determined radiometrically using commercial radiotracers, and assayed *via* gamma spectroscopy using standard procedures. $D_w$ is defined by Equation 2-1:

$$D_w = [(C_0 - C_f)/C_f]\,[V/m] \qquad (2\text{-}1)$$

where $C_0$ and $C_f$ are the counts rates for a tracer-spiked aqueous phase of volume $V$ (mL) prior to and following contact with a mass $m$ (grams) of resin or solid extraction phase, respectively. Each $D_w$ value is the average of at least three replicates with resulting uncertainties based on counting statistics that were generally within 10%. Determination of the dry mass fraction of Diphonix® resin was performed by weighing samples ($n$ = 3, RSD = 0.28%) of resin before and after drying in a vacuum oven at 70 °C for 12 hours.

Column bed densities were determined by measuring the volume occupied by a known mass of resin packed in the column.

The urine sample pretreatment experiments consisted of acidification of urine with concentrated nitric acid or methanesulfonic acid, followed by addition of triplicate aliquots of these stocks to either Amberlite XAD-7 (which is an acrylic ester resin) or activated charcoal in polypropylene snap-cap tubes at phase ratios of 50, 100, or 200 (mL $g^{-1}$ adsorbent). The tubes were vortex mixed for 1 minute and centrifuged for 15 minutes, after which the suspensions were filtered through 0.15-0.45 $\mu$m polypropylene filters to remove microparticles. Retention of $Sr^{2+}$ on the adsorbents was determined by spiking the urine samples with $^{85}Sr$ and measuring the weight distribution ratios after equilibration. The solution pH was measured using universal indicator strips (ThermoFisher Scientific, Pittsburgh, PA).

### 2.2.4 Overview of the procedure

The approach to the separation and preconcentration of radiostrontium from urine is summarized in Figure 2.1. This procedure involves an initial acidification of the urine sample to pH < 2 using methanesulfonic acid (MSA) and pretreatment with activated charcoal (1:100 charcoal:sample) to remove organic constituents. Following filtration, the sample is treated in succession with Diphonix® resin (a strong acid ion exchange resin) to remove the interfering cations and finally with Sr resin (a porous polymeric chromatographic support loaded with 1.0 M 4,4',(5')-di(*tert*-butyl-cyclohexano)-18-crown-6 in 1-octanol) to complete the purification and preconcentration process. Because normal urine samples may contain large amounts of sodium (50 to 200 mM) [2.15] and potassium (20 to 70 mM) [2.15], and because the crown ether on which the Sr resin is

based exhibits measureable affinity for both of these ions [2.16] (see Table 1), it is important that they be removed prior to application of the sample to the Sr resin column. This can be accomplished with Diphonix® resin, which exhibits relatively strong retention of alkaline earth cations and poor retention of $Na^+$ and $K^+$ from dilute (*ca.* 0.1 M) acid solutions. (According to the manufacturer, Diphonix® resin is composed of a polystyrene/divinylbenzene matrix containing carboxylic, 4-benzenesulfonic, and diphosphonic groups.) Once the levels of the alkali ions have been sufficiently reduced (to < 10 mM), a small-volume Sr resin column (*ca.* 10% of the volume of commercially available columns) can be employed to decontaminate and further concentrate the $^{90}Sr$. It is important to note that iron, aluminum, actinides, and lanthanides are very strongly retained ($D_w \sim 10^2$ to $10^3$ for trivalent ions and $D_w \sim 10^4$ for tetravalent ions, where $D_w$ is defined in Eqn. 1 in Section 2.2) by Diphonix® resin up to acidities as high as 4 M $HNO_3$ (due largely to the formation of very strong complexes with the phosphoryl groups by these metal species. [2.17]) Consequently, the presence of $^{90}Y$ in secular equilibrium with $^{90}Sr$ is unproblematic, because $Y^{3+}$ will be retained by the Diphonix column under conditions that permit elution of strontium and thus will be eliminated by this separation step. It is also noteworthy that, although there is little selectivity between alkaline earth metal ions on Diphonix resin, calcium ions have the lowest published retention of these ions on Sr resin, making calcium easily separable from strontium in this process [2.16-2.17]. Moreover, it is expected on the basis of the size selectivity of the crown ether ligand, that magnesium ions will exhibit poorer retention on Sr Resin than calcium ions.

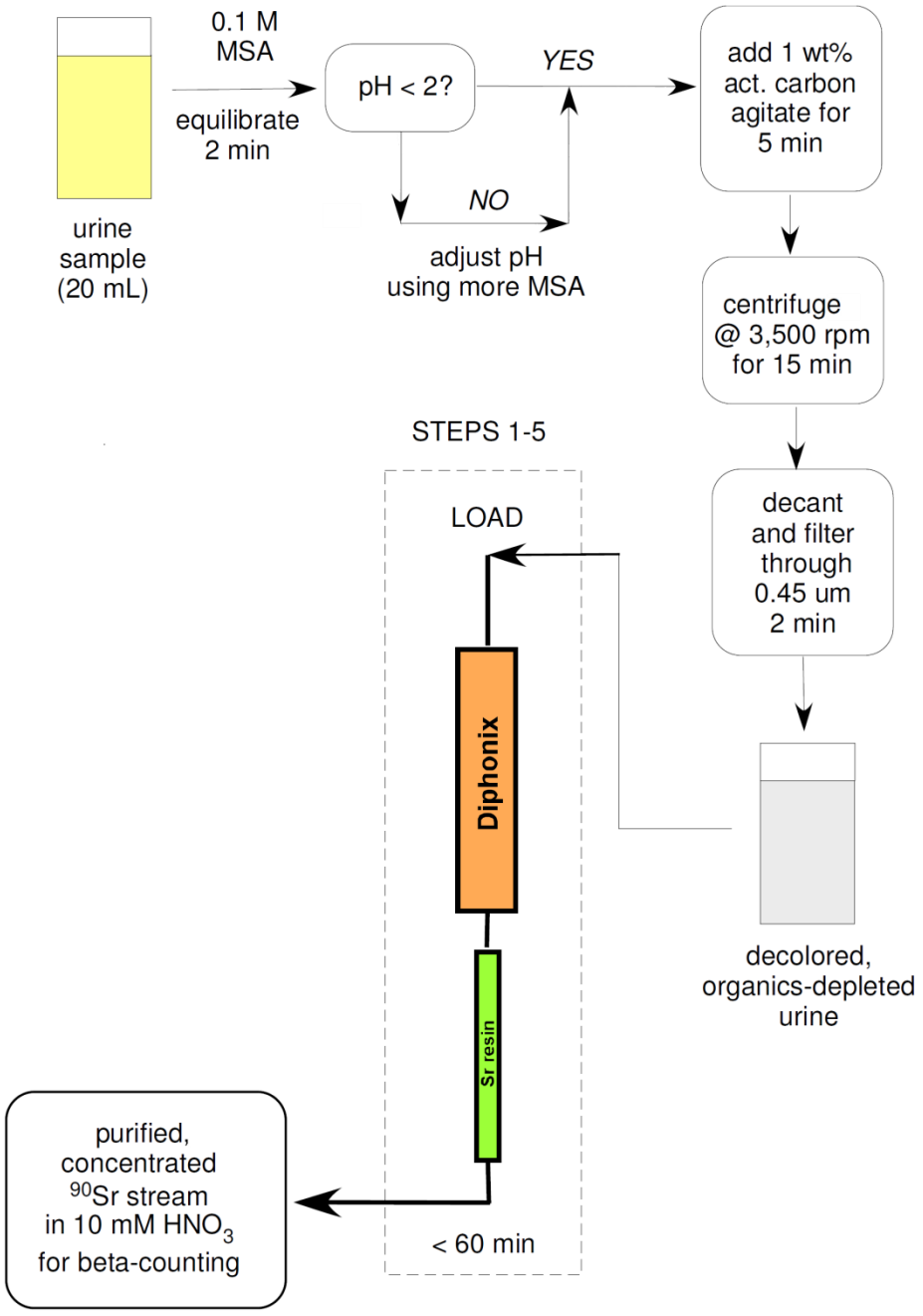


**Figure 2.1: Overview of procedure for rapid $^{90}$Sr sorption, purification, and concentration from human urine samples.**

**Table 2.1**
**Calculated values of Retention Coefficient ($k_{ex}$) for Sr resin**

| Resin & Conditions[a, b] | $[HNO_3]$, M | $k_{ex}$ $K^+$ | $Na^+$ | $Sr^{2+}$ |
|---|---|---|---|---|
| | 0.02 | 0.1 | 0.10 | 0.2 |
| | 0.05 | 0.1 | 0.10 | 0.7 |
| | 0.10 | 0.9 | 0.10 | 1.1 |
| | 0.30 | 1.8 | 0.20 | 6.5 |
| | 0.50 | 2.0 | 0.20 | 11 |
| | 1.00 | 3.5 | 0.30 | 30 |
| | 2.00 | 3.5 | 0.28 | 50 |
| | 4.00 | 3.0 | 0.28 | 70 |
| | 7.00 | 0.8 | 0.10 | 80 |

[a] Calculated by Dr. Ilya Shkrob (Argonne) using Eqn 2-2 and assuming a bed ratio of 0.30 for Sr resin
[b] The parameters are taken from the data supplied by the manufacturer, EiChroM

## 2.3 Development of a Rapid Sample Pretreatment

### 2.3.1 Removal of urine matrix components

As noted in section 2.2.4, the analytical procedure devised here requires pretreatment of the urine sample to remove organic compounds that can foul the chromatographic resins and interfere with liquid scintillation counting by acidification of the raw urine and stirring with an organophilic adsorbent. The efficiency of removal of urine pigments was evaluated by noting the extent of decolorization of the urine and, for XAD-7, any change in the appearance (shade/color) of the sorbent following equilibration (see Table 2.2). While samples treated with charcoal were immediately decolorized upon contact, much slower uptake of color from acidified urine was observed for XAD-7, with apparent equilibrium being reached only after more than five 1-2 minute intervals of vigorous mixing and two 30-minute intervals of standing. Removal or deactivation of high molecular mass substances (*e.g.*, proteins) from the urine was indicated by the fact that

the pretreated samples displayed water-like consistencies and no emulsion or bubble formation upon agitation. Raw urine, in contrast, was found to produce substantial and persistent foam upon shaking.

**Table 2.2**
**Color observed during urine pretreatment**

| **Nitric acid-treated samples** | | | |
|---|---|---|---|
| [Acid], M | Color of urine following acidification | Color of acidified urine following equilibration with XAD-7 | Color of XAD-7 following equilibration with acidified urine |
| 0.001 | light yellow | colorless | light orange |
| 0.01 | light yellow | colorless | light orange |
| 0.1 | light orange | colorless | orange |
| 1 | light orange | colorless | red-brown |
| 4 | brilliant yellow | light yellow | orange |
| 8 | pale yellow | pale yellow | light yellow |
| **MSA-treated samples** | | | |
| [Acid], M | Color of urine following acidification | Color of acidified urine following equilibration with XAD-7 | Color of XAD-7 following equilibration with acidified urine |
| 0.001 | light yellow | colorless | light orange |
| 0.01 | light yellow | colorless | light orange |
| 0.1 | yellow | colorless | orange |
| 1 | orange | colorless | red-brown |
| 4 | red-brown | light yellow | orange |

The extent of urine pigment removal by activated charcoal was assessed (by Ilya Shkrob at Argonne National Labortory) using UV spectroscopy. A sample of certified urine was adjusted to pH < 2 with MSA, after which a portion of the sample was diluted 1:10 with water and the UV spectrum (200 nm to 350 nm) measured. Another aliquot of the acidified urine was treated with activated charcoal (1:50 charcoal:sample), filtered through a 0.2 $\mu$m syringe filter and diluted 10-fold with water before the absorption

spectrum of this solution was obtained. An overlay of these spectra is provided in Figure 2.2, where absorbance is plotted versus wavelength. These results indicate that the treated sample is transparent at wavelengths greater than 240 nm. The significance of this result is that the secondary fluor will receive all of the energy from the solvent and there will be no interference with emission of the fluors. For example, a typical primary fluor, 2,5-diphenyloxazole (PPO) [2.18], has an absorption band with onset at 240 nm and peak at 300 nm. A secondary fluor commonly paired with PPO, *p-bis*-[2-(4-methyl-5-phenyloxazolyl)]benzene (POPOP) [2.18], has an onset of the absorption band at 240 nm and a peak absorption at 275 nm (emission at 290 nm); the onset of the emission band is 270 nm, all of which are in the transparency region. Put succinctly, there will be no interference with scintillation counting due to urine matrix-associated color quench.

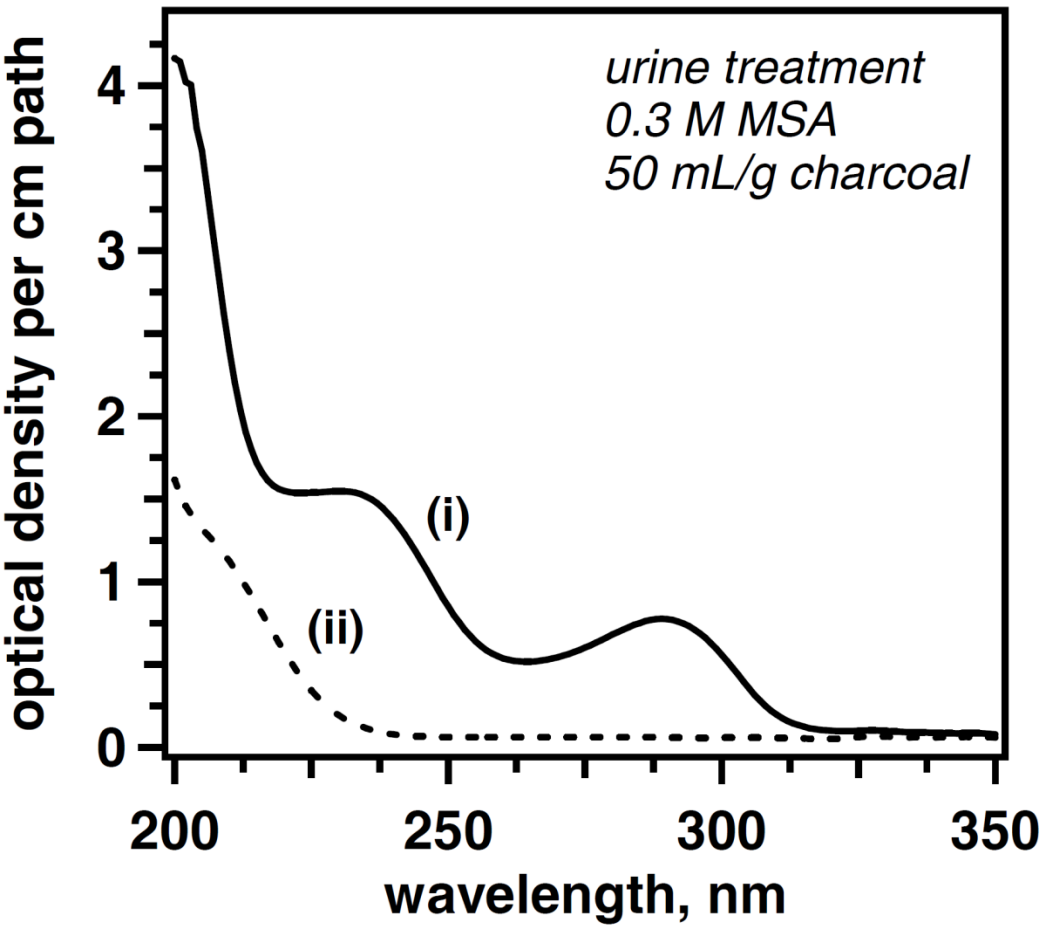


**Figure 2.2: UV spectrum of acidified urine before and after treatment with activated charcoal.** The solid trace (i) is that of the untreated urine sample (diluted 1:10), while the dashed trace (ii) is that of the sample treated with charcoal followed by ten-fold dilution with water. (Data were provided by Dr. Ilya Shkrob, Argonne National Laboratory.)

2.3.2 Uptake of Strontium by Pretreatment Adsorbents

To determine the effect of sample pretreatment on the recovery of strontium, $Sr^{2+}$ uptake by the various sorbents in contact with certified human urine acidified to various nitric acid or methanesulfonic acid concentrations was measured. After treatment with either activated charcoal or XAD-7 (resin:aqueous ratio of 1:100), $Sr^{2+}$ recoveries of between 87% and 114% were obtained. (That is, little or no uptake of $Sr^{2+}$ by either material was observed.) In most cases minimal difference was noted between charcoal

and XAD-7 using either nitric acid or MSA (Table 2.3). Essentially quantitative recovery of strontium in the presence of charcoal was achieved at acid concentrations of 0.10 M and greater. These results stand in contrast to those reported previously [2.10], where up to half of the strontium spiked in HCl-acidified urine was retained on activated charcoal. All conditions for XAD-7 treatment led to quantitative recovery of strontium.

**Table 2.3**
**Recovery of strontium from acidified urine treated with charcoal and XAD-7[a]**

| [Acid], M | $HNO_3$/Charcoal Recovery, % | MSA/Charcoal Recovery, % | $HNO_3$/XAD-7 Recovery, % | MSA/XAD-7 Recovery, % |
|---|---|---|---|---|
| 0.001 | 84.7 ± 2.0 | 91.2 ± 1.8 | 99.1 ± 1.2 | 114 ± 1.8 |
| 0.01 | 96.0 ± 2.1 | 93.3 ± 0.93 | 98.3 ± 2.3 | 100 ± 2.4 |
| 0.1 | 98.4 ± 2.1 | 96.3 ± 1.8 | 97.3 ± 5.4 | 97.2 ± 1.5 |
| 1 | 97.0 ± 2.2 | 99.4 ± 1.6 | 98.5 ± 1.6 | 98.8 ± 3.2 |
| 4 | 98.0 ± 2.5 | 98.8 ± 2.2 | 99.3 ± 1.1 | 99.3 ± 2.0 |
| 8 | 98.2 ± 1.8 | not measured | 99.3 ± 1.6 | not measured |

[a] Uncertainties are calculated from three measurements at the 95% confidence interval.

### 2.3.3 Selected Pretreatment

On the basis of the results described in sections 2.3.1 and 2.3.2, pretreatment involving acidification of the urine sample with MSA (introduced in neat form) to a pH of less than 2 (*e.g.*, 0.1 M to 0.3 M MSA) followed by stirring of the solution with 1% (w/v) activated charcoal was chosen as optimum. After this treatment (< 5 min), the sample is filtered to remove microparticles of activated carbon, rendering it suitable for the next step in the process. Several aspects of this pretreatment process warrant comment. First, at pH < 2, $Sr^{2+}$ is released from the urine components to which it binds. Next, unlike nitric acid, MSA does not react with bile pigments to form highly UV-absorbing nitroaromatic compounds that interfere with liquid scintillation counting.

Lastly, activated charcoal with MSA treatment removes bile pigments and high-molecular mass compounds that foul chromatographic columns. At the same time, activated carbon does not retain $Sr^{2+}$ during the treatment, provided that pH < 2. (Because the pH of urine naturally varies from 4.4 to 8 and urine has mildly buffering properties, addition of 0.1 M MSA may not result in pH <2 for some samples. In this case, the pH is simply adjusted by addition of neat MSA until the pH < 2.)

## 2.4 Retention of Strontium and Sodium on Diphonix® Resin

### 2.4.1 Dependence of strontium and sodium uptake on acid concentration

Because the uptake of alkali and alkaline earth metals by the Diphonix® resin is accompanied by the displacement of a number of protons corresponding to the charge on the ion, it is expected that a plot of $D_w$ for $Sr^{2+}$ uptake by Diphonix® resin vs. $[H_3O^+]$ will exhibit a slope of -2, while an analogous plot for alkali metal ions should yield a slope of -1. Accordingly, the retention of a given alkaline earth metal ion should far exceed that of alkali metal ions over a range of conditions. As shown in Figure 2.3, which depicts the dependence of strontium ion and sodium ion (chosen as a representative alkali metal) uptake by the Diphonix® resin as a function of the concentration of MSA in the aqueous phase, this is indeed the case. As predicted for extraction involving only cation exchange, the slopes of the bilogarithmic data are -1 and -2 for sodium and strontium cations, respectively, in the region where these curves are linear. By performing linear regression analysis of the strontium data from 0.10 M MSA to 2.0 M MSA and sodium data from 0.10 M MSA to 1.5 M MSA ($r^2 > 0.99$), the selectivity of $Sr^{2+}/Na^+$ is estimated to vary from 120 at low acidity to 9 at higher acidities. These data indicate that the reduction of

urine matrix alkali metals (*i.e.*, $Na^+$ and $K^+$) can be accomplished by loading the decolorized urine sample directly on a Diphonix® resin cartridge and washing with a low acidity eluent. The alkali metal ions will be removed by this wash, while strontium is retained for the subsequent preconcentration step. As shown in Figure 2.4, elution with 0.1 M MSA results in $k_{ex} < 10$ for $Na^+$ (and by analogy for $K^+$), whereas for $Sr^{2+}$, $k_{ex} > 100$, indicating that the complete separation of the $Sr^{2+}$ from the alkali ions is feasible on a Diphonix column. Note that the capacity factor is defined as the number of free column volumes needed to reach peak maximum for particular solute, and is related to the weight distribution coefficient ($D_w$) through

$$k_{ex} = D_w \rho V_s/V_m, \qquad (2\text{-}2)$$

where $\rho$ is the density of the resin, $V_s$ is the volume of the stationary phase and $V_m$ is the volume of the mobile phase. Using $\rho = 1.16$ g $mL^{-1}$ and the bed density of 0.30 g $mL^{-1}$, for the Diphonix® resin, $k_{ex} \approx D_w/2.01$. Using this formula, we calculated the capacity factors $k_{ex}$ for $Sr^{2+}$, $K^+$, and $Na^+$ on the Diphonix® resin using the data given in Figure 2.3.

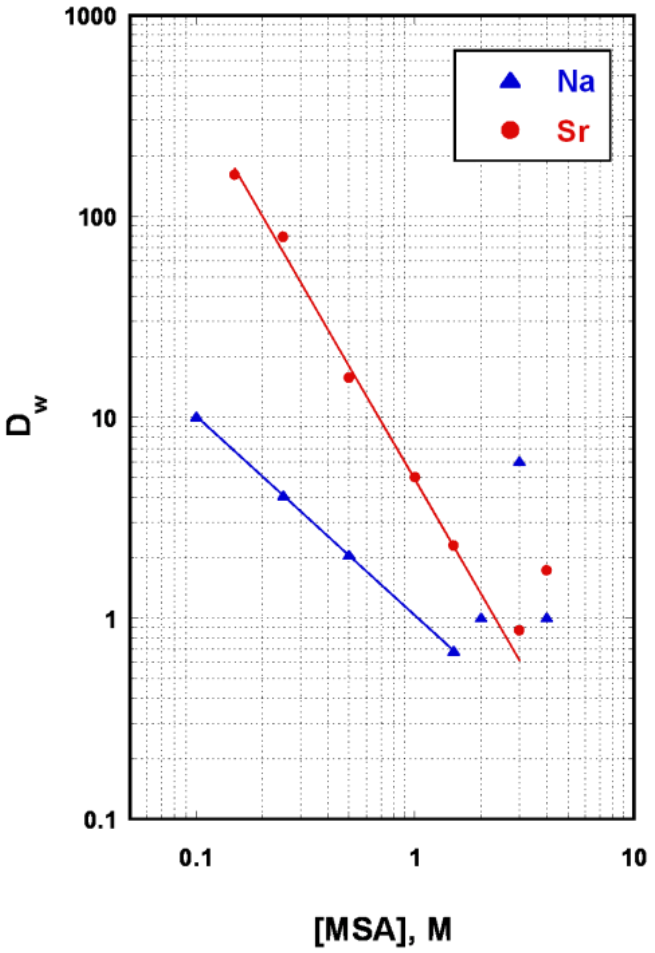


**Figure 2.3: Methanesulfonic acid dependency of $Sr^{2+}$ and $Na^{+}$ retention by Diphonix® resin.** The lines are linear least-squares fits to the data points, intended as visual guides.

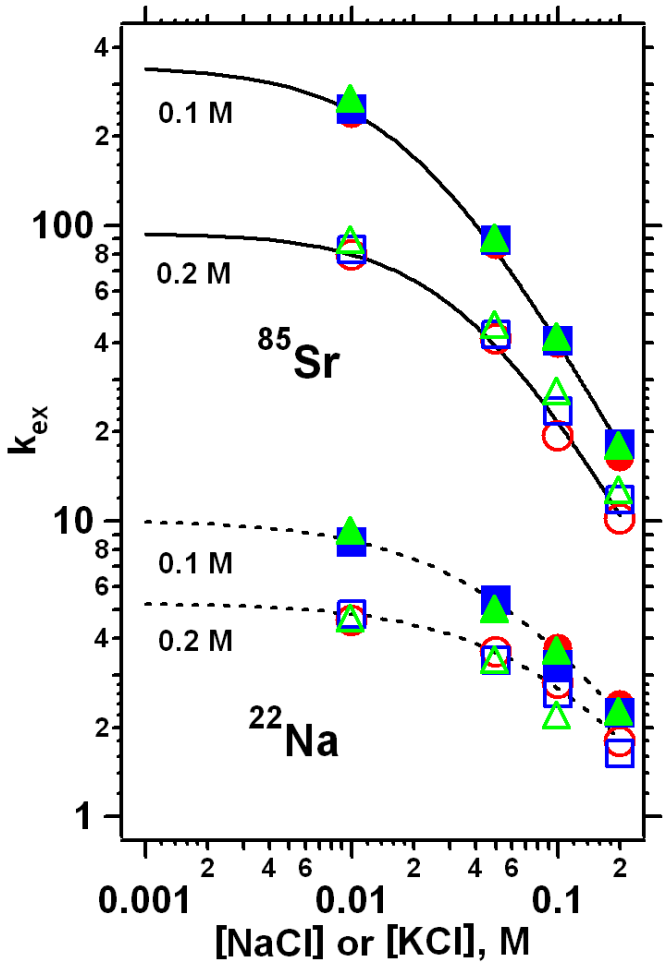


**Figure 2.4: Dependence of $k_{ex}$ for $^{85}Sr$ and $^{22}Na$ on Diphonix® resin on the molar concentration of $Na^+/K^+$ (1:1) ions.** The conditions are indicated by 1:10 phase ratio with 0.1 M MSA (●) and 0.2 M MSA (○), 1:20 phase ratio with 0.1 M MSA (■) and 0.2 M MSA (□), 1:30 phase ratio with 0.1 M MSA (▲) and 0.2 M MSA (△). The lines are fits to Equation 4. (Data were provided by Dr. Ilya Shkrob, Argonne National Laboratory.)

Figure 2.5 compares results for strontium uptake by Diphonix® resin from aqueous phases containing a given concentration of MSA in presence of 0.5 M $HNO_3$. No significant difference is observed in the two sets of results up to approximately 2 M acid, and the data, not unexpectedly, closely resemble published nitric acid dependencies [2.19]. In all instances, $D_w$ for $Sr^{2+}$ uptake falls as the aqueous acidity increases, consistent with cation exchange. Interestingly then, MSA yields essentially the same retention of strontium as nitric acid under a given set of conditions. Thus, our choice of

MSA for sample acidification, which was prompted by consideration of sample decolorization (see section 2.3.3), is further supported by the efficient and selective retention of $Sr^{2+}$ upon the Diphonix® resin achieved with it.

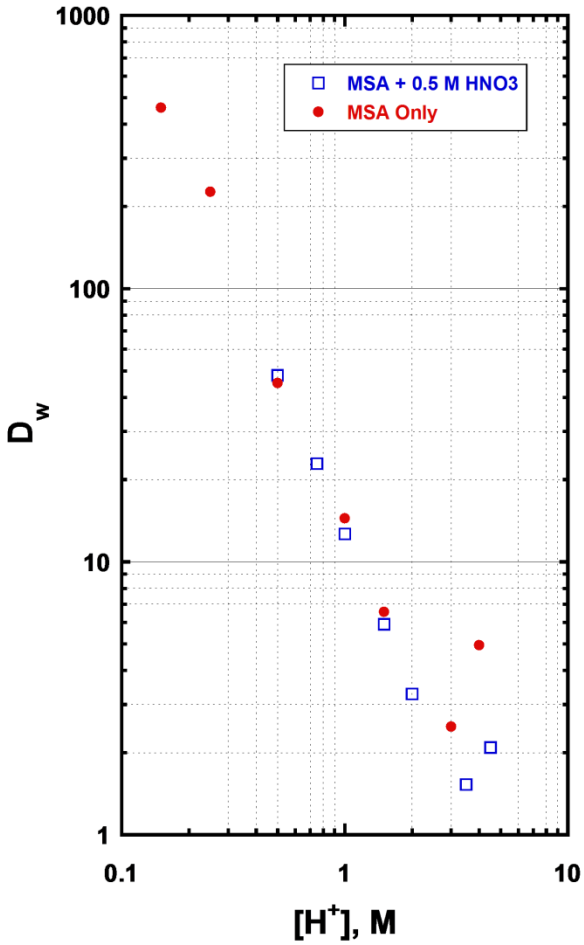


**Figure 2.5: Acid dependency of $Sr^{2+}$ retention by Diphonix® resin.**

2.4.2 Diphonix® column trials

Of course, the performance of a real column is less predictable because the Diphonix® resin column operates far from equilibrium. In the simplest column test (Figure 2.6 panel A), 10 column volumes of the saline solution in 0.1 M MSA were loaded on a 0.54 $cm^2$ x

3.7 cm (2 mL) column. The alkali ions were then eluted at 1.5 mL $min^{-1}$ using 0.1 and 0.2 M MSA as eluent. The alkali ions on the column were eluted down to < 1 mM in 20 column volumes (the minimum column volumes for elution of each ion are given in Table 4. Estimates of the number of column volumes required to elute the alkali ions with 0.1 M MSA after a 10 column volume load on 2 mL Diphonix® resin column (1.5 mL $min^{-1}$ flow rate) were 18 and 10 for $K^+$ and $Na^+$ respectively. Elution with 0.2 M MSA under the same loading conditions required 12 and 7 column volumes for $K^+$ and $Na^+$, respectively. As shown in Figure 2.6 panel B and Table 2.4, stripping the column after elution of 22 column volumes lead to 100% recovery of strontium and reduced the concentration of sodium and potassium to the limits of detection. In this experiment, less than 40% of the alkali ions were retained on the column during loading, while $Sr^{2+}$ was quantitatively retained. The same relates to the experiment with acidified urine (0.1 M MSA) spiked with 6.5 mM strontium (Figure 2.6 panel C and Table 2.4). Less than 30% of the alkali ions were retained during the 10 column volume loading. The alkali ions were eluted down to negligible concentrations in 10 column volume elution with 0.1 M MSA, while 98% of $Sr^{2+}$ was retained at the column. A 15 column volume wash would result in 5% loss of $Sr^{2+}$, while the 22 column volume wash results in 13% loss of strontium. (That is, a strontium recovery of 87% is obtained in the nitric acid strip following a 22 column volume elution.) This experiment suggests that unidentified components of urine decrease the capacity factors below those in the saline solution.

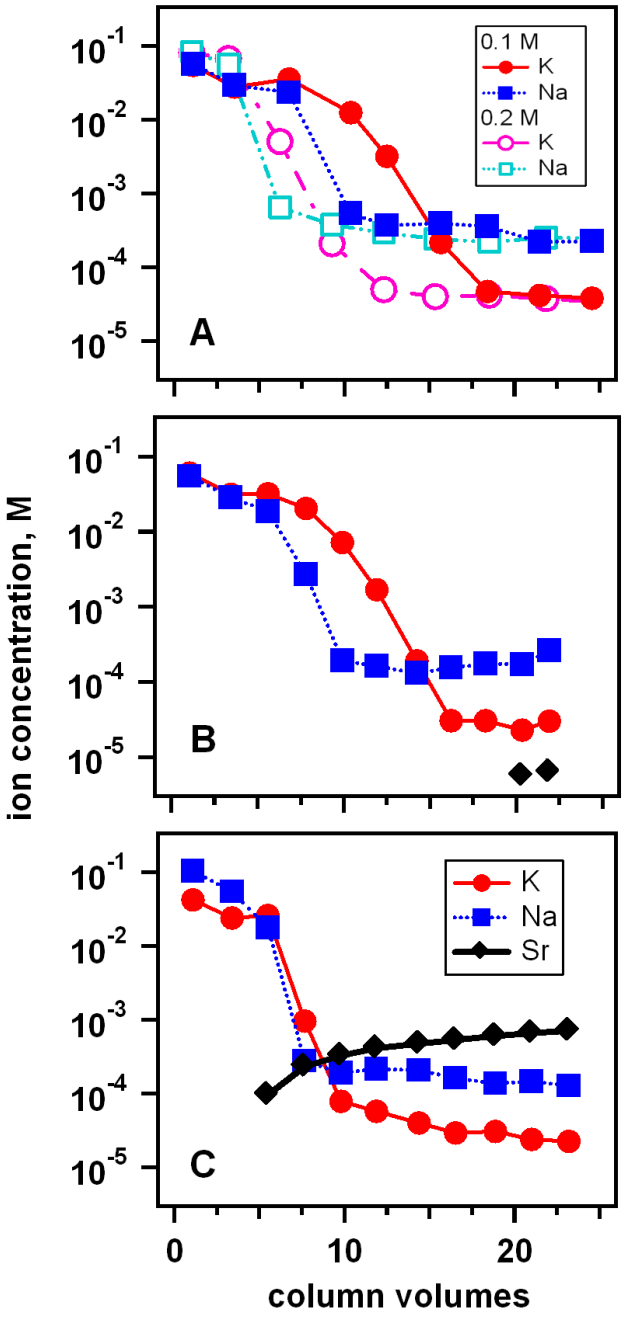


**Figure 2.6. Elution profiles for the column where ion concentrations in the eluate are plotted vs. the number of column volumes.** Panel A: 10 column volume load of saline solution (0.1 M NaCl + 0.1 M KCl) acidified with 0.1 M MSA (2 mL Diphonix resin column, 0.54 $cm^2$ x 3.7 cm) or 0.2 M MSA. Panel B: 10 column volume load of $^{85}Sr$-spiked saline solution acidified with 0.1 M MSA. Load ion concentrations are given. Panel C: 10 column volume load of $^{85}Sr$-spiked human urine acidified with 0.1 M MSA. (Data were provided by Dr. Ilya Shkrob, Argonne National Laboratory.)

**Table 2.4**
**Trial data for Diphonix® column tests in simulated urine and human urine**

| | aqueous matrix[a] (Figure 2.6 panel A) | | | acidified human urine treated with charcoal[a] (Figure 2.6 panel B) | | |
|---|---|---|---|---|---|---|
| | $K^+$ | $Na^+$ | $Sr^{2+}$ | $K^+$ | $Na^+$ | $Sr^{2+}$ |
| Load, mM | 96.4 | 88.7 | 6.4 | 64.2 | 160 | 6.4 |
| Load, mmol | 1.93 | 1.77 | 0.127 | 1.19 | 2.98 | 0.061 |
| Load (effluent), mmol | 1.30 | 1.35 | 0 | 0.84 | 2.28 | 0 |
| % retained | 32.6 | 23.7 | 100 | 29.7 | 23.5 | 100 |
| Column, M | 0.315 | 0.21 | 0.064 | 0.18 | 0.35 | 0.063 |
| recovered, mmol 3M $HNO_3$ strip | $4.35 \times 10^{-5}$ | $2.75 \times 10^{-3}$ | 0.125 | $1.45 \times 10^{-4}$ | $2.57 \times 10^{-3}$ | 0.108 |
| Conc. on the column after 22 volume elution | 21.5 $\mu$M | 1.38 mM | 63 mM | 73 $\mu$M | 1.29 mM | 54 mM |
| Eluent, mmol by integration | 0.56 | 0.36 | < LOD | 0.32 | 0.57 | 0.017 |
| Sr, recovery % after 22 volume elution | | 100 | | | 86.4 | |
| Sr recovery, % after 10 volume elution | | 100 | | | 98.0 | |

[a] Both tests use 0.1 M MSA load solutions eluted with 0.1 M MSA. The load was 10 column volumes (2 mL, 0.54 $cm^2$ x 3.7 cm column) and the elution was to 22-23 column volumes at 1.5 mL $min^{-1}$. (Data were provided by Dr. Ilya Shkrob, Argonne National Laboratory.)

Figure 2.7 shows the elaboration of a column for a raw urine sample after a 10 column volume loading and 15 column volume wash using 0.1 M MSA. Approximately 7% of $Sr^{2+}$ was eluted from the Diphonix® resin column during the wash step, so the recovery of $Sr^{2+}$ was 93%. However, 99.95% of the $Sr^{2+}$ on the Diphonix® resin column was stripped passing just 3 column volumes of 3M $HNO_3$, resulting in 3.2x concentration of $Sr^{2+}$ in the strip eluent. Approximately 82% of $Sr^{2+}$ on the column was eluted with the first column volume of the 3 M nitric acid, resulting in a very concentrated strontium stream. In Figure 2.8, a test on the certified normal human urine is shown. In this test, 5 column volume samples of frozen urine (the form in which it typically arrives from the field assays for laboratory analysis) were loaded onto separate 2 mL Diphonix columns.

In one test, the urine was acidified to pH=1 using 0.22 M MSA (the urine is buffering); in another, 0.1 M MSA was added to achieve pH=1.6. In these experiments, there was no loss of $Sr^{2+}$ during loading and < 0.1% loss of $Sr^{2+}$ during elution, in both cases. Stripping the column after 15 column volumes of 0.1 M MSA with 3 column volumes of 3 M $HNO_3$ resulted in the recovery of 99.7% of Sr on the column. The concentrations of $K^+$ and $Na^+$ in the strip solution were < 0.3 mM (Figure 2.8). Though the 10 column volume load leads to a 7% loss of $Sr^{2+}$ in the wash step (Figure 2.7), the overall recovery is nearly twice that obtained with a 5 column volume load (Figure 2.8), which will result in lower detection limits. Differences between raw urine and frozen urine may also have an effect on the recoveries from these two loading experiments. That is, freezing urine, because it forms ice, denatures many of the proteins that aggregate and remove pigments when they precipitate. Hence, there tends to be less interference with frozen urine than with raw urine, which may lead to higher recoveries from the former.

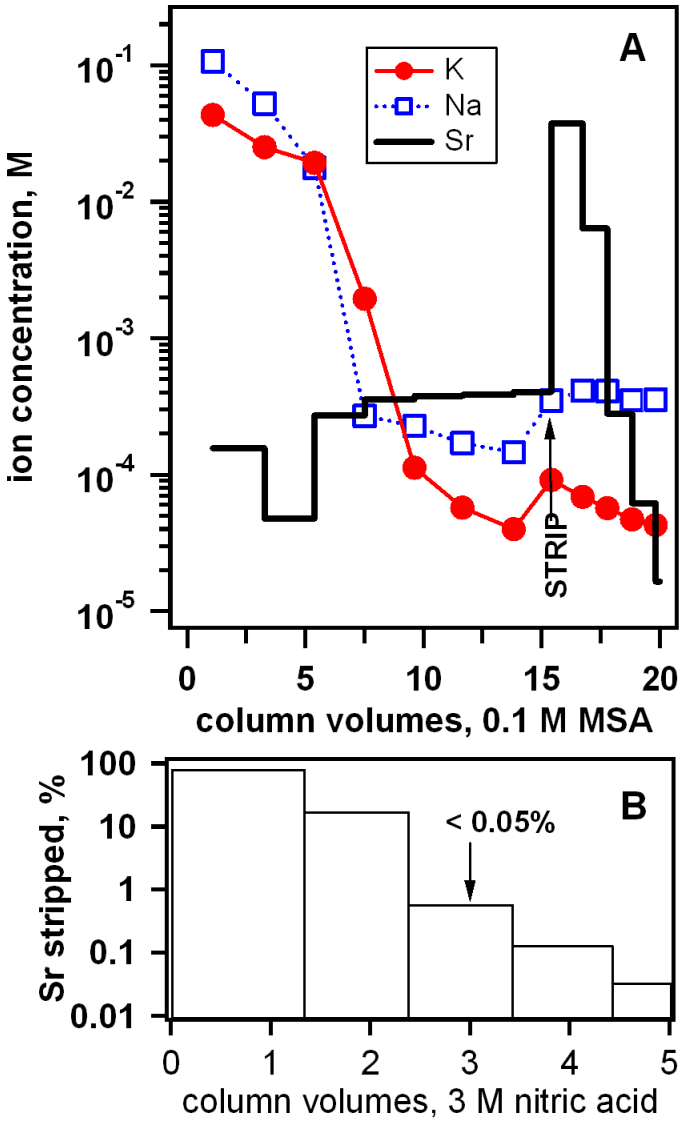


**Figure 2.7. Column test using standardized certified normal human urine.** 10x sample volumes were loaded on the 2 mL Diphonix resin column, 15x volumes of 0.1 M MSA were passed, and the column was stripped using 3 M $HNO_3$. (Data were provided by Dr. Ilya Shkrob, Argonne National Laboratory.)

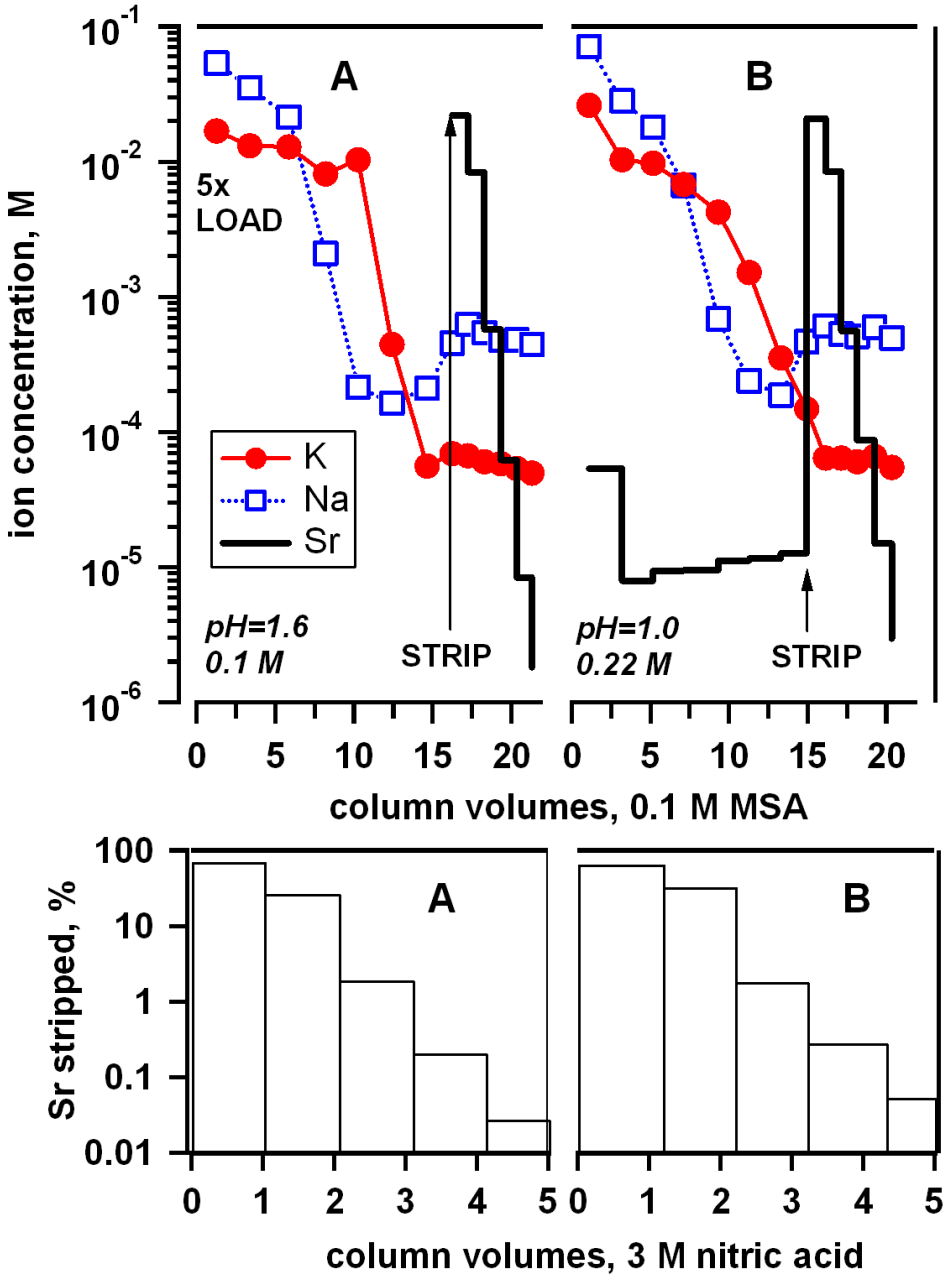


**Figure 2.8. Column test elution profiles and $Sr^{2+}$ stripping data using certified normal human urine on 2 mL Diphonix resin columns.** Panels A: 15 column volumes of 0.1 M MSA were used to wash, Panels B: 15 column volumes of 0.22 M MSA were used to wash. (Data were provided by Dr. Ilya Shkrob, Argonne National Laboratory.)

The retention behavior of alkali and alkaline earth cations on the Sr resin is well documented [2.16, 2.20]. The 3 M $HNO_3$ strip (3 column volumes) corresponds to the conditions under which $k_{ex}$ for strontium on the Sr resin is approximately 60 (Table 2). Assuming that the volume of the Sr resin column is 10% of the volume of Diphonix column, applying the strip solution directly on a 20-plate Sr resin column would correspond to 30 column volume load resulting in a loss of < 0.1% $Sr^{2+}$ during the loading. After passing five more column volumes of nitric acid to wash away undesirable ions and 2 column volumes of 10 mM nitric acid to strip, $Sr^{2+}$ is concentrated 20-fold in addition to the preconcentration on the Diphonix® resin column. This strontium stream is decontaminated from any residual potassium, calcium, and trivalent ions including yttrium.

**2.5 The suggested process**

The results given in the previous sections provide the basis for the suggested process (Figure 2.1). At the heart of this process are two columns: a larger column filled with the Diphonix® resin and a smaller one (10% of the volume of the former) filled with Sr resin and connected to the other by a three-way valve. To save processing time, while one of the columns is loaded/eluted, the other column is washed/conditioned for the next run, as shown in Figure 2.9. In step 1, the two columns are offline and the Diphonix column is conditioned for loading of $Sr^{2+}$ with 0.1 M MSA while the Sr column is washed with 10 mM nitric acid. In step 2, 10-30 column volumes of treated urine are loaded on the Diphonix® resin column, while the Sr resin column is still washed by 10 mM nitric acid. In step 3, the alkali ions are eluted using 15-20 column volumes of 0.1 M MSA, while the Sr resin column is conditioned for loading by passing 3 M nitric acid. In step 4, $Sr^{2+}$ is

stripped from the Diphonix® resin column using 3 M nitric acid and the effluent from the column is loaded directly on the Sr resin column. In step 5, 2 column volumes of 10 mM nitric acid are used to strip $Sr^{2+}$ from the Sr resin column, while the Diphonix column is washed with 3 M nitric acid. Following the stripping of $Sr^{2+}$, the two columns return to the conditions of step 1. The whole process takes approximately one hour. The typical volumes of the two columns are 2 mL and 200 μL, respectively. For a 20 mL load, the first column would concentrate $Sr^{2+}$ by a factor of 2.5-3.5 and the second by a factor of 20, resulting in the overall concentration factor > 50. Higher concentration factors are possible for Diphonix® resin columns with 30-40 theoretical plates.

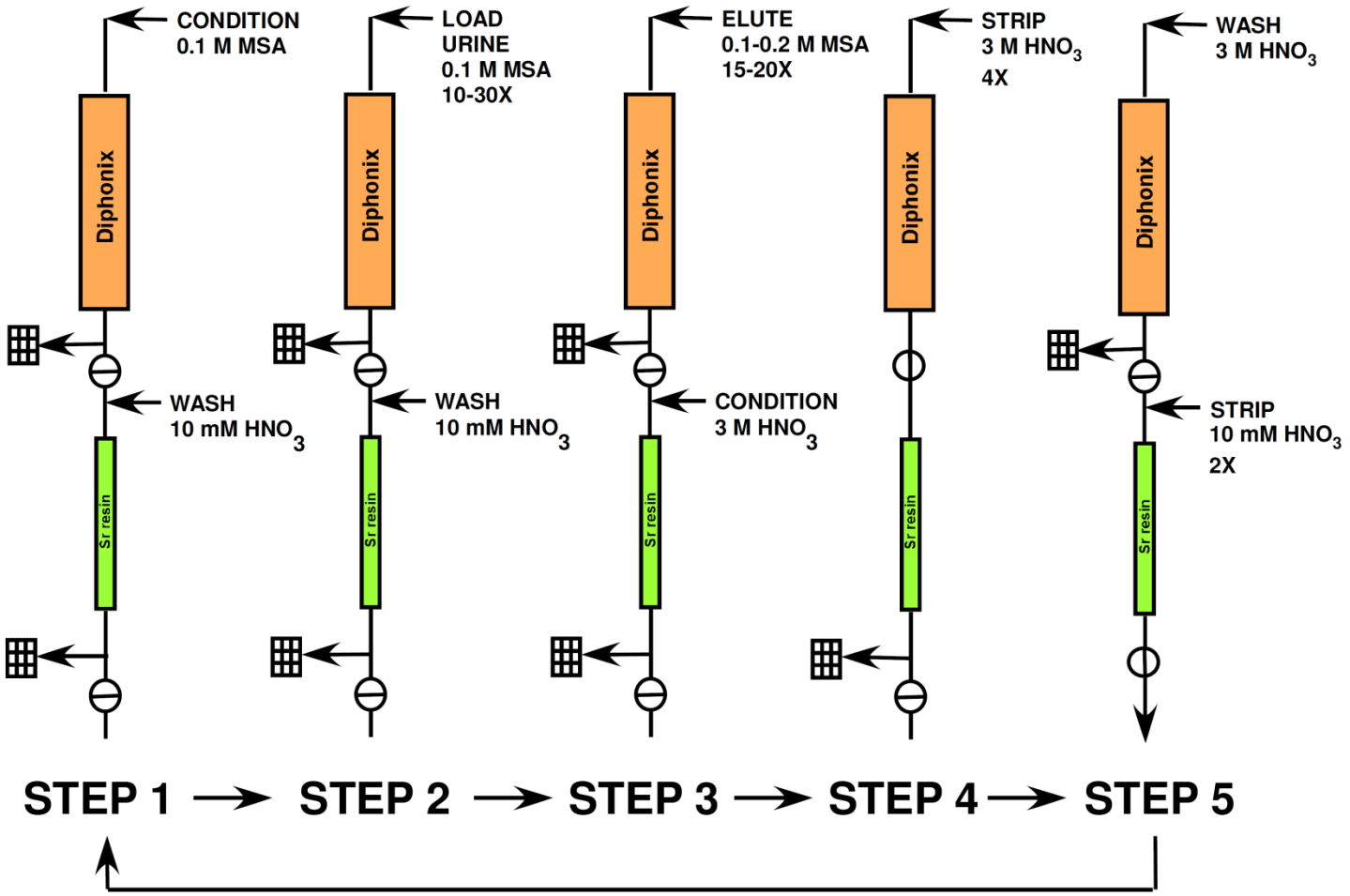


**Figure 2.9. Tandem Diphonix®-Sr Resin column treatment steps in the proposed scheme for rapid sorption, decontamination, and concentration of $^{90}$Sr from human urine samples.**

## 2.6 Conclusion

The procedure described here constitutes a simple method for the separation and preconcentration of radiostrontium from human urine comprising an acidification and decolorization step followed by the use of Diphonix® resin (instead of tedious and time-consuming ashing and precipitation steps[2.8, 2.9, 2.20] or multiple ion exchange resins in tandem[2.9, 2.10]) and final concentration by Sr resin. Importantly, the rapid depigmentation method devised here can be used for direct and efficient detection of other radioisotopes in urine, including tritium, using common scintillation cocktails, as color quenching is completely eliminated and MSA (unlike nitric acid) does not quench fluorescence. By employing the recommended conditions, greater than 98% recovery of $Sr^{2+}$, a concentration factor higher than 50-fold, and a processing time of approximately one hour can be achieved. Notably, the suggested Sr resin column volume is 10-fold smaller than the typical cartridges supplied by the manufacturer, leading to significant cost savings. Furthermore, this method could be a simpler and more cost-effective alternative to the sample processing techniques currently utilized for emergency purposes.

Although the approach described here does represent a significant improvement in the available methodology for determination of radiostrontium in human urine, certain features of it may render it difficult to implement for high-throughput analysis of large numbers of samples. First, if emergency responders require immediate information about an individual's exposure to radiostrontium, then the procedure clearly must be further simplified. For instance, when the combination of acidity and other urine components results in high ionic strength, premature $Sr^{2+}$ breakthrough may occur. This fact, taken

together with the differences in the levels of various urine constituents among individuals, suggests that highly skilled workers may be required to operate the procedure. Next, although the Diphonix resin in this scheme does provide a means of eliminating certain interferences before the Sr resin column, the fact remains that the capacity of Diphonix® is limited (by the availability of active phosphoryl ligands). Likewise, the amount of crown ether that can be loaded onto the Sr resin (and thus the retention of $Sr^{2+}$) is limited, both by the substrate capacity and the solubility of the crown in 1-octanol. These limitations restrict the extent to which the size of the columns can be reduced. Finally, Sr retention is further limited by its modest extractability into a 1-octanol solution of the crown ether. All of this suggests that truly meeting the requirements of a high-throughput method may necessitate innovative approaches to sample processing. For example, high capacity sorbents capable of being loaded with much higher levels of extractant [2.21] could be devised. Along the same lines, improved extractants with strong metal ion binding could be developed. Another more exotic possibility would be to devise an easily retrievable strontium-specific solvent based on a magnetic ionic liquid [2.22-2.24]. Such a system could, in principle, combine high capacity and rapid kinetics with the ease of handling and high rates of sample throughput. All of these approaches, however, require substantial additional fundamental research before their feasibility can be assessed. In the case of ionic liquids, for example, significant gaps remain in our understanding of the processes involved in the transfer of metal ions from an aqueous phase into an ionic liquid in the presence of various extractants. In the chapters that follow, our efforts to address this deficiency, in particular, to elucidate the details of the processes involved in the extraction of

radiostrontium by a crown ether into various ionic liquids, are described. Only after such details are understood might ionic liquid-based systems be developed to meet the demands of high-throughput bioassays.

## 2.7 Acknowledgements

This study [2.1] was conducted in collaboration with the Chemical Sciences and Engineering Division at Argonne National Laboratory. Because this work was performed, in part, by the author, and because it serves as the inspiration for the remaining work described in this dissertation, details of the study are provided in this chapter. The results are reproduced with the permission of the authors, and those results obtained by others are clearly indicated in the text or tables and figures provided.

## 2.8 References

[2.1] C.A. Hawkins, I.A. Shkrob, C.J. Mertz, M.L. Dietz, M.D. Kaminski, *Anal. Chim. Acta*, 534, **2012**, 271–279.

[2.2] G. Choppin, J. Rydberg, J.-O. Liljenzin, *Radiochemistry and Nuclear Chemistry*, 3rd Ed.; Butterworth-Heinemann, **2001**.

[2.3] M. Bé, C.C. Delieu, X. Mougeot, *Radioactive Decay Data Tables, Monography*, Bureau International des Poid et Mesures; 1-5, **2010**, 201-204.

[2.4] U.S. Environmental Protection Agency, *Radiation Protection*, http://www.epa.gov/rpdweb00/radionuclides/strontium.html#environment, Accessed 27 September 2012.

[2.5] Agency for Toxic Substances and Disease Registry (ATSDR), *Toxicological Profile for Ionizing Radiation*. U.S. Dept. of Health and Human Services, Atlanta, GA, September **1999.**

[2.6] Ž. Grahek, M. R. Mačefat, *Anal. Chim. Acta*, 534, **2005**, 271–279.

[2.7] S. L. Maxwell, B. K. Culligan, *J. Radioanal. Nucl. Chem*., 279, **2009**, 757–760.

[2.8] M.L. Dietz, E.P. Horwitz, *Health Phys.* 61, **1991**, 871-877.

[2.9] S. L. Maxwell, B. K. Culligan, *J. Radioanal. Nucl. Chem*. 275, **2008**, 497-502.

[2.10] B.B. Sadi, C. Li, S. Jodayree, E.P.C. Lai, V. Kochermin, G.H. Kramer, *Rad. Prot. Dos.*, 140, **2010**, 41-48.

[2.11] D.R. McAlister, E.P. Horwitz, J.T. Harvey, *Health Phys.*, 101, **2011**, 176-179.

[2.12] M.H. Lee, H.J.Ahn, J.H.Park, Y.J.Park, K.Song, *Appl. Rad. and Isotopes*, 69, **2011**, 295–298.

[2.13] J. Mellado, M. Llauradó, G. Rauret, *Anal. Chim. Acta*, 458, **2002**, 367-374.

[2.14] G.A. Taylor, *The Evolution of Internal Dosimetry Bioassay Methods at the Savannah River Site*, http://www.c-n-t-a.com/srs50_files/253taylor.pdf, (accessed 02 March 2012).

[2.15] D.F. Putnam, *Composition and Concentrative Properties of Human Urine*, NASA CR-1802, **1971**, http://ntrs.nasa.gov/archive/nasa/casi.ntrs.nasa.gov/19710023044_1971023044.pdf. Accessed 02 March 2012.

[2.16] E.P. Horwitz, R. Chiarizia, M.L. Dietz, *Solvent Extr. Ion Exch.*, 10, **1992**, 313–336.

[2.17] R. Chiarizia, E.P. Horwitz, S.J. Alexandratos, M.J. Gula, *Sep. Sci. Technol.*, 32, **1997**, 1-35.

[2.18] R. Chang, *Physical Chemistry for the Biosciences*, 1st Ed., University Science Books, **2005**, 556.

[2.19] R. Chiarizia, J.R. Ferraro, K.A. D'Arcy, E.P. Horwitz, *Solv. Extr. Ion Exch.*, 13, **1995**, 1063-1082.

[2.20] E.P. Horwitz, M.L. Dietz, D.E. Fisher, *Anal. Chem.*, 63, **1991**, 522-525.

[2.21] C. van den Berg, C.P.M. Roelands, P.Bussman, E.L.P. Goetheer, D. Verdoes, L.A.M. van der Weilen.

[2.22] S. Hayashi, H. Hamaguchi, *Chemistry Letters*, 33, **2004**, 1590-1591.

[2.23] Y. Yoshida, G. Saito, *J. Mat. Chem.* 16, **2006**, 1254-1262.

[2.24] R.E. Del Sesto, T.M. McCleskey, A.K. Burrell, G.A. Baker, J.D. Thompson, B.L. Scott, J.S. Wilkes, P.Williams, *Chem. Commun*. **2008**, 447-449.

# CHAPTER 3:
# THREE-PATHWAY MODEL OF METAL ION EXTRACTION INTO IONIC LIQUIDS

## 3.1 Introduction

Growing recognition of the extraordinary physicochemical properties and unique solvation environment afforded by ionic liquids (ILs) has drawn increasing attention to these solvents as media for chemical separations and analysis [3.1-3.3]. In recent years, ILs have found use in such diverse areas as gas chromatography [3.4], mass spectrometry [3.5-3.7], fluorescence spectroscopy [3.8], and capillary electrophoresis [3.9], among others. Work in this laboratory has primarily concerned the potential utility of ILs, (particularly those that are liquid at room temperature) as replacements for the molecular organic solvents (*e.g.*, paraffinic and chlorinated hydrocarbons) typically employed in liquid-liquid extraction (LLE) [3.10-3.16]. These and other studies have demonstrated that a variety of organic molecules (*e.g.*, dyestuffs [3.17-3.20], amino acids [3.21, 3.22]) and inorganic species [3.23-3.27] readily partition into ILs under appropriate conditions. In the case of metal ion partitioning, these conditions most often involve the presence of a complexing agent/extractant to render the metal ion more hydrophobic and thus, extractable. Of the variety of reagents available for this purpose, neutral extractants (*e.g.*, organophosphorus reagents, crown ethers, and calixarenes) are generally regarded as most desirable from a practical perspective, as (at least in conventional molecular solvent systems) the extent of metal ion partitioning can be varied simply by altering the concentration of the aqueous phase anion (*e.g.*, nitrate) present. Prior work, however, indicates that metal ion partitioning in IL-based systems incorporating neutral extractants

can be a far more complex process than that observed in analogous conventional systems [3.10-3.16]. Studies of the extraction of strontium and sodium ion by the macrocyclic polyether (*i.e.*, crown ether, CE) dicyclohexano-18-crown-6 (DCH18C6), for example, suggest that in contrast to ordinary organic solvent-based extraction systems, for which partitioning proceeds by extraction of a neutral complex, partitioning into ILs can involve as many as three distinct pathways: extraction of a neutral complex, ion-exchange (IX) involving exchange of a cationic metal-DCH18C6 complex for the cationic constituent of the IL, and a second type of IX involving exchange of the metal ion for a hydronium ion (or proton) bound to the extractant (Figure 3.1).

In attempting to evaluate the suitability of ILs as extraction solvents and to develop guidelines for the design of separation systems employing them, it is essential to establish the extent to which these observations are "generic". To this end, a systematic examination of the extraction of several alkali and alkaline earth cations by DCH18C6 from acidic nitrate media has been performed. As will be shown, in addition to providing much-needed fundamental information concerning the extraction behavior of these ions with neutral extractants, the results obtained may have practical significance in efforts to devise improved systems for metal ion separations employing ILs. Several of the results discussed in this chapter have been previously published [3.28]. Their reproduction here has been approved by the authors.

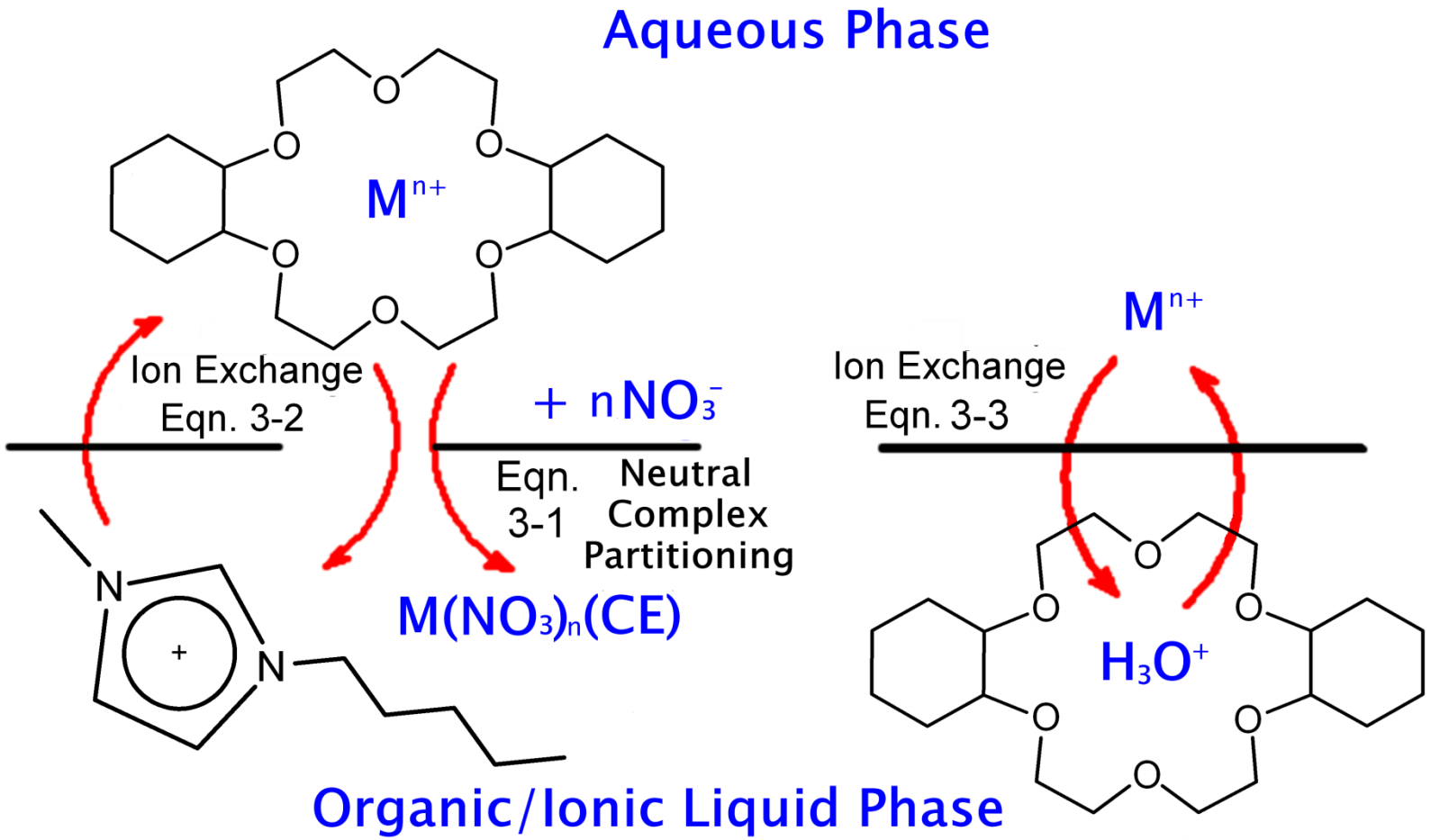


**Figure 3.1: The three-path model for metal ion partitioning between nitric acid solution and $C_nC_1imTf_2N$ ionic liquids in the presence of DCH18C6.**

## 3.2 Experimental

### 3.2.1 Materials

The ionic liquids were prepared and purified using established methods [3.29, 3.30]. All $Tf_2N$ IL products were tested for residual halides by contacting a measured volume three times with an equal volume of water and analyzing the combined aqueous fractions by ion chromatography. All were found to contain less than 1 ppm bromide or chloride. Ion chromatographic eluents were prepared from either saturated sodium hydroxide solution (puriss., Fluka, Milwaukee, WI) or methanesulfonic acid (puriss., Fluka, Milwaukee, WI). Primary alcohols and inorganic salts were obtained from Sigma-Aldrich (Milwaukee, WI). The DCH18C6 (Parish Chemical, Orem, UT) used was a mixture of the *cis-syn-cis* and *cis-anti-cis* isomers and was used as received. Nitric acid solutions were prepared from trace-metal grade concentrated acid (Optima™, Fisher Scientific, Pittsburg, PA) and standardized by titration with standard sodium hydroxide solutions (Ricca, Arlington, TX) using phenolphthalein indicator (Ricca, Arlington, TX). Radiotracers of $^{22}Na$, $^{45}Ca$, $^{85}Sr$, $^{135}Ba$, and $^{137}Cs$ were purchased as nominal solutions from Eckert and Ziegler Isotope Products, Inc. (Valencia, CA).

### 3.2.2 Instruments

Gamma spectroscopy was performed using a PerkinElmer model 2480 automatic gamma counter equipped with WIZARD2 software. Liquid scintillation counting was performed using a PerkinElmer Tri-Carb 2810 TR Series liquid scintillation counter equipped with QuantaSmart software. NMR spectra were acquired on a Bruker DPX300 NMR spectrometer operating at 300.13 MHz for proton and 75.47 MHz for carbon-13,

and equipped with a z-gradient broadband (BBO) probe. Spectra were obtained using solutions of dimethylsulfoxide-$d_6$ (Aldrich, 99.96 atom% D), and all chemical shifts were reported relative to tetramethylsilane. Where appropriate (*i.e.*, for ILs not previously reported) elemental (CHN) analysis of the ionic liquids was performed by the combustion method (Galbraith Laboratories, Knoxville, TN). Other elements (*e.g.*, oxygen) were determined from the theoretical mass balance. Potassium concentrations for acid dependencies were determined using a spectroscopic standard solution (Ultra Scientific, North Kingstown, RI) and assayed using a Varian Liberty Series II sequential inductively coupled plasma atomic emission spectrometer (ICP-AES) using parameters listed in Table 3.1 or a MicroMass inductively coupled plasma mass spectrometer (ICP-MS) using settings similar to those listed in Table 3.2. Nitrate and halide concentrations were determined using a Dionex ICS-1000 ion chromatograph equipped with equipped with a 25 μL fixed-loop manual injection port, an ASRS 300 cation self-regenerating eluent suppressor,a conductivity detector, Dionex AS18/AG18 analytical and guard columns (4 X 250 and 4 X 50 mm), a Dionex ASRS 300 (4 mm) conductivity suppressor, and 37 mM NaOH eluent. The instrument was operated using Chromeleon software version 6.80. Potassium and cesium concentrations for the determination of anion co-extraction were measured using the same ion chromatograph equipped with a CSRS 300 cation self-regenerating eluent suppressor, a Dionex CS12A analytical and CG12A guard columns (4 X 250 and 4 X 50 mm), and 20 mM methanesulfonic acid eluent. IC eluent flow rates were 1.00 mL/min, and the column temperature was maintained at 30°C.

**Table 3.1**
**Parameters employed for potassium ion determination by ICP-AES[a]**

| | | | |
|---|---|---|---|
| Peak | 766.490 nm | Viewing Height | 10 mm |
| Window | 0.080 nm | Sample Uptake Delay | 25 seconds |
| Integration Time | 5.00 seconds | Pump Rate | 15 rpm |
| Replicates | 3 | Instrument Stabilization | 15 seconds |
| Power | 1.00 kW | Rinse Time | 30 seconds |

[a] Operated with Varian Plasma96 software version 1.12

**Table 3.2**
**Parameters employed for potassium ion determination by ICP-MS[a]**

| **Analyzer** | | **Gas** | | **Torch** | |
|---|---|---|---|---|---|
| Cone Lens | 85 | Cool | 13.59 | X-Axis | 2.00 |
| Hex Exit Lens | 400 | Intermediate | 0.90 | Y-Axis | -0.06 |
| Hex Bias | 0 | Nebulizer 1 | 0.87 | Z-Axis | -0.36 |
| LM Resolution | 12.5 | Nebulizer 2 | 0.00 | Forward Power | 1350 |
| High Resolution | 12.5 | He | 8.0 | | |
| Ion Energy | 2.0 | $H_2$ | 4.0 | | |
| Multiplier | 400 | Hexapole Aux | 0.00 | | |
| Mass Monitored | 39 m/z | Laser | 2.40 | | |

[a] Operated with MassLynx software version 3.4

3.2.3 Methods

Distribution ratios ($D_M$) were determined as a ratio of the count rate in the organic phase to that of the aqueous phase using commercial radiotracers, assayed *via* gamma spectroscopy or liquid scintillation counting using standard procedures. In each metal

distribution experiment, the organic phase consisted of DCH18C6 dissolved in the designated ionic liquid, and the aqueous phase nitric acid concentration was systematically adjusted either by conducting separate experiments for each condition, or adding acid after each condition had been sampled. Unless otherwise noted, acid dependencies for metal extraction were performed at 0.1 M DCH18C6 in the organic phase. All organic phases were pre-equilibrated with aqueous phase prior to the introduction of the metal ions or radiotracer. Each equilibrated phase was sampled for analysis in at least duplicate with resulting uncertainties based on counting statistics that were generally within 10%, although the uncertainty interval was considerably wider for the highest distribution ratios values ($D_M \geq 1000$). Additionally, for radiometric measurements, the sum of the count rates in each phase yielded recoveries within 10% of the radiotracer stock solution used, indicating that equilibrium was established with only two phases involved. Nitric acid concentrations were determined by titration with a standard sodium hydroxide solution (Ricca Chemical Company, Arlington, TX). Due to considerable background signal in the ICP-MS associated with carryover from biological samples for which this instrument is most often used, a cesium internal standard (ICP Standard, Ricca, Arlington, TX) was used to improve the quantification of various samples with low (< 25 ppb) potassium concentrations.

## 3.3 Generality of the Three-Path Model for Groups 1 and 2 Ions

### 3.3.1 Nitric acid dependency of $D_M$ for extraction into aliphatic alcohols by DCH18C6

In their initial studies to explore the possible utility of ionic liquids as solvents in the extraction of metal ions, Dai *et al.* [3.23] reported astonishingly efficient extraction of

strontium from water into a series of *N,N'*-dialkylimidazolium-based ILs containing DCH18C6. Indeed, for several ILs, the values obtained for the strontium distribution ratio ($D_{Sr}$) far exceeded (*i.e.*, $D_{Sr} > 10^3$ *vs.* $D_{Sr} \approx 1$) those achieved with conventional molecular diluents (*e.g.*, chloroform) under the same conditions, a surprising result given the low aqueous phase anion concentration (1.5 mM $NO_3^-$) present and the nature of the expected partitioning process (*i.e.*, extraction of a neutral complex, as per Eqn. 3-1):

$$Sr^{2+} + 2\ NO_3^- + DCH18C6_{org} \leftrightharpoons Sr(NO_3)_2 \bullet DCH18C6_{org} \qquad (3\text{-}1)$$

In an effort to discern the source of the unexpectedly high strontium extraction efficiencies observed, a systematic comparison of the extraction of $Sr^{2+}$ by DCH18C6 into several *N,N'*-dialkylimidazolium *bis*[(trifluoromethyl)sulfonyl]imide ILs to that observed for a series of aliphatic alcohols (*n*-pentanol to *n*-decanol) was carried out [3.10]. This work, along with a subsequent study of sodium ion extraction under similar conditions [3.14], suggested that the enhanced extraction efficiency can be attributed to differences in the predominant mode by which the metal ion partitions between the IL (or organic) and aqueous phases (*i.e.*, ion-exchange for the IL *vs*. extraction of a neutral complex for the conventional diluent). In this work, these studies have been extended to other alkali and alkaline earth cations to determine both the generality of these earlier observations and to establish the influence upon extraction selectivity of changing system conditions.

Figures 3.2 and 3.3 depict the dependence of the distribution ratio ($D_M$) of several Group 1A and 2A metal ions on aqueous nitric acid concentration for extraction into 0.1

M solutions of DCH18C6 in various *n*-alcohols. For these and other such conventional solvents, $D_M$ initially rises with increasing nitric acid (*i.e.*, nitrate) concentration, as the extraction of metal ions into these diluents requires anion co-extraction to maintain electroneutrality (Eqn. 3-1). The leveling-off and eventual sharp decrease in $D_M$ for alkali metal ions at high acidity can be attributed to a decrease in the free DCH18C6 concentration arising from nitric acid extraction by this crown ether [3.31]. Such competition for the extractant is obviously less pronounced in the case of alkaline earth cations, a result of their greater electrostatic charge and the accompanying increase in the metal ion-crown ether complex formation constant [3.32]. As expected, an increase in the hydrophobicity of the alcohol results in a decline in extraction efficiency for all of the alkali and alkaline earth cations under any given set of conditions, a consequence of the decrease in organic phase water content that accompanies this greater hydrophobicity and the importance of organic phase water in facilitating co-extraction of the nitrate anion [3.33]. (Further details of this phenomenon will be discussed in Chapter 4.) Regardless of conditions (*e.g.*, the nature of the metal ion or the alkyl chain length of the solvent), however, the process responsible for metal ion partitioning into the alcohols remains unchanged (*i.e.*, extraction of a neutral metal-nitrato crown ether complex).

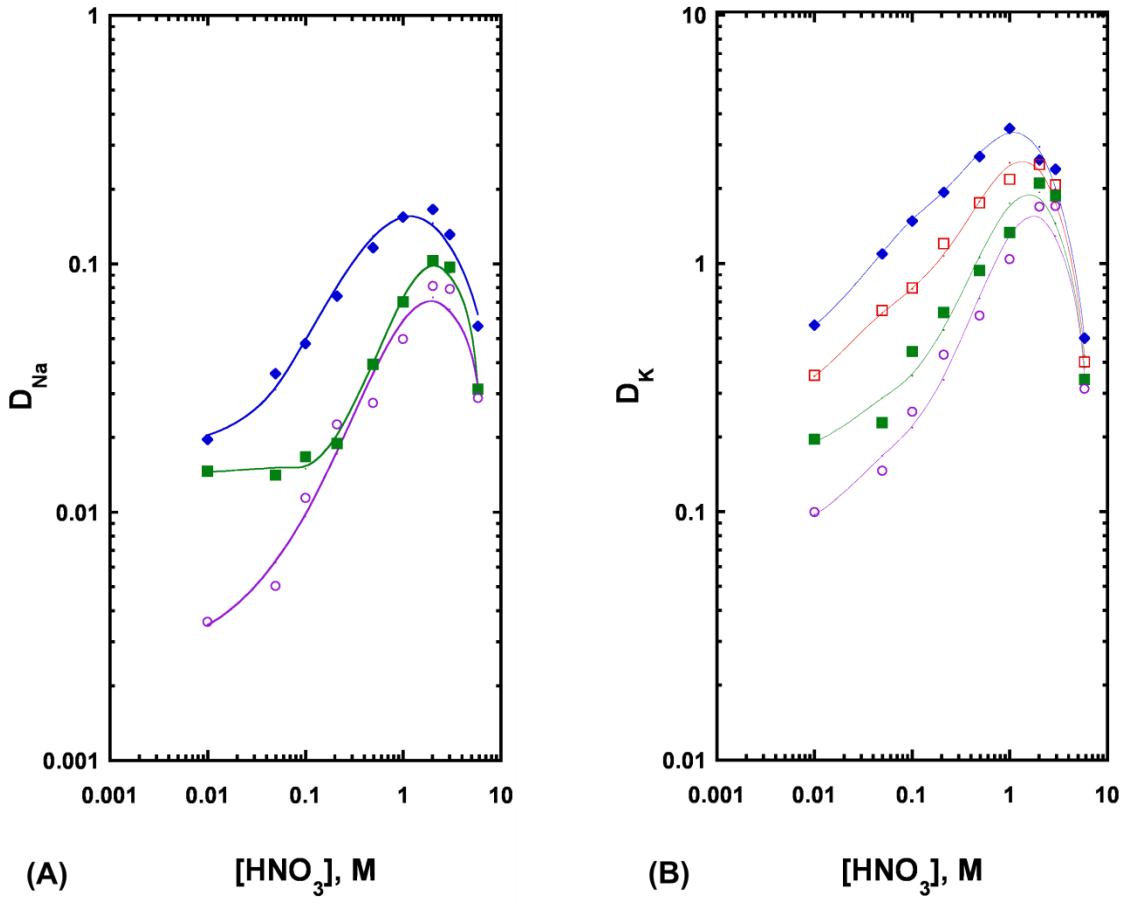


**Figure 3.2: Effect of nitric acid concentration on the extraction of $Na^+$ (panel A) and $K^+$ (panel B) by DCH18C6 (0.10 M) in 1-pentanol (◆), 1-hexanol (□), 1-octanol (■), and 1-decanol (○).** The smooth curves are intended only as guides to the eye.

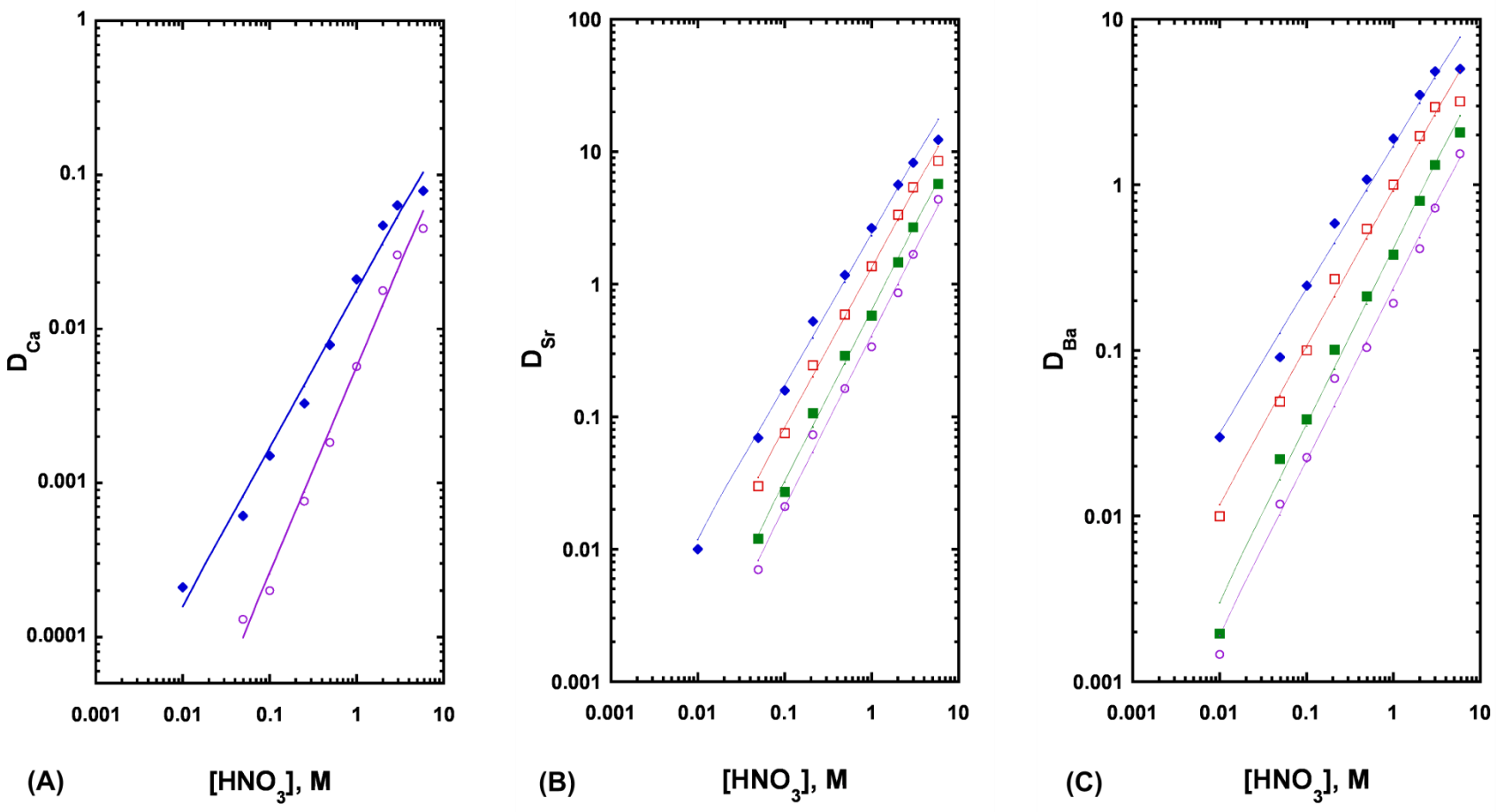


**Figure 3.3: Effect of nitric acid concentration on the extraction of $Ca^{2+}$ (panel A), $Sr^{2+}$ (panel B), and $Ba^{2+}$ (panel C) by DCH18C6 (0.10 M) in 1-pentanol (◆), 1-hexanol (□), 1-octanol (■), and 1-decanol (○).** Curves are least-squares linear fits.

3.3.2 Metal ion vs. nitrate extraction into $C_nC_1imTf_2N$ ILs by DCH18C6

That this is not the case for the ionic liquids is readily evident from an examination of the results presented in Tables 3.3 and 3.4, which summarize measurements of the partitioning of nitrate anions and five alkali and alkaline earth cations between water and several $C_nC_1imTf_2N$ ILs in the presence of DCH18C6. If the partitioning of a neutral complex were the sole mode of cation extraction in these systems as well, then the percentage extraction of nitrate and of the metal ion would correspond throughout. As can be seen, however, this is not observed. Rather, in most instances, the fraction of nitrate extracted is far less than the corresponding fraction of metal ion extracted, consistent with a significant contribution of ion exchange involving the cationic constituent of the IL (a process which, as shown in Eqn. 3-2, does not require anion co-extraction) to the observed metal ion partitioning [3.12]:

$$M\bullet DCH18C6^{n+} + x\ IL^{+}{}_{IL} \leftrightharpoons M\bullet DCH18C6^{n+}{}_{IL} + n\ IL^{+} \qquad (3\text{-}2)$$

As has been shown previously for strontium [3.12], for all of the metal ions examined here, increasing IL cation hydrophobicity is accompanied by a diminished contribution of ion exchange to the overall extraction process. For $Ba^{2+}$, for example, the amount of nitrate extracted corresponds to only *ca*. 9% of that required for extraction of a neutral complex when $C_5C_1imTf_2N$ is employed, indicating that barium partitioning proceeds primarily by ion exchange in this solvent. However, for the homologue, $C_{10}C_1imTf_2N$, the percentages of nitrate and barium ion extracted are essentially identical, consistent with neutral complex partitioning as the sole mode of extraction. It is obvious from the

results shown that an increase in IL cation hydrophobicity is more effective at inducing a shift toward neutral complex extraction for divalent metal ions (such as $Ba^{2+}$) than for monovalent cations. Undoubtedly, it is the greater charge of the Group 2A cations and the accompanying stronger interaction of these ions with nitrate that account for this difference. Additionally, the limited water solubility of the ionic liquid cation will render the extraction of an equivalent of the cationic metal-crown ether complex (Eqn. 3-2) less favorable for divalent complexes than for monovalent complexes.

**Table 3.3**
**The effect of IL cation chain length on strontium, barium, and nitrate ion partitioning between water and 0.20 M DCH18C6 in $C_nC_1imTf_2N$**

| Metal | Organic Phase | $\%E_M$ [a, b] | $\%E_{NO_3^-}$ [a, b] | Ratio $\%E_M/\%E_{NO_3^-}$ | Partitioning Mode Indicated |
|---|---|---|---|---|---|
| Sr | $C_5C_1imTf_2N$ | 96.4<br>96.5 | 10.7 ± 0.3<br>9 ± 7 | 9.01 | cation exchange |
| | $C_6C_1imTf_2N$ | 83.4 ± 5.1<br>82.6 | 17.6 ± 0.5<br>16.1 ± 0.8 | 4.74 | cation exchange |
| | $C_8C_1imTf_2N$ | 45.7<br>39.0 | 25.4 ± 0.8<br>20.9 ± 1.0 | 1.80 | mixed |
| | $C_{10}C_1imTf_2N$ | 23.4 ± 3.0<br>20.2 | 23.1 ± 0.2<br>20.0 ± 1.0 | 1.01 | neutral complex |
| Ba | $C_5C_1imTf_2N$ | 98.6 | 8.92 ± 0.18 | 11.1 | cation exchange |
| | $C_6C_1imTf_2N$ | 93.6 ± 5.0 | 18.4 ± 0.2 | 4.53 | cation exchange |
| | $C_8C_1imTf_2N$ | 58.0 | 28.7 ± 0.1 | 2.02 | mixed |
| | $C_{10}C_1imTf_2N$ | 31.4 ± 2.3 | 28.0 ± 0.1 | 1.12 | neutral complex |

[a] The two values shown are from the present study and reference [3.12], respectively.
[b] Uncertainties were calculated at the 95% confidence interval (n=3).
Values without uncertainties were calculated from duplicate measurements.

**Table 3.4**
**The effect of IL cation chain length on sodium, potassium, cesium, and nitrate ion partitioning between water and 0.20 M DCH18C6 in $C_nC_1imTf_2N$**

| Metal | Organic Phase | $\%E_M$ [a] | $\%E_{NO_3^-}$ [a] | Ratio $\%E_M/\%E_{NO_3^-}$ | Partitioning Mode Indicated |
|---|---|---|---|---|---|
| Na | $C_5C_1imTf_2N$ | 94.1 | 1.34 ± 0.02 | 70.2 | cation exchange |
| | $C_6C_1imTf_2N$ | 85.1 ± 4.7 | 5.08 ± 0.03 | 16.7 | cation exchange |
| | $C_8C_1imTf_2N$ | 50.3 | 12.4 ± 0.1 | 4.06 | cation exchange |
| | $C_{10}C_1imTf_2N$ | 28.2 ± 2.5 | 21.0 ± 0.1 | 1.34 | mixed |
| K | $C_5C_1imTf_2N$ | 99.9 ± 0.1 | 0.214 ± 0.031 | 476 | cation exchange |
| | $C_6C_1imTf_2N$ | 99.8 ± 0.1 | 6.67 ± 0.02 | 15.0 | cation exchange |
| | $C_8C_1imTf_2N$ | 98.4 ± 0.1 | 50.4 ± 0.1 | 1.95 | cation exchange |
| | $C_{10}C_1imTf_2N$ | 92.7 ± 0.1 | 60.8 ± 0.0 | 1.52 | mixed |
| Cs | $C_5C_1imTf_2N$ | 99.2 ± 0.4 | 1.64 ± 0.68 | 60.4 | cation exchange |
| | $C_6C_1imTf_2N$ | 98.2 ± 0.4 | 3.55 ± 0.32 | 27.7 | cation exchange |
| | $C_8C_1imTf_2N$ | 85.1 ± 0.4 | 17.8 ± 0.1 | 4.78 | cation exchange |
| | $C_{10}C_1imTf_2N$ | 56.4 ± 0.4 | 26.3 ± 0.1 | 2.14 | mixed |

[a] Uncertainties were calculated at the 95% confidence interval (n=3).
Values without uncertainties were calculated from duplicate measurements.

### 3.3.3 Nitric acid dependency of $D_M$ for extraction into $C_nC_1imTf_2N$ ILs by DCH18C6

The significant differences between the behavior of mono- and divalent cations in the ionic liquid systems (as well as the differences in the behavior of ionic liquids and aliphatic alcohols as extraction solvents) are also readily apparent from an examination of the nitric acid dependencies of the metal ion distribution ratios (Figures 3.4 and 3.5) for the various alkali and alkaline earth cations. Prior work with strontium ion [3.12] has shown that a systematic shift in the predominant mode of its transfer into ILs in the presence of DCH18C6 accompanies an increase in IL cation hydrophobicity. Specifically, this shift manifests itself as a change in the acid dependency from one in which rising nitric acid concentration is accompanied by falling $D_{Sr}$ values to one in

which these values generally increase as the acidity increases. This conclusion, however, was based on a somewhat limited range of acid concentrations (*i.e.*, those expected to be encountered either in the analytical-scale separation and preconcentration of Sr-89/90 from typical environmental samples [3.34, 3.35] or in the process-scale removal of radiostrontium from nuclear waste samples [3.36, 3.37]). As can be seen from Figure 3.4, when considered over a wide range of acidities, the variation in $D_M$ with nitric acid concentration for divalent cations can be a rather complex one. In contrast, each of the monovalent cations is seen to exhibit a nearly monotonic decrease in $D_M$ with rising aqueous acidity (Figure 3.5).

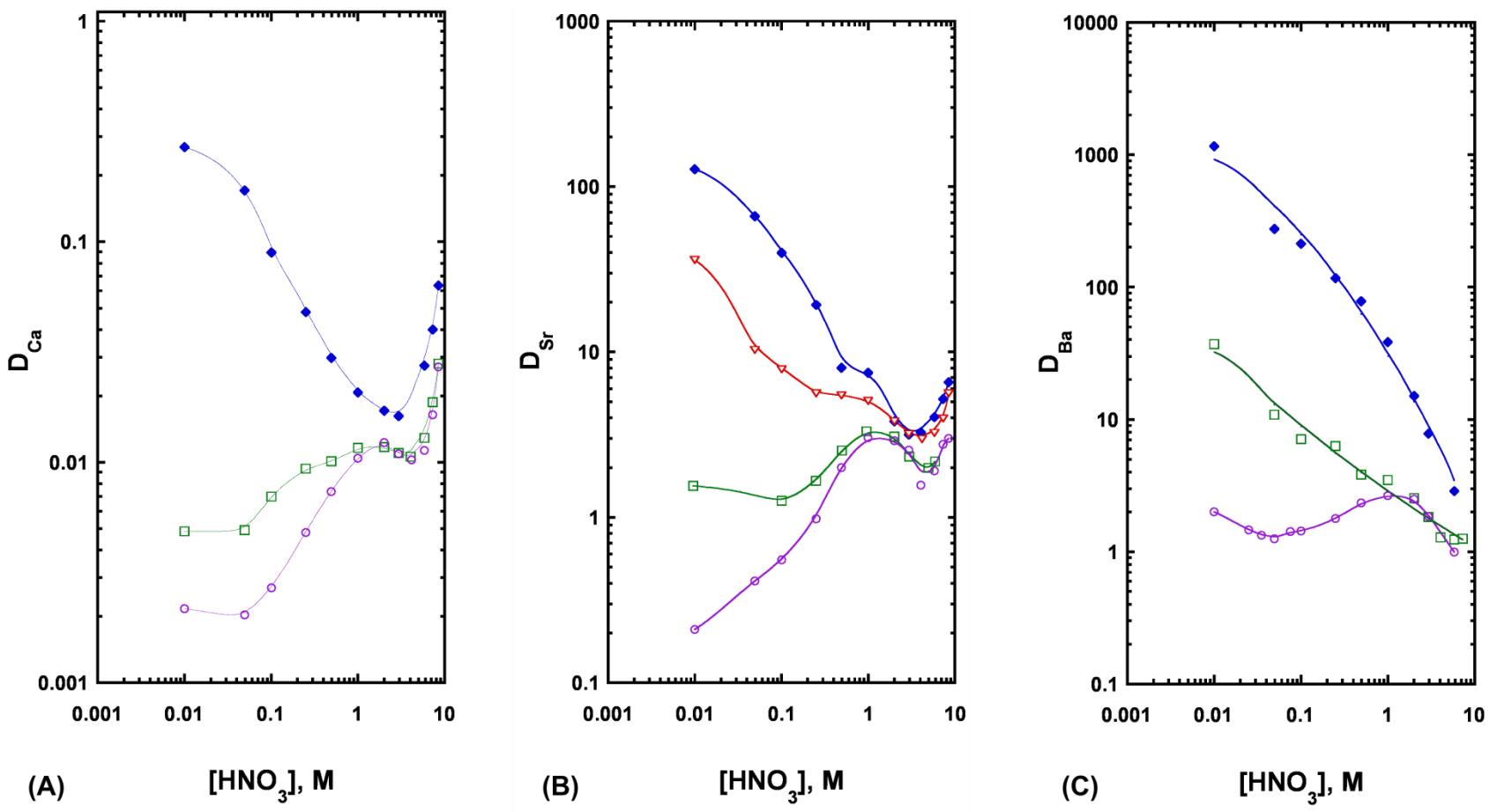


**Figure 3.4: Effect of nitric acid concentration on the extraction of $Ca^{2+}$(panel A), $Sr^{2+}$ (panel B), and $Ba^{2+}$ (panel C) by DCH18C6 (0.10 M) in $C_5C_1imTf_2N$ (◆), $C_6C_1imTf_2N$ (▽), $C_8C_1imTf_2N$ (□), and $C_{10}C_1imTf_2N$ (○).** The smooth curves are intended only as guides to the eye.

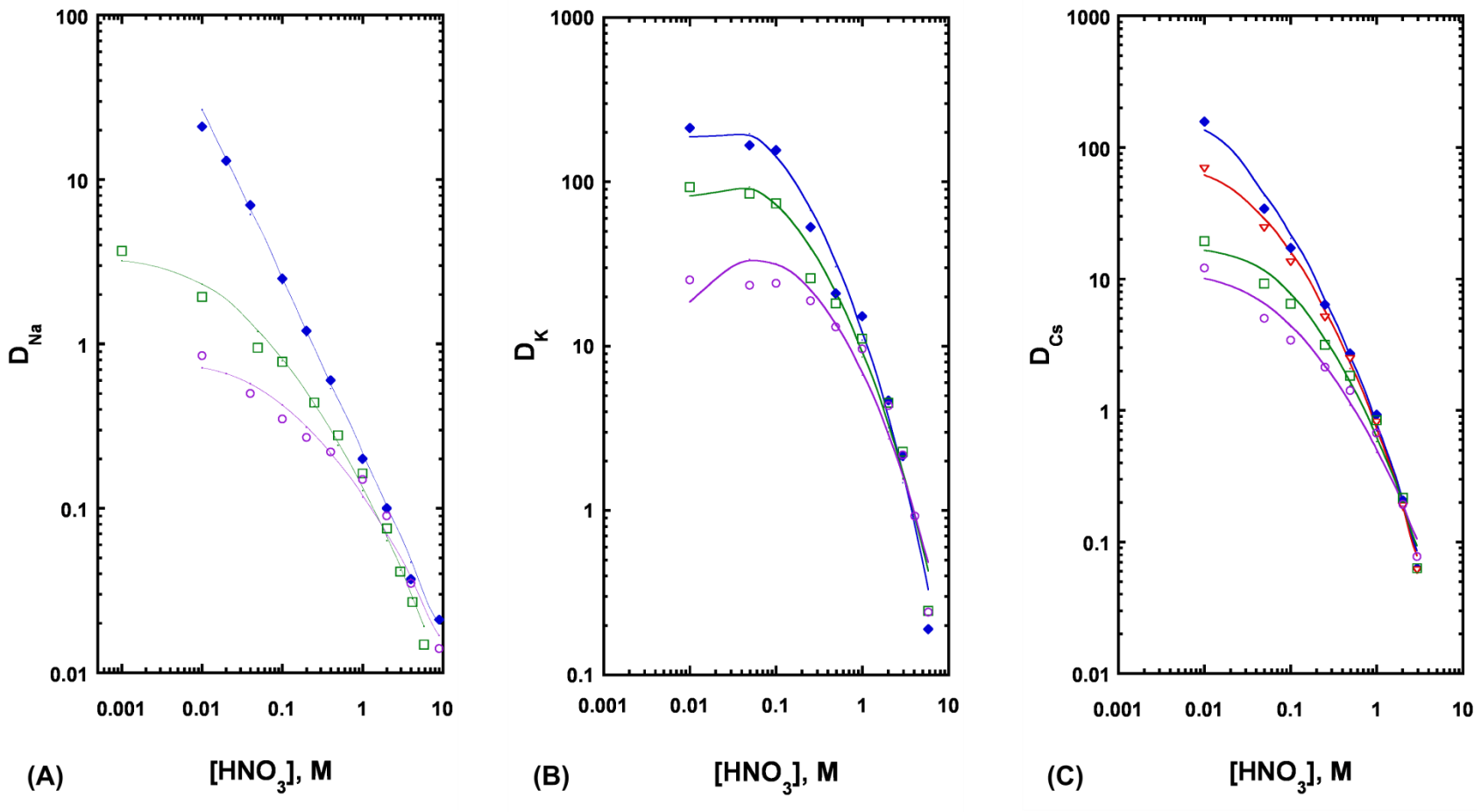


**Figure 3.5: Effect of nitric acid concentration on the extraction of $Na^+$ (panel A) and $K^+$ (panel B), and $Cs^+$ (panel C) by DCH18C6 (0.10 M) in $C_5C_1imTf_2N$ (◆), $C_6C_1imTf_2N$ (▽), $C_8C_1imTf_2N$ (□), and $C_{10}C_1imTf_2N$ (○).** The smooth curves are intended only as guides to the eye.

To understand these results, it must be recalled that prior work with $Sr^{2+}$ and $Na^{+}$ [3.12, 3.14] suggests the presence of three distinct pathways by which a metal ion can be extracted into an IL in the presence of a crown ether (Figure 3.1): the processes described by Equations 3-1 and 3-2 above (*i.e.*, partitioning of a neutral metal-nitrato crown ether complex and exchange of a cationic metal-crown ether complex for the cationic component of the IL, respectively) and a third process in which the metal ion is exchanged for a hydronium ion extracted by the crown ether, as depicted for sodium ion:

$$Na^{+} + H_3O{\bullet}DCH18C6\,^{+}{}_{IL} \leftrightharpoons H_3O^{+} + Na{\bullet}DCH18C6^{+}{}_{IL} \qquad (3\text{-}3)$$

Prior work further suggests that the balance among these pathways will vary with the experimental conditions (*e.g.*, the hydrophobicity of the IL cation and the aqueous acidity) [3.12]. Examination of the variation in $D_M$ with aqueous nitric acid concentration for potassium and cesium ion indicates that these dependencies, like those of $Na^{+}$, are consistent with a partitioning process involving two types of ion exchange. That is, for each of these ions, at low aqueous acidities, $D_M$ under a given set of conditions is seen to fall as the chain length of the IL cation (*i.e.*, its hydrophobicity) rises. Such a result is that expected when the dominant mode of extraction involves exchange of the metal-crown ether complex for the cationic constituent of the IL (Eqn. 3-2 above) [3.12]. As the acidity rises, however, the extractant dependencies converge, indicating that the same process (here, exchange of the metal ion for hydronium ion complexed with the crown ether as per Eqn. 3-3 [3.14]) is likely the primary factor determining the extraction efficiency ($D_M$) observed in all three ILs. That a third mode of

partitioning (*i.e.*, extraction of a neutral metal-nitrato-crown ether complex) must also be operative in the extraction of monovalent cations is demonstrated by the results presented earlier in Table 3.2, where co-extraction of measureable quantities of nitrate from water into the ILs is frequently observed. It is important to note, however, that this mode is apparently of significance only in the absence of appreciable quantities of aqueous acid.

Contrary to conventional organic solvents (in which the acid adducts with DCH18C6 typically comprise molecules of undissociated $HNO_3$ [3.30]), spectroscopic analysis [3.14] has revealed that acid extraction by the crown ether into an IL phase results in the formation of a DCH18C6 : hydronium complex. Although the process described in Eqn. 3-3 does not lead to the *direct* loss of the IL cation to the aqueous phase, it is important to note that the formation and partitioning of the DCH18C6 : hydronium adduct would be expected to result in the loss of an equivalent of the IL cation upon preconditioning of the IL phase with acid:

$$H_3O\bullet DCH18C6^{+} + IL^{+}IL^{-}_{IL} \leftrightharpoons H_3O\bullet DCH18C6^{+}IL^{-}_{IL} + IL^{+} \qquad (3\text{-}4)$$

That an increase in the initial concentration of the crown ether in the ionic liquid is accompanied by a corresponding increase in the equilibrium concentration of the IL cation in the aqueous phase [3.14] confirms that extraction of a metal ion by either ion-exchange pathway (Eqn. 3-2 or Eqn. 3-3) undoubtedly requires the transfer of the IL cation to the aqueous phase. From a practical standpoint, these are not conditions for a sustainable metal ion separation system.

In contrast to the trends observed in the acid dependencies of the alkali cations, the contribution of neutral complex extraction to the overall partitioning process is readily evident for the divalent metal ions, even at high acidities. Again beginning by considering the results obtained at low (*ca.* ≤ 0.5 M) acid concentrations (Figure 3.3), it can be seen that as was the case for the monovalent metal ions, increasing IL cation hydrophobicity is accompanied by a decrease in the value of $D_M$ at a given acidity for each of the Group 2A metal ions, consistent with the dominant role of ion-exchange involving the IL cation (Eqn. 3-2) under these conditions. As the nitric acid concentration is increased, competition between the two other possible modes of metal ion partitioning determines the direction and shape of the acid dependency, a consequence of the fact that nitric acid addition introduces both acid (*i.e.*, $H_3O^+$) and nitrate anion to the system. For the ILs comprising a short-chain (*i.e.*, low hydrophobicity) cation, increasing nitric acid concentration is initially accompanied by falling values of $D_M$, indicating that ion exchange between crown ether-complexed hydronium ion and the aqueous metal ion is an important contributor to extraction.

Consideration of the competition among the various possible routes for partitioning can be used to rationalize the shape of the acid dependencies for the longer chain (*i.e.*, more hydrophobic) ILs as well. For calcium ion extraction into the $C_8$ and $C_{10}$ ILs, for example, the difference between the dependencies at low acidity is consistent with a contribution to the observed partitioning of ion exchange involving the cationic component of the IL (Eqn. 3-2) [3.12]. As the $HNO_3$ concentration (and thus, the nitrate concentration) rises, $D_M$ also increases, indicating that partitioning of the neutral metal-nitrato-crown ether complex is the primary contributor to the observed extraction [3.12].

The eventual convergence and rollover of the dependencies suggests that at least over a limited range of acidities, the contribution of ion exchange involving the protonated crown ether is significant [3.14]. Eventually, however, rising nitrate concentration leads to re-establishment of neutral complex partitioning as the predominant mode of extraction. This same approach can be used to rationalize the results obtained for the other divalent metal ions under the same conditions.

It is important to note here that a variation in the preferred mode of extraction with aqueous acidity is not without precedent. Similar results have, in fact, been reported in the extraction of uranium with tri-n-butyl phosphate into the same series of ILs considered here, for which the predominant route for uranium partitioning has been reported to change from ion exchange to neutral complex extraction as the nitric acid concentration rises [3.15].

### 3.3.4 Influence of Hard-Soft Lewis Acid Character of Extracted Metal Ions

In addition to providing data that support the generality of the three-pathway model as a means to describe the balance of pathways that may contribute to the extraction of metal ions by crown ethers in ILs, comparing the results for different metal ions reveals the significant role that the Lewis acidity of the metal ion plays in determining the predominant mode of partitioning in the crown ether-IL system. That is, as the Lewis acidity of the divalent cations rises ($Ba^{2+} < Sr^{2+} < Ca^{2+}$), so too does the prevalence of a positive slope in the nitric acid dependencies of $D_M$ (Figure 3.3) and thus, the significance of neutral complex extraction. For instance, although the downward trend in the nitric acid dependency for barium extraction into $C_8C_1imTf_2N$ continues even at

relatively high acidities, for both $Ca^{2+}$ and $Sr^{2+}$, $D_M$ eventually begins to rise with increasing nitric acid concentration. As noted previously (and as observed in conventional molecular solvents), increasing $D_M$ with rising nitric acid (*i.e.*, nitrate) concentration is consistent with partitioning of a neutral metal-nitrato-crown ether complex [3.12]. These trends may be explained by the hard-soft theory of complexation [3.38], whereby the nitrate ion (as a hard base) interacts most strongly with a harder acid (*i.e.*, $Ca^{2+}$ *vs.* $Ba^{2+}$). Apparently then, for metal cations with an appropriately high charge density (*i.e.*, $Ca^{2+}$ and $Sr^{2+}$), the interaction between the cation and nitrate anion is sufficiently strong as to disfavor ion exchange processes.

### 3.3.5 Crown ether dependency of $D_M$ for extraction into $C_nC_1imTf_2N$ ILs by DCH18C6

It is also worth noting that despite obvious differences in the acid dependencies of $D_M$ for the various monovalent and divalent metal ions, in all cases, the extractant dependencies observed are consistent with the partitioning of a 1:1 metal ion: crown ether complex. Specifically, as can be seen from Figure 3.6, a log-log plot of $D_M$ *vs.* DCH18C6 concentration at constant nitric acid concentration yields a line of unit slope for each of the Group I cations. For the divalent metal ions, some deviation from unit slope is observed at sufficiently high extractant concentrations, as is observed for 1-ocatnol [3.31]. To understand the origin of this deviation, it is necessary to first consider in some detail the extraction of strontium from acidic nitrate media by DCH18C6 into 1-octanol.

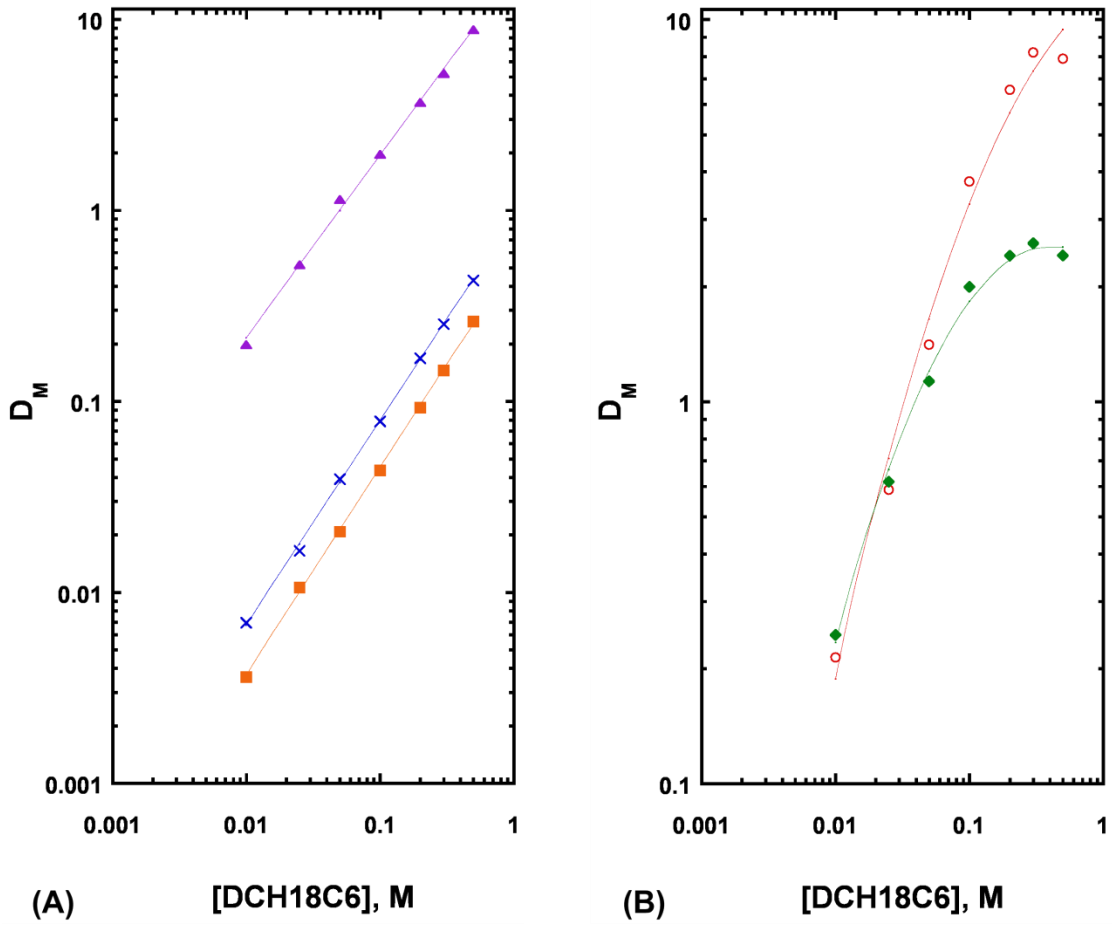


**Figure 3.6: Effect of DCH18C6 concentration on the extraction of $Na^+$ (■), $K^+$ (▲), $Cs^+$ (×) (panel A); $Sr^{2+}$ (○) and $Ba^{2+}$ (◆) (panel B) from 3.0 M nitric acid into $C_{10}C_1imTf_2N$.** Curves are least-squares linear fits.

Dietz *et al*. [3.31] have derived an expression relating $D_{Sr}$ to various experimental parameters for this system. Specifically, for the cases in which the nitric concentration is maintained constant, the the distribution ratio of strontium (and by analogy, other alkaline earth cations) can be expressed as follows

$$D_M = \frac{K'_{ex}\ NO_3^{-\ 2}\alpha_f C_{crown}}{1+K'_c\ \frac{C_{crown}}{D+1}} \qquad (3\text{-}5)$$

where $K'_{ex}$ is the conditional extraction constant and $K'_c$ is the conditional formation constant for the metal ion - crown ether complex, $\alpha_f$ is the fraction of free (not complexed by acid) crown ether in the organic phase, $C_{crown}$ is the formal crown ether concentration, and *D* (in the denominator) is the distribution ratio of the crown ether itself under the experimental conditions.

Equation 3-5 may be useful in interpreting the differences observed between conventional solvent systems and those based upon of ILs. That is, the denominator of Eqn. 3-5 includes a crown ether concentration term, the magnitude of which (relative to 1) will determine the extent to which $D_M$ will rise with increasing extractant concentration. At low $C_{crown}$, $K'_c$ ($C_{crown}$/D+1) << 1, and the value of $D_M$ will thus rise linearly with $C_{crown}$ (for a given nitric acid concentration, which fixes [$NO_3^-$] and $\alpha_f$). At higher $C_{crown}$, however, $K'_c$ ($C_{crown}$/D+1) eventually approaches 1, or exceeds 1, and the result is a dimunition in the slope of the $D_M$ *vs*. [DCH18C6] plot, and eventually, a leveling off of the plot. Indeed, as might be expected, the curves for the extractant dependencies of alkaline earth cation extraction in Figure 3.6 panel B appear to level off. However, at still higher concentrations of the crown ether, the plot actually exhibits a decrease in $D_M$ with rising extractant concentration, an observation not explained by Eqn. 3.5. Apparently then, the dependence of the distribution ratios for divalent metal ions on the extractant concentration is more complicated for ILs than that for molecular diluents. When the same measurements are made at lower nitric acid concentrations (Figure 3.7), the lower nitrate concentration is reflected in the overall lower $D_{Sr}$ values, consistent with

the acid dependency of $D_{Sr}$ (Figure 3.3). More importantly, a greater decline in the values of of $D_{Sr}$ at high extraction concentrations is observed at these lower acidities, indicating that the acid concentration also plays a role in defining the extractant dependencies. All of these observations can be explained by recognizing that, over the range of acidities considered, a not insignificant contribution to the overall extraction is made by a crown-mediated ion exchange reaction analogous that shown for $Na^+$ in Eqn. 3-3. As can be seen from the equation for this reaction (Eqn. 3-6), the only acid adduct that is formed in systems comprising these ILs is a 1:1 hydronium: crown ether complex [3.14]. Thus, if $M^{2+}$ (*e.g*, $Sr^{2+}$) is substituted for $Na^+$, electroneutrality demands that for every metal ion extracted, *two* hydronium: DCH18C6 adducts be involved. Accordingly, the general equation for the partitioning pathway involving cationic metal ion: DCH18C6 complexes is

$$M^{n+} + n\ H_3O{\bullet}DCH18C6\ ^{+}{}_{IL} \leftrightharpoons n\ H_3O^+ + M{\bullet}DCH18C6^{n+}{}_{IL} + (n\text{-}1)\ DCH18C6_{IL} \qquad (3\text{-}6)$$

From the perspective of chemical equilibria, the production of free DCH18C6 molecules in the presence of increased concentrations of this species would not be favorable. Thus, as the initial concentration of the free ligand in the IL phase increases, the propensity to extract a divalent metal ion by crown-mediated cation exchange is likely to diminish. In fact, under some conditions (*i.e.*, those that tend to support the extraction of divalent metal ions by this pathway), the decrease in the rate of change in $D_M$ with increasing crown concentration is apparently sufficient to produce a noticeable decline in the extractant dependencies.

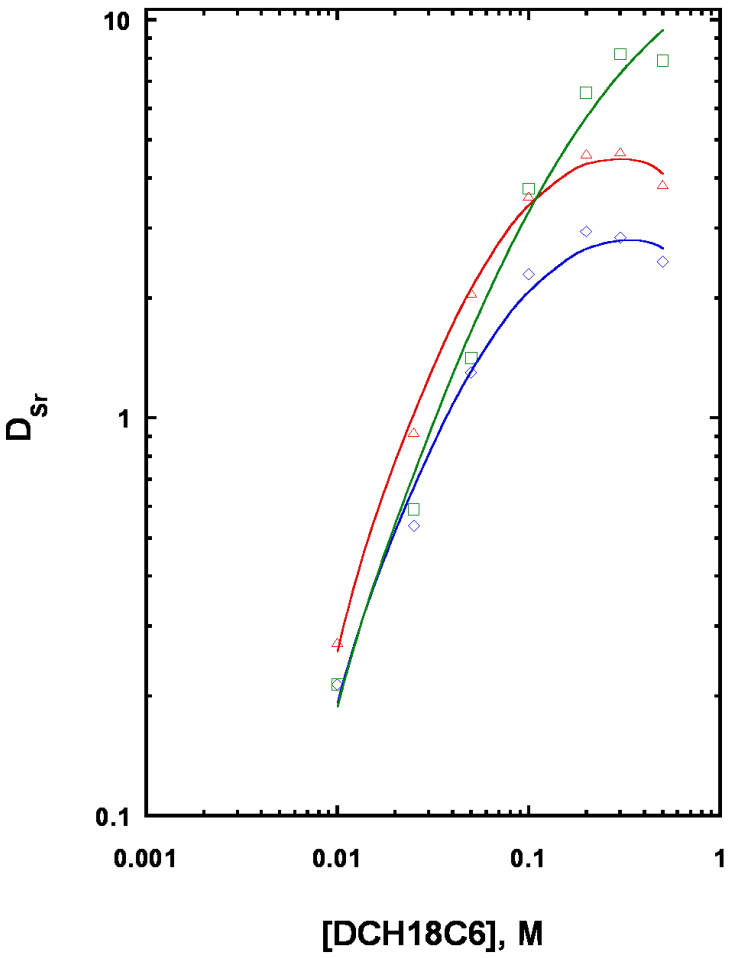


**Figure 3.7: Effect of DCH18C6 concentration on the extraction of $Sr^{2+}$ from 0.050 M $HNO_3$ (◇) 1.0 M $HNO_3$ (△) and 3.0 M $HNO_3$ (□) into $C_{10}C_1imTf_2N$.** The smooth curves are intended only as guides to the eye.

### 3.3.6 Implications for Extraction Efficiencies and Selectivities

In considering the possible practical significance of these results, it is important to point out that certain separations important in radiation dosimetry require (among other things) high divalent/monovalent cation extraction selectivity. For example, in the determination of radiostrontium in biological samples, isolation of a pure strontium

fraction requires a separation method exhibiting strontium/sodium selectivity ($\alpha_{Sr/Na}$) sufficient to take up traces of Sr-89/90 in the presence far larger quantities of sodium ions and calcium ions [3.34, 3.35]. In conventional solvent extraction systems employing an aliphatic alcohol diluent (*e.g.*, 1-octanol), as depicted in Figure 3.8 panel A, DCH18C6 can provide adequate $\alpha_{Sr/Na}$ only at certain acidities. For $C_{10}C_1imTf_2N$ (Figure 3.8 panel B), in contrast, the tendency of the extraction of monovalent cations to fall with increasing acidity while that of the divalent cations rises results in an improvement in $\alpha_{Sr/Na}$ *vs*. that seen in 1-octanol over a range of acidities. Especially useful from a practical perspective is the improvement in the 1-3 M $HNO_3$ region, the range over which extraction/sorption is commonly carried out. As shown in Table 3.3, at 2 M $HNO_3$ for example, the Sr/Na selectivity is improved by a factor of five upon changing the organic diluent from 1-octanol to $C_{10}C_1imTf_2N$. (Also noteworthy is that this change also results in a 10-fold improvement in the Sr/Ca extraction selectivity.) The Sr/Na selectivity in $C_{10}C_1imTf_2N$ peaks in the 1-3 M nitric acid region as a consequence of the decline of strontium extraction above this acidity. It remains to be determined if a modification of the structure of the crown ether to render it more hydrophobic might preserve these improvements in selectivity, while affording higher extraction efficiencies.

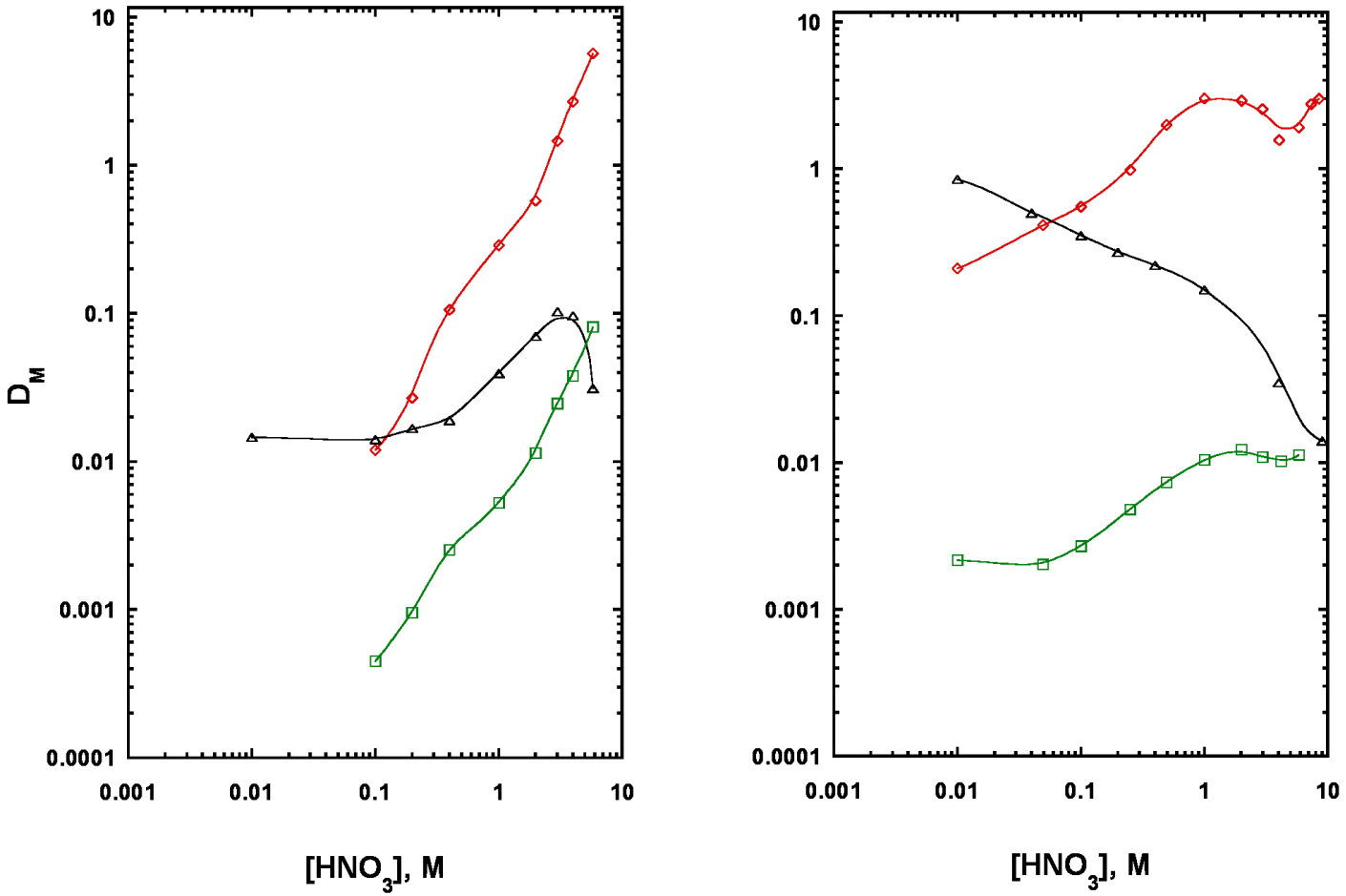


**Figure 3.8: Effect of nitric acid concentration on the extraction of $Sr^{2+}$ (◇), $Na^{+}$ (△), and $Ca^{2+}$ (□) into 1-octanol (left panel) and $C_{10}C_1imTf_2N$ (right panel).** Data for calcium distribution ratios in the left panel were estimated as an average of those for 1-pentanol and 1-decanol. The smooth curves are intended only as guides to the eye.

**Table 3.3**

**Effect of nitric acid concentration on $\alpha_{Sr/Na}$ and $\alpha_{Sr/Ca}$ values[a] in extraction from aqueous solution by 0.10 M DCH18C6 in 1-octanol and $C_{10}C_1imTf_2N$**

| $[HNO_3]$, M | $\sigma_{Sr/Na}$ in 1-octanol | $\sigma_{Sr/Na}$ in $C_{10}C_1imTf_2N$ | $\sigma_{Sr/Ca}$ in 1-octanol[b] | $\sigma_{Sr/Ca}$ in $C_{10}C_1imTf_2N$ |
|---|---|---|---|---|
| 0.1 | 0.85 | 1.3 | 12.6 | 206 |
| 0.2 | 1.6 | 2 | 13.6 | 150 |
| 0.4 | 5.61 | 7.5 | 25.3 | 267 |
| 1 | 7.35 | 25.8 | 25.4 | 291 |
| 2 | 8.22 | 42.6 | 23.6 | 237 |
| 3 | 14.2 | 68.4 | 38.0 | 234 |
| 4 | 27.8 | 60.2 | 50.6 | 157 |
| 5.8 | 182 | 32 | 70.4 | 169 |

[a] Distribution ratios used in these calculations are derived from least-squares regression of the empirical data.

[b] Data for calcium distribution ratios estimated as an average of those for pentanol and decanol.

### 3.4 Conclusions

Taken together, the results presented in this chapter indicate that the three-path description of metal ion partitioning into imidazolium-based ILs in the presence of a neutral crown ether suggested by prior studies of strontium and sodium ion constitutes a "generic" representation of alkali and alkaline earth cation extraction in these systems. This model, therefore, can be utilized to gain a qualitative understanding of the balance of the partitioning pathways by interpretation of the trends in the acid dependencies, and perhaps the extractant dependencies, over a wide range of conditions for metal ions that do not form anionic complexes. Such interpretation has been useful in explaining, for instance, how the hard-soft acid nature of the metal ion may affect which of the pathways predominates under given conditions, and in turn, provides significant selectivity between metal ions differing in this aspect. Although it remains to be demonstrated, it is expected that analogous processes describe the partitioning of any of a number of other metal ions into a variety of ILs in the presence of other neutral extractants as well. Because the interplay between the various pathways has shown to be considerably dependent on the structure (*e.g.*, hydrophobicity) of the IL, the effect of systematic variations in the structure of the cationic component of the IL will be explored in subsequent chapters.

### 3.4 Acknowledgements

This work was supported by the Single Investigator Small Group Research (SISGR) Program of the Office of Basic Energy Sciences of the United States Department of Energy under sub-contract from Brookhaven National Laboratory. The measurements of the nitric acid dependence of the strontium distribution ratios and those of sodium in *n*-

alcohols were performed by Sarah Garvey. Dan McAlister of EiChroM Technologies, Inc. (Darien, IL) and Sue Krezoski of the UWM Department of Chemistry and Biochemistry are gratefully acknowledged for assistance with ICP-AES and ICP-MS measurements, respectively.

### 3.6 References

[3.1] X. Han, D.W. Armstrong, *Acc. Chem. Res.* **2007**, 40, 1079–1086.

[3.2] P. Sun, D.W. Armstrong, *Anal. Chim. Acta*, **2010**, 661, 1-16.

[3.3] M. Koel, *Crit. Rev. Anal. Chem.* **2005**, 35, 177-192.

[3.4] J.L. Anderson, D.W. Armstrong, *Anal. Chem.* **2005**, 77, 6453-6462.

[3.5] D.W. Armstrong, L-K. Zhang, L. He, M.L. Gross, *Anal. Chem.* **2003**, 73, 3679-3686.

[3.6] S. Carda-Broch, A. Berthod, D.W. Armstrong, *Rapid Comm. Mass Spec.* **2003**, 17, 553-560.

[3.7] I. Romero-Sanz, J. Fernandez de la Mora, *J. Appl. Phys.* **2004**, 95, 2123-2129.

[3.8] P.K. Chowdhury, M. Halder, L. Sanders, T. Calhoun, J.L. Anderson, D.W. Armstrong, X. Song, J. W. Petrich, *J. Phys. Chem. B*, **2004**, 108, 10245-10255.

[3.9] E.G. Yanes, S.R. Gratz, M.J. Baldwin, S.E. Robinson, A.M. Stalcup, *Anal. Chem.* **2001**, 73, 3838-3844.

[3.10] M.L. Dietz, J.A. Dzielawa, *Chem. Commun.* **2001**, 20, 2124-2125.

[3.11] M.P. Jensen, J.A. Dzielawa, P. Rickert, M.L. Dietz, *J. Am. Chem. Soc.* **2002**, 124, 10664-10665.

[3.12] M.L. Dietz, J.A. Dzielawa, I. Laszak, B.A. Young, M.P. Jensen, *Green Chem.* **2003**, 5, 682-685.

[3.13] D.C. Stepinski, M.P. Jensen, J.A. Dzielawa, M.L. Dietz, *Green Chem.* **2005**, 7, 151-158.

[3.14] D.C. Stepinski, M.L. Dietz, *Green Chem.* **2005**, 7, 747-750.

[3.15] M.L. Dietz, D.C. Stepinski, *Talanta*, **2008**, 75, 598-603.

[3.16] D.C. Stepinski, G.F. Vandegrift, I.A. Shkrob, J.F. Wishart, K. Kerr, M.L. Dietz, D.T.D. Qadah, S.L. Garvey, *Ind. Eng. Chem. Res.* **2010**, 49, 5863-5868.

[3.17] A.E. Visser, R.P. Swatloski, R.D. Rogers, *Green Chem.* **1999**, 2, 1-4.

[3.18] R. Vijayaraghavan, N. Vedaraman, M. Surianarayanan, D.R. MacFarlane, *Talanta*, **2006**, 69, 1059-1062.

[3.19] Y.C. Pei, J.J. Wang, X.P. Xuan, J. Fan, M. Fan, *Environ. Sci. Technol.* **2007**, 41, 5090-5095.

[3.20] A. Safavi, H. Abdollahi, N. Maleki, S. Zienali, *J. Colloid Interface Sci.* **2008**, 332, 274-280.

[3.21] Wang, J. Pei, Y. Zhao, Y. Hu, Z., *Green Chem.* **2005**, 7, 196-202.

[3.22] L.I.N. Tomé, M. Domínguez-Pérez, A.F.M. Cláudio, M.G. Freire, I.M. Marrucho, O. Cabeza, J.A.P. Coutinho, *J. Phys. Chem. B*, **2009**, 113, 13971-13979.

[3.23] S. Dai, Y.H. Ju, C.E. Barnes, *J. Chem. Soc., Dalton Trans.* **1999**, 1201-1202.

[3.24] A.E. Visser, R.P. Swatloski, W.M. Reichert, S.T. Griffin, R.D. Rogers, *Ind. Eng. Chem. Res.* **2000**, 39, 3596-3604.

[3.25] J. Huang, A. Riisager, P. Wasserscheid, R. Fehrmann, *Chem. Commun.* **2006**, 38, 4027-4029.

[3.26] H. Luo, S. Dai, P. Bonnesen, *Anal. Chem.* **2004**, 76, 2773-2779.

[3.27] K. Binnemans, *Chem. Rev.* **2007**, 107, 2592-2614.

[3.28] C.A. Hawkins, S.L. Garvey, M.L. Dietz, *Sep. Purif. Technol.* **2012**, 89, 31-38.

[3.29] P. Bonhote, A.P. Dias, N. Papageorgiou, K. Kalyanasundaram, M. Grätzel, *Inorg. Chem.* **1996**, 35, 1168-1178.

[3.30] M. Deetlefs, K.R. Seddon, *Green Chem.* **2003**, 5, 181-186.

[3.31] Dietz, M.L. Bond, A.H. Clapper, M. Clapper, J.W. Finch, *Radiochim. Acta*, **1999**, 85, 119-129.

[3.32] R.M. Izatt, J.S. Bradshaw, S.A. Nielsen, J.D. Lamb, J.J. Christensen, D. Sen, *Chem. Rev.* **1985**, 85, 271-339.

[3.33] E.P. Horwitz, M.L. Dietz, and D.E. Fisher, *Solvent Extr. Ion Exch.* **1990**, 8, 199-208.

[3.34] E.P. Horwitz, M.L. Dietz, and D.E. Fisher, *Anal. Chem.* **1991**, 63, 522-525.

[3.35] E.P. Horwitz, R. Chiarizia, M.L. Dietz, *Solvent Extr. Ion Exch.* **1992**, 10, 313–336.

[3.36] E.P. Horwitz, M.L. Dietz, D.E. Fisher, *Solvent Extr. Ion Exch.* **1991**, 9, 1-25.

[3.37] M.L. Dietz, E.P. Horwitz, R.D. Rogers, *Solvent Extr. Ion Exch.* **1995**, 13, 1-17.

[3.38] R.G. Pearson, *J. Am. Chem. Soc.* **1963**, 85, 3533-3539.

# CHAPTER 4:
# THE ROLE OF IONIC LIQUID PHASE WATER CONTENT

## 4.1 Introduction

In the interest of providing a clear description of the current understanding of metal ion extraction into ILs it is worth summarizing the main points found in Chapter 3, where our fundamental knowledge of the extraction of metal ions into conventional solvents has been applied to interpret their extraction behavior into ILs. Put simply, the similarities between these types of solvents quickly disappear when a wide range of conditions are evaluated. Metal ion extraction into the conventional (*i.e.*, molecular) solvents (*e.g.*, paraffinic and chlorinated hydrocarbons) traditionally employed in liquid-liquid extraction (LLE) generally involves the complexation of the metal ion by a ligand (*i.e.*, extractant) to produce a hydrophobic (and thus, extractable) species [4.1]. Of the many extractants available, neutral extractants are the most widely employed, in large part because the extent of metal ion partitioning can be adjusted simply by changing the aqueous phase anion (*e.g.*, nitrate) concentration. In such systems, electroneutrality requires that the cationic metal-extractant complex initially formed be accompanied by an aqueous phase anion (or anions) upon extraction, thus producing a neutral (and therefore extractable) species. Such a process is depicted in Eqn. 4-1 for the extraction of an alkali or alkaline earth cation from a nitrate-containing aqueous phase by a crown ether (here, dicyclohexano-18-crown-6, henceforth abbreviated as DCH18C6):

$$M^{n+} + n\ NO_3^- + DCH18C6_{org} \leftrightharpoons M(NO_3)_n \bullet DCH18C6_{org} \qquad (4\text{-}1)$$

Prior work with these systems has shown that when oxygenated, aliphatic solvents (*e.g.*, *n*-alcohols) are employed, the magnitude of the metal ion distribution ratio (a measure of the extent to which a given metal ion is extracted, defined as $[M]_{org}/[M]_{aq}$ at equilibrium) under a given set of conditions is related to the organic phase water content, with metal extraction efficiency increasing as the hydrophilicity (and thus, the water content) of the organic diluent rises [4.2, 4.3].

In contrast to the straightforward nature of extraction into conventional solvents (*e.g.*, *n*-alcohols), alkali and alkaline earth cation extraction by DCH18C6 into ionic liquids has been found to be far more complex [4.4-4.9], with as many as three distinct pathways for partitioning possible: extraction of a ion paired (neutral) complex (Eqn. 4-1); exchange of the cationic metal complex for the IL cation (Eqn. 4-2); and a third process in which the metal ion is exchanged for the proton (*i.e.*, hydronium ion) extracted by the crown ether during preconditioning of the system, as depicted in Eqn. 4-3 [4.4-4.8].

$$M\bullet DCH18C6^{n+} + x\ IL^{+}_{IL} \leftrightharpoons M\bullet DCH18C6^{n+}_{IL} + n\ IL^{+} \qquad (4\text{-}2)$$

$$M^{n+} + n\ H_3O\bullet DCH18C6\ ^{+}_{IL} \leftrightharpoons n\ H_3O^{+} + M\bullet DCH18C6^{n+}_{IL} + (n\text{-}1)\ DCH18C6_{IL} \qquad (4\text{-}3)$$

Work in this and other laboratories concerning the factors governing the balance among these various pathways suggests that numerous factors can play a role in determining the predominant mode of extraction, among them the hydrophobicity of the IL cation [4.6] and anion [4.10], the nature of the metal ion (in particular, its charge density [4.9, 4.11]), and the aqueous phase anion [4.9]. Most often, the interaction of

these factors is such as to favor one or both of the ion exchange processes, rather than neutral complex extraction [4.4, 4.6, 4.7, 4.9, 4.11]. Given that ion exchange inevitably results in loss of the IL to the aqueous phase [4.4, 4.7], this is a problematic observation from the perspective of the development of practical IL-based extraction processes.

Clearly, an ideal extraction system would combine the highly efficient metal ion partitioning often observed for some ILs [4.12] with the uncomplicated behavior (*i.e.*, neutral complex partitioning as the sole mode of extraction) of a conventional organic solvent. Yet, the vast diversity of available IL structures complicates the selection of IL solvents without an understanding of their correlated physicochemical properties. To this end, we have examined the effect of incorporating a primary alcohol group into the long chain of the imidazolium ion for a series of 1-alkyl-3-methylimidazolium and 1-alkyl-3-butylimidazolium *bis*[(trifluoromethyl)sulfonyl]imides on the extraction of alkali and alkaline earth cations by DCH18C6. It was anticipated that such structural modification, by raising the water content of the solvent (versus that of the corresponding IL lacking a hydroxyl group), would favor extraction of a neutral complex, in analogy to aliphatic alcohols. Although ILs incorporating hydroxyl groups have been described previously [4.13-4.15], this work, which explores the mutual solubility of the ILs and water [4.16], and the follow-up studies described here represent the first systematic effort to evaluate them as solvents for metal ion extraction.

## 4.2 Experimental

### 4.2.1 Materials

All chemicals were reagent grade and used without additional purification, unless noted otherwise. All aqueous solutions were prepared using deionized water with a

specific resistance of at least 18 $M\Omega \cdot cm^{-1}$. Dicyclohexano-18-crown-6 ether (DCH18C6) was purchased from Parish Chemical (Orem, UT) as a mixture of the *cis-syn-cis* and *cis-anti-cis* isomers. Strontium-85 and sodium-22 radiotracers were purchased as nominal solutions from Eckert and Ziegler Isotope Products, Inc. (Valencia, CA).

Imidazolium-based ionic liquids including the 3-methyl, 3-ethyl, and 3-butyl substituents were synthesized by the two-step process shown in Scheme 4.1. The 1-alkyl-3-methylimidazolium based ILs have been prepared previously by similar methods [4.17]. In the first step, a halogenated alkane or alcohol (in 3% molar excess) and an *N*-alkylimidazole were combined neat, and the mixture subjected to microwave irradiation (using a CEM Discover BenchMate Model 908005), yielding an 1,3-dialkylimidazolium halide. The product was washed with ethyl acetate (unless noted otherwise) four times to remove unreacted starting materials. Halide salts that were solid were either heated slightly until melted or dissolved in a small amount of deionized water to facilitate contact with the ethyl acetate. Excess solvent was removed under reduced pressure by rotary evaporation in a water bath held at 60°C. In the second step, the water-miscible salts were dissolved in deionized water and combined with an aqueous solution containing a 3 mol% excess of lithium *bis*[(trifluoromethyl)sulfonyl]imide ($LiTf_2N$). Although in each case, the IL phase formed readily following the addition of the aqueous $LiTf_2N$ solution, samples were allowed to stir overnight to ensure completion of the reaction. The IL (lower) layer was then allowed to settle, separated from the aqueous phase, and washed with deionized water until a test of the water washes for the presence of halide ion (by precipitation with silver nitrate) was negative. The final products, which were nearly colorless to yellow free-flowing liquids, were dried under vacuum at 80°C

for at least 24 hours. It is worth noting that the impurities imparting visible color to the ILs are compounds with high molar extinction coefficients, and these compounds are estimated to be present in concentrations less than 1 μM [4.18, 4.19]. They are thus unlikely to affect partitioning experiments. The ionic liquids used in these experiments (all $Tf_2N$ salts) were tested for residual halides by contacting them three times with equal volumes of water and analyzing the combined aqueous fractions by ion chromatography. In all cases, analysis indicated that the IL contained less than 10 ppm bromide or chloride. Where appropriate (*i.e.*, for ILs not previously reported) elemental (CHN) analysis of the ionic liquids was performed by the combustion method (Galbraith Laboratories, Knoxville, TN). Other elements (*e.g.*, oxygen) were determined from the theoretical mass balance.

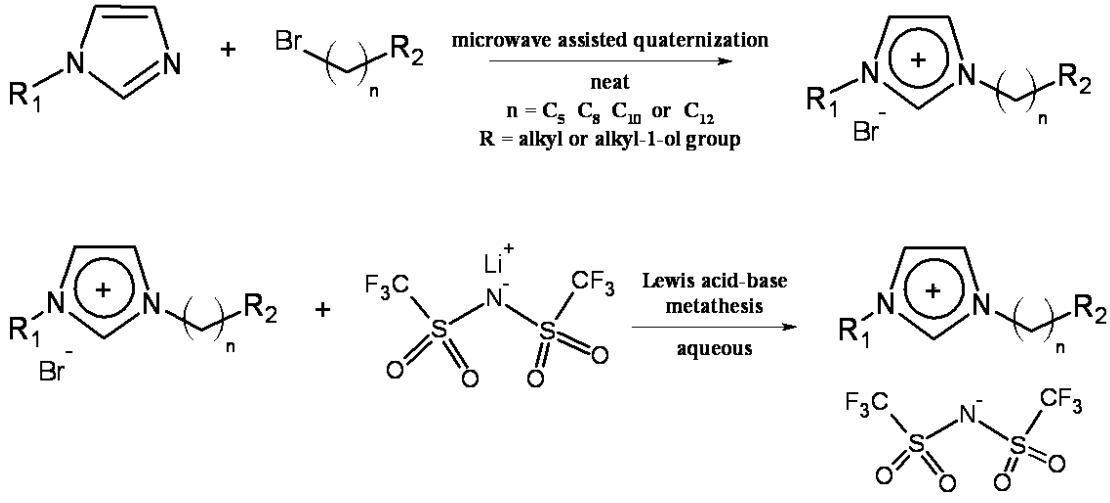


**Figure 4.1: Synthesis of Imidazolium-based RTILs.**

Because of the absence of commercially available 1-hexylimidazole or 1-octylimidazole precursors, ionic liquids incorporating the 3-hexyl or 3-octyl substituents were synthesized in a five step process starting with the three steps shown in in Scheme 4.2 and finishing with the two steps in Scheme 4.1. The procedure to synthesize the 1-alkylimidazoles were adapted from reference [4.20]. In the first step, protection of one imidazole amine was performed in a methanol solution by adding excess acrylonitrile and heating to 60°C while stirring under an atmosphere of nitrogen gas for at least 12 hours. The 1-(2-cyanoethyl)imidazole product was obtained by vacuum-assisted rotary evaporation in a water bath held at 80°C. Significant amounts (*ca.* 3-5%) of a 3-methoxypropanenitrile side-product were also recovered due to Michael addition of the solvent to acrylonitrile. This molecular impurity was removed from the ionic liquid by solvent washes. Proton NMR spectra also revealed that 3-5% unprotected imidazole was also recovered, because the side-reaction eliminated the active excess of acrylonitrile. Thus, the reaction was started again with the addition of a smaller amount of acrylonitrile. After recovery of this product by rotary evaporative, the 1H-NMR spectrum was free of imidazole signals, suggesting that the reaction was complete. In the second step, either 1-bromohexane or 1-bromooctane was combined with the crude product from the first step and the mixture dissolved in acetonitrile because the two reactants are immiscible. The solution was subjected to microwave irradiation (using a CEM Discover BenchMate Model 908005), yielding an 3-alkyl-1-(2-cyanoethyl)limidazolium bromide. After rotary evaporation of the solvent at 80°C, the product was washed with ethyl acetate four times to remove unreacted starting materials. Excess solvent was removed by vacuum-assisted rotary evaporation in a water bath held at 60°C. The third step

comprised the deprotection of the amine in a biphasic reaction between 15% (w/w) aqueous sodium hydroxide and the second product dissolved in dichloromethane by vigorously stirring overnight. The resulting organic phase was removed and washed with water to remove excess salt and sodium hydroxide. The solvent was then removed by rotary evaporation in a water bath held at 40°C, Finally, other volatiles were removed in the same manner with the water bath held at 80°C.

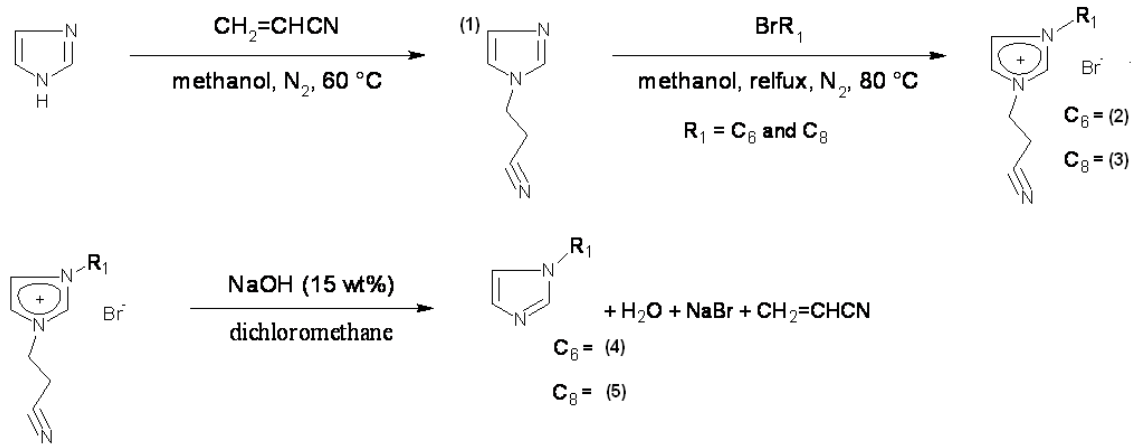


**Figure 4.2: Synthesis of Hexylimidazole and Octylimidazole.**

## ***N*-Alkylimidazole Synthesis**

### 1-(2-cyanoethyl)imidazole (1)

Dissolve 1*H*-imidazole (35.6 g, 0.52 mol) in 80 mL methanol. Add (36.2 mL, 29.3 g, 0.55 mol) acrylonitrile and dissolv while bubbling nitrogen gas into the solution. Stir at 60°C under flowing nitrogen for at least 12 hours. Evaporate solvent and excess volatiles. Add 50 mL of methanol and an additional 2 mL of acrylonitrile and continued the reaction for at least 8 hours. Evaporate solvent and volatiles to obtain a crude product free of imidazole, but replete with 3-methoxypropanenitrile, a by-product of methanol and

acrylonitrile. $^{1}$H-NMR in $CDCl_3$: δ, 7.58 (s, 1H), 7.11 (s, 1H), 7.03 (s, 1H), 4.27 (t, 2H), 3.60 (t, 2H, by-product), 3.40 (s, 3H, by-product), 2.82 (t, 2H), 2.60 (t, 2H, by-product).

**1-(2-cyanoethyl)-3-hexyl-imidazole (2)**

From compound 1 (1.89 g, 0.015 mol nominally), and 1-bromohexane (2.70 g, 0.016 mol) (in 2.5 mL acetonitrile, microwave: power = 200 W, 120°C, t = 20 min), 4.31 g (0.019 mol) of 3-hexyl-1-(2-cyanoethyl)imidazole (97% recovery). $^{1}$H-NMR in $CDCl_3$: δ, 10.23 (s, 1H), 8.16 (s, 1H), 7.45 (s, 1 H), 4.90 (t, 2H), 4.26 (t, 2H), 3.37 (t, 2H), 1.88 (m, 2H), 1.29 (m, 6H), 0.90 (t, 3H).

**(2-cyanoethyl)-3-octyl-1-imidazole (3)**

From compound 1 (1.58 g, 0.013 mol nominally), and 1-bromooctane (2.64 g, 0.014 mol) (in 2.5 mL acetonitrile, microwave: power = 200 W, 120°C, t = 20 min), 3.90 g (0.012 mol) of 3-octyl-1-(2-cyanoethyl)imidazole (91% recovery). $^{1}$H-NMR in $CDCl_3$: δ, 10.17 (s, 1H), 8.11 (s, 1H), 7.44 (s, 1 H), 4.91 (t, 2H), 4.32 (t, 2H), 3.39 (t, 2H), 1.91 (m, 2H), 1.24 (m, 10H), 0.86 (t, 3H).

**1-hexylimidazole (4)**

Dissolve compound 2 (62.1 g, 0.22 mol) in 130 mL dichloromethane. Add 125 mL 15% (w/w) sodium hydroxide and stir vigorously overnight. Separate the organic phase and wash it repeatedly with water until a silver nitrate test reveals no residual bromide. Remove the solvent by vacuum-assisted rotary evaporation at 40°C, then any residual volatiles at 80°C. A light yellow more less viscous liquid of 1-hexylimidazole was

recovered (31.1 g, 0.20 mol, 94% recovery). $^{1}$H-NMR in $CDCl_3$: δ, 7.47 (s1, H), 7.28 (s, 1H), 6.89 (s, 1 H), 3.91 (t, 2H), 1.75 (qt, 2H), 1.26 (m, 6H), 0.86 (t, 3H).

**1-octylimidazole (5)**

Dissolve compound 3 (73.8 g, 0.26 mol) in 130 mL dichloromethane. Add 135 mL 15% (w/w) sodium hydroxide and stir vigorously overnight. Separate the organic phase and wash it repeatedly with water until a silver nitrate test reveals no residual bromide. Remove the solvent by vacuum-assisted rotary evaporation at 40°C, then any residual volatiles at 80°C. A yellow, less viscous liquid of 1-hexylimidazole was recovered (38.3 g, 0.35 mol, 95% recovery). $^{1}$H-NMR in $CDCl_3$: δ, 7.60 (s1, H), 7.14 (s, 1H), 6.87 (s, 1 H), 3.93 (t, 2H), 1.67 (qt, 2H), 1.23 (m, 10H), 0.85 (t, 3H).

**1,3-Dialkylimidazolium IL Synthesis (compounds not described in Chapter 3)**

**1-octyl-3-butylimidazolium bromide (6)**

From *N*-butylimidazole (2.37 g, 0.019 mol), and 1-bromooctane (3.87 g, 0.020 mol) (neat, microwave: power = 240 W, 110°C, t = 8 min), 6.00 g (0.019 mol) of $C_8C_4$imBr was obtained as a yellow liquid (yield of 99%). $^{1}$H-NMR (DMSO): δ, 9.32 (s, 1H), 7.84 (d, 2H), 4.19 (dt, 4H), 1.80 (m, 4H), 1.24 (m, 12H), 0.90 (m, 6H).

**1-decyl-3-ethylimidazolium bromide (7)**

From *N*-ethylimidazole (1.83 g, 0.019 mol), and 1-bromodecane (4.49 g, 0.020 mol) (neat, microwave: power = 240 W, 90°C, t = 10 min), 5.76 g (0.018 mol) of $C_{10}C_2$imBr

was obtained as a yellow liquid (yield of 94%). $^{1}$H-NMR (DMSO): δ, 9.34 (s, 1H), 7.85 (d, 2H), 4.19 (t and q, 4H), 1.80 (m, 4H), 1.42 (t, 3H), 1.24 (m, 14H), 0.86 (m, 3H).

**1-decyl-3-butylimidazolium bromide (8)**

From *N*-butylimidazole (2.37 g, 0.019 mol), and 1-bromodecane (4.49 g, 0.020 mol) (neat, microwave: power = 240 W, 90°C, t = 10 min), 6.60 g (0.019 mol) of $C_{10}C_4$imBr was obtained as a yellow liquid (yield of 99%). $^{1}$H-NMR (DMSO): δ, 9.34 (s, 1H), 7.85 (d, 2H), 4.18 (dt, 4H), 1.80 (m, 4H), 1.24 (m, 16H), 0.90 (m, 6H).

**1-decyl-3-hexylimidazolium bromide (9)**

From compound 3 (2.33 g, 0.015 mol), and 1-bromodecane (3.55 g, 0.016 mol) (neat, microwave: power = 240 W, 100°C, t = 15 min), 5.33 g (0.014 mol) of $C_{10}C_6$imBr was obtained as a pale yellow liquid (yield of 94%). $^{1}$H-NMR ($CDCl_3$): δ, 10.63 (s, 1H), 7.38 (d, 2H), 4.37 (t, 4H), 1.91 (m, 4H), 1.29 (m, 20H), 0.88 (t, 6H).

**1-decyl-3-octylimidazolium bromide (10)**

From compound 4 (2.50 g, 0.014 mol), and 1-bromodecane (3.25 g, 0.015 mol) (neat, microwave: power = 240 W, 100°C, t = 15 min), washes were performed using *n*-hexane 5.06 g (0.013 mol) of $C_{10}C_8$imBr was obtained as a yellow liquid (yield of 91%). in ($CDCl_3$): δ, 10.46 (s, 1H), 7.41 (d, 2H), 4.36 (t, 4H), 1.89 (m, 4H), 1.28 (m, 24H), 0.86 (t, 6H).

**1-octyl-3-butylimidazolium *bis*[(trifluoromethyl)sulfonyl]imide (11)**

From compound 6 (5.99 g, 0.019 mol), and 6.04 g (0.021 mol) $LiTf_2N$ (both predissolved in D.I. water), 9.44 g (0.018 mol) of $C_8C_4imTf_2N$ was obtained as a colorless liquid (yield of 95%).$^1$H-NMR (DMSO): δ, 9.19 (s, 1H), 7.80 (s, 2H), 4.16 (q, 4H), 1.80 (m, 4H), 1.25 (m, 12H), 0.90 (m, 6H).

**1-decyl-3-ethylimidazolium *bis*[(trifluoromethyl)sulfonyl]imide (12)**

From compound 7 (6.41 g, 0.020 mol), and 6.38 g (0.022 mol) $LiTf_2N$ (both predissolved in D.I. water), 10.25 g (0.020 mol) of $C_{10}C_2imTf_2N$ was obtained as a colorless liquid (yield of 98%).$^1$H-NMR (DMSO): δ, 9.93 (s, 1H), 7.84 (d, 2H), 4.20 (t and d, 4H), 1.79 (m, 2H), 1.42 (t, 3H), 1.24 (m, 14H), 0.89 (m, 3H).

**1-decyl-3-butylimidazolium *bis*[(trifluoromethyl)sulfonyl]imide (13)**

From compound 8 (7.01 g, 0.020 mol), and 6.11 g (0.021 mol) $LiTf_2N$ (both predissolved in D.I. water), 10.85 g (0.020 mol) of $C_{10}C_4imTf_2N$ was obtained as a colorless liquid (yield of 98%).$^1$H-NMR (DMSO): δ, 9.19 (s, 1H), 7.80 (s, 2H), 4.16 (dt, 4H), 1.78 (m, 4H), 1.30 (m, 16H), 0.89 (m, 6H).

**1-decyl-3-hexylimidazolium *bis*[(trifluoromethyl)sulfonyl]imide (14)**

From compound 9 (7.21 g, 0.019 mol), and 6.09 g (0.021 mol) $LiTf_2N$ (both predissolved in D.I. water), 9.98 g (0.017 mol) of $C_{10}C_6imTf_2N$ was obtained as a yellow liquid (yield of 90%).$^1$H-NMR ($CDCl_3$): δ, 8.83 (s, 1H), 7.34 (s, 2H), 4.20 (q, 4H), 1.88 (m, 4H), 1.30 (m, 20H), 0.89 (m, 6H).

**1-decyl-3-octylimidazolium *bis*[(trifluoromethyl)sulfonyl]imide (15)**

From compound 10 (7.63 g, 0.019 mol), and 6.09 g (0.021 mol) $LiTf_2N$ (both predissolved in D.I. water), 10.4 g (0.017 mol) of $C_{10}C_8imTf_2N$ was obtained as a yellow liquid (yield of 91%).$^1$H-NMR ($CDCl_3$): δ, 8.81 (s, 1H), 7.36 (s, 2H), 4.19 (t, 4H), 1.87 (m, 4H), 1.26 (m, 24H), 0.88 (m, 6H).

**1-(Hydroxyalkyl)-3-alkylimidazolium IL Synthesis**

**1-(5-hydroxypentyl)-3-methylimidazolium bromide (16)**

From *N*-methylimidazole (2.37 g, 0.029 mol), and 5-bromo-1-pentanol (4.69 g, 0.028 mol) (neat, microwave: power = 250 W, 70°C, t = 20 min), 6.58 g (0.026 mol) of $C_5OHC_1imBr$ was obtained as a pale yellow solid (yield of 94%). $^1$H-NMR: δ, 9.20 (s, 1H), 7.80 (d, 1H), 7.73 (s, 1H), 4.41 (broad peak, 1H), 4.16 (t, 2H), 3.85 (s, 3H), 3.31 (t, 2H), 1.79 (m, 2H), 1.44 (m, 2H), 1.25 (m, 2H).

**1-(8-hydroxyoctyl)-3-methylimidazolium bromide (17)**

From *N*-methylimidazole (1.86 g, 0.023 mol), and 8-bromo-1-octanol (4.61 g, 0.022 mol) (neat, microwave: power = 250 W, 60°C, t = 30 min), 5.86 g (0.020 mol) of $C_8OHC_1imBr$ was obtained as a slightly yellow solid (yield of 91%). $^1$H-NMR: δ, 9.15 (s, 1H), 7.90 (s, 1H), 7.72 (s, 1H), 4.34 (broad peak, 1H), 4.16 (t, 2H), 3.85 (s, 3H), 3.35 (m, 2H, obscured by water peak), 1.78 (m, 2H), 1.40 (m, 2H), 1.26 (m, 8H).

**1-(10-hydroxydecyl)-3-methylimidazolium bromide (18)**

From *N*-methylimidazole (2.03 g, 0.025 mol), and 10-bromo-1-decanol heated to melt (5.75 g, 0.024 mol) (neat, microwave: power = 250 W, 60°C, t = 30 min), 7.36 g (0.023 mol) of $C_{10}OHC_1$imBr was obtained as a colorless solid (yield of 96%). $^1$H-NMR (DMSO): δ, 9.18 (s, 1H), 7.79 (s, 1H), 7.73 (s, 1H), 4.34 (broad peak, 1H), 4.16 (t, 2H), 3.85 (s, 3H), 3.37 (m, 2H, obscured by water peak ), 1.78 (m, 2H), 1.40 (m, 2H), 1.26 (m, 12H).

**1-(8-hydroxyoctyl)-3-butylimidazolium bromide (19)**

From *N*-butylimidazole (2.43 g, 0.020 mol), and 8-bromo-1-octanol (3.89 g, 0.019 mol) (neat, microwave: power = 250 W, 70°C, t = 30 min) 6.03 g (0.018mol) of $C_8OHC_4$imBr was obtained as a slightly yellow liquid (yield of 97%). $^1$H-NMR (DMSO): δ, 9.17 (s, 1H), 7.82 (s, 2H), 4.34 (broad peak, 1H), 4.17 (dt, 4H), 3.85 (s, 3H), 3.33 (m, 2H, obscured by water peak ), 1.80 (m, 4H), 1.42 (m, 2H), 1.30 (m, 10H), 0.90 (t, 3H).

**1-(10-hydroxydecyl)-3-butylimidazolium bromide (20)**

From *N*-butylimidazole (1.75 g, 0.014 mol), and 10-bromo-1-decanol heated to melt (3.25 g, 0.014 mol) (neat, microwave: power = 250 W, 70°C, t = 30 min), 4.65 g (0.013 mol) of $C_{10}OHC_4$imBr was obtained as slightly yellow liquid (yield of 94%). $^1$H-NMR (DMSO): δ, 9.31 (s, 1H), 7.84 (s, 2H), 4.33 (broad peak, 1H), 4.19 (dt, 4H), 3.85 (s, 3H), 3.33 (m, 2H, obscured by water peak ), 1.80 (m, 4H), 1.42 (m, 2H), 1.30 (m, 10H), 0.90 (t, 3H).

**1-(12-hydroxydodecyl)-3-methylimidazolium bromide (21)**

From *N*-methylimidazole (1.94 g, 0.024 mol), and 12-bromo-1-dodecanol heated to melt (5.98 g, 0.023 mol) (neat at 60°C to melt the bromoalcohol and mix), microwave: power = 250 W, 60°C, t = 30 min), 7.58 g (0.022 mol) of $C_{12}OHC_1$imBr was obtained as a slightly colored solid (yield of 97%). $^1$H-NMR (DMSO): δ, 9.16 (s, 1H), 7.79 (s, 1H), 7.72 (s, 1H), 4.33 (broad peak, 1H), 4.16 (t, 2H), 3.85 (s, 3H), 3.36 (m, 2H, obscured by water peak ), 1.78 (m, 2H), 1.40 (m, 2H), 1.26 (m, 16H).

**1-(12-hydroxydodecyl)-3-ethylimidazolium bromide (22)**

From *N*-ethylimidazole (1.04 g, 0.011 mol), and 12-bromo-1-dodecanol heated to melt (2.95 g, 0.011 mol) (neat, microwave: power = 250 W, 70°C, t = 30 min), 3.70 g (0.010 mol) of $C_{12}OHC_2$imBr was obtained as slightly yellow liquid (yield of 94%). $^1$H-NMR ($CDCl_3$): δ, 10.63 (s, 1H), 7.36 (s, 1H), 7.30 (s, 1H), (4.48 (q, 2H), 4.33 (t, 2H), 3.365 (t, 2H), 1.94 (m, 2H), 1.63 (t, 3H), 1.58 (m, 2H), 1.30 (m, 17H).

**1-(12-hydroxydodecyl)-3-butylimidazolium bromide (23)**

From *N*-butylimidazole (1.38 g, 0.011 mol), and 12-bromo-1-dodecanol heated to melt (3.04 g, 0.011 mol) (neat, microwave: power = 250 W, 70°C, t = 30 min), 4.36 g (0.011 mol) of $C_{12}OHC_4$imBr was obtained as slightly yellow liquid (yield of 98%). $^1$H-NMR (DMSO): δ, 9.25 (s, 1H), 7.82 (d, 2H), 4.33 (t, 1H), 4.18 (dt, 4H), 3.38 (m, 2H, obscured by water signal), 1.78 (m, 4H), 1.40 (m, 2H), 1.21 (m, 18H), 0.90 (t, 3H).

**1-(12-hydroxydodecyl)-3-octylimidazolium bromide (24)**

From compound 5 (1.93 g, 0.011 mol), and 12-bromo-1-dodecanol heated to melt (2.93 g, 0.011 mol) (neat, microwave: power = 240 W, 120°C, t = 30 min), 4.20 g (0.0094 mol) of $C_{12}OHC_8imBr$ was obtained as yellow liquid (yield of 85%). $^1$H-NMR ($CDCl_3$): δ, 10.72 (s, 1H), 7.25 (d, 2H), 4.38 (t, 4H), 3.66 (t, 2H), 1.89 (m, 2H), 1.58 (m, 2H), 1.36 (m, 14H), 1.28 (m, 14H), 0.91 (t, 3H).

**1-(5-hydroxypentyl)-3-methylimidazolium *bis*[(trifluoromethyl)sulfonyl]imide (25)**

From compound 16 (6.51 g, 0.026 mol), and 7.42 g (0.026 mol) $LiTf_2N$ (both predissolved in D.I. water), 11.0 g (0.024 mol) of $C_5OHmimTf_2N$ was obtained as a colorless liquid (yield of 95%). $^1$H-NMR (DMSO): δ, 9.10 (s, 1H), 7.75 (s, 1H), 7.70 (s, 1H), 4.37 (broad peak, 1H), 4.16 (t, 2H), 3.85 (s, 3H), 3.39 (m, 2H, obscured by water peak), 1.79 (m, 2H), 1.45 (m, 2H), 1.29 (m, 2H).

**1-(8-hydroxyoctyl)-3-methylimidazolium *bis*[(trifluoromethyl)sulfonyl]imide (26)**

From compound 17 (5.81 g, 0.020 mol), and 5.74 g (0.020 mol) $LiTf_2N$ (both predissolved in D.I. water), 9.28 g (.019 mol) of $C_8OHmimTf_2N$ was obtained as a colorless liquid (yield of 95%). $^1$H-NMR (DMSO): δ, 9.10 (s, 1H), 7.77 (s, 1H), 7.70 (s, 1H), 4.334 (t, 1H), 4.16 (t, 2H), 3.85 (s, 3H), 3.38 (m, 2H, obscured by water peak ), 1.78 (m, 2H), 1.40 (m, 2H), 1.27 (m, 8H). Elemental analysis data: Theoretical: %C = 34.21, %H = 4.72, %N = 8.55; Empirical: %C = 34.07, %H = 4.61, %N = 8.58.

**1-(10-hydroxydecyl)-3-methylimidazolium *bis*[(trifluoromethyl)sulfonyl]imide (27)**

From compound 18 (7.72 g, 0.024 mol), and 6.96 g (0.025 mol) $LiTf_2N$ (both predissolved in D.I. water), 12.02 g (0.023 mol) of $C_{10}OHmimTf_2N$ was obtained as a colorless liquid (yield of 96%). $^1$H-NMR (DMSO): δ, 9.11 (s, 1H), 7.79 (s, 1H), 7.73 (s, 1H), 4.34 (t, 1H), 4.16 (t, 2H), 3.85 (s, 3H), 3.40 (m, 2H, obscured by water peak ), 1.80 (m, 2H), 1.40 (m, 2H), 1.24 (m, 12H). Elemental analysis data: Theoretical: %C = 36.99, %H = 5.24, %N = 8.09; Empirical: %C = 36.94, %H = 5.05, %N = 8.00.

**1-(8-hydroxyoctyl)-3-butylimidazolium *bis*[(trifluoromethyl)sulfonyl]imide (28)**

From compound 19 (7.67 g, 0.023 mol), and 6.64 g (0.024 mol) $LiTf_2N$ (both predissolved in D.I. water), 11.65 g (0.023 mol) of $C_8OHbimTf_2N$ was obtained as a colorless liquid (yield of 95%). $^1$H-NMR (DMSO): δ, 9.10 (s, 1H), 7.80 (s, 2H), 4.33 (t, 1H), 4.16 (dt, 4H), 3.35 (m, 2H, obscured by water peak ), 1.78 (m, 4H), 1.40 (m, 2H), 1.26 (m, 10H), 0.91 (t, 3H). Theoretical: %C = 38.27%, %H = 5.48, %N = 7.88; Empirical: %C = 37.47, %H = 5.46, %N = 7.61.

**1-(10-hydroxydecyl)-3-octyllimidazolium *bis*[(trifluoromethyl)sulfonyl]imide (29)**

From compound 20 (9.62 g, 0.025 mol), and 7.31 g (0.026 mol) $LiTf_2N$ (both predissolved in D.I. water), 13.38 g (0.024 mol) of $C_{10}OHbimTf_2N$ was obtained as a colorless liquid (yield of 94%). $^1$H-NMR (DMSO): δ, 9.19 (s, 1H), 7.79 (s, 2H), 4.31 (t, 1H), 4.16 (dt, 4H), 3.39 (m, 2H, obscured by water peak ), 1.79 (m, 4H), 1.40 (m, 2H), 1.25 (m, 13H) 0.93 (t, 3H). Theoretical: %C = 40.63, %H = 5.92, %N = 7.48; Empirical: %C = 39.32, %H = 5.86, %N = 6.98.

**1-(12-hydroxydodecyl)-3-methylimidazolium *bis*[(trifluoromethyl)sulfonyl]imide (30)**

From compound 21 (7.50 g, 0.022 mol), and 6.21 g (0.022 mol) $LiTf_2N$ (both predissolved in D.I. water), 11.44 g (.021 mol) of $C_{12}OHC_1imTf_2N$ was obtained as a slightly colored liquid (yield of 97%). $^1$H-NMR (DMSO): δ, 9.10 (s, 1H), 7.80 (s, 1H), 7.69 (s, 1H), 4.32 (t, 1H), 4.15 (t, 2H, J = ), 3.85 (s, 3H), 3.41 (m, 2H, obscured by water peak ), 1.80 (m, 2H), 1.40 (m, 2H), 1.25 (m, 21H). Theoretical: %C = 39.48, %H = 5.71, %N = 7.68; Empirical: %C = 38.19, %H = 5.64, %N = 7.29.

**1-(12-hydroxydodecyl)-3-ethylimidazolium *bis*[(trifluoromethyl)sulfonyl]imide (31)**

From compound 22 (3.70 g, 0.010 mol, suspended in water), and 3.28 g (0.011 mol) $LiTf_2N$ (dissolved in D.I. water), 5.62 g (0.010 mol) of $C_{12}OHC_2imTf_2N$ was obtained as a colorless liquid (yield of 98%). $^1$H-NMR ($CDCl_3$): δ, 8.86 (s, 1H), 7.35 (d, 2H), 4.30 (q, 2H), 4.17 (t, 4H), 3.65 (t, 2H), 1.89 (m, 2H), 1.58 (t, 3H), 1.30 (m, 19H).

**1-(12-hydroxydodecyl)-3-butylimidazolium *bis*[(trifluoromethyl)sulfonyl]imide (32)**

From compound 23 (13.17 g, 0.034 mol), and 10.65 g (0.037 mol) $LiTf_2N$ (both predissolved in D.I. water), 18.93 g (0.032 mol) of $C_{12}OHC_4imTf_2N$ was obtained as a colorless liquid (yield of 95%). $^1$H-NMR (DMSO): δ, 9.18 (s, 1H), 7.80 (d, 2H), 4.31 (t, 1H), 4.17 (dt, 4H), 3.38 (q, 2H, unresolved from water signal), 1.78 (m, 4H), 1.40 (m, 2H), 1.21 (m, 18H), 0.91 (t, 3H).

**1-(12-hydroxydodecyl)-3-ethylimidazolium *bis*[(trifluoromethyl)sulfonyl]imide (33)**

From compound 24 (4.17 g, 0.0094 mol, suspended in water), and 2.96 g (0.010 mol) $LiTf_2N$ (predissolved in water), 4.96 g (0.077 mol) of $C_{12}OHC_4imTf_2N$ was obtained as a colorless liquid (yield of 81%). $^1$H-NMR: δ, 9.18 (s, 1H), 7.80 (d, 2H), 4.31 (t, 1H), 4.17 (dt, 4H), 3.38 (q, 2H, unresolved from water signal), 1.78 (m, 4H), 1.40 (m, 2H), 1.21 (m, 18H), 0.91 (t, 3H).

The names and structures of all of the ionic liquid cations prepared, along with the shorthand notation employed to represent them, are summarized in Table 4.1.

**Table 4.1**
**Structures and Nomenclature of the Ionic Liquid Cations Studied**

| IL Cation Name | IL Cation Shorthand | IL Cation Structure |
|---|---|---|
| 1-pentyl-3-methylimidazolium | $C_5C_1$im | 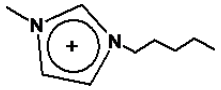 |
| 1-hexyl-3-methylimidazolium | $C_6C_1$im | 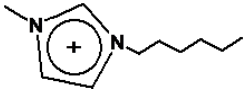 |
| 1-octyl-3-methylimidazolium | $C_8C_1$im | 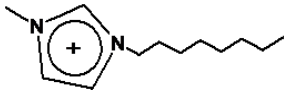 |
| 1-decyl-3-methylimidazolium | $C_{10}C_1$im | 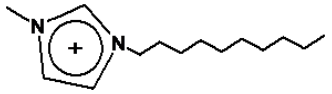 |
| 1-decyl-3-ethylimidazolium | $C_{10}C_2$im | 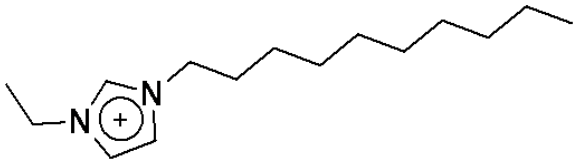 |
| 1-decyl-3-butylimidazolium | $C_{10}C_4$im | 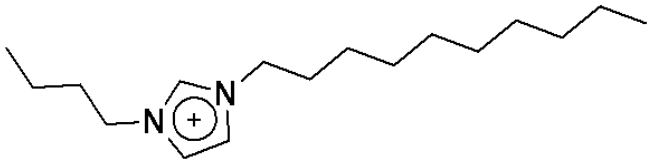 |
| 1-decyl-3-hexylimidazolium | $C_{10}C_6$im | 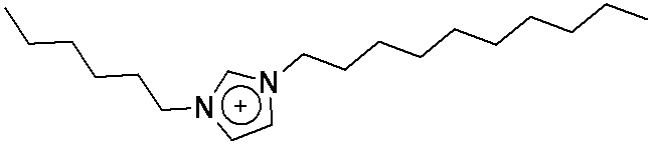 |

**Table 4.1 Continued**

| | | |
|---|---|---|
| 1-decyl-3-octylimidazolium | $C_{10}C_8$im | 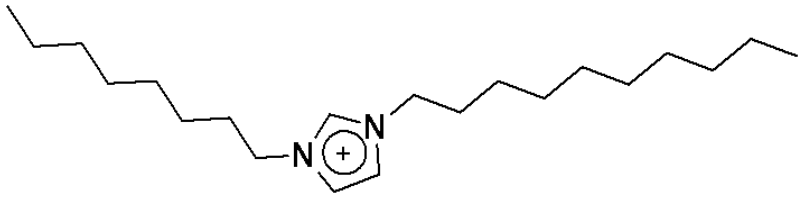 |
| 1-(5-hydroxypentyl)-3-methylimidazolium | $C_5OHC_1$im | 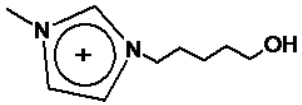 |
| 1-(8-hydroxyoctyl)-3-methylimidazolium | $C_8OHC_1$im | 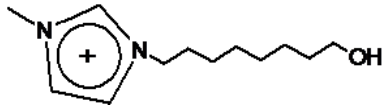 |
| 1-(8-hydroxyoctyl)-3-butyl-imidazolium | $C_8OHC_4$im | 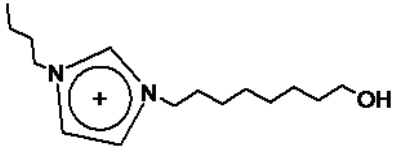 |
| 1-(10-hydroxydecyl)-3-methylimidazolium | $C_{10}OHC_1$im | 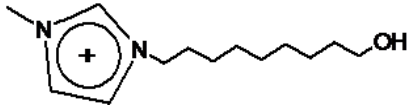 |
| 1-(10-hydroxydecyl)-3-butyl-imidazolium | $C_{10}OHC_4$im | 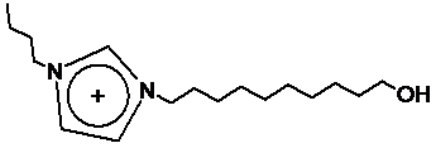 |

**Table 4.1 Continued**

| | | |
|---|---|---|
| 1-(12-hydroxydodecyl)-3-methylimidazolium | $C_{12}OHC_1im$ | 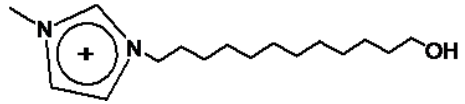 |
| 1-(12-hydroxydodecyl)-3-ethyl-imidazolium | $C_{12}OHC_2im$ | 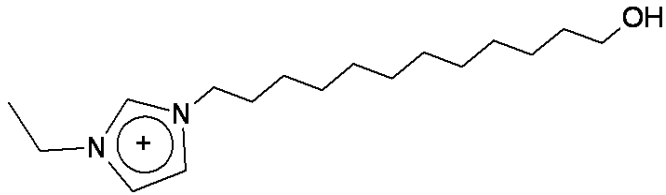 |
| 1-(12-hydroxydodecyl)-3-butyl-imidazolium | $C_{12}OHC_4im$ | 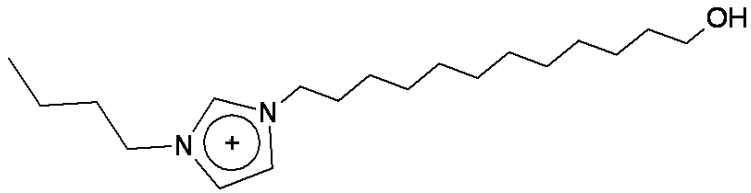 |
| 1-(12-hydroxydodecyl)-3-octyl-imidazolium | $C_{12}OHC_8im$ | 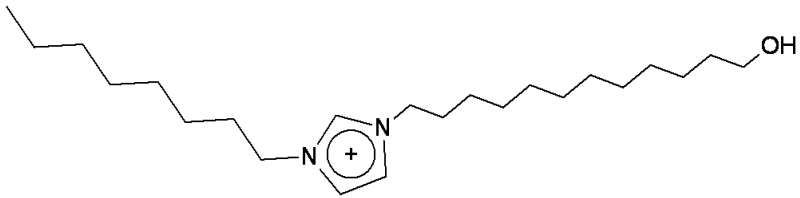 |

4.2.2 Instruments

Gamma spectroscopy was performed using a PerkinElmer model 2480 automatic gamma counter equipped with WIZARD2 software. NMR spectra were acquired on a Bruker DPX300 NMR spectrometer operating at 300.13 MHz for proton and 75.47 MHz for carbon-13, and equipped with a z-gradient broadband (BBO) probe. Unless otherwise noted, spectra were obtained using solutions of dimethylsulfoxide-$d_6$ or chloroform-$d_3$ (Aldrich, 99.96 atom% D), and all chemical shifts were reported relative to tetramethylsilane. Thermogravimetric analysis (TGA) was performed using a TA Instruments Q50 TGA in a nitrogen atmosphere at a scan rate of 10°C/min with sample sizes of approximately 5 mg. Differential scanning calorimetry data were obtained with a TA Instruments Q20 DSC. The DSC scanning sequence involved freezing the sample to -90°C, then ramping to 200°C, followed by cooling to -90°C, and finally ramping to 40°C, all at a rate of 5°C $min^{-1}$. The water content of the ILs was measured using a Metrohm 670 KF coulometer. The water solubility of ILs was measured using a Shimadzu UV-2450 UV-Visible Spectrophotometer with matching 10 mm path length quartz cuvettes. Halide impurities were determined using a Dionex ICS-1000 ion chromatograph equipped with equipped with a 25 μL fixed-loop manual injection port, an, a conductivity detector, Dionex AS18/AG18 analytical and guard columns (4 X 250 and 4 X 50 mm), a Dionex ASRS 300 anion self-regenerating eluent suppressor (4 mm), and 37 mM NaOH eluent. The instrument was operated using Chromeleon software version 6.80.

4.2.3 Methods

Distribution ratios ($D_M$ ) were determined as the ratio of the count rate in the organic phase to that of the aqueous phase using commercial radiotracers. Assays were carried out *via* gamma spectroscopy using standard procedures. In each metal ion distribution experiment, the organic phase consisted of DCH18C6 dissolved in the designated ionic liquid, and the aqueous phase nitric acid concentration was systematically adjusted either by conducting separate experiments for each condition, or adding the appropriate amount of acid after each sampling. All organic phases were pre-equilibrated with aqueous phase prior to the introduction of the metal radiotracer. Additionally, the sum of the count rates in each phase yielded recoveries within 10% (most often < 10%) that of the radiotracer stock solution used, indicating that equilibrium was established with only two phases involved. Room temperature was maintained at 23 ± 2°C. Each equilibrated phase was sampled for analysis in at least duplicate, with resulting uncertainties based on counting statistics that were generally within 10%, although the uncertainty interval was considerably wider for the highest $D_M$ values ($D_M \geq 1000$). The determination of the conditional extraction constant for strontium extraction was performed as an average of three experiments, each with four replicate analyses. Nitric acid concentrations were determined by titration with a standard sodium hydroxide solution (Ricca Chemical Company, Arlington, TX). The density of the ionic liquids (ILs) was determined by weighing volumes accurately measured by calibrated micropipettes. All measurements for "dry" ionic liquids were performed using materials that were dried *in vacuo* at 80°C for at least 24 hours in small quantities (≤ 3 mL) to facilitate the loss of water vapor. Samples used in the measurement of the mutual solubility of ionic liquids with water

were prepared by contacting a 1:1 ratio of the neat IL with deionized water in glass culture tubes and vortex mixing. Following 12 hours or more of standing at 25 ± 2°C, samples were centrifuged at 3000 rcf to ensure complete disengagement. The water solubility of ILs was measured by UV spectrophotometry at the wavelength characteristic of the imidazolium ring (210 nm) using standards prepared from a known weight of the dry IL. The water content of solutions of DCH18C6 in ILs was measured after vortex equilibration with 1.0 M nitric acid. The tubes were allowed to stand overnight in a 25°C water bath and centrifuged for 30 minutes to completely disengage the phases.

## 4.3 Effect of Ionic Liquid Water Content on Strontium Extraction

### 4.3.1 Relationship between ionic liquid-water mutual solubilities and metal ion extraction into $C_nC_1imTf_2N$ and $C_nOHC_1imTf_2N$ ionic liquids

Prior work in this laboratory has demonstrated that insight into the partitioning of metal ions into ionic liquids in the presence of a neutral extractant can be obtained by a comparison to the behavior of the ions in various conventional (*i.e.*, molecular) solvents [Chapter 3]. In the interest of providing a comprehensive illustration of how these earlier results relate to the studies performed in this chapter, it is worth reviewing our understanding, as developed on the basis of the results described in Chapter 3. With this in mind, we first consider the extraction of monovalent and divalent cations from acidic nitrate media into several *n*-alcohols in the presence of DCH18C6. The general rise in the distribution ratios with increasing nitric acid concentration for the extraction of alkali and alkaline earth ions into *n*-alcohols shows that extraction proceeds *via* the partitioning of a neutral complex (Eqn. 4-1). At sufficiently high acidity, however, the extraction of the monovalent cation declines, the apparent result of competition for the crown ether

between the cation and extracted nitric acid [4.21]. From a practical perspective, reactions of the type described by Eqn. 4-1 are highly desirable as the basis for metal ion separations, as they permit the extraction of the ion of interest from an acidic aqueous phase (such as are encountered in waste processing applications [4.22] or result from the leaching or dissolution of a sample for subsequent analysis [4.23]) and its facile recovery (*i.e.*, back-extraction) into dilute acid or water.

In contrast, results obtained in the extraction of alkali and alkaline earth ions into $C_nC_1imTf_2N$ ILs, containing DCH18C6 from nitric acid solutions of increasing concentration show quite different trends. In the case of the sodium ion, a monotonic decrease in $D_M$ with acidity is observed, while for strontium ion, the dependency obtained is a complex relationship in which $D_M$ may either fall or rise with acidity, depending on the hydrophobicity of the IL cation and the precise acid concentration. In both instances, the substantial difference between the behavior of the conventional solvents and the ionic liquids is readily apparent. Prior work [4.4, 4.6, 4.7, 4.9] has demonstrated that the unusual acid dependencies observed in these ILs have their origins in the multi-path extraction process operative, in which three distinct reactions contribute to the observed metal ion distribution. That is, in addition to the extraction of a neutral complex (as per Eqn. 4-1), two other processes are observed, both (as noted above) involving ion exchange (Eqn. 4-2 and 4-3).

Figure 4.1 and 4.2 depict the results obtained in analogous extraction studies employing a series of 1-hydroxyalkyl-3-methylimidazolium ionic liquids (hereafter designated as $C_nOHC_1imTf_2N$ ILs), while Table 4.2 summarizes several physicochemical properties of these ILs, as well as those for three $C_nC_1imTf_2N$ ILs, relevant to their

behavior as extraction solvents. As can be seen from the table, for a given alkyl chain length, incorporation of a hydroxyl group, while not appreciably affecting the IL density and only modestly reducing the liquidus range, significantly increases the water content of the solvent, typically by a factor of nearly four. For all of the $C_nOHC_1$im-based ILs examined, in fact, the solvent water content is comparable to or exceeds that measured for 1-octanol (36,000 ppm), the solvent upon which are based processes for the recovery of Sr-90 from nuclear wastes [4.22] and commercial sorbents for its recovery from various samples for subsequent determination [4.23]. This functionalization also increases the water solubility of the IL rather substantially, however. In all instances, in fact, the water solubility of the $C_nOHC_1$im IL is an order of magnitude or larger than that of the corresponding $C_nC_1$im-based IL. Thus, while hydroxyl-functionalization does have the desired effect on the solvent water content, it also significantly raises the hydrophilicity of the IL, likely rendering it more prone to function as a liquid ion-exchanger (Eqn. 4-2) [4.4, 4.6]. Of these two effects, the increase in solvent hydrophilicity is apparently the more important, as is suggested by Figures 4.1 and 4.2. That is, for alkali cations, a monotonic decrease in extraction is observed as the nitric acid concentration is raised. For alkaline earth cations, nearly the same type of dependency is observed, especially for barium. Although a slight upturn in $D_{Sr}$ is seen at the highest acidities, and $D_{Ca}$ increases from 4 M to 8 M $HNO_3$ (a trend that has been attributed to the metal ion charge density and thus, nitrato stability constants), for all of the metal ions considered, ion exchange, not neutral complex extraction, predominates under the experimental conditions. Thus the increased water content associated with hydroxyl-functionalization of the IL is apparently insufficient to outweigh the increased

tendency toward ion exchange resulting from the presence of a relatively hydrophilic IL cation.

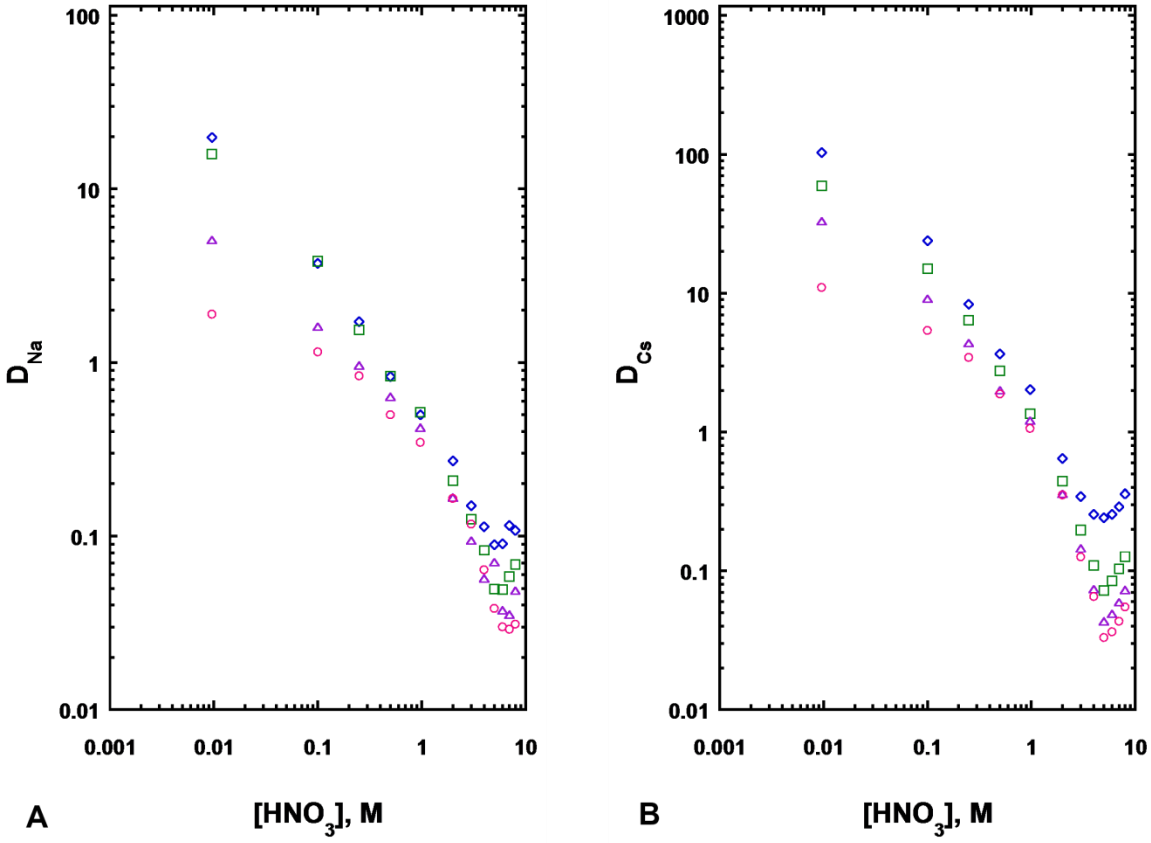


**Figure 4.1: Effect of nitric acid concentration on the extraction of $Na^+$(panel A) and $Cs^+$ (panel B) by DCH18C6 (0.10 M) in $C_5OHC_1imTf_2N$ (◇), $C_8OHC_1imTf_2N$ (□), $C_{10}OHC_1imTf_2N$ (△), and $C_{12}OHC_1imTf_2N$ (○).**

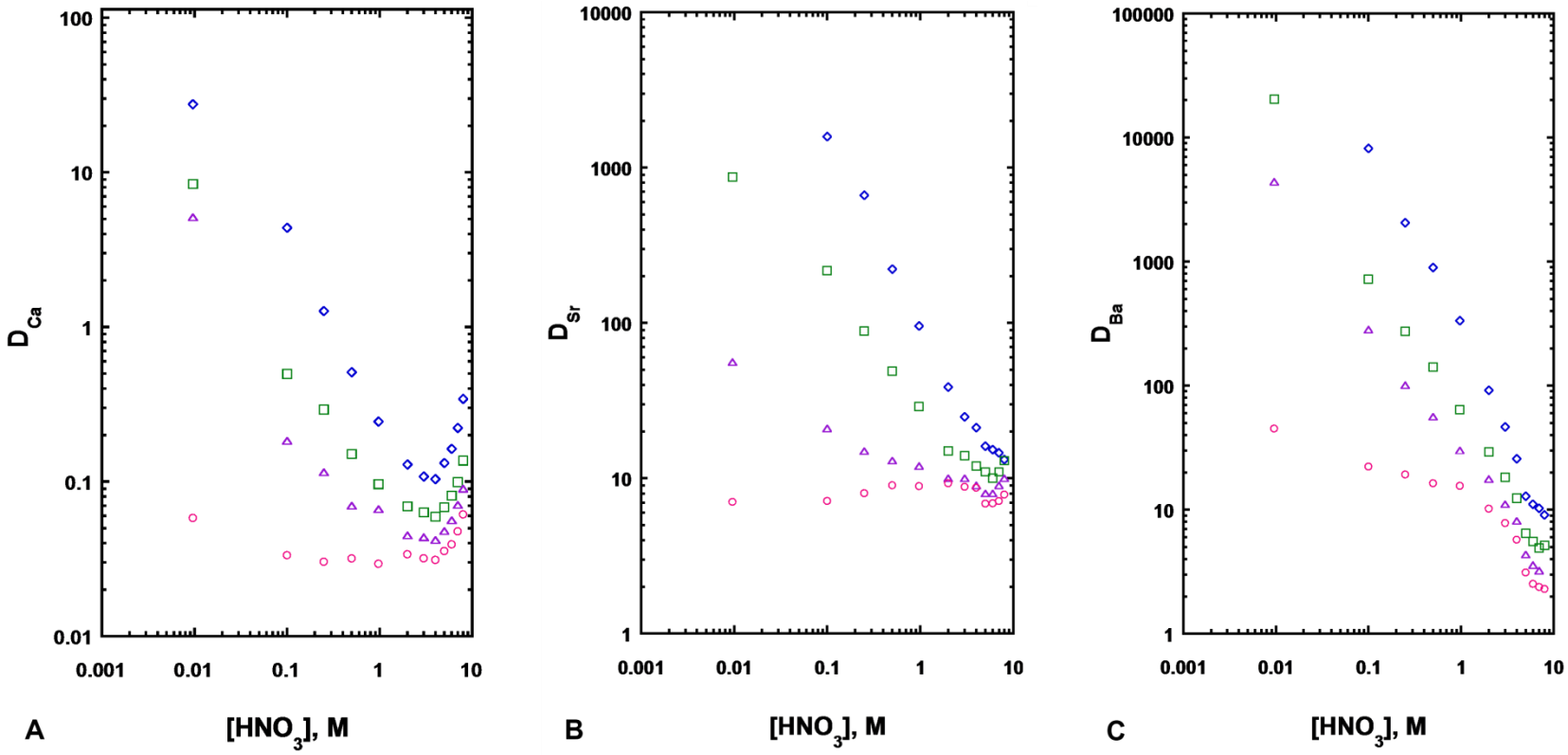


**Figure 4.2: Effect of nitric acid concentration on the extraction of $Ca^{2+}$(panel A), $Sr^{2+}$ (panel B), and $Ba^{2+}$ (panel C) by DCH18C6 (0.10 M) in $C_5OHC_1imTf_2N$ (◇), $C_8OHC_1imTf_2N$ (□), $C_{10}OHC_1imTf_2N$ (△), and $C_{12}OHC_1imTf_2N$ (○).**

**Table 4.2**
**Various Physicochemical Properties of Some Ionic Liquids Studied**

| IL | Density (dry), g/mL | Density (wet), g/mL | Water Content (wet), ppm | Water Solubility, ppm | $T_g$ / $T_m$, °C | $T_d$, °C |
|---|---|---|---|---|---|---|
| $C_5OHC_1imTf_2N$ | 1.51 ± 0.02 | 1.41 ± 0.01 | 66700 ± 144 | 33900 ± 400 | -72 | 383 |
| $C_8OHC_1imTf_2N$ | 1.27 ± 0.08 | 1.28 ± 0.02 | 48000 ± 39 | 12400 ± 160 | -72 | 385 |
| $C_{10}OHC_1imTf_2N$ | 1.31 ± 0.02 | 1.24 ± 0.03 | 39800 ± 42 | 3700 ± 380 | -71 | 403 |
| $C_{12}OHC_1imTf_2N$ | 1.23 ± 0.06 | 1.18 ± 0.05 | 34200 ± 110 | 568 ± 20 | -63 / -40 | 413 |
| $C_8OHC_4imTf_2N$ | 1.28 ± 0.04 | 1.27 ± 0.02 | 34100 ± 1901 | 4700 ± 380 | -72 | ND |
| $C_{10}OHC_4imTf_2N$ | 1.23 ± 0.02 | 1.21 ± 0.01 | 25600 ± 80 | 6800 ± 150 | -71 | ND |
| $C_{12}OHC_4imTf_2N$ | 1.23 ± 0.03 | 1.18 ± 0.02 | 23800 ± 727 | 2600 ± 140 | ND | ND |
| $C_5mimTf_2N$ | 1.35 ± 0.04 | 1.36 ± 0.01 | 17100 ± 56 | 2150 ± 76 | -85 / -9[a] | 444 |
| $C_8mimTf_2N$ | 1.28 ± 0.06 | 1.24 ± 0.03 | 11500 ± 65 | 990 ± 28 | -85[a] | 425[b] |
| $C_{10}mimTf_2N$ | 1.29 ± 0.02 | 1.22 ± 0.04 | 10400 ± 45 | 310 ± 33 | -83 / -29[a] | 395 |

Uncertainties are based on the 95% confidence interval, where n = 5 measurements of density and n = 4 measurements of water mutual solubility
ND = not determined
[a] Reference [4.24]
[b] Reference [4.25]

### 4.3.2 Relationship between ionic liquid-water mutual solubilities and metal ion extraction into $C_nC_4imTf_2N$ and $C_nOHC_4imTf_2N$ ionic liquids

Although the overall trends indicate that ion-exchange pathways will dominate the extraction of $Sr^{2+}$ into $C_nOHC_1imTf_2N$ ILs, the relatively flat acid dependency of $D_{Sr}$ in $C_{12}OHC_1imTf_2N$ suggests that an improvement (*i.e.*, a greater propensity toward neutral complex extraction) might be realized by a combination of hydroxyl-functionalization of one of the alkyl groups of the dialkylimidazolium cation (to boost the water content of the ionic liquid) and a lengthening of the other (to reduce the IL cation hydrophilicity). Accordingly, the *n*-butyl analogs of $C_8OHC_1imTf_2N$ and $C_{10}OHC_1imTf_2N$ (designated as $C_8OHC_4imTf_2N$ and $C_{10}OHC_4imTf_2N$, respectively) were prepared and evaluated as extraction solvents. Figure 4.3 shows the acid dependency of the extraction of strontium ion by DCH18C6 into $C_8OHC_4imTf_2N$, along with (for purposes of comparison) the corresponding results for $C_8OHC_1imTf_2N$, $C_8C_1imTf_2N$, and 1-octanol. As might be anticipated for the slightly more hydrophobic IL (for which a lesser tendency toward ion exchange would be expected), the decline in $D_{Sr}$ with acidity is less pronounced for $C_8OHC_4imTf_2N$ than for $C_8OHC_1imTf_2N$. Unfortunately, however, the fact that $D_{Sr}$ still declines with increasing nitric acid concentration is a clear indication that the contribution of neutral complex partitioning (Eqn. 4-1) to the overall extraction remains insignificant.

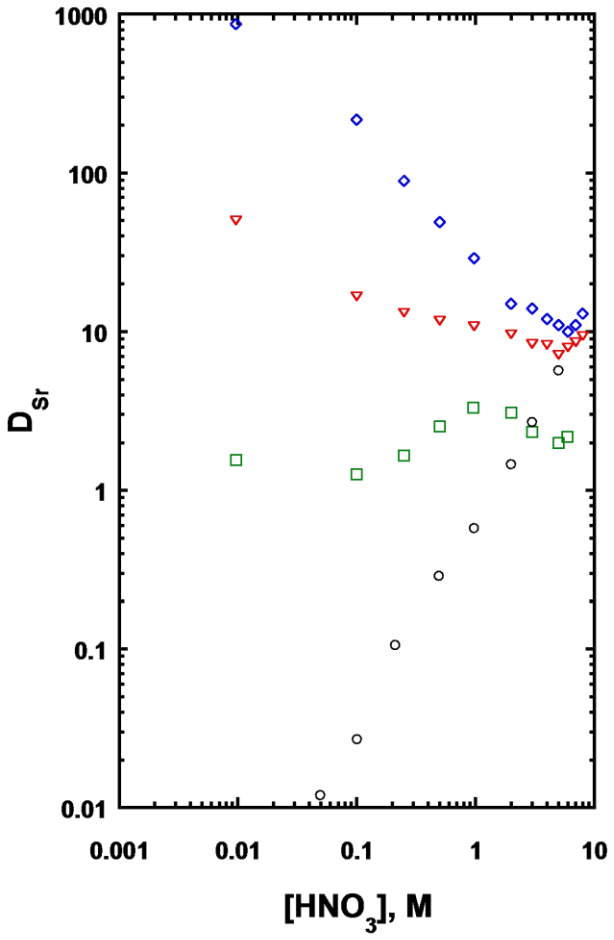


**Figure 4.3: Effect of nitric acid concentration on the extraction of $Sr^{2+}$ by DCH18C6 (0.10 M) in $C_8OHC_1imTf_2N$ (◇), $C_8OHC_4imTf_2N$ (▽), $C_8C_1imTf_2N$ (□), and 1-octanol (○).**

Figure 4.4 shows the acid dependency of $D_{Sr}$ for extraction by DCH18C6 into $C_{12}OHC_4imTf_2N$. Also shown (to facilitate comparison) are the corresponding results for $C_{10}OHC_1imTf_2N$, $C_{10}OHC_4imTf_2N$, $C_{10}C_1imTf_2N$, and 1-decanol. As is immediately apparent, the slightly greater alkyl chain length of $C_{10}OHC_4imTf_2N$ *vs*. $C_{10}OHC_1imTf_2N$ results in a change from an acid dependency in which $D_{Sr}$ falls with rising acidity to one in which $D_{Sr}$ generally increases as the nitric acid concentration is raised. The addition of two more methylene groups to the long alkyl chain, producing the more hydrophobic $C_{12}OHC_4imTf_2N$, further reduces $D_{Sr}$ at low acidities. In this respect then, the behavior of

$C_{12}OHC_4imTf_2N$ mimics that of $C_{10}C_1imTf_2N$, an IL previously shown to be sufficiently hydrophobic as to favor neutral complex extraction [4.6]. Interestingly, however, the values of $D_{Sr}$ under a given set of conditions are up to a factor of two higher for $C_{12}OHC_4imTf_2N$ than for $C_{10}C_1imTf_2N$. The much greater water content of the OH-functionalized IL (25,600 ppm *vs*. 10,400 ppm) and the accompanying greater ease of transfer of the co-extracted nitrate anion likely accounts for the improvement in $Sr^{2+}$ extraction. As shown in Table 4.3, this increased extraction efficiency is not accompanied by a significant decrease in the extraction selectivity for strontium over sodium ion, an important issue in any potential practical application of these extraction systems [4.14, 4.15]. Curiously, the water solubility of $C_{10}OHC_4imTf_2N$ (6830 ppm) is higher than that of both $C_{10}C_1imTf_2N$ (300 ppm) and $C_{10}OHC_1imTf_2N$ (3700 ppm), and on this basis, a greater propensity toward ion exchange would be anticipated. That this is not observed suggests that the water solubility of the ionic liquid, considered alone, is not adequate as a predictor of the predominant mode of metal ion partitioning to be expected in these extraction systems.

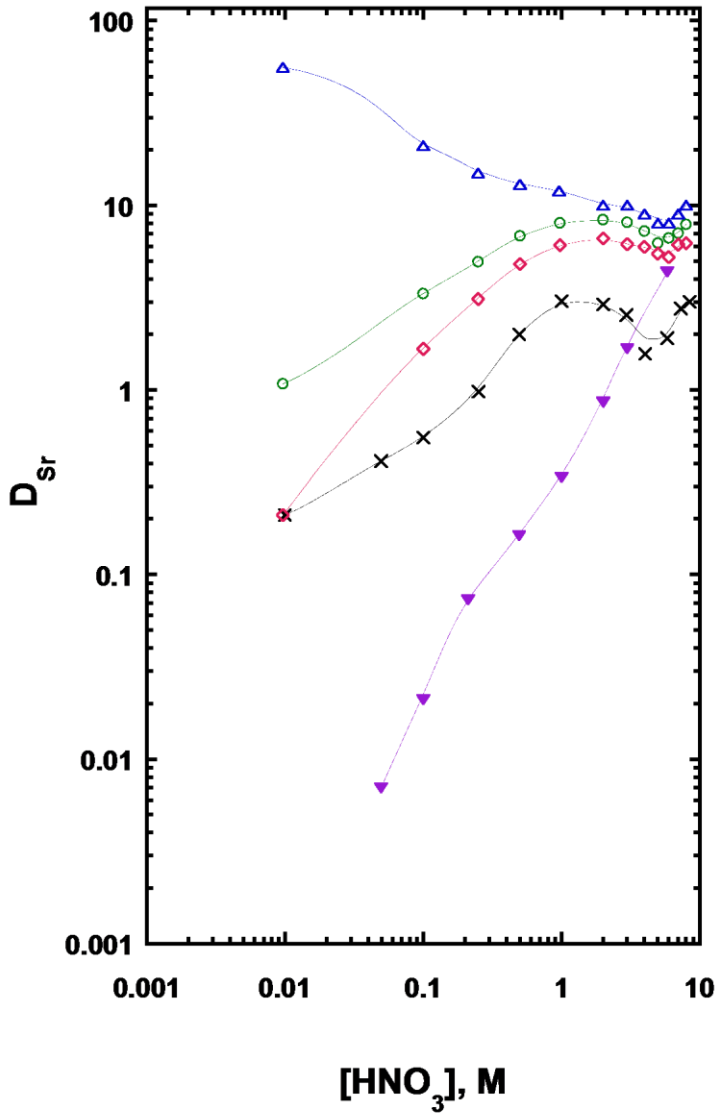


**Figure 4.4: Effect of nitric acid concentration on the extraction of $Sr^{2+}$ by DCH18C6 (0.10 M) in $C_{10}OHC_1imTf_2N$ (△), $C_{10}OHC_4imTf_2N$ (○), $C_{12}OHC_4imTf_2N$ (◇), $C_{10}C_1imTf_2N$ (×), and 1-decanol (▼).**

**Table 4.3**
**Extraction Selectivity for Strontium over Sodium in 1-Octanol, $C_{10}C_1imTf_2N$, and $C_{12}OHC_4imTf_2N$**

| $[HNO_3]$, M | $D_{Sr}/D_{Na}$ in 1-octanol | $D_{Sr}/D_{Na}$ in $C_{10}C_1imTf_2N$ | $D_{Sr}/D_{Na}$ in $C_{12}OHC_4imTf_2N$ |
|---|---|---|---|
| 0.01 | ND | 0.3 | 0.5 |
| 0.1 | 0.9 | 1.3 | 2.3 |
| 0.25 | 1.7 | 1.9 | 4.8 |
| 0.5 | 5.8 | 13 | 10 |
| 1 | 7.4 | 26 | 19 |
| 2 | 8.2 | 43 | 32 |
| 3 | 14 | 68 | 53 |
| 4 | 28 | 60 | 80 |
| 5 | 75 | 50 | 130 |
| 6 | 190 | 30 | 180 |

ND = not determined

### 4.3.3 Direct correlation of strontium nitrate extraction with ionic liquid phase water content

The importance of organic phase water content in determining the extent of strontium nitrate extraction into oxygenated, aliphatic solvents (*e.g.*, *n*-alcohols) was established by Horwitz *et al*. in 1990 [4.2]. In this work, a correlation was observed between the conditional extraction constant for the neutral strontium nitrato-crown ether complex and the water content of the organic phase. This observation served as the basis for understanding the higher extraction efficiencies observed for these diluents than for other classes of conventional solvents (*e.g.*, alkanes). In particular, high solvent water contents were shown to support the extraction of the strontium nitrate because the energies involved in the formation and extraction of its complex with DCH18C6 are not sufficient to dehydrate the co-extracted nitrate anion. High organic phase water contents, by eliminating the need for anion dehydration, thus favor extraction of the strontium-nitrato-crown ether complex. While for molecular diluents, the correlation between $K'_{ex}$ and $[H_2O]_{org}$ is expected to persist over a wide range of acidities and within the range of DCH18C6 concentrations where the extractant dependencies are linear, for ILs, the situation is less clear. Prior studies of the extraction of strontium into ILs have, in fact, yielded contradictory results [4.12, 4.26] concerning the role played by IL phase water content in determining the efficiency with which Sr is extracted by a crown ether [4.12, 4.26, 4.27]. In certain instances, no correlation with water content was observed, while in others, a relationship opposite that seen in conventional solvents was seen [4.27]. In these studies, however, the lack of understanding of the underlying processes involved in the extraction meant that the observed extraction represented a composite of the contributions of three partitioning pathways. In each of these studies, in fact,

investigations were carried out under conditions in which ion-exchange processes contribute significantly to the observed partitioning. Systematic exploration of the role of water content in metal ion extraction into ILs, however, requires the conditions be carefully chosen so as to favor extraction of a metal-nitrato-crown ether complex (product of Eqn. 4-1), in analogy to the process observed in conventional molecular solvents. If conditions are chosen that promote a significant and varying contribution to the extraction from ion exchange processes (Eqn. 4-2 and Eqn. 4-3), it is unreasonable to anticipate a correlation between the observed extraction efficiency and the IL water content. One must also exercise caution in attributing a particular mechanism to a correlation with solvent water content. For instance, in Figure 4.5, although a strong correlation is found between the extraction of strontium from water into a series of 1-alkyl-3-methylimidazolium ILs and the solubility of water in those ILs, it is merely a correlation, not an indicator that water is playing a direct role in the extraction of the complex. Rather, the extraction efficiency, in these instances, is directly related to the hydrophobicity of the IL cation, which similarly dictates the solubility of water in the IL.

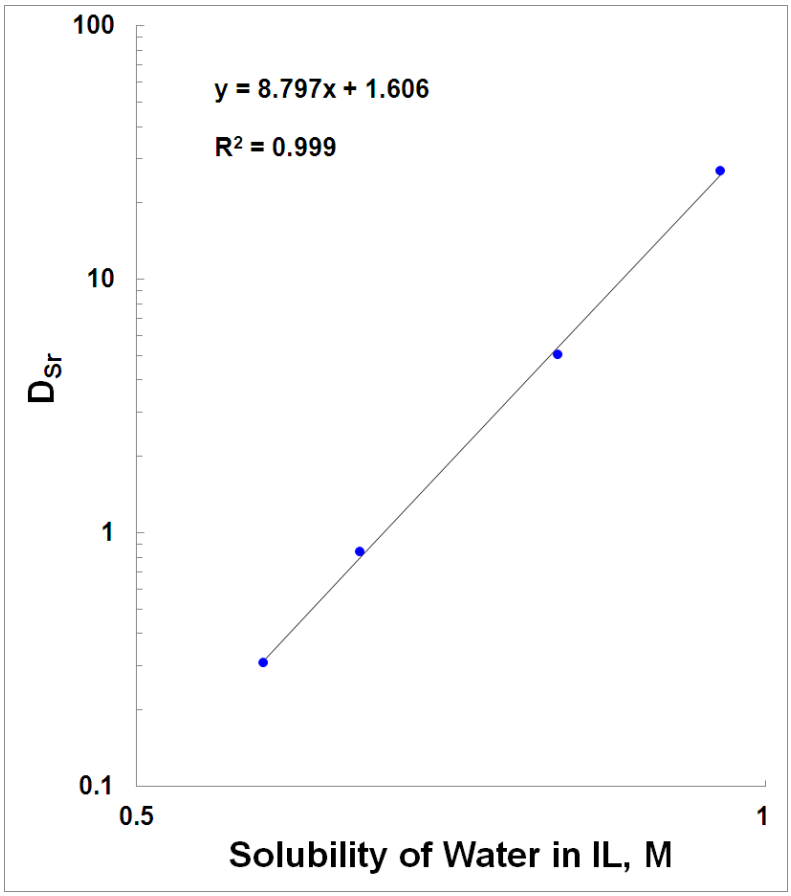


**Figure 4.5: Extraction of Strontium from Water into 1-Alkyl-3-methylimidazolium ILs Containing 0.20 M DCH18C6.** Extraction efficiency data obtained from Table 3.3

With this in mind, strontium extractions into a series of increasingly hydrophobic ILs was evaluated, starting with an IL known to behave much like a traditional solvent (*i.e.*, $C_{10}C_1imTf_2N$), where the extracted species is an ion-paired (*i.e.*, neutral) complex. The IL cation structures chosen comprise a homologous series, in which the short alkyl chain is augmented while the long alkyl chain is held constant. For the systems tested, in which the nitric acid and DCH18C6 concentrations were held constant, the relationship between the conditional extraction constant (Eqn. 4-4 [4.2]) and the aqueous nitrate ion activity ($\alpha_{\pm}$), crown ether concentration, and the measured $D_{Sr}$ values are given by:

$$K'_{ex,Sr} = D_{Sr} [DCH18C6]^{-1} \alpha_{\pm}^{-2} \qquad (4\text{-}4)$$

Several issues regarding this calculation must be noted. First, no measureable extraction of $^{85}Sr$ was found in the absence of DCH18C6. Next, the DCH18C6 concentration chosen must lie in the region of first-order extractant dependency. In addition, the nitric acid concentration chosen must be such that not only is $D_{Sr}$ readily measureable, but also the activity of the nitrate ion in that solution is known (here, 0.75 for a 1.0 M $HNO_3$ solution [4.28]). Lastly, to facilitate measurements, the crown ether concentration was the highest possible in the range for which the extractant dependence of $D_{Sr}$ is linear.

As can be seen from in Figure 4.6, at any given DCH18C6 concentration, $D_{Sr}$ declines as the hydrophobicity of the ILs increases. For all of the ILs, a significant deviation from linearity is evident above 0.1 M DCH18C6. Therefore, a concentration of 0.05 M DCH18C6 was chosen for the experiments to determine if a correlation exists between strontium extraction and the water content of the acid-equilibrated IL phases. As it happens, these are the same conditions employed by Horwitz *et al*. in their studies of conventional solvents.

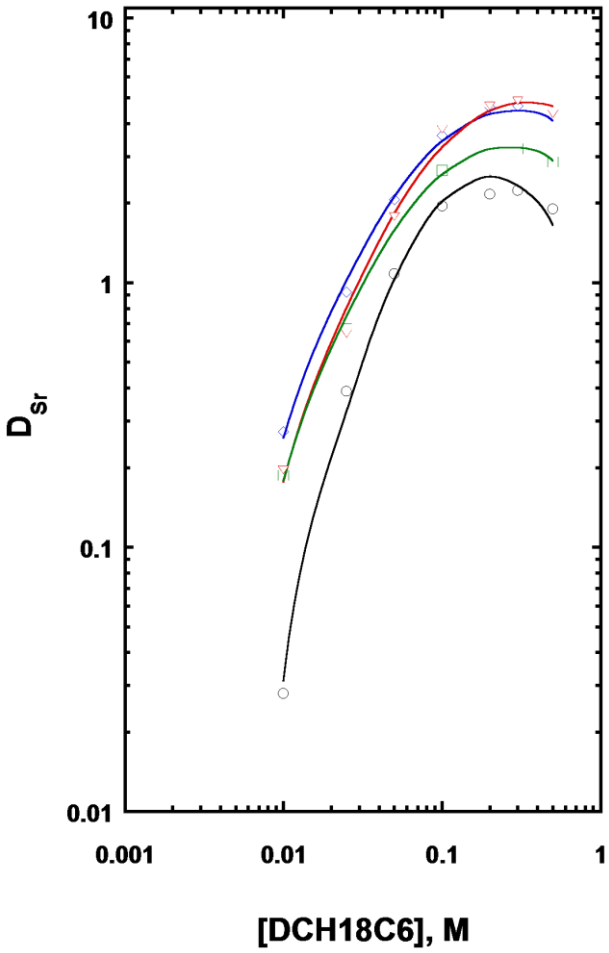


**Figure 4.6: Effect of DCH18C6 concentration in $C_{10}C_1imTf_2N$ (◇), $C_{10}C_2imTf_2N$ (▽), $C_{10}C_4imTf_2N$ (□), and $C_{10}C_6imTf_2N$ (○) on the extraction of $Sr^{2+}$ at 1.0 M nitric acid.** The solid lines are intended only as guides to the eye.

The results of the linear least-squares regression of the conditional strontium extractant constant with the water content of the equilibrated ILs are presented in Figure 4.7 and Table 4.4. Considering the complexities involved in these system, with ion-pair/neutral complex extraction (Eqn. 4-1) and a contribution from crown ether-mediated ion exchange (Eqn. 4-3, section 3.3.5), the merits of this regression ($R^2 = 0.95$) and the fact that the overall uncertainties based on counting statistics and replicates (7% to 13% RSD) are comparable to those expected for these types of measurements, support the

hypothesis that water content plays a important role in the extraction, provided that care is taken to select conditions strongly disfavoring ion-exchange processes.

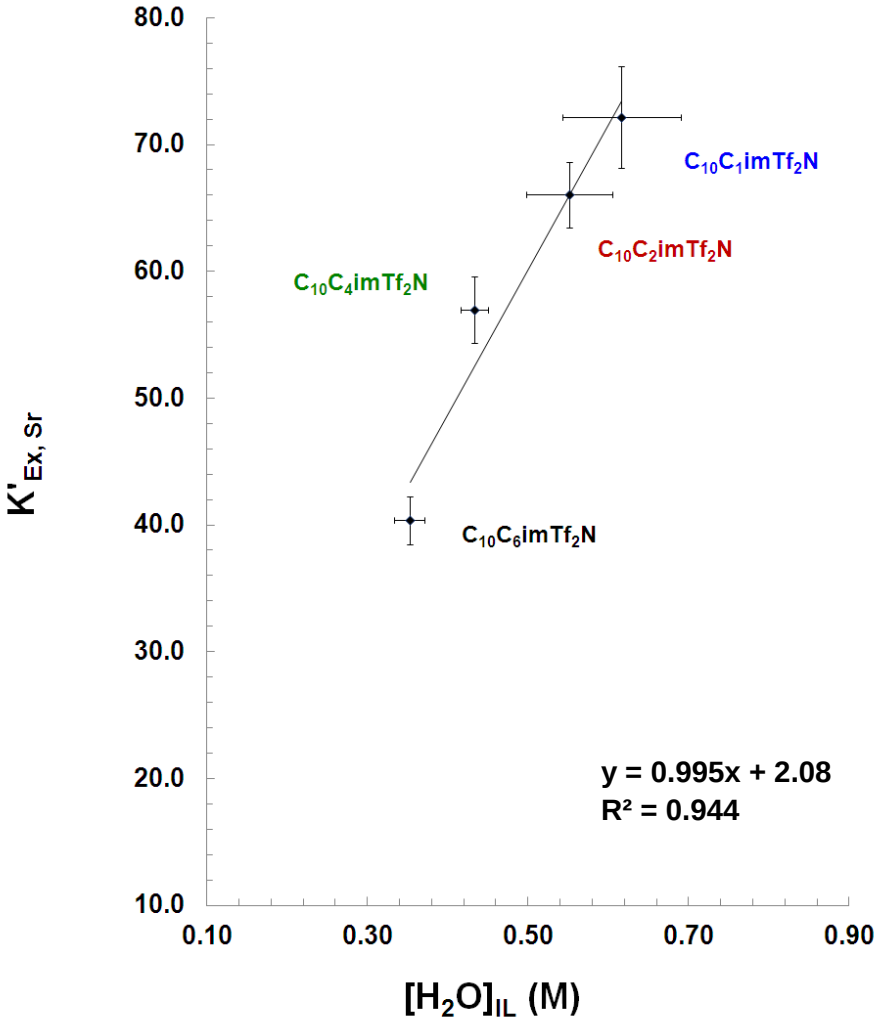


**Figure 4.7: Correlation of the conditional extraction constant with the water content of the IL phase for strontium extraction into a series of $C_{10}C_n$imTf$_2$N ILs at 1.0 M $HNO_3$ and 0.050 M DCH18C6.** Error bars are based on the standard deviations (n=4) and counting error (for $K'_{ex}$) at the at the 95% confidence interval. Regression is of the bilogarithmic relationship.

**Table 4.4**
**Experimental and calculated values of the linear least-squares regression of the conditional extractant constant with the water content of the IL phase for strontium extraction in Figure 4.6**

| IL | $[H_2O]$, M [a] | $K'_{ex,Sr}$ [a] | $K'_{ex,Sr}$ Calc. [b] | %Deviation |
|---|---|---|---|---|
| $C_{10}C_1imTf_2N$ | 0.62 | 72 | 73 | -1.8% |
| $C_{10}C_2imTf_2N$ | 0.55 | 66 | 66 | -0.1% |
| $C_{10}C_4imTf_2N$ | 0.43 | 57 | 51 | 8.3% |
| $C_{10}C_6imTf_2N$ | 0.35 | 40 | 43 | -7.0% |

[a] Experimental results were for 4 replicates of water content and 4 replicates with 3 replicate determinations of Sr-85 distribution ratios
[b] Calculated values are those predicted and %deviations are calculated from the residuals

In considering these results, it is important to note that data from the $C_{10}C_8imTf_2N$ system were excluded as outliers because of higher-than-expected water content (0.39 ± 0.01 M $H_2O$, higher than that for $C_{10}C_6imTf_2N$), while the $K'_{ex,Sr}$ (29) continued to diminish as expected. A clue as to the source of these aberrant results is found in observations made during sample preparation. That is, upon disengagement of the IL from the equilibrated acid, the IL phase became cloudy. When these samples were centrifuged or warmed by hand the cloudiness vanished. In addition, upon standing, the IL phase became cloudy. Both observations strongly indicate that the formation of a microemulsion is responsible for the higher water content observed for this ILs. This same conclusion may apply, albeit to a lesser extent, to $C_{10}C_6imTf_2N$, for which a slightly higher than anticipated water content was observed. Although surface tension data are required to confirm this, it appears that, as the shorter alkyl chain of the imidazolium ion exceeds half the length of the longer chain the surface activity of the IL may increase to

the point that formation of surfactant aggregates contribute to the overall water content. The extraction of the strontium complex, however, is apparently not enhanced proportionately. If this is the case, then the role that water plays in the solubilization of the complex is dependent on how water itself is solubilized. Lower extraction with increased IL hydrophilicity indicates that the IL may have formed either reversed-micelles in which the complex is not soluble, or normal micelles too small to accommodate the strontium-nitrato-crown ether complex. These results may corroborate the hypothesis of Horwitz *et al*. that, "the water dissolved in the system is, in all probability, hydrogen-bonded to the solvent molecules" [4.2], and suggest that the formation of micelles or entrainment of microdroplets of acid or water in the organic phase may not significantly contribute to the solubilization of the complex.

Although the water contents of these ILs were approximately an order of magnitude lower than those of *n*-alcohols, improvements upon extraction by way of higher IL water content were expected with the hydroxy-functionalized ILs. Care was taken to avoid ILs that display a significant amount of ion exchange behavior under the same conditions as the $C_{10}C_n$im$Tf_2$N series. Figure 4.8 is a combined plot of the effect of water content in the equilibrated IL phase on the calculated conditional extraction constant for both the $C_{10}C_n$im$Tf_2$N (n = 1, 2, 4, 6) series and the $C_{12}OHC_n$im$Tf_2$N (n = 1, 2, 4, 8) series. A striking feature of these plots is the obvious continuity between the separate series of ILs. Taking into consideration the uncertainties involved in the measurements of the distribution ratios, water contents, and the densities of the contacted IL phases, the correlation is remarkable. In fact, the combined linear bilogarithmic regression yields a

straight line with slope of nearly 1, suggesting that the co-extraction of nitrate in the ion-paired complex requires the same number of water molecules.

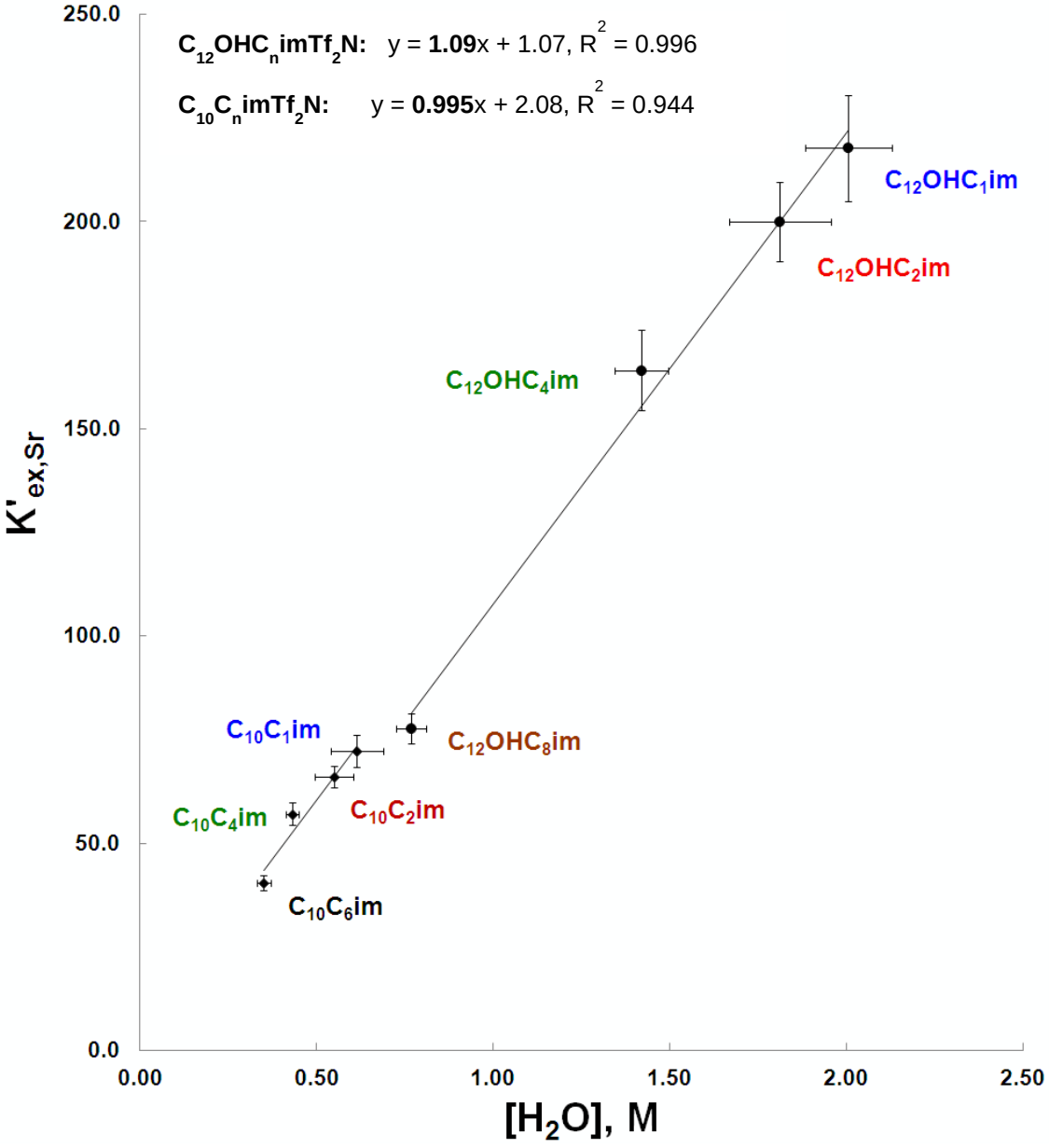


**Figure 4.8: Correlation of the conditional extraction constant with the water content of the IL phase for strontium extraction into the homologous series of $C_{10}C_nimTf_2N$ and $C_{12}OHC_nimTf_2N$ ILs at 1.0 M $HNO_3$ and 0.050 M DCH18C6.** Error bars are based on the standard deviations (n=4) and counting error (for $K'_{ex}$) at the 95% confidence interval. Regression is of the bilogarithmic relationship for the combined data points.

### 4.4 Conclusions

The results presented here represent an important step toward clarifying the factors responsible for determining the "balance of pathways" among the various possible modes of alkali and alkaline earth cation extraction by crown ethers into RTILs. As had been anticipated, hydroxyl-functionalization does increase the water content of an *N,N'*-dialkylimidazolium *bis*[(trifluoromethyl)sulfonyl]imide IL. At the same time, however, it increases the water solubility of the IL cation. The net effect of these changes can be a greater tendency toward either ion exchange (as is observed for $C_{10}OHC_1imTf_2N$) or towards neutral complex extraction (as is observed for $C_{12}OHC_4imTf_2N$) as a mode of metal ion partitioning. It appears then that neither IL water content nor IL cation solubility in water *by itself* is sufficient to permit the prediction of the favored mode of metal ion extraction. Additional studies to better define the complicated interplay among various IL characteristics, the nature of the metal ion, and the aqueous phase conditions are clearly needed to realize such predictive capabilities. In following the work of Horwitz *et al*. to determine the relationship between the conditional strontium extraction constant and the equilibrium water content of a variety of oxygenated aliphatic diluents, homologous series of hydrophobic 1,3-dialkylimidazolium (*e.g.*, $C_{10}C_nimTf_2N$) and 1-(ω-hydroxyalkyl-3-alkylimidazolium ILs (*e.g.*, $C_{12}OHC_nimTf_2N$) ILs were evaluated. Both families exhibited a meaningful correlation, suggesting that under certain conditions (*i.e.*, those that suppress ion exchange as a mode of partitioning), IL phase water does play a central role in the partitioning of the complex(es). If the log-log relationship with water actually correlates with the metal complex coordination environment, then the number of water molecules associated with the extracted complex in these systems is one. This is

the first time that a set of ionic liquid solvents has been evaluated in this manner. Furthermore, the water content has been shown to be a directly related to the structure (*i.e.*, hydrophobicity) of the ILs, a topic that will be examined in more detail in Chapter 5.

## 4.5 Acknowledgements

This work was supported by the Single Investigator Small Group Research (SISGR) Program of the Office of Basic Energy Sciences of the United States Department of Energy under sub-contract from Brookhaven National Laboratory.

## 4.6 References

[4.1] J. Rydberg, *Solvent Extraction Principles and Practice, Revised and Expanded*, CRC Press, New York, **2004**.

[4.2] E.P. Horwitz, M.L. Dietz, D.E. Fisher, *Solv.Ext. Ion Exch*. **1990**, 8, 199-208.

[4.3] M.L. Dietz, E.P. Horwitz, S. Rhoads, R.A. Bartsch, J. Krzykawski, *Solv.Extr. Ion Exch*. **1996**, 14,1-12.

[4.4] M.L. Dietz, J.A. Dzielawa, *Chem. Commun*., **2001**, 2124-2125.

[4.5] M.P. Jensen, J.A. Dzielawa, P. Rickert, M.L. Dietz, *J. Am. Chem. Soc*., **2002**, 124, 10664-10665.

[4.6] M.L. Dietz, J.A. Dzielawa, I. Laszak, B.A. Young, M.P. Jensen, *Green Chem*. **2003**, 5, 682-685.

[4.7] D.C. Stepinski, M.L. Dietz, *Green Chem*. **2005**, 7, 747-750.

[4.8] D.C. Stepinski, M.P. Jensen, J.A. Dzielawa, M.L. Dietz, *Green Chem*., **2005**, 7, 151-158.

[4.9] M.L. Dietz, S.L. Garvey, C.A. Hawkins, *Proceedings of the 19$^{th}$ International Solvent extraction Conference (ISEC)*, Santiago, Chile, **2011**, Chapter X, 208-213.

[4.10] H. Luo, S. Dai, P. V. Bonnesen, T. J. Haverlock, B. A. Moyer, A. C. Buchanan III *Solv. Extr. Ion Exch*. **2006**, 24, 19-31.

[4.11] C.A. Hawkins, S.L. Garvey, M.L. Dietz, *Sep. Purif. Technol*., **2012**, 89, 31-38.

[4.12] S. Dai, Y.H. Ju, C.E. Barnes, *J. Chem. Soc., Dalton Trans.* **1999**, 1201-1202.

[4.13] S.V. Dzyuba, R.A. Bartch, *Tet. Lett.*, **2002**, 43, 4657-4659.

[4.14] J.D. Holbrey, M.B. Turner, W.M. Reichert, R.D. Rogers, *Green Chem*., **2003**, 5, 731-736.

[4.15] K. Shimojo, K. Nakashima, N. Kamiya, M. Goto, *Biomacromolecules*, **2006**, 7, 2-5.

[4.16] C.A. Hawkins, A. Rud, S.L. Garvey, M.L. Dietz, *Sep. Sci. and Technol.* 10.1080/01496395.2012.697527, 27 June 2012.

[4.17] M. Detleefs, K.R. Seddon, Green Chem., **2003**, 5, 181-186.

[4.18] M.J. Earle, C.L. Gordon, N.V. Plechkova, K.R. Seddon, T.Welton, *Anal. Chem*. **2007,** 79, 758-764

[4.19] F. Tang, K. Wu, L. Ding, J.Yuan, Q. Liu, L. Nie, S. Yao, *Sep. Purif. Technol*. **2008**, 60, 45-50.

[4.20] Y.S. Ding, M. Zha, J. Zhang, S.S. Wang, Chin. Chem. Let. **2007**, 18, 48-50

[4.21] M.L. Dietz, A.H. Bond, M. Clapper, J.W. Finch, *Radiochim. Acta*, **1999**, 85, 119-129.

[4.22] E.P. Horwitz, M.L. Dietz, D.E. Fisher, *Solvent Extr. Ion Exch*. **1991**, 9, 1-25.

[4.23] E.P. Horwitz, M.L. Dietz, D.E. Fisher, *Anal. Chem*. **1991**, 63, 522-525.

[4.24] S.V. Dzyuba, R.A. Bartsch, *ChemPhysChem*, **2002**, 3, 161–166.

[4.25] H. Tokuda, K. Hayamizo, K. Ishii, Md. A.B.H. Susan, M. Watanabe, *J. Phys. Chem. B*, **2005**, 109, 6103-6110.

[4.26] A.E. Visser, R.P. Swatloski, W.M. Reichert, S.T. Griffin, R.D. Rogers, *Ind. Eng. Chem. Res.* **2000**, 39, 3596–3604.

[4.27] M.L. Dietz, J.A. Dzielawa, M.P. Jensen, M.A. Firestone, ACS Symposium Series (Ionic Liquids as Green Solvents), **2003**, 856, 526-543

[4.28] W. Davis Jr., H.J. De Bruin *et al., J. Inorg. Nucl. Chem.*, **1964**, 25, 1065-1083.

# CHAPTER 5:
# DEVELOPMENT AND EVALUATION OF A HIGH PERFORMANCE LIQUID CHROMATOGRAPHIC METHOD FOR IONIC LIQUID DETERMINATION

## 5.1 Introduction

The determination of IL concentrations in aqueous solution has generally been carried out spectrophotometrically, exploiting the presence of a chromophore in the cation, or less frequently, in the anion. Imidazolium ions, for example, strongly absorb UV radiation, undergoing $\pi \rightarrow \pi^*$ transitions with a maximum absorbance at approximately 210 nm, thus providing a facile means for their quantification. Yet UV spectrophotometry can be fraught with interferences at such low wavelengths, particularly from organic solvents, which can lead to poor sensitivity. Additionally, because our objective was to measure the octanol-water partition coefficients of selected ILs, for UV spectrophotometry, it would be necessary to use references of octanol-saturated water and water-saturated octanol, as well as standard calibrators in these solvents, to measure the extinction coefficients for each compound in each phase. This can be laborious and generate significant amounts of waste octanol. To address these issues, a new method for IL determination using HPLC-UV has been developed and evaluated.

A number of previous studies have examined the separation of ILs by various liquid chromatographic methods. These methods can be classified as either normal- or reversed-phase depending on the relative polarity of the mobile and stationary phases. In normal-phase liquid chromatography, the stationary phase is more polar than the mobile phase. Retention therefore increases as the polarity of the mobile phase decreases, and polar analytes are more strongly retained than nonpolar ones [5.1]. (The opposite situation

occurs in reversed-phase liquid chromatography, which employs a hydrophobic stationary phase and water-rich mobile phase [5.1].) Normal-phase liquid chromatography has been used to separate a variety of substances, ranging from nonpolar to highly polar compounds [5.1]. Although historically less frequently used than reversed-phase systems, normal-phase methods are currently undergoing a resurgence, particularly for small polar or charged analytes.

To date, the efficient separation of ILs in a rapid and efficient manner has using reversed-phase HPLC proven difficult. To achieve a separation of polar or charged analytes in reversed-phase systems, either ion-pairing agents or high salt concentrations can be employed [5.2-5.4]. For the analysis of imidazolium-based ILs, for example Stepnowski *et al*. [5.2, 5.3] used an octylsiloxane-bonded stationary phase, and studied the effects of organic modifiers (acetonitrile or methanol) and phosphate buffer concentration on the separation of various 1,3-dialkylimidazolium and *N*-alkylpyridinium ILs by gradient elution. They noted that while acetonitrile provided the best peak shape and detection limits, some of the most polar solutes (*i.e.*, $C_2C_1$im and $C_4C_1$im) were difficult to retain and separate. In addition, ionic interactions led to less-than-desirable retention time precision, necessitating the addition of trifluoroacetic acid as an ion-pairing agent to increase the retention times. More recently, the effect of various added salts and a variety of reversed-phase stationary phases has been investigated by Ruiz-Angel and Berthod [5.4]. It was shown that retention of ILs could be increased by the addition of salts, but that several adsorption isotherms overlap, resulting in poor peak shapes. In particular, excessive peak tailing or even peak splitting was observed as a consequence of significant ionic interactions with exposed silanols and ion-exchange

with adsorbed ions from added salts. The loss in efficiency and distorted peak shapes were overcome by the use of fast or stepwise gradients.

Taking advantage of the dominance of ionic interactions observed with IL solutes, several researchers have explored ion chromatography (IC) with direct conductivity detection as an approach to the determination of IL cations and anions [5.5-5.7]. Satisfactory results have been obtained by employing low conductivity buffers (*e.g.*, phthalate) and an acetonitrile modifier in the eluent. The advantage of IC methods is that by using tandem cation/anion exchange columns, both the IL cations and anions can be determined simultaneously, often with excellent sensitivity and linearity (1-300 μM). IC systems utilizing tandem orthogonal separations and gradient elution programs are quite expensive and can be difficult to maintain, however.

Encouraging results have also been obtained using HPLC employing either polar or mixed-mode stationary phases for the separation of ILs [5.8- 5.11]. Some of the most intriguing approaches have employed a technique known as hydrophilic interaction liquid chromatography (HILIC). The term HILIC was coined by Alpert in 1990 [5.12] to differentiate the partitioning mechanism involved in the separation of relatively polar or charged analytes (*e.g.*, carbohydrates, amino acids, oligonucleotides) on a polar stationary phase (*e.g.*, silica, amino, amide, cyano, diol, sulfobetaine, zwitterionic) to which is adsorbed a stagnant layer of water under conditions of high organic solvent strength (usually 70-95% acetonitrile). Solute retention in the HILIC mode is directly proportional to the polarity of the solute and inversely proportional to the polarity of the mobile phase, resulting in a normal-phase retention order. Although the HILIC separation mechanism has yet to be satisfactorily explained, it appears to be based on the differential

distribution of the solute molecules between the organic-rich mobile phase and a water-enriched layer retained on the hydrophilic stationary phase [5.13, 5.14]. Retention in separations involving the HILIC mode therefore has a significant partitioning component, thus differing from typical normal-phase separations, which are based on the adsorption of solutes on a polar stationary phase using purely organic solvents. Of course, hydrogen bonding and dipole-dipole interactions will be present to some extent, due to the polar column packing and the presence of the water-rich layer. In all cases, this technique utilizes buffers, salts and/or acids in the eluent that tend to mask ionic interactions with surface silanols. Still, because the residual silanols cannot be completely suppressed, particularly with non-bonded silica phases, a HILIC separation can exhibit ionic interactions as another significant component [5.13]. Note that the buffers employed often comprise volatile salts (*e.g.*, ammonium acetate or trifluoroacetate), primarily because of their solubility in highly polar aprotic organic mobile phases. An added benefit of such salts is that their use often renders the method compatible with mass spectrometry [5.15], a particular advantage over reverse-phase techniques, which tend to have much lower sensitivity due to the higher mobile phase water content.

## 5.2 Experimental

### 5.2.1 Materials

All chemicals were reagent grade and used without additional purification, unless noted otherwise. All aqueous solutions were prepared using deionized water with a specific resistance of at least 18 $M\Omega \cdot cm^{-1}$. The HPLC mobile phase buffer was prepared by combining equal parts of 500 mM formic acid (puriss. Grade, Sigma-Aldrich, St. Louis, MO) and 500 mM ammonium formate (J.T. Baker, supplied by VWR Chicago,

IL), which resulted in a pH of 3.7. The HPLC mobile phase was prepared by combining 10.0 mL of this formate buffer with 40.0 mL of water and 450 mL of acetonitrile (Honeywell Burdick and Jackson, HPLC grade, supplied by VWR Chicago, IL) to produce a 10 mM buffer concentration in 90:10 acetonitrile:water for analysis. Imidazolium-based ionic liquids including the 3-methyl, 3-ethyl, and 3-butyl substituents were synthesized by the two-step process described in Chapter 4.

### 5.2.2 Instruments

The HPLC system comprised a set of Agilent 1200 series analytical binary pumps equipped with an online degasser, a fixed loop manual injection port, and a variable wavelength UV-VIS flow cell, and operated using ChemStation software. The column was a 75 mm x 3.0 mm Agilent Zorbax HILIC Plus silica column with 3.5 μm average particle size. The final conditions for HPLC analysis were an isocratic flow rate of 0.800 mL $min^{-1}$ with 10 mM ammonium formate buffer (pH 3.7) in 90:10 acetonitrile:water. The column temperature was maintained at 30°C, and an injection volume of 20 μL was employed. The detection of eluting species was carried out at 210 nm, near the absorbance maximum for the imidazolium cation.

### 5.2.3 Methods

All retention factors (k'), were calculated as per Eqn. 5-1, where $t_R$ is the retention time of the solute of interest and $t_0$ is the peak retention time for an unretained solute. Toluene is known to have no significant interactions with silica under these conditions; thus it was chosen as the unretained solute in the determination of k'.

$$k' = \frac{(t_R - t_0)}{t_0} \qquad 5\text{-}1$$

Initial experiments investigating the retention of different ILs were performed using 60 μM solutions of $C_{10}C_1$imBr and $C_{10}C_1$im$Tf_2$N in acetonitrile at a 0.400 mL/min flow rate. The mobile phase composition was modified for the determination of the effect of water content by online mixing of the 10 mM ammonium formate buffer (pH 3.7) in 90:10 acetonitrile:water mobile phase with the appropriate amount of 10 mM ammonium formate buffer (pH 3.7) in water, and by preparing a solution in a 95:5 acetonitrile:water mobile phase. The temperature range and step for the van't Hoff correlation with retention was 25-60°C in 5°C increments. Investigating the effect of buffer concentration was accomplished with individual solutions of 2, 5, 8, 9, 10, 20, 30, and 50 mM buffer in 90:10 acetonitrile:water. Before each new set of chromatographic conditions were examined, the column was equilibrated with at least 20 column volumes (*i.e.*, for at least 11 minutes) of mobile phase. A steady baseline UV signal and stable column temperature were taken as indicators that the system was, in fact, equilibrated.

## 5.3 Development of an HPLC-UV Method for IL Analysis

### 5.3.1 Method optimization

Because samples and standards must be analyzed in identical chemical environments for UV spectrophotometry, samples derived from octanol-water partition experiments must either be analyzed in octanol-saturated water or water-saturated octanol, or in a diluent that is compatible with both water and 1-octanol. For ease of sample preparation, the latter strategy was typically employed. (See, for example, the determination of IL

water solubility in Chapter 4 using a 50% aqueous methanol diluent.) This technique does not, however, exhibit the sensitivity and selectivity necessary to determine $D_{o,w}$ values that are much greater than 10 or lower than 0.1, given the micromolar concentrations expected. A more sensitive technique is necessary to achieve the detection limits sought.

In considering the array of possible chromatographic approaches, HILIC appears to offer the most promise, in that it has been found to be much less prone to severe peak tailing than are reversed-phase separations [5.9]. Unfortunately, the best retention factor (k') windows to date [5.11] are very wide ($\Delta k' \geq 30$ separating $C_2C_1imTf_2N$ and $C_8C_1imTf_2N$), too wide for the rate of throughput sought. Better results (*i.e.*, good peak shape and narrower retention factor windows; $\Delta k' \sim 5$ in the separation of 8 neutral ionizable solutes) were obtained, however, using underivatized silica columns and ammonium formate buffer [5.10]. Method development therefore began with conditions similar to these (*i.e.*, a mobile phase consisting of 10 mM ammonium formate buffer at pH 3.7 in 90:10 acetonitrile:water and an Agilent Zorbax HILIC Plus silica column that had been previously shown to be a very robust stationary phase, capable of tolerating high ionic strength and strong acids.)

Figure 5.1 shows the chromatogram obtained upon injection of $C_{10}C_1imBr$ and its $Tf_2N$ analog. In considering these results, it is important to note that in order to maintain electroneutrality during the separation, the imidazolium ion must be paired with an anion and the ions cannot migrate independently. As can be seen, although the bromide and $Tf_2N$ salt have vastly different properties (*e.g.*, water miscibility), they exhibit the same retention factor This suggests that formate, the most common anion in the system, is the anion with which the $C_{10}C_1im^+$ ion is paired during migration under these conditions.

Reports of such IL anion-independent retention behavior have appeared previously [5.3, 5.4, 5.9]. The very symmetrical peak (asymmetry factor of less than 1.2, as calculated by the ratio of the widths of the trailing edge to the leading edge of the peak at 10% peak height) is a benefit when separating members of a homologous series, and minimal baseline noise suggests that detection limits should be in the low μM range. As a fortunate consequence of having chosen appropriate conditions to start method development, with the direction provided by prior efforts [5.9-5.11], only a change in flow rate from to 0.800 mL $min^{-1}$ was necessary to obtain the elution profile for the nine 1,3-dialkylimidazolium-based ILs shown in Fig. 5.2. As can be seen, excellent results were obtained. With the exception of $C_8C_1$im and $C_7C_1$im, there is baseline resolution among the homologous ILs. In addition, the retention window for these compounds is suitably narrow, with retention factors falling between 3 and 11. Lastly, the diluent impurity is well resolved from the analytes of interest.

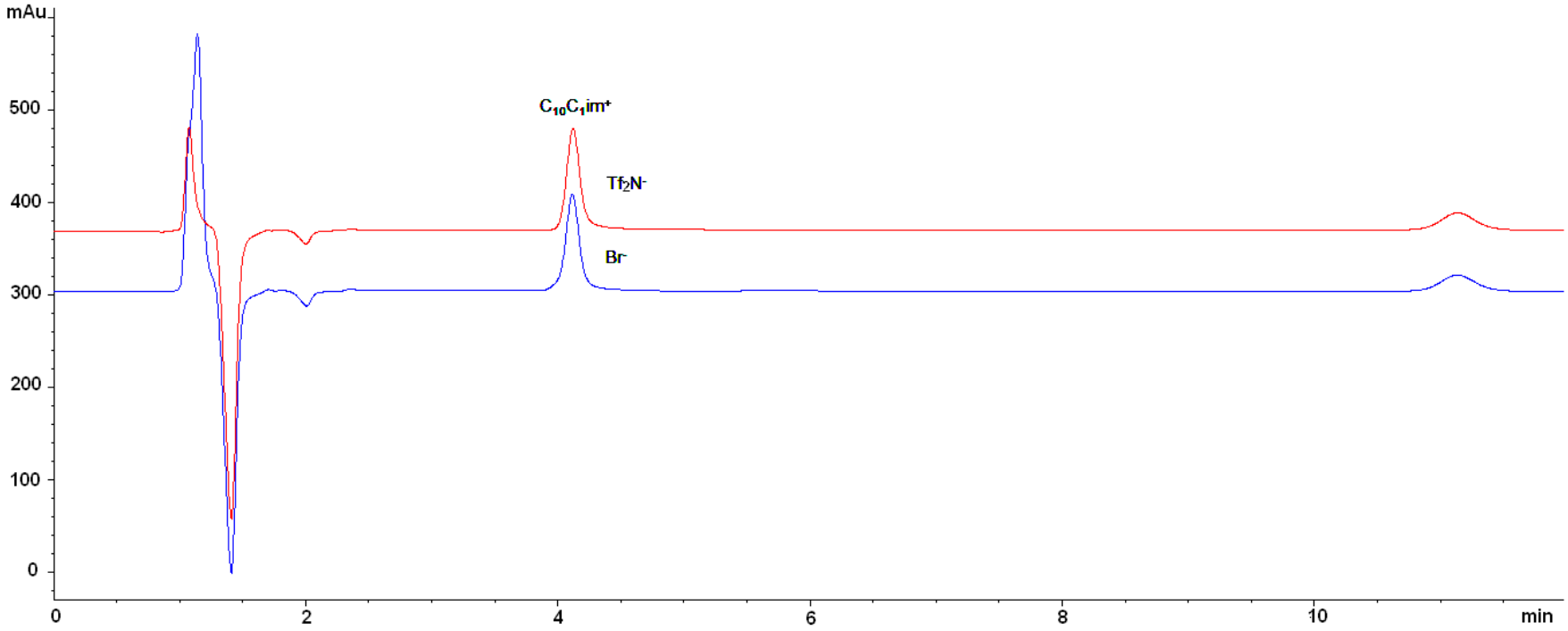


**Figure 5.1: Overlay of Chromatograms from Injections of 60 µM $C_{10}C_1imTf_2N$ (top trace in red) and $C_{10}C_1imBr$ (lower trace in blue) in ACN;** 20 µL injection volume, mobile phase: 10 mM ammonium formate buffer pH 3.7 in 90:10 ACN:water, flow rate: 0.400 mL $min^{-1}$, Zorbax HILIC Plus 3.0 mm I.D. x 75 mm 3.5 µm $d_p$, column temp. 30°C, UV detection 210 nm. Analysis of an acetonitrile blank indicates that the peak at *ca.* 11.5 minutes is a polar, UV-active contaminant common to all lots the HPLC grade acetonitrile (ACN) used.

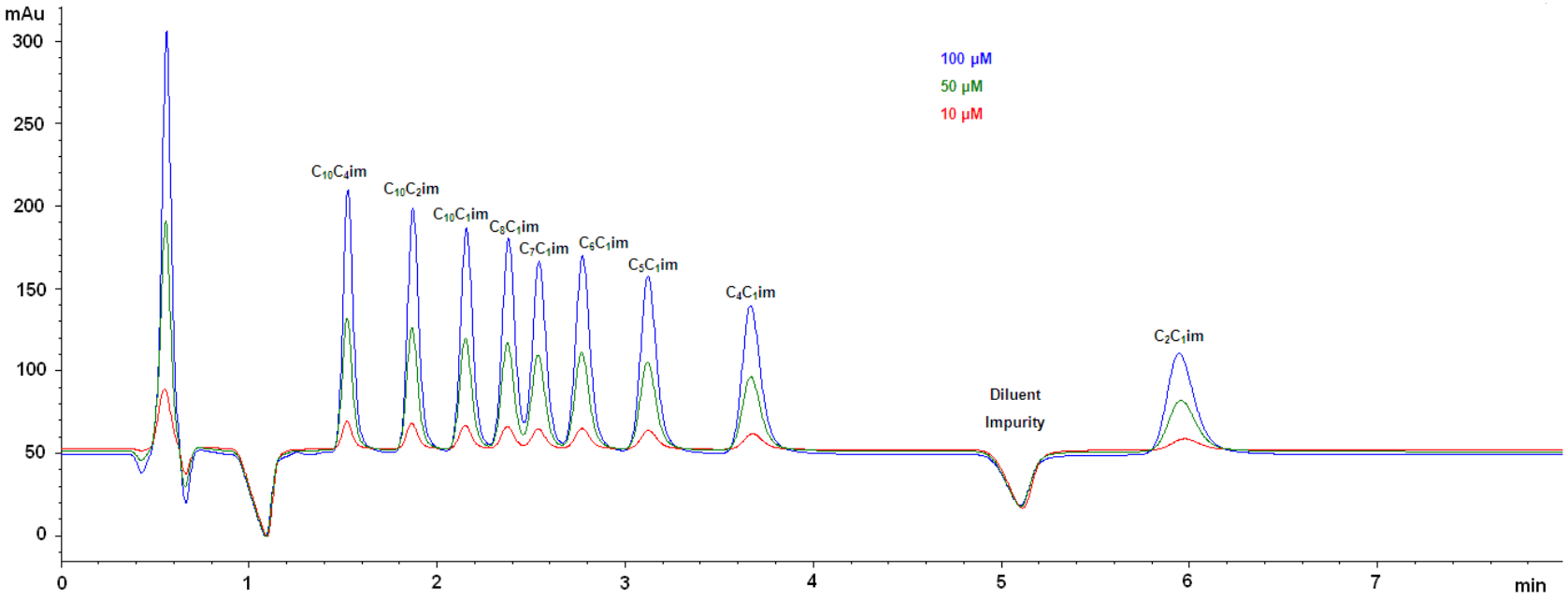


**Figure 5.2: Overlay of Chromatograms from the injection of a cocktail composed of nine homologous 1,3-dialkylimidazolium bis[(trifluoromethyl)sulfonyl]imide ionic liquids in 90:10 ACN:water;** 20 µL injection volume, mobile phase: 10 mM ammonium formate buffer pH 3.7 in 90:10 ACN:water, flow rate: 0.800 mL $min^{-1}$, Zorbax HILIC Plus 3.0 mm I.D. x 75 mm 3.5 µm $d_p$, column temp. 30°C, UV detection 210 nm

5.3.2 Evaluation of the method merits

Using $C_8C_1$im as a representative analyte with intermediate retention, the lower limit of detection can be calculated as $5.6 \times 10^{-7}$ mol $L^{-1}$, and the lower limit of quantification as $1.87 \times 10^{-6}$ mol $L^{-1}$. This sensitivity corresponds to a 30-fold improvement over previously described HPLC-based analytcal methods [5.9-5.11] and compares favorably to that of IC methods with conductivity detection [5.6]. The reproducibility of peak retention times ranged from 0.16% to 0.90% RSD, and the precision of peak areas ranged from 1.26% RSD to 5.80% RSD for 10 nmol and 0.2 nmol on column per IL in the cocktail, respectively. Good linearity ($R^2 > 0.999$) was observed for 0.01 nmol to 20 nmol on column per IL in the cocktail. However, at 40 nmol on column, significant fronting of the peaks was observed due to overloading of the column. (The column capacity could be increased substantially by increasing the column size to more standard analytical dimensions (150 mm x 4.6 mm), at the cost of sample throughput.) Carryover was found to be 0.1% by injecting a blank diluent sample after the injection of a high standard, which is suitable for a manual injection system. Over one-thousand injections have been performed on the same column without a significant deterioration in efficiency or resolution.

## 5.4 Characterization of the Retention Mechanisms of the HPLC Method

### 5.4.1 Silica column characteristics

The use of an underivatized silica stationary phase remains the major difference between this method and that of Lamouroux *et al*. [5.11], in which a diol-derivatized silica stationary phase was described as exhibiting HILIC retention behavior. Because silica and diol phases afford approximately the same polarity, they tend to provide similar retention characteristics for polar and ionic solutes. There are, however, major differences between the diol and silica phases. First, diol phases are bonded to the silica, resulting in fewer free silanol sites to provide a means of adsorptive ion-exchange. In addition, they have a greater tendency to form hydrogen bonds, and therefore, they acquire thicker layers of water on the stationary phase, enhancing the partitioning mechanism. In general, satisfactory retention and selectivity on a diol stationary phase come at the cost of long elution times and poor peak shapes for the many retained species (*i.e*., $C_2C_1$im). As Lamouroux *et al*. noted [5.9], the considerable tailing observed in the separation of Ils on a diol phase is due, in large part, to secondary ionic interactions with free silanols. Such drastic differences in elution profiles, coupled with the expectation that a HILIC mode may be involved in the retention observed in Fig. 5.2, prompted an investigation of the retention mechanism under these conditions.

The chemistry of the surface of silica is not straightforward [5.18]. While only two types of functional groups (*i.e*., silanols and siloxane bridges) exist on the surface, the interrelationships between them are many and complex. For example, the silanol groups can exist either independently or hydrogen bonded to near neighbors. Although they are primarily weakly acidic, some of these silanols are strongly acidic and thus, ionized at

even low pH [5.1]. The siloxane bridges, while often assumed to be inactive, can contribute to retention through hydrophobic interactions [5.1]. Not unexpectedly then, chromatography performed on silica-based stationary phases is not always reproducible or understandable.

Normal-phase elution order with a significant partitioning component is a hallmark of HILIC mode separations [5.12]. For ionized solutes, ion exchange often constitutes a secondary component [5.10, 5.13]. In an effort to assess the relative contributions of these two components, the first of our studies involved determining the relationship between the retention of the IL cations and their hydrophobicity. Figure 5.3 illustrates the relationship between the logarithm of the retention factor and the carbon number of the same two homologous series of ILs ($C_{10}C_n$im and $C_nC_1$im) in Fig. 5.2. Consistent with typical normal-phase separations, the retention is observed to decrease with increasing hydrophobic character of the IL. Additionally, the correlations are more or less linear, suggesting that retention (and therefore selectivity) is largely driven by the hydrophobicity of the ILs. The slightly parabolic shape of the plots, however, suggests that more than one retention mode influences the retention of these solutes, despite their vastly different polarities.

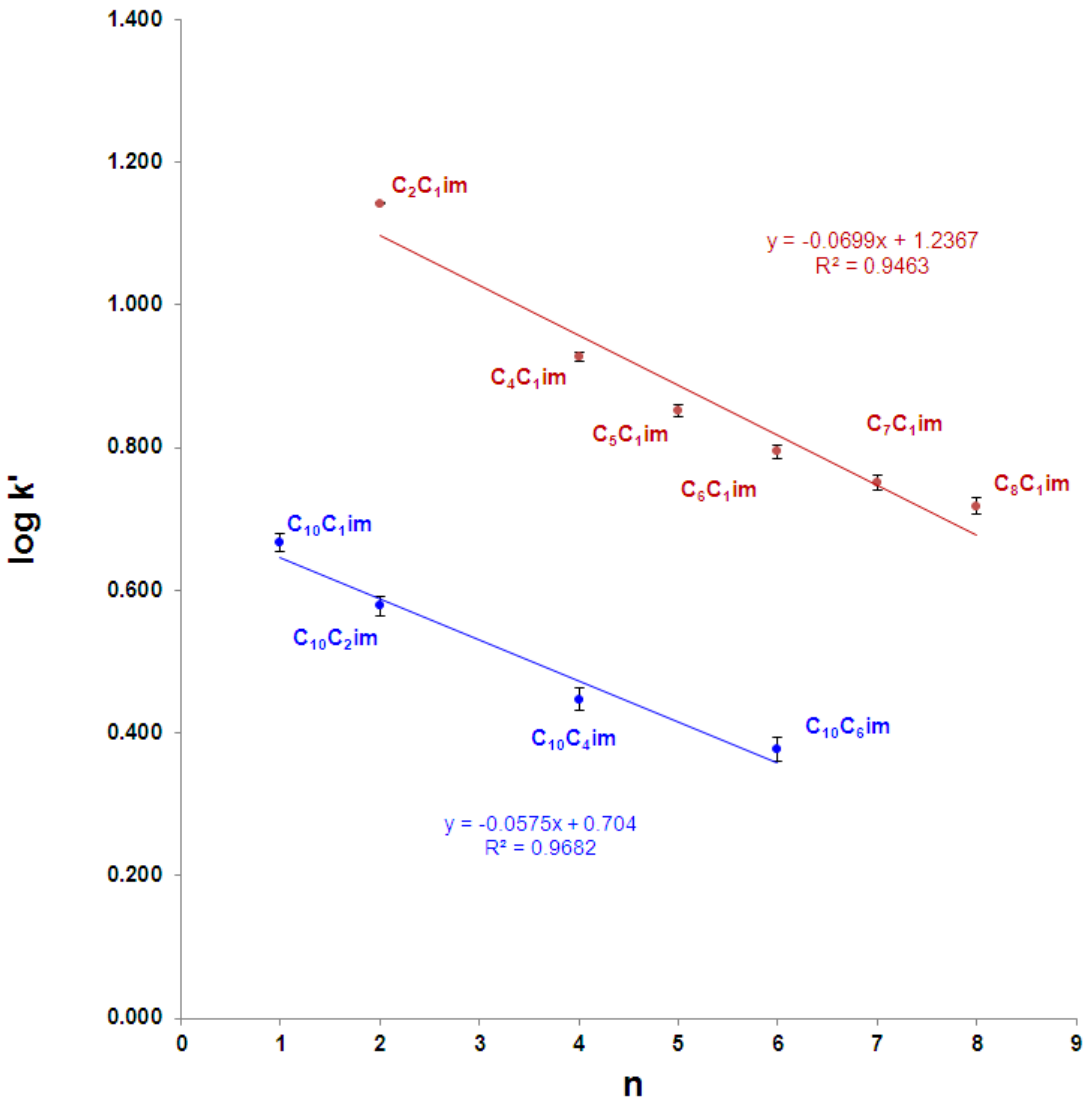


**Figure 5.3: Variation of logarithmic retention factor with carbon number of homologous series of 1,3-dialkylimidazolium-based ILs.** Fitted lines are of linear least-squares regressions. Error bars are standard deviations (n=3) at the 95% confidence interval. Conditions are the same as in Fig. 5.2.

5.4.2 Effect of solvent strength on retention

These results raise the question of whether the most important factor governing IL retention is partitioning or adsorption. Obviously, electrostatic interactions often play an

important role in the behavior of ILs [5.19], and these interactions are thus likely to be a significant factor in their chromatographic retention. The basic relationship governing solute retention derives from reversed-phase chromatography, for which retention is determined (ideally) by partitioning. Equation 5-2 describes the relationship between the retention factor and solvent strength for a separation system [5.16].

$$\log k' = \log k'_A - SV_B \qquad (5\text{-}2)$$

where $k'_A$ is the theoretical value of retention factor with only the weak solvent as the mobile phase, $V_B$ is the volume fraction of the strong solvent in the mobile phase, and S is a constant for a given solute (all other conditions constant). In conventional normal-phase systems, where retention is based on surface adsorption and subsequent displacement of the analyte by the eluent, the relationship between retention and the volume fraction of the strong solvent (*i.e.*, water), will conform to the following expression [5.17]

$$\log k' = \log k'_A - \frac{A_s}{n_b} log V_B \qquad (5\text{-}3)$$

where $A_s$ and $n_b$ are the cross-sectional areas occupied by the solute and the eluent molecules, respectively, on the surface. Plots of logarithmic retention factor *vs*. the linear and logarithmic functions of the water contents in the eluents should thus produce one straight line and one curve, depending on whether the dominant retention mechanism is partitioning or adsorption. While there are many examples of such plots in the literature, it remains unclear if these mechanisms can be resolved in such a simple manner.

Figure 5.4 shows the effect of varying the volume fraction of water in the mobile phase on log k'. That the plot is not linear is clear evidence that partitioning cannot be the only mechanism contributing to the retention of the ILs (if indeed it is present at all), in agreement with previous studies [5.20, 5.9] which proposed that for ionic solutes, retention is likely to be controlled by adsorption. A closer look at Fig. 5.4 shows that the plot can be divided into three distinct regions. In the first, which corresponds to the volume fraction of water from 0.05 to 0.6, IL retention decreases with increasing water content, thus defining a region of normal-phase behavior that might be considered HILIC mode. In the next region, which encompasses water volume fractions from 0.6 to 0.8, the retention factor remains essentially constant and all nine IL peaks co-elute. Lastly, in the third region (water fraction of 0.8 and above), a subtle shift to reversed-phase behavior (increasing k' with increased water in the mobile phase) is observed. These shifts in retention mode lead to the default "U" shape of the curves [5.21].

When the logarithmic retention factors of several representatives ILs are plotted versus the logarithmic volume fraction of water for region 1 (Fig. 5.5), an excellent linear fit is obtained (as per Eqn. 5-3), which is consistent with an adsorptive process [5.8]. Thus, adsorption (most likely ion-exchange) plays a dominant role in the retention and selectivity under the operating conditions of this method. Note, that to attain these fits, the range of the water contents was truncated from 60% for $C_2C_1$im to 50% for $C_4C_1$im, and 40% for $C_7C_1$im and $C_{10}C_2$im, because of a shift toward more reversed-phase behavior with increasing solute hydrophobicity. Regardless of the apparent role of adsorption, no single approach can definitively elucidate the retention mechanism(s).

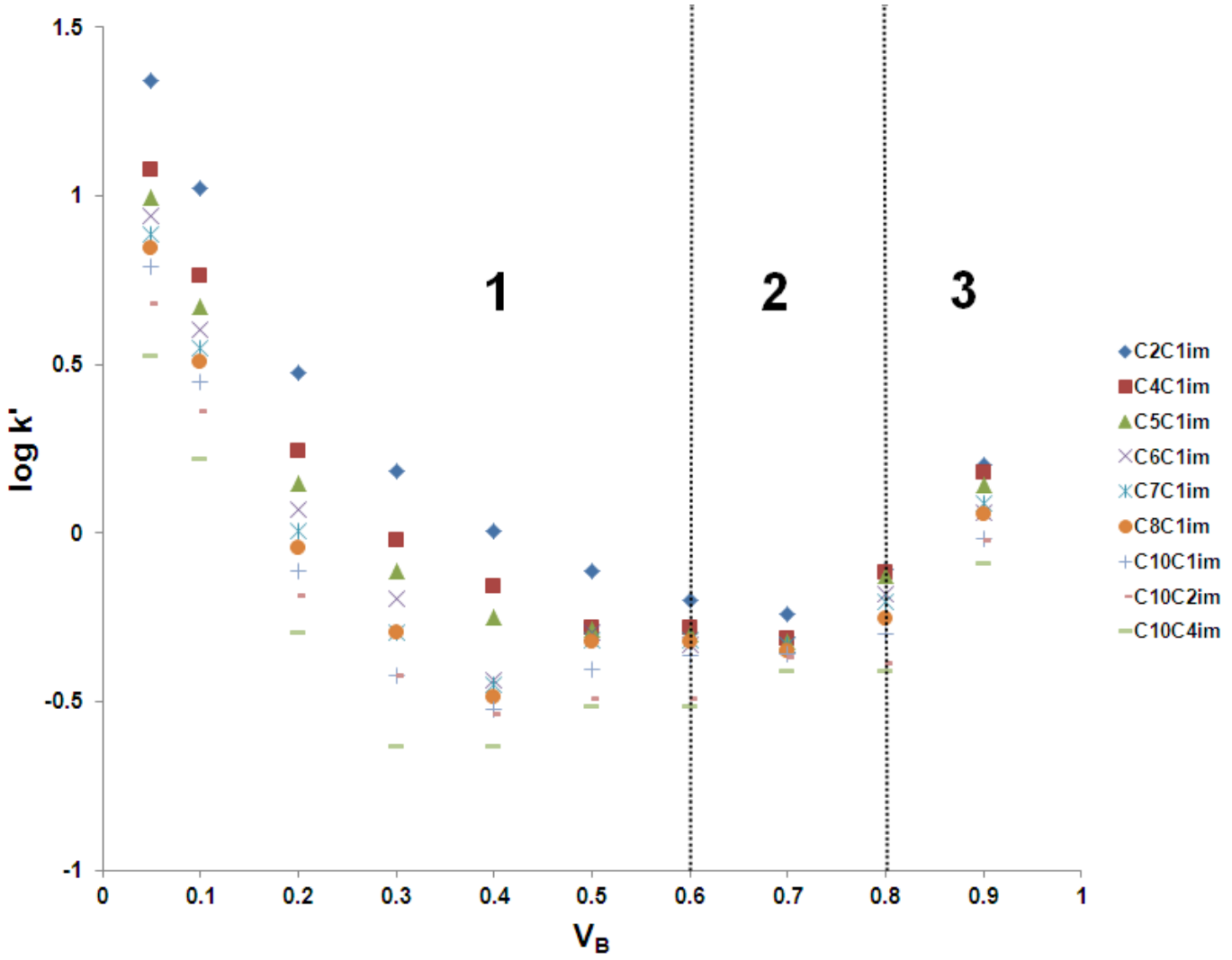


**Figure 5.4: The effect of varying the volume fraction of water in the eluent ($V_B$) on the logarithmic retention factor.**

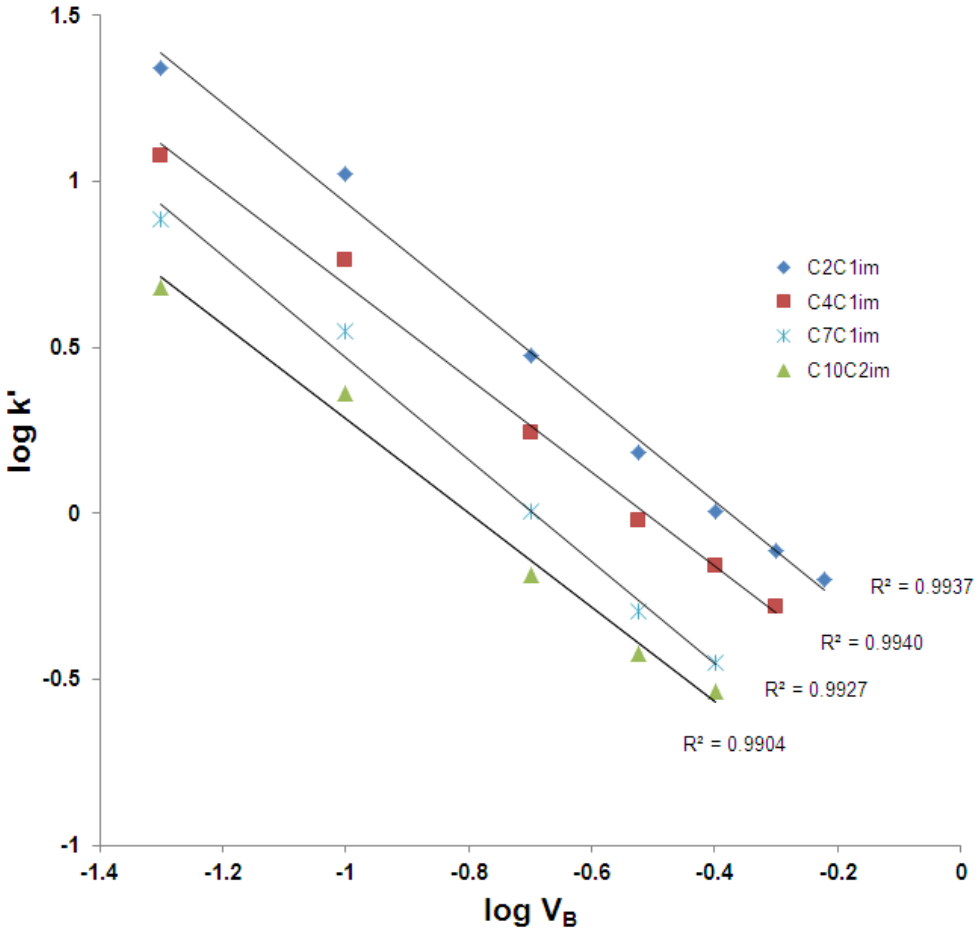


**Figure 5.5: Bilogarithmic relationship of retention factor on the varying volume fraction of water in the eluent ($V_B$).**

Previous studies of the retention of hydrophobic solutes on silica have estimated that, from 70% to 95% ACN, the water-rich layer occupies 4% to 13% of the pore volume, leading to significantly exclusion of those solutes from the pores and reduced retention [5.22]. That an estimated 7% of the pore volume may be occupied by the water-rich layer at the 90% ACN operating mobile phase composition suggests that the exclusion of the ILs from the pores may be a factor leading to the trend of decreasing k' with increasing

IL hydrophobic surface area. This process may also play a significant role in the selectivity observed with this method.

5.4.3 Influence of temperature on the separation process

Temperature has a significant effect on retention, especially for charged or ionizable solutes [5.1]. Several previous studies have explored the effect of temperature on retention for a variety of solutes and stationary phases [5.20, 5.25-5.27], and the results have provided the means for fundamental thermodynamic interpretations of the retention mechanisms involved. The relationship between the retention factor and thermodynamic temperature (T in Kelvin) is described by the van't Hoff equation [5.23, 5.24] (Eqn. 5-4):

$$ln\ k' = -\frac{\Delta H^{\circ}}{RT} + \frac{\Delta S^{\circ}}{R} + ln\frac{V_S}{V_M} = A_i + \frac{B_i}{T} \qquad (5\text{-}4)$$

where the parameter $B_i$ is proportional to the partial standard molar enthalpy of transfer of a solute *i* from the mobile phase to the stationary phase (ΔH°), $A_i$ involves the standard partial molar entropy of transfer of the solute from the mobile phase to the stationary phase (ΔS°), and the last term is the phase ratio (ratio of the volume of the stationary phase, Vs, to that of the mobile phase, $V_M$). Accordingly, the dependence of ln k' on inverse temperature is expected to be linear. Thus, by plotting ln k' versus 1/T over a sufficiently wide temperature range, the enthalpic and entropic contributions to the retention and selectivity can be calculated - ΔH° from the slope and ΔS° from the intercept. A van't Hoff plot exhibiting nonlinearity indicates that a change in retention mechanism has occurred over the range of temperatures studied [5.23].

Before one can calculate the entropic contribution to retention from the intercept ($A_i$), the phase ratio of the column must be known. Because it is impossible to know exactly the boundary between the space occupied by the stationary phase and the mobile phase in the column, however, the ratio must be calculated (Eqn. 5-5) using the total column porosity ($\varepsilon_T$) provided by Eqn. 5-6 [5.28].

$$\frac{V_S}{V_M} = \frac{1-\varepsilon_T}{\varepsilon_T} \qquad (5\text{-}5)$$

$$\varepsilon_T = \frac{V_0}{V_C} \qquad (5\text{-}6)$$

where $V_0$ is the hold-up time determined as the elution volume of a small unretained solute (toluene), and $V_C$ is the volume of the empty column. The retention time for toluene was 0.539 ± 0.001 min, resulting in a $V_0$ of 0.431 mL and a phase ratio ($V_S/V_M$) of 0.230.

Figure 5.6 is a plot of ln k' versus 1/T for the various 1,3-dialkyimidazolium ILs as well as the diluent impurity. At first glance, the curves appear to be quite linear. Although the retention of the $C_4C_1$im through $C_{10}C_4$im ILs increases with increasing temperature, the retention of the diluent impurity and $C_2C_1$im exhibit *decrease* with increasing temperature (with that of the impurity being more dependent on temperature). Evidently, there is a difference, from a thermodynamic perspective, between the overall retention process for $C_2C_1$im and the impurity versus that of the remaining ILs. To gain more insight into the processes involved, it is helpful to examine the trends in the thermodynamic contributions for the various solutes. Table 5.1 shows the results of linear least-squares regression of the experimental ln k' versus 1/T data and the calculated thermodynamic contributions for each IL, as well as those for the diluent impurity.

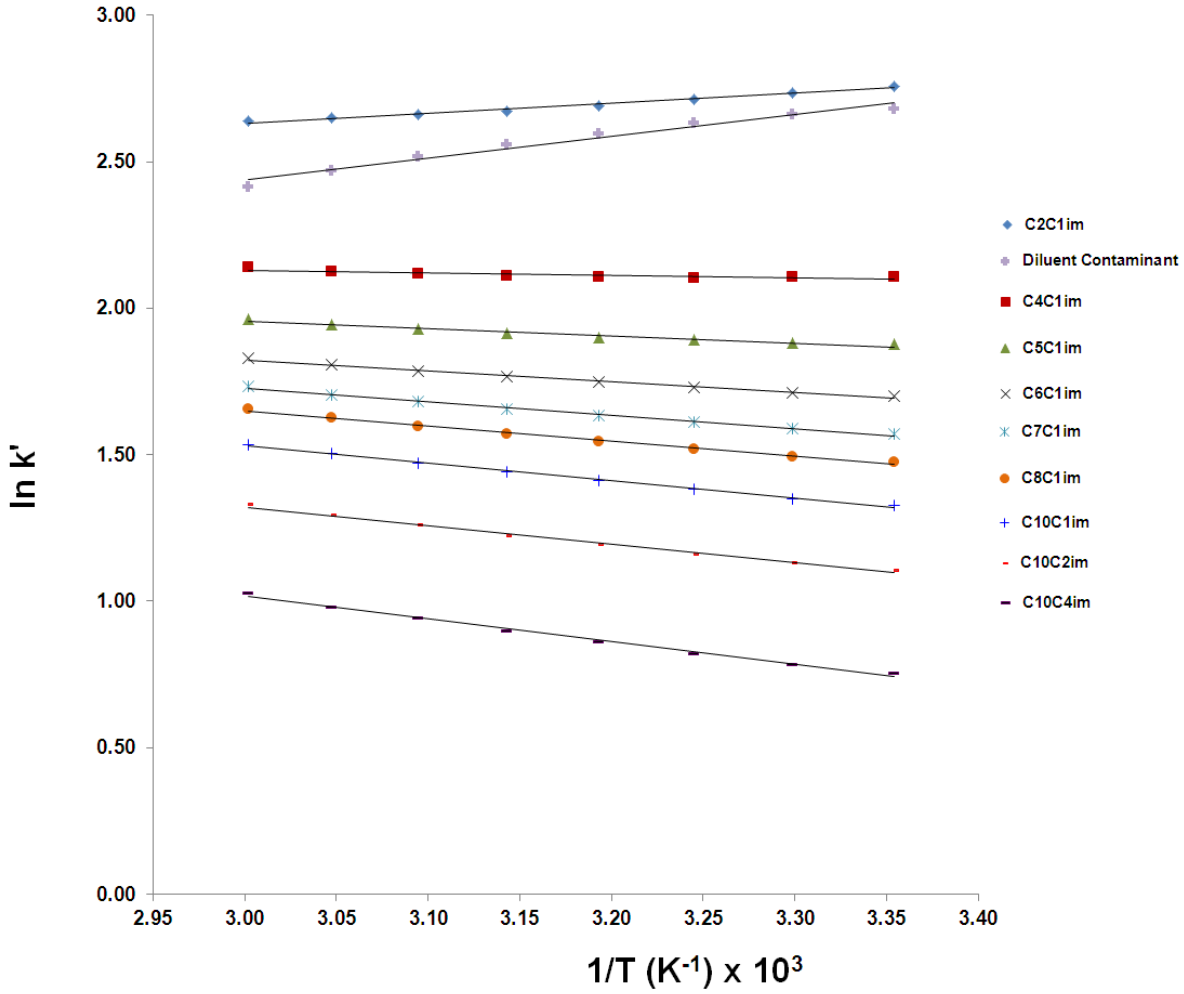


**Figure 5.6: Temperature dependence of retention factors for ILs and the diluent impurity.** Temperature range was 25°C to 60°C

Given that the shift in enthalpy from negative to positive (*i.e.*, exothermic to endothermic) coincides with significant changes in the hydrophilicity of the ILs, it can be surmised that the retention mechanism of $C_2C_1$im and the impurity includes a larger contribution from specific adsorptive interactions with the silica stationary phase than is the case for the remaining ILs. These observations are in accord with prior work [5.26] suggesting that retention by direct electrostatic interactions results in significantly more negative enthalpies than does retention dominated by ion-exchange with adsorbed eluent ions. Moreover, all of the processes are dominated by the partial molar change in entropy from the mobile phase to the stationary phase. That the entropic contribution is observed to rise with increasing IL alkyl chain length indicates that the driving force behind the retention process ion exchange that, to some extent, it is governed by hydrophobicity. Theory of ion-exchange involving non-adsorptive interactions has been developed in terms of Gouy-Chapman theory [5.29], where the analyte ions interact with the electric field formed by the buffer cation concentration gradient established in the eluent layers closest to the stationary phase. Under the conditions of the current method, an entropically-driven process might be one where the IL cations entering those layers from the bulk eluent exchange for ammonium ions without specific adsorptive interactions with the stationary phase. The correlation coefficients suggest that the dependence of ln k' on 1/T is linear ($R^2 > 0.95$), except for $C_4C_1$im (for which $R^2 = 0.712$). Assessment of the seemingly low correlation coefficient for the latter must take into account that temperature has little effect on the retention of $C_4C_1$im, whose small positive enthalpy lies in the region of transition from an endothermic process to an exothermic process. Therefore, even though the residuals from this regression are comparable to those of the

other curves, they result in a much larger sum of deviations. Upon closer inspection of the residuals for each regression, it can be seen that there is a slightly parabolic nature. But, whether this is a result of slight variations in the relative contributions of the different retention mechanisms or merely an artifact of bias in the column temperature at 25°C and 60°C (not determined by an online thermocouple) cannot be determined, however.

**Table 5.1**
**Best fit parameters, $A_i$, $B_i$ of Eqn. 5-3, correlation coefficients $R^2$, and the calculated thermodynamic contributions[a] to retention.**

| Solute | $A_i$ | $B_i$ | $R^2$ | $-\Delta H°$ (kJ mol$^{-1}$) | $\Delta S°$ (J K$^{-1}$ mol$^{-1}$) |
|---|---|---|---|---|---|
| $C_2C_1$im | 1.61 ± 0.06 | 342 ± 18 | 0.984 | -2.84 | 25.6 |
| Diluent Impurity | 0.18 ± 0.16 | 753 ± 51 | 0.973 | -6.26 | 13.7 |
| $C_4C_1$im | 2.39 ± 0.07 | -85.5 ± 22 | 0.712 | 0.71 | 32.0 |
| $C_5C_1$im | 2.69 ± 0.06 | -246 ± 19 | 0.964 | 2.05 | 34.6 |
| $C_6C_1$im | 2.94 ± 0.06 | -371 ± 18 | 0.987 | 3.08 | 36.6 |
| $C_7C_1$im | 3.10 ± 0.05 | -457 ± 17 | 0.992 | 3.80 | 38.0 |
| $C_8C_1$im | 3.20 ± 0.05 | -517 ± 17 | 0.994 | 4.30 | 38.8 |
| $C_{10}C_1$im | 3.31 ± 0.05 | -594 ± 17 | 0.995 | 4.94 | 39.7 |
| $C_{10}C_2$im | 3.23 ± 0.07 | -636 ± 21 | 0.994 | 5.29 | 39.1 |
| $C_{10}C_4$im | 3.34 ± 0.08 | -774 ± 24 | 0.994 | 6.43 | 40.0 |

[a] Uncertainties are based on the standard error of the coefficients at the 95% confidence interval

5.4.4 Effect of changing buffer concentration on retention

The extent to which ionic interactions play a role in the retention of solutes can be assessed by observing the effect of changing buffer concentration on retention. In traditional ion-exchange chromatography, the relationship between the retention factor (k') of a solute and the buffer or salt concentration [*C*] is described by Eqn. 5-7 [5.30], where *s* is a constant dependent on the charge of the solute and counter-ion.

$$\log k' = -s \log C + constant \qquad (5\text{-}7)$$

If we define the retention of a solute ($A^+$) by silanol-mediated ion-exchange as the equilibrium constant of the process in Eqn. 5-8

$$K_A = \frac{SiO^-{:}A^+{}_s[C^+]_m}{SiO^-{:}C^+{}_s[A^+]_m} \qquad (5\text{-}8)$$

where $SiO^-$ and $C^+$ represent the ionized silanol group and its counter ion (*i.e.*, $NH_4^+$), respectively, and the subscripts s and m denote the stationary phase and mobile phase, respectively. Expressed for a singly charged solute and a monovalent counter-ion, the slope of the relationship in Eqn. 5-7 would be -1. Although the relationship for our compounds is linear, as shown in Fig. 5.7, the deviation from unit slope observed for all of the curves (-0.37 to -0.10) may be indicative of the existence of retention mechanisms other than ion exchange [5.31, 5.32]. However, the activity of the ammonium ion may be significantly less due to diminished dissociation of the buffer salt in a largely aprotic solvent [5.31], which would also account for the deviation of the slope from unity.

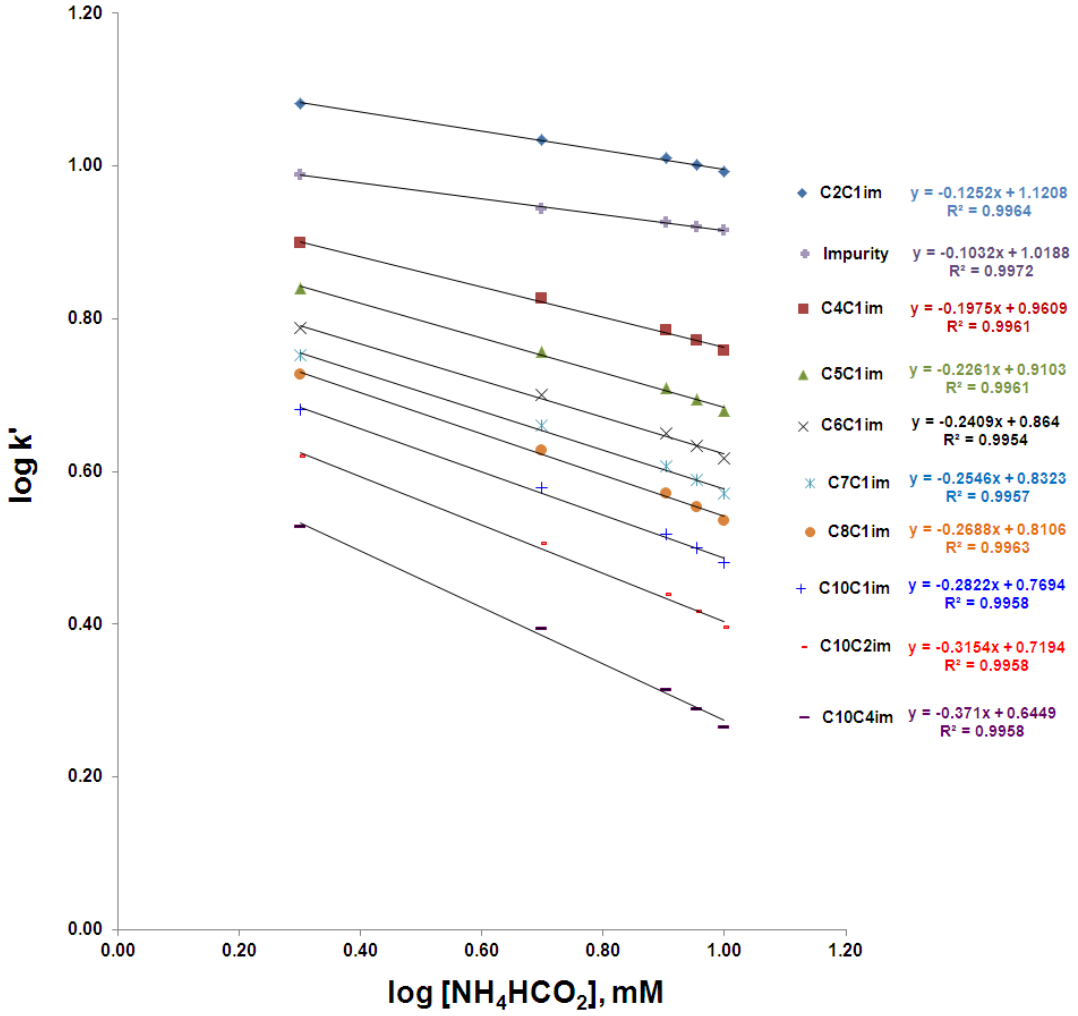


**Figure 5.7: The effect of varying the ammonium formate buffer concentration on the retention factor.**

To better define the contribution of ion-exchange to the overall retention, a "two-site model" described by Yang *et al*. [5.32] for the determination of the contribution from ion-exchange behavior of hydrophobic bases on reversed-phase columns was employed. Rearrangement of Eqn. 5-8 results in an ion-exchange distribution ratio for the solute, $A^+$, according to Eqn.5-9.

$$\frac{[A^+]_s}{[A^+]_m} = \frac{SiO^-:A^+{}_s}{[A^+]_m} = \frac{K_A * SiO^-:C^+{}_s}{[C^+]_m} \qquad (5\text{-}9)$$

Using the appropriate phase ratio ($\phi_{IX}$) and distribution ratio ($K_{IX}$), the retention factor for $A^+$ can be obtained, as in Eqn. 5-10.

$$k'_{IX} = \phi_{IX} * K_{IX} = \frac{K_A \times SiO^-:C^+{}_s}{[C^+]_m} \qquad (5\text{-}10)$$

For a given column, all of the terms in Eqn. 5-10 except for $[C^+]_m$ can be combined into a single constant, $B_{IX}$, which is proportional to is the total number of free silanol sites per unit area, $[SiO^-: C^+]$, and the equilibrium constant for the process, $K_A$. This leads to the simplified Eqn. 5-11:

$$k'_{IX} = \frac{B_{IX}}{[C^+]_m} \qquad (5\text{-}11)$$

It is noteworthy that for a 1:1 displacement reaction, Eqn. 5-11 leads to the conclusion that there will be no retention upon extrapolation to $1/[C^+] = 0$. The key assumption of the two-site model is that the solute molecules interact with two types of sites independently. Therefore, applying this approach the present system is indicative of a combination of a normal-phase and ion-exchange contribution to retention, as per Eqn. 5-12.

$$k' = \phi_{NP}K_{NP} + \phi_{IX}K_{IX} = k'_{NP} + k'_{IX} \qquad (5\text{-}12)$$

where $\phi_{NP}$ and $K_{NP}$ are the phase ratio and distribution ratio for a pure normal-phase partitioning process, and $k'_{NP}$ and $k'_{IX}$ are the respective retention factors for these two mechanisms, the sum of which is the observed retention factor, k'. No assumption is made as to the details of the normal-phase interaction, but it is taken to be a partitioning process like that described by HILIC theory. As long as these two components are independent of one another, and the normal-phase mechanism is only weakly dependent on the buffer concentration, then Eqn. 5-11 and Eqn. 5-12 can be rewritten as:

$$k' = \phi_{NP} K_{NP} + \frac{B_{IX}}{[C^+]_m} \qquad (5\text{-}13)$$

This expression provides the means to interpret a plot of k' versus $1/[C^+]$, where the slope of the curve is $B_{IX}$ and the y-intercept is the contribution to retention by mechanisms other than ion-exchange. It is not unprecedented to apply this approach to a normal-phase separation [5.33, 5.34]. In fact, the first such use of a plot of k' versus the inverse counter-ion concentration was performed in pursuit of a second non-ion-exchange process in a system utilizing bare silica phases [5.34].

Figure 5-8 is a plot of the retention factor versus the reciprocal ammonium concentration from the mobile phase buffer. (Conspicuously absent is the impurity peak, which was not observed for the highest buffer concentration (20 mM).) In accordance with Eqn. 5-13, the plots are rather linear ($R^2 \geq 0.98$). All of the intercepts observed are positive, consistent with the existence of an additional retention mechanism at "infinite" buffer concentration [5.34]. The decreasing intercepts with respect to increasing

hydrophobicity (*i.e.*, alkyl chain length) of the ILs reveal that there are vast differences in the contribution from the normal-phase mode, with a very small contribution from that to the retention of $C_{10}C_4$im. With the exception of $C_2C_1$im, the slopes of the curves decrease in that same order, reinforcing the idea that the silica particle pores are less accessible to the more hydrophobic solutes.

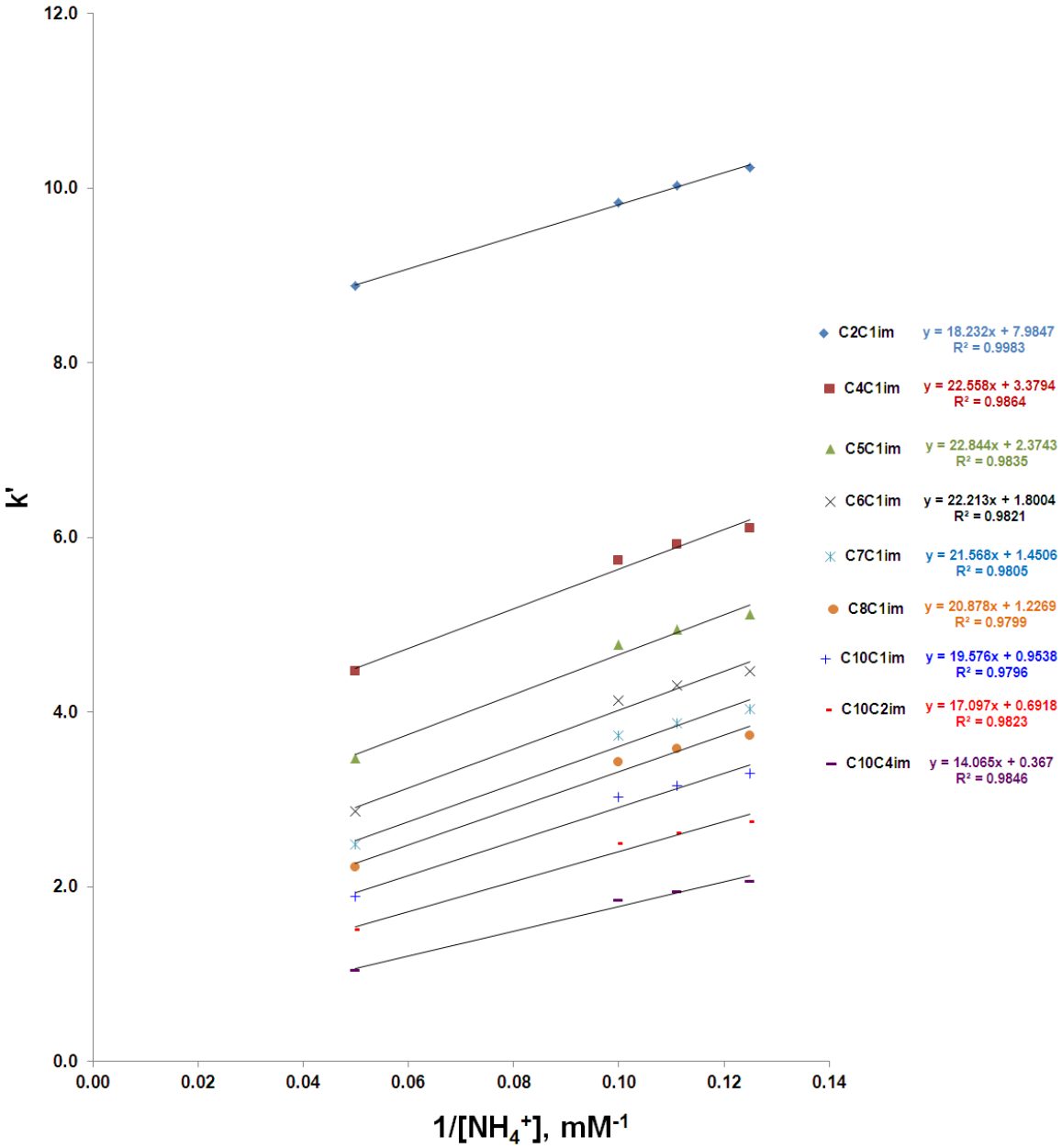


**Figure 5.8: Plot of retention factor versus the reciprocal buffer concentration.**

That the slopes of these curves are much greater than the intercepts reinforces view that the ion-exchange process is dominant for all of the ILs tested. Values of the regression parameters, however, should not be taken as a direct measure of the relative contributions

from normal-phase retention modes, because the activity of the ammonium ion under these conditions is not known. Yet again, the diminishing slopes ($B_{IX}$) along with increasing alkyl chain carbon number suggest that the interactions become somewhat less significant with increasing hydrophobicity of the solute. Considering the normal-phase behavior of the solute bands, and the likelihood that the high organic content of the mobile phase has led to a water-rich boundary on the silica phase, it is noted that the more hydrophobic ILs may be significantly excluded from pores that are enriched in water, and will, therefore, exhibit lower retention.

### 5.5 Conclusions

The method outlined here represents a significant improvement over previously developed HPLC and IC methods for the separation of ILs [5.9, 5.6], as nine imidazolium cations can be separated in the span of 7 minutes with exceptionally good peak shape. In addition, the method provides a means for rapid determination of a number of ILs with excellent sensitivity and precision. Because the 90% ACN mobile phase employed is miscible with both organic solvents and water, as long as the water (*i.e.*, strong solvent) content of an injected sample is 10% or less (*i.e.*, a 10-fold dilution of a purely aqueous sample) , the method provides a facile approach for the determination of ILs in a wide variety of samples.

The retention of 1,3-dialkylimidazolium IL homologues was found to vary with carbon number with some deviation from linearity. A thorough evaluation of the retention mechanism showed that ion-exchange is the predominant mode of retention for the ionic liquid cations on underivatized silica, which is consistent with several prior

studies [5.11, 5.20, 5.35, 5.36] and reviews [5.13, 5.21] on the subject of the interaction modes on various polar stationary phases. The van't Hoff correlation indicates that the retention mechanisms do not change with temperature and phase transfer of the analytes is driven primarily by entropy. Taken together with a predominantly ion-exchange mode of retention under conditions that favor the sorption of water on the silica surface, these thermodynamic data suggests that analyte adsorption may not be the dominant retention mechanism, but that ion-exchange may occur in the boundary layer formed near the stationary phase surface. Additionally, retention of the IL cations is controlled by their hydrophobicity, suggesting that increased exclusion from the pores and resulting decrease in retention with increasing alkyl chain length is, in part, responsible for the selectivity observed.

## 5.6 References

[5.1] L.R. Snyder, J.J. Kirkland, J.L. Glajch, *Practical HPLC Method Development*, Wiley and Sons, Inc., New York, **1997**.

[5.2] P. Stepnowski, A. Müller, P. Behrend, J. Ranke, J. Hoffmann, B. Jastorff, *J. Chromatogr. A*, **2003**, 993, 173-178.

[5.3] P. Stepnowski, W. Mrozik, *J. Sep. Sci*. **2005**, 28, 144-148.

[5.4] M.J. Ruiz-Angel, A. Berthod, *J. Chromatogr. A*, **2008**, 1189, 476-482.

[5.5] A. Markowska, P. Stepnowski, *Jap. Anal. Sci.* 2008, 24, 1359-1361.

[5.6] S. Stolte, S. Steudte, A. Markowska, J. Arning, J. Neumann, P. Stepnowski, *Anal. Methods*, **2011**, 3, 919-926.

[5.7] W. Gao, H. Yu, *Analytical Letters*, **2011**, 44, 922–931.

[5.8] S. Kowalska, B. Buszewski, *J. Sep. Sci*. **2006**, 29, 2625-2634.

[5.9] G. Le Rouzo, C. Lamouroux, C. Bresson, A. Guichard, P. Moisy, G. Moutiers, *J. Chromatogr. A*, **2007**, 1164, 139-144.

[5.10] D.V. McCalley, *J. Chromatogr. A*, **2007**, 1171, 46-55.

[5.11] C. Lamouroux, G. Foglia, G. Le Rouzo, *J. Chromatogr. A*, **2011**, 1218, 3022-3028.

[5.12] A.J. Alpert, *J. Chromatogr. A*, **1990**, 499, 177-196.

[5.13] P. Hemström, K. Irgum, *J. Sep. Sci*. **2006**, 29, 1784-1821.

[5.14] E. Wikberga, T. Sparrmana, C. Viklundb, T. Jonssonb, K. Irgum, *J. Chromatogr. A*, **2011**, 1218, 6630-6638.

[5.15] H.P. Nguyen, K.A. Shug, *J. Sep. Sci*. **2008**, 31, 1465-1480.

[5.16] C.F. Poole, *The Essence of Chromatography*, Elsevier, Amsterdam, **2003**, 302.

[5.17] L.R. Snyder, H. Poppe, *J. Chromatogr. A*, **1980**, 184, 363-413.

[5.18] R.K. Iler, The Chemistry of Silica, and Sons, Inc., New York, **1979**.

[5.19] H. Tokuda, K. Hayamizu, K. Ishii, Md.A.B.H. Susan, M. Watanabe, *J. Phys. Chem. B*, **2005**, 109, 6103-6110.

[5.20] Y. Guo, S. Gaiki *J. Chromatogr. A*, **2005**, 1074, 71-80.

[5.21] B. Buszewski, S. Noga, Anal. Bioanal. Chem. 2012, 402, 231-247.

[5.22] D.V. McCalley, U.D. Neue, J. Chrom. A, **2008**, 1192, 225-229.

[5.23] L.A. Cole, J.G. Dorsey, Anal. Chem. **1992**, 64, 1317-1323.

[5.24] D. Haidacher, A. Vailaya, C. Horváth, *Proc. Natl. Acad. Sci*. **1996**, 93, 2290-2295.

[5.25] Z. Hao, B. Xiao, N. Weng, *J. Sep. Sci*. **2008**, 31, 1449-1464.

[5.26] J. Wu, W. Bicker, W. Linder, *J. Sep. Sci*. **2008**, 31, 1492-1503.

[5.27] J. J. Soukup, P. Jandera, Biologija, 2011, 57, 85-91.

[5.28] J. Urban, P. Jandera, Z. Kučerová, M.A. van Straten, H.A. Claessens, , *J. Chromatogr. A*, **2007**, 1167, 67-75.

[5.29] J. Stråhlberg, *Anal. Chem*. **1994**, 66, 440-449.

[5.30] H.F. Walton, R.D. Rochlin, *Ion Exchange in Analytical Chemistry*, CRC Press, Boca Raton, FL, **1990**.

[5.31] G.W. Tindall, J.W. Dolan, *LC-GC North America*, **November 2002**, 1028-1032.

[5.32] X. Yang, J. Dai, P.W. Carr, *J. Chromatogr. A*, **2003**, 996, 13-31.

[5.33] M. Liu, J. Ostovic, E.X. Chen, N. Cauchon, *J. Chromatogr. A*, **2009**, 1216, 2362-2370.

[5.34] G.B. Cox, R.W. Stout, *J. Chromatogr. A*, **1987**, 384, 315-336.

[5.35] N.P. Dihn, T. Jonsson, K. Irgum, *J. Chromatogr. A*, **2011**, 1218, 5880-5891.

[5.36] Y. Guo, S. Gaiki *J. Chromatogr. A*, **2011**, 1218, 5920-5938.

# CHAPTER 6:
# THE ROLE OF IONIC LIQUID CATION HYDROPHOBICITY

## 6.1 Introduction

### 6.1.1 Impetus for studies of ionic liquid hydrophobicity

The ease with which an imidazolium ion can be derivatized has led to a vast array of imidazolium-based ILs that are potential candidates for a wide range of applications. In fact, there are over 30,000 1,3-dialkyl imidazolium entries recorded in the ACS Chemical Abstracts Service database [6.1]. The array of possible structures, however, presents a challenge in determining what structural features will likely afford the physicochemical properties sought for a given application. The selection of an appropriate IL is further complicated by the sensitivity of properties to the IL structure. For example, studies of the effect of systematically varying the alkyl chain length of 1,3-dialkylimidazolium-based ILs have demonstrated that the certain properties (*e.g.*, water solubility) of these compounds can be substantially altered by addition or deletion of a single methylene group.

The goal of a substantial portion of this work has been to provide information to establish guiding principles for the rational selection of the ILs most appropriate for use in metal ion extraction. Clearly, the most effective guidelines would be those based on the fundamental physicochemical properties of ILs and their relationship to the behavior of ILs as solvents. As the three-path model for metal ion extraction has informed our understanding, it has become clear that the desired solvent characteristics (*e.g.*, mimicking the behavior of conventional solvents but with extraction efficiencies and extraction selectivities that are superior to conventional solvents) can be achieved under certain conditions simply by making the IL cation sufficiently hydrophobic as to render

exchange of this species for the cationic metal complex much less favorable. As described in Chapter 4, the switch in the predominant mode of partitioning from ion exchange to ion-pair extraction comes at the cost of lower extraction efficiency. Often among the results of this change in pathway are values of $D_{Sr}$ (at acidities where extraction is normally performed) no better than those observed with 1-octanol as the solvent. Despite the lack of overall improvement in extraction efficiencies when using a relatively hydrophobic IL (*e.g.*, $C_{10}C_1imTf_2N$), these solvents have been shown to offer greater selectivities, a result of the switch in partitioning mode which occurs for $Sr^{2+}$, but not for $Na^+$ (see Chapter 3). Although these studies have proven to be important in understanding the factors that contribute to the trends seen in the acid dependencies, they have not provided a means of quantitatively relating IL structure to the propensity for ion-pair extraction. From a practical standpoint, such a goal would likely be best served by developing a scale of hydrophobicity that relates the structure of the IL to its extraction properties, a scale that could provide a means of solvent selection. With this in mind, in this chapter we describe our efforts to devise a system for determining IL hydrophobicity (lipophilicity) and its correlation to metal ion extraction behavior in biphasic systems employing ILs as the organic phase.

### 6.1.2 The hydrophobic effect

Although hydrophobicity has been invoked in previous chapters as a fundamental property involved in determining both the balance of pathways in the extraction of metal ions (Chapters 3 and 4) and the chromatographic retention mechanism(s) of retention of an IL on a chromatographic column (Chapter 5), it has not been strictly defined. Initially,

a conceptual description of hydrophobicity will be the most useful. The phenomenon underlying the property is the hydrophobic effect, which arises from the fact that hydrocarbon molecules have a greater solubility in hydrocarbon (*i.e*, organic) solvents than in water [6.2]. More exactly, the hydrophobic effect is defined by the free energy transfer of a hydrocarbon from water into a hydrocarbon solvent [6.3]. Let us start by noting that due to the presence of a hydrogen bond network, water is a highly ordered substance. The introduction of a solute into an aqueous environment will therefore disrupt this hydrogen bond network. To some extent, the hydrogen bonding requirements can be satisfied by forming new interactions with a polar solute. For a nonpolar solute, however, or one with extensive nonpolar functionalities, those bonds are unable to reform. Instead, the water molecules at the surface of the cavity formed by the inclusion of the nonpolar solute must rearrange tangentially to that surface to reform the broken hydrogen bonds. In the process of rearranging, a higher degree of local order (a negative change in entropy) is established, with more rigid hydrogen bonds between water molecules. The extent to which this reorganization is necessary to maintain the hydrogen bonds in the presence of a solute is related to the overall hydrophobicity of the solute. The thermodynamic interpretation of this situation is that hydrocarbon (*i.e*., non-polar) moieties have a tendency to be expelled from an aqueous environment because of the unfavorable free energy of the process. This so-called "hydrophobic effect" is the source of many spontaneous molecular phenomena in aqueous solution including protein folding [6.4, 6.5], the formation of membranes [6.2, 6.7], and gas solubility in water [6.8].

In order to draw the relationship between the hydrophobic effect and the solution chemistry we seek to explain, it is best to take a more quantitative approach to the

phenomenon. Partitioning of a solute between an aqueous phase and an immiscible hydrocarbon solvent is a process that is described well by fundamental chemical thermodynamics, beginning with a general expression for the chemical potential of a solute, *i*, in Eqn. 6-3

$$\mu_i = \mu^\circ + RT\ ln\ \gamma X_i \qquad (6\text{-}3)$$

where μ° is the standard chemical potential, R is the gas constant, T is absolute temperature, and γ is the activity coefficient in a solution of $X_i$ concentration of the solute. The chemical potential of a hydrocarbon dissolved in water is given by Eqn. 6-4.

$$\mu_w = \mu_w^\circ + RT\ ln\ X_w + RT\ ln\ \gamma_w \qquad (6\text{-}4)$$

where $X_w$ is the mole fraction of the solute, $\gamma_w$ is the activity coefficient at that concentration, and $\mu_w^\circ$ is the standard chemical potential. The reference standard state for the standard chemical potential is the state of "infinite dilution" in water. The third term on the right-hand side of the equation represents only the partial excess chemical potential that stems from interactions of solute molecules with each other, and because of the very low solubility of hydrocarbons in water, may be assumed to be zero. The second term on the right-hand side is the contribution made by the entropy of mixing. Accordingly, $\mu_w^\circ$ is a measure of the internal free energy of the solute molecule and its interaction with the solvent. A corresponding term, $\mu_{hc}^\circ$, is obtained from the counterpart expression of chemical potential for a solute dissolved in a hydrocarbon solvent, shown in Eqn. 6-5.

$$\mu_{hc} = \mu^{\circ}_{hc} + RT\ ln\ X_{hc} + RT\ ln\ \gamma_{hc} \qquad (6\text{-}5)$$

Because the internal free energy is the same in both solvents, $\mu_{hc}$ - $\mu_w$, therefore represents the difference in free energy between the solute in a hydrocarbon solvent and the solute in water. This difference is deemed the free energy of transfer from water to hydrocarbon, and its assessment provides a basis for understanding the hydrophobic effect.

The values of $\mu^{\circ}_{hc}$ for different hydrocarbon solvents differ only slightly in comparison to the difference in $\mu^{\circ}_{hc}$ and $\mu^{\circ}_{w}$, and therefore, Eqn 6-5 can be applied to a solution of a hydrocarbon in itself (*i.e.*, pure liquid hydrocarbon). In this case, the second and third terms on the right-hand side of Eqn. 5-5 would be zero and $\mu_{hc}$ would equal to $\mu^{\circ}_{hc}$ within the limits of approximations made. When a hydrocarbon dissolves in water to form a saturated solution, the chemical potentials of that solute in the two phases will be the same because of the established equilibrium. Therefore, for a solute partitioned between a hydrocarbon liquid and water, $\mu_w = \mu_{hc}$. Substitution of the expression for $\mu_w$ from Eq. 6-4 in Eq. 6-5, results in an expression for the free energy of transfer that is only dependent on the solubility in water:

$$\mu^{\circ}_{hc} - \mu^{\circ}_{w} = RT\ ln\ X_w \qquad (6\text{-}6)$$

In the case of the distribution of solutes between octanol and water, where the solute concentration can be determined in both phases, the overall expression for the difference in free energy between the phases can be applied, as in Eqn. 6-7.

$$\Delta G = \mu^{\circ}_{hc} - \mu^{\circ}_{w} = RT\ ln\ X_{hc} - RT\ ln\ X_{w} \qquad (6\text{-}7)$$

6.1.3 Octanol-water partition coefficients for ionic liquids

Of the parameters describing the hydrophobicity of small molecular substances, the octanol-water partition coefficient ($K_{ow}$) is perhaps the most well-established, a result of its ease of measurement, the extensive set of values available for a wide range of solutes [6.8], and the demonstrated relationship between the parameter and a variety of other important solute properties. For example, because the dielectric properties of 1-octanol are similar to those of a generalized lipid phase [6.8], $K_{ow}$ can be used to model the partitioning of solutes across biological membranes [6.9-6.11]. Along these same lines, this parameter is useful in correlating the hydrophobicity of a wide variety of substances to processes that depend on their lipophilicity, including the prediction of the transport of chemical species in ecosystem risk analysis and the distribution and pharmacodynamics of drug substances in the human body [6.12, 6.13]. Briefly, the $K_{ow}$ represents a thermodynamic property of a pure substance under specified conditions that is defined precisely (by Eqn. 6-8) as the ratio of the equilibrium concentration of an identical pure chemical species (X) distributed between an octanol-rich phase (saturated with water, org) to that in a water-rich phase (saturated with 1-octanol, aq) at a given temperature.

$$K_{ow} = \frac{[X]_{org}}{[X]_{aq}} \qquad (6\text{-}8)$$

Applying the rule for the difference in logarithms to Eqn. 6-7 will provide the proportionality between the free energy of transfer and the distribution ratio at

equilibrium (Eqn. 6-8). Therefore, the logarithm of the distribution ratio is directly proportional to the free energy change in the transfer of the solute, as shown for the octanol-water distribution ratio in Eqn. 6-9.

$$\Delta G = RT\ ln\ \frac{X_{hc}}{X_w} \qquad (6\text{-}9)$$

The resulting proportionality provided in Eqn. 6-10 demonstrates that the octanol-water partition coefficient is a direct measurement of the hydrophobic effect. It follows from this that a logarithmic plot of the partition coefficient may be a linear function of some condition (*e.g.*, carbon number of the solute, aqueous modifier concentration) on which the partitioning of the solute is dependent.

$$\Delta G = RT\ ln\ \frac{X_{hc}}{X_w} \propto log\ \frac{solute_{\ org}}{solute_{\ aq}} = \log K_{ow} \qquad (6\text{-}10)$$

$K_{ow}$ is defined for the undissociated species of the solute in both phases. As a result, it can be difficult to determine for acids, bases, and salts, for which the degree of ionization in the aqueous phase is greater than that in the octanol phase. Like these more conventional compounds, ILs are expected to undergo greater dissociation in the water-rich phase (Fig. 6.1), thus complicating $K_{ow}$ determination. (The dissociation constants of $C_4C_1imTf_2N$ in water and 1-octanol have been determined to be 115 and 0.07, respectively [6.16], indicating the significant degree of dissociation in the aqueous phase versus the octanol phase for this particular IL.)

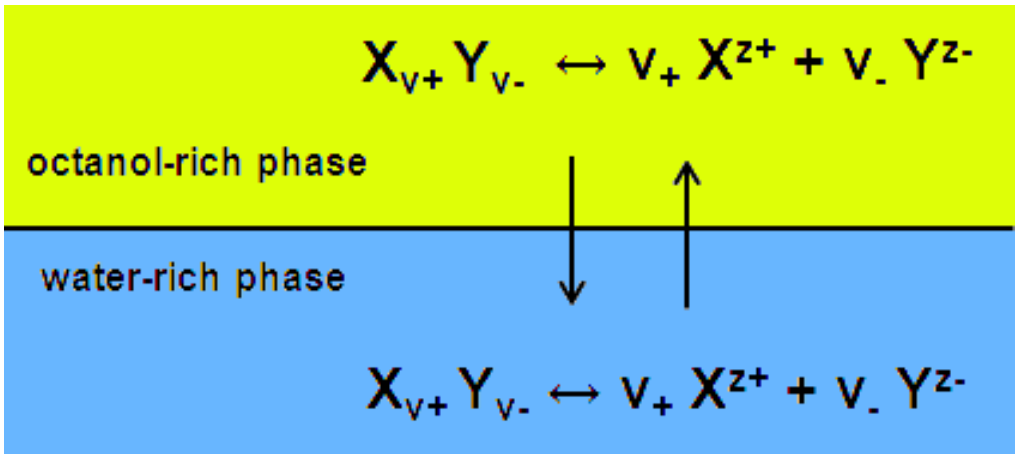


**Figure 6.1: A model for the partitioning of ILs in an mctanol/water biphasic system.** The symbols represent the ion pair, $X_{v+}Y_{v-}$, the respective dissociated ions $X^{z+}$ $Y^{z-}$, and their stoichiometric coefficents v+ and v-.

For ionizable substances, the octanol-water partition coefficient is often reported as the ratio of the sum of the concentration of both undissociated and dissociated salt in the octanol-rich phase to that in the water-rich phase [6.15-6.17]. Although by definition this value cannot be considered the $K_{ow}$, it can be deemed an octanol-water distribution ratio ($D_{ow}$), as described by Eqn. 6-11, where the dissociated and undissociated IL cation may be measured in both phases.

$$D_{o,w} = \frac{X_{v+}Y_{v-\ oct} + [X^{z+}]_{oct}^{v+}}{X_{v+}Y_{v-\ aq} + [X^{z+}]_{aq}^{v+}} \qquad (6\text{-}11)$$

Large databases of log $K_{ow}$ values estimated by structural-property models (*e.g*, linear solvation free energy relationships [6.18], quantitative structure-property relationships [6.19], and atom/fragment contribution models [6.20]) have been compiled in an effort to predict the biological behavior of potential drugs or pollutants. In cases where a wide variety of structures are possible, and therefore an multiplicity of properties that can affect the transport of solutes, these correlation models have provided a means to identify structures with important properties prior to their synthesis [6.21]. To facilitate estimation of the physicochemical properties of ionic liquids, these and other models and empirical correlations have been successful, but in ways that are often not mutually comparable [6.22]. However, the variables encountered in solvent extraction are far fewer than those in biological systems transport and distribution, and hence, these models may be too complicated for the hydrophobicity scale pursued in this work.

Techniques for the experimental determination of octanol-water partition coefficients (or distribution ratios) include the shake-flask method, the generator column method, high-performance liquid chromatography (HPLC), and the slow-stirring method. The shake-flask method establishes the equilibrium by shaking or rotating suitable vessels containing the mutually saturated phases in the presence of the solute of interest. The phases are disengaged by centrifugation. Although its simplicity makes this is the most common technique used, the method can yield erroneous results for solutes with very high (> 4) or very low (< -4) log $D_{ow}$, due to the formation of emulsions and/or entrainment of microdroplets of one phase in the other [6.23]. As an alternative to the shake-flask method, the generator column technique [6.24] utilizes a column is packed with an inert material (Chemosorb W or glass beads) that has been coated with water-

saturated octanol containing the test solute. Water is then pumped through the column, resulting in the equilibrium of the phases. The solute that elutes with the water and that passes through the column is then processed by solvent extraction and or concentrated by solid phase extraction to be analyzed. A tremendously high phase ratio allows the measurement of extremely high $K_{ow}$ values ($> 10^8$) [6.23]. Although this method prevents the formation of emulsions by slowly passing the phases through one another, it is a tedious and time-consuming procedure, and thus, is probably well-suited only for the most hydrophobic of solutes.

Liquid chromatography, particularly in reversed-phase mode, lends itself well to the estimation of partition coefficients because the principle retention mechanism is based on the partitioning of the test solute between an aqueous mobile phase and lipophilic stationary phase. Additionally, automated instrument for simultaneous analysis of substances with a wide range of polarities can rapidly generate a large number of results without the need for quantifying solute concentrations [6.25-6.28]. Partition coefficients are estimated from linear equations relating retention indices on RP-$C_{18}$ columns to $K_{ow}$, as derived for a set of reference chemicals. Among the disadvantages of this are the difficulty in extrapolating the results (*i.e.*, the linearity of the equations) beyond the range of the test solutes, and the variability in the density of the bonded phase between columns and manufacturers. (Specifications such as the carbon-load and end-capping of silanols must remain the same between columns to compare retention factor indices. Over the last decade, column manufacturers and chromatographers have made significant efforts to classify the selectivity of alkyl-silica columns on the market, resulting in selection guides for column equivalency [6.29].) Despite these limitations, recent attempts to catalog the

chemical toxicity of various 1,3-dialkylimidazolium-, 1-alkylquinolinium-, and 1-alkylpyridinium-based ILs by Ranke *et al*. [6.30] employing linear regression of reversed-phase gradient elution retention and IL lipophilicity or cytotoxicity data resulted in significant correlations. The results confirmed that hydrophobicity dominates the biological transport properties of IL cations over a wide range of structures. Ranke *et al*. [6.31] subsequently derived equations from first principles that relate the retention of ILs in the same chromatographic systems to their aqueous solubility and partitioning behavior.

The slow-stirring method was introduced [6.32] as a direct alternative to the shake-flask method for the measurement of the partition coefficient of very hydrophobic solutes (*e.g*., polychlorinated biphenyls) [6.23]. By equilibrating the phases through non-turbulent mixing this technique prevents the formation of emulsions as well as the mutual entrainment of the phases, to which the shake-flask method is prone. Recently, the slow-stirring method was applied to the determination of the $D_{ow}$ values of various ILs by Brenneke *et al*. [6.15], and confirmed by Ventura *et al*. [6.17]. Because the slow-stirring method was used with satisfactory accuracy for the difficult determination of the $D_{ow}$ of ILs, this technique was explored as a means for measuring the $D_{ow}$ of the ILs in the current study.

A complication noted by prior investigations in the determination of $D_{ow}$ values for ILs is the considerable concentration dependence of the values obtained. For instance, the log $D_{ow}$ values of $C_4C_1imTf_2N$ between the octanol and water have been shown to decrease with decreasing initial concentrations [6.15- 6.17]. Rigorous evaluation of the equilibria for this compound in each phase by Lee *et al*. [6.16] and later by Ventura *et al*.

[6.17] demonstrated that the $D_{ow}$ is a composite of the equilibria shown in Fig. 6.1, and that, the $D_{ow}$ is a linear function of IL concentration at sufficiently low initial concentrations. In light of these complications, the model proposed by Ventura *et al*. [6.17] is based on an ion-pair extraction into the octanol phase. It is worthy to note, however, that at the lowest values of initial IL concentration, Ventura *et al*. reported equilibrium concentrations for $C_2C_1imTf_2N$ and $C_4C_1imTf_2N$ in the octanol phase that were at or below the detection limit of the UV-VIS spectrophotometer (0.01 in absorbance). Therefore, these studies have called into question the use of a direct method for the determination of IL octanol-water distribution ratios.

For the purpose of these studies, $D_{ow}$ (as a basic representation of solute hydrophobicity) has been sought as a means to correlate the extraction of metal ions (*i.e*., $Sr^{2+}$) by DCH18C6 from acidic nitrate solutions into ILs, to the hydrophobicity of 1,3-dialkylimidazolium *bis*[(trifluoromethyl)sulfonyl]imide ILs. Establishing a scale with a simple relationship would provide a relatively facile means of evaluating ILs for a variety of processes where solvent hydrophobicity is a primary factor. As in previous studies, in this work, the hydrophobic anion *bis*[(trifluoromethyl)sulfonyl]imide is common to all of the ILs, thus simplifying the assessment of the differences in the hydrophobicity of the IL cation.

## 6.2 Experimental

### 6.2.1 Materials

All chemicals were reagent grade and used without additional purification unless noted otherwise. All aqueous solutions were prepared using deionized water with a

specific resistance of at least 18 MΩ·cm$^{-1}$. The DCH18C6 (Parish Chemical, Orem, UT) used was a mixture of the *cis-syn-cis* and *cis-anti-cis* isomers and was used as received. The 1-octanol employed for partitioning experiments was spectroscopic grade purchased from Alfa Aesar (distributed by VWR Chicago, IL) The HPLC mobile phase buffer was prepared by combining equal parts 500 mM formic acid (puriss. Grade, Sigma-Aldrich, St. Louis, MO) and 500 mM ammonium formate (J.T. Baker, supplied by VWR Chicago, IL) which resulted in a pH of 3.7. The HPLC mobile phase was prepared by combining 10.0 mL of the formate buffer with 40.0 mL of water and 450 mL of acetonitrile (Honeywell Burdick and Jackson, HPLC grade, supplied by VWR Chicago, IL) to produce a 10 mM buffer concentration in 90:10 acetonitrile:water. Imidazolium-based ionic liquids including the 3-methyl, 3-ethyl, and 3-butyl substituents were synthesized by the two-step process described in Chapter 4.

### 6.2.2 Instruments

NMR spectra were acquired on a Bruker DPX300 NMR spectrometer operating at 300.13 MHz for proton and 75.47 MHz for carbon-13, and equipped with a z-gradient broadband (BBO) probe. Unless otherwise noted, spectra were obtained using solutions of dimethylsulfoxide-$d_6$ or chloroform-$d_3$ (Aldrich, 99.96 atom% D), and all chemical shifts were reported relative to tetramethylsilane. Initial attempts to determine IL concentrations from octanol-water partition devices were made using a Shimadzu UV-2450 UV-Visible Spectrophotometer (sensitivity of ±0.01 absorbance units) with matching 10 mm path length quartz cuvettes. Measurements of IL concentrations from octanol-water partition devices were made using a set of Agilent 1200 series analytical

binary pumps equipped with an online degasser, a fixed loop manual injection port, and a variable wavelength UV-VIS flow cell, and operated using ChemStation software. The column used was a 75 mm x 3.0 mm I.D. Agilent Zorbax HILIC Plus silica column with 3.5 μm average particle size. The conditions for HPLC analysis were an isocratic flow rate of 0.800 mL $min^{-1}$ with 10 mM ammonium formate buffer (pH 3.7) in 90:10 acetonitrile:water. The column temperature was maintained at 30°C. An injection volume of 20 μL was employed, along with detection at 210 nm.

### 6.2.3 Methods

Slow-stirring devices were prepared according to the work of Brenneke *et al.* [6.15]. The apparatus shown in Fig. 6.2 consisted of a 40 mL (24 mm diameter 93 mm height) clear, glass vial (National Scientific Company, Claremont, CA, supplied by Thermo-Fisher Scientific), fitted with an open-top screw cap incorporating a Teflon-coated silicone septum, and containing a 1 cm Teflon-coated magnetic stir bar. Prior to adding the octanol phase, a 12 gauge Teflon tube (Hamilton Company, Reno, NV) topped with a polypropylene Luer Lug style female hub with a 1/16" barb (Value Plastics, Fort Collins, CO) was immersed in the water phase, drawn through a similar sized hole in the vial septum, and sealed with parafilm.

It has been noted previously that IL concentrations in the aqueous phase must be less than the critical micelle concentration (CMC) [6.33]. For even the most hydrophilic ILs studied here (*i.e.* $C_5C_1imTf_2N$), the CMC is expected to be greater than the aqueous solubility [6.34]. Additionally, a dependence of $D_{ow}$ on concentration (deviation from Henry's Law) was investigated by Lee *et al*. [6.17], suggesting that the concentrations used in previous experiments [6.15] were too high. Consideration of these and other data

[6.17] determined that indeed $D_{ow}$ does diminish with decreasing initial concentration of the IL, and that the initial concentration of the solute must be exceedingly low to avoid a significant bias. Our approach to achieving this goal while maintaining measureable concentrations was to employ initial concentrations of ILs in the octanol-rich phase that were less than the water solubility of the ILs, and at least 10-fold less than those used in the original studies [6.15]. Accordingly, all devices were prepared with an initial IL concentration of less than or equal to $1 \times 10^{-3}$ M in water-saturated 1-octanol. The octanol-rich phase was gently added on top of the water-rich phase in equal volumes and stirred for at least 40 days at 23 ± 2°C, until the $D_{ow}$ did not change by more than ± 0.3. Sampling of the octanol-phase was accomplished by penetrating the vial septum with a syringe. Samples were withdrawn from the aqueous phase by inserting a stainless steel syringe needle into the Teflon tube to avoid contamination with the octanol phase.

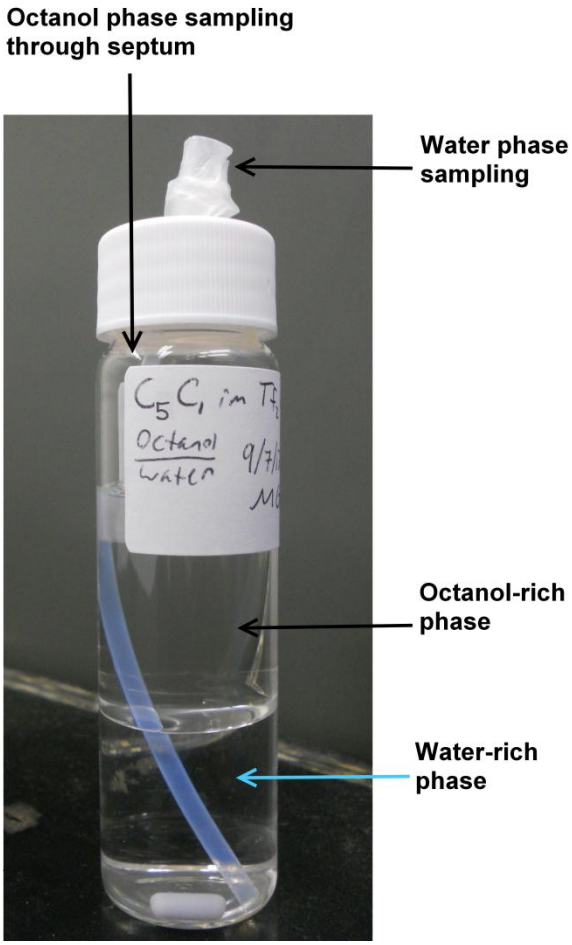


**Figure 6.2: Photo of a slow-stirring device for $D_{o,w}$ measurement of $C_5C_1imTf_2N$.**

Shake-flask devices were prepared in quadruplicate by simply adding equal volumes of 1.0 mM IL in water-saturated octanol and octanol-saturated water to 50 mL polypropylene centrifuge tubes (Becton Dickinson, Franklin Lakes, NJ, supplied by Thermo-Fisher Scientific). The tubes were mixed for 12 hours on a horizontal rotary shaker at 250 rpm, allowed to settle for 24 hours, and centrifuged at 3000 rcf for 5 minutes to disengage the phases. Aliquots of each phase were separated from the other and stored in 15 mL polypropylene tubes (Becton Dickinson, Franklin Lakes, NJ, supplied by Thermo-Fisher Scientific).

Aqueous phase samples were diluted 10-fold in acetonitrile prior to analysis by HPLC, as required to maintain efficiency in the separation. In cases where the aqueous IL cation concentrations were less than the lower limit of quantification of the HPLC-UV method (*ca*. 2 μM), an aliquot of the water-rich phase was evaporated and reconstituted with acetonitrile to a concentration factor of at least five. Octanol phase samples that contained higher concentrations than the highest standard calibrator were diluted at least 10-fold with acetonitrile, resulting in a peak area response within the range of the calibration curve. Note that 1-octanol is a weaker solvent than acetonitrile in a normal phase chromatographic system, and because it is miscible in the eluent, samples from that phase do not require solvent strength modification as do aqueous phase samples.

Distribution ratios of metal ions ($D_M$) were determined as the ratio of the count rate in the organic phase to that of the aqueous phase using commercial radiotracers. Assays were carried out *via* gamma spectroscopy using standard procedures. In each metal ion distribution experiment, the organic phase consisted of DCH18C6 dissolved in the designated ionic liquid, and the aqueous phase nitric acid concentration was systematically adjusted either by conducting separate experiments for each condition, or by adding the appropriate amount of acid after each sampling. All organic phases were pre-equilibrated with aqueous phase prior to the introduction of the metal radiotracer. Additionally, the sum of the count rates in each phase yielded recoveries within 10% (most often < 10%) that of the radiotracer stock solution used, indicating that equilibrium was established with only two phases involved. Room temperature was maintained at 23 ± 2°C. Each equilibrated phase was sampled for analysis in at least duplicate, with resulting uncertainties based on counting statistics that were generally within 10%,

although the uncertainty interval was considerably wider for the highest $D_M$ values ($D_M \geq$ 1000).

## 6.3 Determination of Ionic Liquid Hydrophobicity

### 6.3.1 Methods comparison of the slow-stirring and shake-flask techniques

Before studies relating $D_{ow}$ to IL solvent properties can commence, a workable method of equilibration for the octanol and water phases must be chosen. The most facile of these is the shake-flask technique, but owing to its various drawbacks [6.15, 6.16, 6.23], the slow-stirring technique is considered the more reliable approach. For ease of measuring the octanol-water distribution ratios of ILs, however, it would be preferable to use the shake-flask method. Avoiding a time-intensive equilibration would allow for a higher throughput analysis of the distribution ratios for a broader range of ILs. Although there is ample data to support the assertion that a bias is common with this technique, it is incumbent upon the analyst to determine whether such a bias is prevalent for a particular set of solutes and whether that bias is acceptable or not.

In the present work, a single slow-stirring device was prepared for the partitioning determination for each solute.. This device (Fig. 6.2) may require several months to equilibrate the phases due to the small contact area between them. To evaluate the necessity of using the slow-stirring technique for 1,3-dialkylimidazolium-based ILs, quadruplicate shake-flask experiments were also performed for several of the ILs to permit a direct method comparison. A simple “student t-test” (taking the slow-stirring results as the accepted value) as per Eqn. 6-12 was applied for this comparison.

$$t_{calc} = \frac{\mu - \bar{x} * \overline{N}}{s} \qquad (6\text{-}12)$$

where μ is the slow-stirring $D_{ow}$ value, $\bar{x}$ is the mean of the shake-flask $D_{ow}$ values, N is the degrees of freedom, s is the standard deviation, and $t_{calc}$ is to be compared to the tabulated t statistic at the 95% confidence interval. If the average $D_{ow}$ values for the shake flask results show no sign of determinant error, then we can reasonably assume that the shake-flask and slow-stirring techniques are equivalent.

The results of the methods comparison are provided in Table 6.1 In every case, the t-test resulted in $t_{calc} > t_{critical}$ ($t_{critical} = 3.18$ for four separate measurements), suggesting that significant systematic error has been introduced to the $D_{ow}$ values obtained using the shake-flask technique. The shake-flask $D_{ow}$ for $C_5C_1imTf_2N$ is approximately 70% higher than that for the slow-stirring method. Likewise, $D_{ow}$ for $C_8C_1imTf_2N$ generated by the shake-flask technique is significantly lower than that of the slow-stirring method.

**Table 6.1**
**T-test comparison of the shake-flask method to the slow-stirring method**

| IL | Shake-flask $D_{o,w}$ | Slow-stirring $D_{o,w}$ | $t_{calc\ (N=3)}$ |
|---|---|---|---|
| $C_5C_1imTf_2N$ | 0.17 ± 0.02 | 0.064 | 8.3 |
| $C_6C_1imTf_2N$ | 0.50 ± 0.01 | 0.38 | 20 |
| $C_8C_1imTf_2N$ | 5.90 ± 0.4 | 7.65 | 8.6 |

At these moderate distribution ratios, the differences are too large to be attributed to the entrainment of one phase in the other. If one places these differences in the context of the

$D_{ow}$ values determined, however, they are relatively small. Yet, combined with the difficulties encountered in previous studies [6.15-6.17], the differences between the method results suggest that the concentration dependence of $D_{ow}$ may be responsible. Additionally, although it may be possible to prevent or remove emulsions incurred during the shaking process, literature data for $K_{ow}$ values measured by the shake-flask technique indicate that formation of emulsions influences the observed $K_{ow}$ values [6.23]. Overall, the t-test results are consistent with misgivings of previous investigators [6.15, 6.17, 6.23], who questioned the validity of the shake-flask technique as a means of making $D_{ow}$ measurements of ILs. Stated another way, the shake-flask method is not valid for our purposes for the present studies, therefore, the octanol-water distribution ratios will be measured for our ILs using only with the slow-stirring technique.

### 6.3.2 Relationship of $D_{ow}$ to carbon number of the IL cation

One of the most straightforward structural descriptors is the number of carbon atoms in a molecule or within a particular functional group. Linear relationships between phase transfer parameters like log $K_{ow}$ and carbon number generally hold true for in particular classes of compounds containing the same kind and number of functional groups such as *n*-alkanes, alkenes, *n*-alcohols, and esters (*i.e.*, series of homologues) [6.2]. From a practical perspective, correlating the carbon number of ILs to the $D_{ow}$ values determined can provides a simple means of verifying the consistency of data obtained by a particular method. The plot in Fig. 6.3 depicts the relationship between the slow-stirring log $D_{ow}$ values for a series of 1,3-dialkylimidazolium ILs and either the carbon number of individual alkyl chains or the total number of carbons in both alkyl chains.

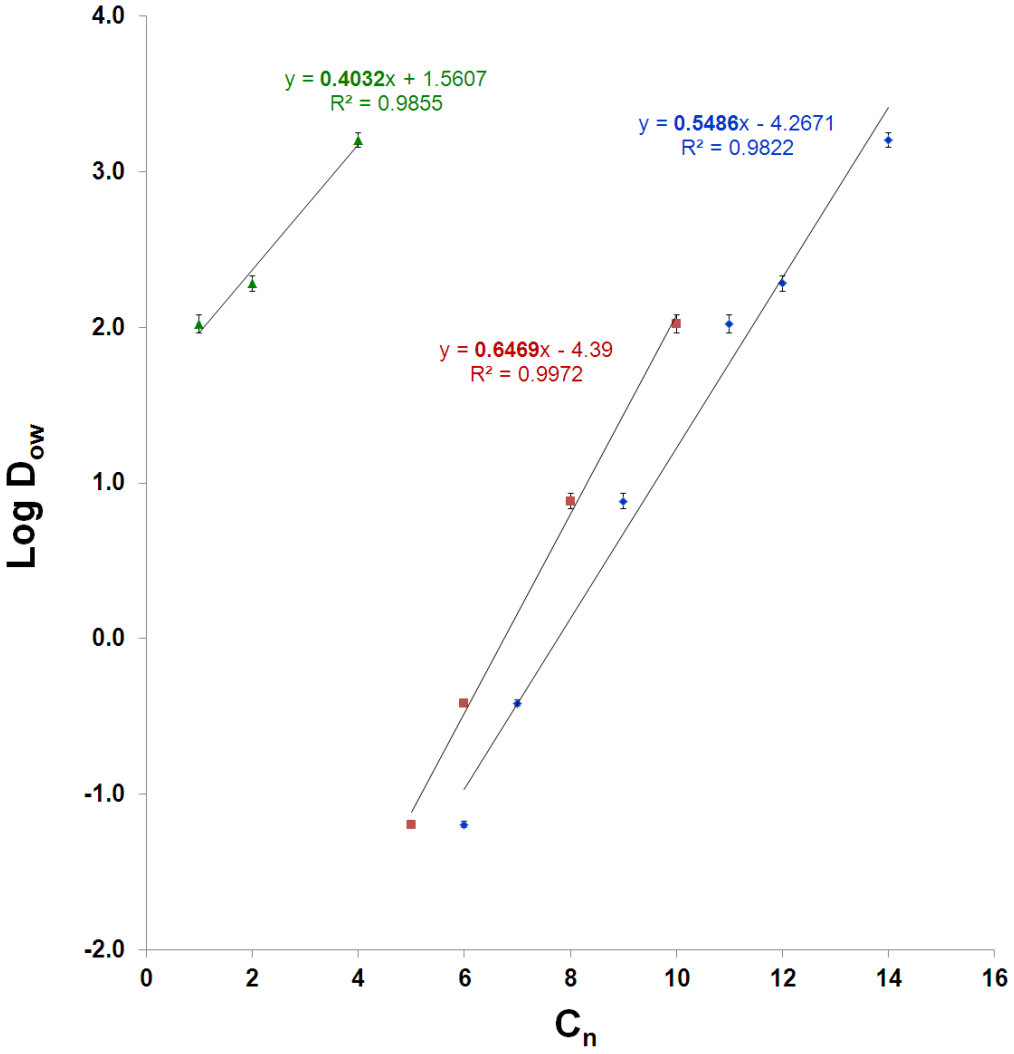


**Figure 6.3: Correlation of log Do,w for ILs obtained using the slow-stirring method with the carbon number ($C_n$) of the long alkyl chain of $C_nC_1imTf_2N$ (■), short alkyl chain of $C_{10}C_nimTf_2N$ (▲) and the sum of chains (◆).** The values are for $C_5C_1imTf_2N$, $C_6C_1imTf_2N$, $C_8C_1imTf_2N$, $C_{10}C_1imTf_2N$, $C_{10}C_2imTf_2N$, and $C_{10}C_4imTf_2N$. Error bars are the relative standard deviations of triplicate analysis at the 95% confidence interval.

If variations in the partitioning of the various ILs arise from differences in the free energy of transfer from one phase to the other (Eqn. 6-10), then previously reported values of ΔG associated with the transfer of a methylene group from water to the water-hydrocarbon interface (-3.0 to -3.5 kJ $mol^{-1}$) [6.35] or from water to the bulk hydrocarbon

solvent (-3.7 kJ $mol^{-1}$) [6.3], imply that a plot of log $D_{ow}$ versus carbon number should yield a curve with a slope that lies in the range of -0.53 to -0.66. That this is consistent with the correlation for the long chain increments and the sum of the alkyl chains, is not just interesting, but suggests that the methodology is performing well for our purposes of IL solvent behavior predictions. There appears, however, to be some significant deviation from that trend with in correlation to the short alkyl chain of the $C_{10}C_nimTf_2N$ homologous series. In attempting to understand these results, it must be recalled that solvent-solute interactions occur over a rather short range, and therefore, for amphiphiles like 1,3-dialkylimidazolium salts, the contributions from the hydrophobic tails and the hydrophilic head group may be, to some extent, considered independent [6.2]. The ordering of polar solvent groups by strong attractive forces in the polar imidazolium head group environment, especially by water molecules, is likely to predominate. Also, it is not probable that the head group will influence interactions distal to the point of attachment to the amine groups. Therefore, because the ILs studied here share a common head group, it is reasonable to assume that, for the same side-chain, the contribution to partitioning from the addition of methylene groups will in interval values, leading to a slope of the same proportion. Nevertheless, because the slope for the variation in the short chain of the $C_{10}C_nimTf_2N$ series is significantly less than that for the variation in the long chain length of $C_nC_1imTf_2N$, there must be a physical explanation. These results are consistent with prior studies [6.36, 6.37] demonstrating that the addition of a second, shorter alkyl tail to a charged head group (*i.e.*, sulfate and quaternary ammonium) already possessing a longer chain, will make a smaller contribution to a phase change (*i.e.*, free energy of critical micelle formation) than will the longer tail. Conversely, the effect of the

incremental augmentation of the longer chain will not be influenced by the presence of a shorter chain [6.36]. Although the aggregation of the solutes investigated is a different process than partitioning, both are governed by the hydrophobic effect, and will therefore be determined, at least in part, by the free energy change associated with the solute-solvent interactions. Taken together, these concepts suggest that of the data point for $C_{10}C_1imTf_2N$ in the short chain increment were replaced by that for another homologue with more methylene groups (*e.g.*, where n = 3, 5, or 6), then the slope would be closer to that for the long chain homologues. Unfortunately, not only are the *N*-propylimidazole and *N*-pentylimidazole precursors not commercially available, but they are difficult to synthesize. Along the same lines, the measurement of $D_{ow}$ for $C_{10}C_6imTf_2N$ has been stymied by its very low water solubility, making its detection difficult.

### 6.3.3 Correlation of $D_{ow}$ to the strontium extraction behavior of ionic liquids

For the distribution of ILs in the octanol-water partitioning system to be used as a parameter to design a scale of hydrophobicity related to their metal ion extraction behavior, a meaningful correlation must be obtained. That is, the equilibrium for metal ion extraction must be established by a process similar to that for the octanol-water biphase. Thus, the conditions chosen for metal ion extraction must be those for which ion-exchange of the IL cation for the metal-crown ether complex (Eqn. 3-2) predominates. Because this pathway dominates at very low nitric acid concentration for the most hydrophilic ILs, the correlation of log $D_{Sr}$ versus log $D_{ow}$ in Fig. 6.4 is based on data for extraction from 0.01 M $HNO_3$ into the $C_nC_1imTf_2N$ homologous series.

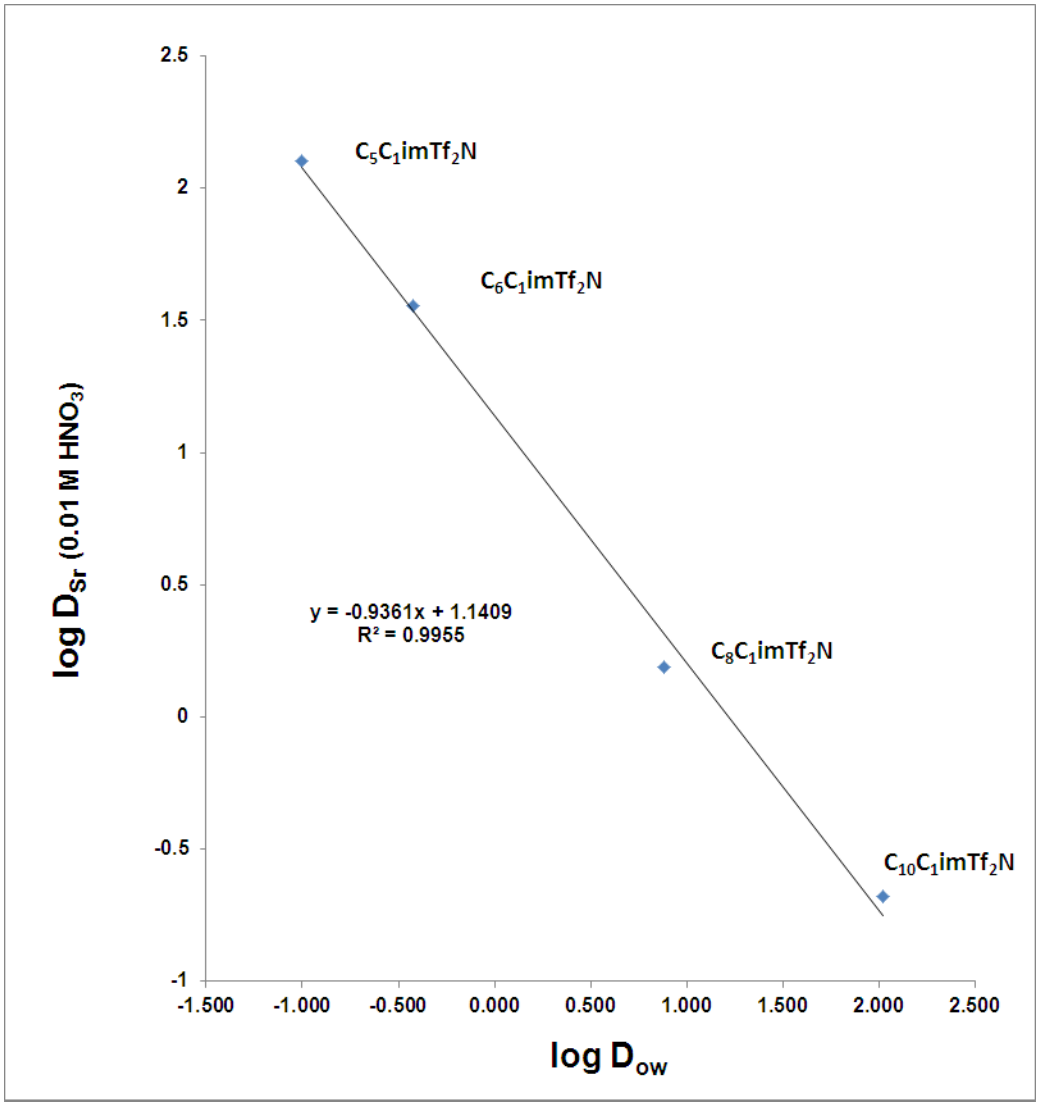


**Figure 6.4: Correlation of log $D_{Sr}$ with log $D_{ow}$ for various $C_nC_1imTf_2N$ ILs .** The $D_{Sr}$ experiments were performed using 0.10 M DCH18C6 in the IL.

The fact that the slope of the plot obtained at 0.01 M $HNO_3$ versus log $D_{ow}$ is nearly negative 1 is not surprising, given that it has been previously demonstrated that plot of log $K_{ex,Sr}$ versus carbon number [6.38] provides a line with a slope similar to the $C_nC_1imTf_2N$ series evaluated in section 6.3.2, which were both in accord with the free energy of the transfer of a $CH_2$ group between the phases. That both the relatively

hydrophobic $C_{10}C_1imTf_2N$ and hydrophilic $C_5C_1imTf_2N$ fit well on this curve, indicates again that, at low nitrate concentrations, the predominant pathway by which extraction occurs is ion exchange. Given that $C_{10}C_1imTf_2N$ has been recognized for $Sr^{2+}$ extraction behavior like that of a conventional solvent (Chapter 3), the log $D_{ow}$ of 2 for this compound may be considered as a benchmark for ILs which are to mimic the behavior of a conventional (molecular) solvent.

### 6.3.4 Chromatographic prediction of $D_{ow}$

Clearly, there is a direct relationship between the partitioning that occurs in the octanol-water system and the partitioning model of reversed-phase retention. However, normal-phase retention is also driven by solute polarity, and whether or not a partitioning mechanism is involved, a correlation may be possible. As a result of the evaluation of this HPLC method (see Chapter 5 section 5.4.2), the selectivity has been shown to be related to the hydrophobicity of the ILs. Therefore the retention of the ILs under these conditions should be comparable with other processes that are governed by their hydrophobicity. The plot in Figure 6.5 shows the relationship between log $D_{ow}$ and the retention factors of several $C_nC_1im$ ionic liquids, using the HPLC method developed and evaluated for their measurement (see Chapter 5). Reciprocal retention factors were used to display the relationship in terms of increasing IL hydrophobicity.

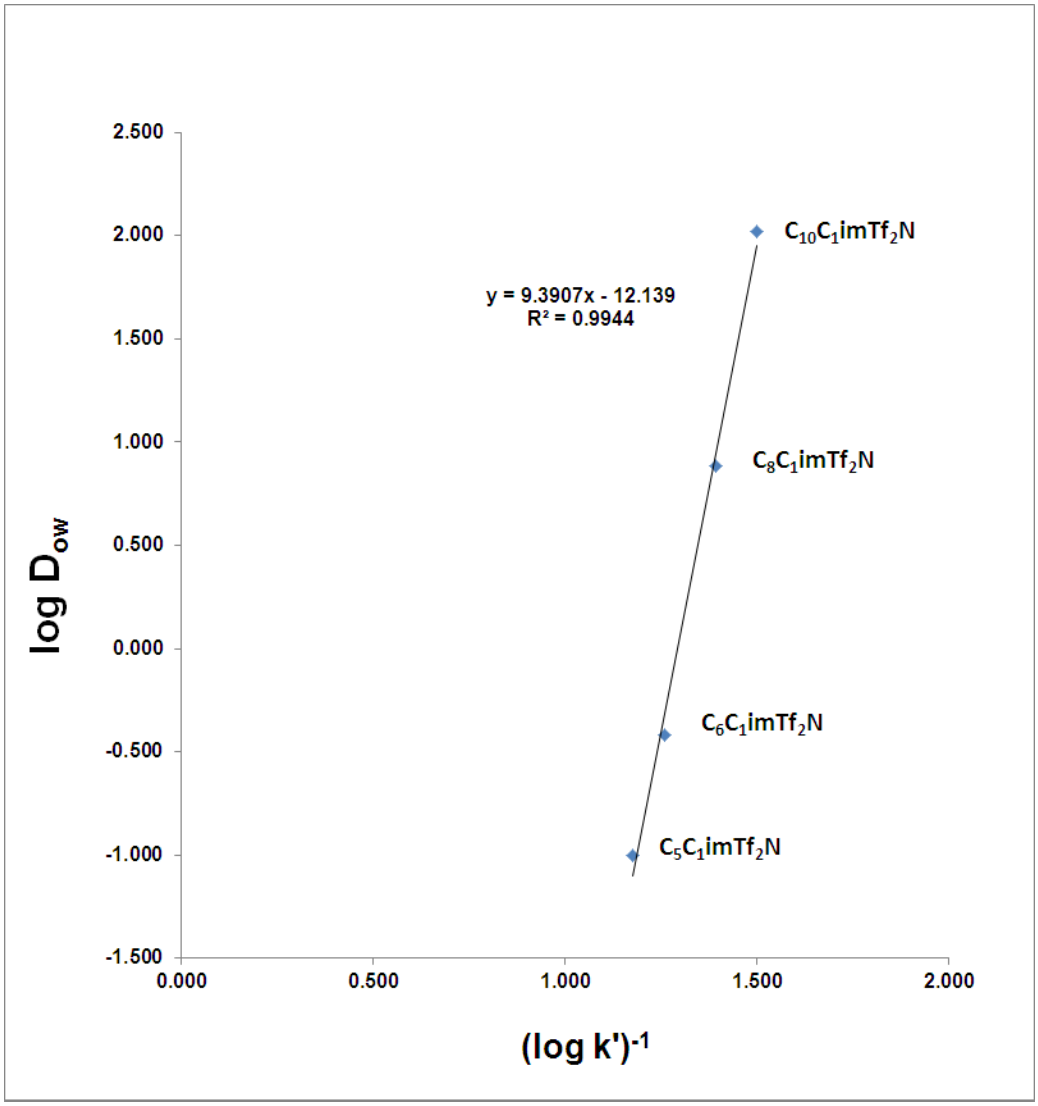


**Figure 6.5: Correlation of log $D_{ow}$ with the reciprocal log k' for various $C_nC_1imTf_2N$ ILs.**

These results contrast with previous reports [6.23] stating that retention mechanisms differing from strict partitioning by solvophobic interactions will not provide reliable correlations with octanol-water partition coefficients, suggesting that, at least for this system, the relationship between a normal phase ion-exchange mode of retention and $D_{ow}$ is correlatable, but not necessarily causal. It is understood that caution should be applied

when attempting to provide general guidelines for families of compounds on the basis of variables with such fundamental differences. Nevertheless, predictions can be made, at least within this homologous series. Furthermore, using the same systems, it may be possible to predict the log $D_{ow}$, and therefore estimate metal ion extraction behavior, for various other ILs that have chromophores (e.g., *N*-alkylpyridinium- and *N*-alkylquinolinium-based ILs) given a few homologues from either family.

### 6.4 Conclusions

The results reported here, while preliminary, provide important insight into the trends of IL hydrophobicity that can potentially form the basis of a practical hydrophobicity scale. Most importantly, by combining the correlation with $D_{ow}$ of the extraction of $Sr^{2+}$ from very dilute nitric acid into $C_nC_1imTf_2N$ and the shape of the nitric acid dependency of extraction into $C_{10}C_1Tf_2N$, a benchmark has been set for the observation of ion-pair extraction behavior into this family of ILs at a log $D_{ow}$ value of *ca*. 2. The relationship of partitioning of ILs with carbon number has afforded appropriate linear best fits to the $D_{ow}$ values determined by slow-stirring and are validated by the relationship of the slope to the free energy of transfer of a $CH_2$ group from water to 1-octanol. Interestingly, differences in results for log $D_{ow}$ versus carbon number of either alkyl tail indicate that evaluating the partitioning of 1,3-dialkylimidazolium ILs as solutes, and perhaps the partitioning of solutes in biphasic systems comprising these ILs may be approached from the standpoint of two-tailed amphiphiles. Differences observed between the shake-flask and slow-stirring method results are statistically significant, but they are quite small compared to the range of values measured. To determine truly accurate $D_{ow}$ values,

however, a systematic evaluation of the concentration dependence of the $D_{ow}$ for these ILs would yield values that are comparable to others [6.16, 6.17], who obtained data by a rigorous treatment (*i.e.*, extrapolation to infinite dilution). Although the accuracy of the octanol-water distribution ratios reported here remains in question due to their possible concentration dependence, the compelling correlations provided therefrom speak to the validity of the intervals generated. Provided that the experimental results are reproducible, then their absolute accuracy is not essential to predict IL hydrophobicity for the means of this laboratory. Furthermore, to put these issues of accuracy into perspective, the concentrations employed for the $D_{ow}$ measurements are comparable to those that might be found in our extraction studies, thus providing data valuable to the prediction of the metal ion extraction behavior of ILs.

### 6.6 References

[6.1] SciFinder Scholar, web version September 2012; Chemical Abstracts Service: Columbus, OH, 2007; RN 58-08-2 (accessed 30 November 2012).

[6.2] C. Tanford, *The Hydrophobic Effect: Formation of Micelles and Biological Membranes*, Wiley, New York, **1973**.

[6.3] F. MacRitchie, *Chemistry at Interfaces,* Academic Press, Inc. San Diego, CA, **1990**.

[6.4] W. Kauzmann, *Adv. Protein Chem.* **1959**, 14, 1.

[6.5] K.A. Dill, *Biochemistry*, **1990**, 29, 7133-7155.

[6.6] E. Wilhelm, R. Battino, R.J. Wilcock, *Chem. Rev*. 1977, 77, 219-262.

[6.7] C. Tanford, Science, 1978, 200, 1012-1018.

[6.8] J. Sangster, *J. Phys. Chem. Ref. Data*, **1989**, 18, 1111-1229.

[6.9] R. Collander, *Ann. Rev. Plant Physiol*.**1957**, 8, 335-348.

[6.10] C. Hansch, J.E. Quinlan, G.L. Lawrence,. *J. Org. Chem*. **1968**, 33, 347-350.

[6.11] A. Leo, C. Hansch, D. Elkins, *Chem. Rev. 1971*, 71, 525-616.

[6.12] C.J. van Leeuwen, T.G. Vermeire, *Risk Assessment of Chemicals: An Introduction*, Springer, 2007.

[6.13] N.P. Franks, W.R. Lieb, *Nature*, 1994, 367, 607-614.

[6.14] N.V. Plechkova, K.R. Seddon, Chem. Soc. Rev. **2008**, 37, 123–150.

[6.15] L. Ropel, L.S. Belvéze, S.N.V.K. Aki, M.A. Stadtherr and J.F. Brennecke, Green Chem. **2005**, 7, 83-90.

[6.16] S.H. Lee, S.B. Lee, *J. Chem. Technol. Biotechnol*. **2009**, 84, 202-207.

[6.17] S.P.M. Ventura, R.L. Gardas, F. Gonçalves, J.A.P. Coutinho, *J. Chem. Technol. Biotechnol*., 2011, 86, 957-963.

[6.18] M.J. Kamlet, R.M. Doherty, M.H. Abraham, Y. Marcus, and R. W. Taft, *J. Phys. Chem.* **1988,** 92, 5244-5255.

[6.19] L. P. Burkhard, A. W. Andrew, D. E. Armstrong, *Chemosphere*, **1983**, 12, 935. 943.

[6.20] A.J. Leo, *Chem. Rev.* **1993**, 93, 1281-1306.

[6.21] E.H. Kerns, *J. Pharm. Sci*. 2001, 90, 1838-1858.

[6.22] C-W. Cho, U. Preiss, C. Jungnickel, S. Stolte, J. Arning, J. Ranke, A. Klamt, I. Krossing, J. Thöming, *J. Phys. Chem. B*, **2011**, 115, 6040–6050.

[6.23] J. De Bruijn, F. Busser, W. Seinen, J. Hermens, *Environ. Toxicol.Chem*. 1989, 8, 499-512.

[6.24] H. DeVoe, M.M. Miller, S.P. Wasik, *J. Res. Natl. Bur.Stand. (U.S.)* **1981**, 86, 361-366.

[6.25] G.D. Veith, N.M. Austin, R.T. Morris, *Wat. Res.* **1979**, 13, 43-47.

[6.26] M-M. Hsieh, J.G. Dorsey, *Anal. Chem*. **1995**, 67, 48-57.

[6.27] K. Valcó, C. Bevan, D. Reynolds, *Anal. Chem*. **1997**, 69, 2022-2029.

[6.28] J.G. Krass, B. Jastorff, H-G. Genesier, *Anal. Chem.* **1997**, 69, 2575-2581.

[6.29] J.W. Dolan, A. Mauleb, D. Bingley, L. Wrisley, C.C. Chan, M. Angod, C. Luntee, R. Krisko, J.M. Winston, B.A. Homeier, D.V. McCalley, L.R. Snyder, J. Chrom. A, 2004, 1057, 59-74.

[6.30] J. Ranke, A. Müller, U. Bottin-Weber, F. Stock, S Stolte, J. Arning, R. Störmann, N Jastorff, *Ecotoxicol. Environ. Safety*, **2007**, 67, 430-438.

[6.31] J. Ranke, A. Othman, P Fan, A. Müller, *Int. J. Mol. Sci*. **2009**, 10, 1271-1289.

[6.32] D.N. Brooke, A.J. Dobbs, N. Williams, Ecotoxicol. Environ. Safety, **1986**, 11 251-260.

[6.33] S. Gocan, G. Cimpan, J. Comer, *Advances in Chromatography v. 44: Lipophilicity Measurements by Liquid Chromatography*, , CRC Press, Boca Raton, FL, **2006**, 79-176.

[6.34] M. Blesic, M.H. Marques, N. V. Plechkova, K.R. Seddon, L.P. N. Rebelo, A. Lopes, *Green Chem*. **2007**, 9, 481–490.

[6.35] M.J. Rosen, *Surfactants and Interfacial Phenomena*, Wiley, New York, **1989**.

[6.36] H.C. Evans, *J. Chem. Soc*., **1956**, 579-586.

[6.37] K.T. Shinoda, T. Nakagawa, B. Tamamushi, T. Isemura, *Colloid Surfactant*, Academic Press, New York, **1963**.

[6.38] M.L. Dietz, J.A. Dzielawa, *Chem. Commun*. 2001, 2124-2125.

# CHAPTER 7:

# PLACING QUALITATIVE TRENDS OF METAL ION EXTRACTION INTO A QUANTITATIVE CONTEXT

## 7.1 Introduction

The analysis in Chapters 3 and 4 described our current understanding of the extraction of metal ions into room-temperature ionic liquids, highlighting the similarities and differences versus extraction systems utilizing molecular diluents (*i.e.*, 1-octanol) and providing insight into the key factors (*e.g.*, metal cation charge density, IL hydrophobicity, the nature of the aqueous phase anion) that determine the balance among the possible modes of extraction. Trends observed in the nitric acid dependencies of alkali and alkaline earth cation extraction, for instance, were explained by a three-path model including ion-pair (neutral complex) extraction, ion exchange of the cationic complex for the IL cation, and crown ether-mediated ion exchange. To date, the information provided by evaluating these acid dependencies has been largely qualitative in nature. Understanding the origins of the observed trends, however, requires a more quantitative approach, in which the interplay among the three equilibria is considered. Therefore, to provide a less ambiguous description of the processes involved in extraction, methods to measure their separate contributions must be developed. It is anticipated that by elucidating the individual contributions of the pathways over the range of conditions employed in the acid dependencies, an improved understanding of the conditions that may provide the best extraction behavior may result. For instance, an understanding of the magnitude of the contribution from ion-exchange modes under various conditions could guide the development of processes for which these pathways

are either required or undesirable. As noted previously, an ideal process for the extraction of strontium is one in which the contribution from ion exchange is minimized, high extraction efficiencies and selectivities at modest acidities are maintained, and the stripping of the IL phase with dilute acid is feasible. The present study is aimed at developing techniques to facilitate in the investigation of the effects of individual pathways on the overall metal ion distribution ratios.

The approach by which the contributions to extraction from individual pathways can be elucidated is not as straightforward as it might seem. In the case of the determination of the co-extraction of nitrate (*i.e.*, ion-pair extraction), for instance, the typical technique employed involves the measurement of the aqueous phase depletion by analysis of the solution before and after extraction using ion chromatography (IC) [7.2, 7.3]. The cadmium reduction colorimetric method could be employed as an alternative to IC [7.4], but wet chemical methods are laborious and time-consuming. Neither of these methods, however, are viable for samples taken under the conditions of a typical extraction, which ivolves molar concentrations of acid, while the depletion of the aqueous phase anion is likely to be orders of magnitude lower. To accurately measure a small change superimposed on such a large background presents a significant challenge. In a few cases, another method that can be used to avoid such difficulties is $^{15}$N-NMR [7.2]. Yet performing this measurement on a regular basis using a $^{15}$N-labelled nitrate source would be prohibitively expensive. Perhaps the best choice of methodology for high acid conditions would be one that measures the anion concentration directly in the IL phase. Anion determination in organic solvents has been performed primarily using modern IC techniques [7.5, 7.6]. These usually involve the simultaneous analysis of various anions

(e.g., carboxylates, chloride, nitrate, sulfate) in water-miscible solvents such as alcohols, ketones, dimethyl sulfoxide, and acetonitrile. The organic phase to be tested in the current studies, however, is a water-immiscible solution of DCH18C6 in a hydrophobic IL. Therefore, a water-miscible diluent will be evaluated for use as a sample diluent. The details of this method development will be provided in the Methods section (7.2.3).

## 7.2 Experimental

### 7.2.1 Materials

All chemicals were reagent grade and used without additional purification, unless noted otherwise. All aqueous solutions were prepared using deionized water with a specific resistance of at least 18 $M\Omega \cdot cm^{-1}$. Strontium nitrate solutions were prepared from the dried (110°C for at least 4 hours) salt (Aldrich, Milwaukee, WI) and diluted with water to the appropriate concentrations. The DCH18C6 (Parish Chemical, Orem, UT) employed was a mixture of the *cis-syn-cis* and *cis-anti-cis* isomers and was used as received. The HPLC mobile phase buffer was prepared by combining equal parts 500 mM formic acid (puriss., Sigma-Aldrich, St. Louis, MO) and 500 mM ammonium formate (J.T. Baker, supplied by VWR Chicago, IL) which resulted in a pH of 3.7. The HPLC mobile phase was prepared by combining 10.0 mL of the formate buffer with 40.0 mL of water and 450 mL of acetonitrile (Honeywell Burdick and Jackson, HPLC grade, supplied by VWR Chicago, IL) to produce a 10 mM buffer concentration in 90:10 acetonitrile:water for analysis. Ion chromatographic eluents were prepared from either saturated sodium hydroxide solution (puriss., Fluka, Milwaukee, WI) or methanesulfonic acid (puriss., Fluka, Milwaukee, WI). Methanol used as a diluent was HPLC grade,

manufactured by Honeywell Burdick and Jackson, and purchased from VWR Chicago, IL. A strontium standard solution (J.T. Baker, INSTRA-ANALYZED®) was used to determine (by IC) the concentration of strontium nitrate solutions. A $^{85}Sr$ radiotracer of was purchased as a nominal solution from Eckert and Ziegler Isotope Products, Inc. (Valencia, CA).

7.2.2 Instruments

Gamma spectroscopy was performed using a PerkinElmer model 2480 automatic gamma counter equipped with WIZARD2 software. The HPLC system comprised a set of Agilent 1200 series analytical binary pumps equipped with an online degasser, a fixed loop manual injection port, and a variable wavelength UV-VIS flow cell, and ChemStation software. The column was a 75 mm x 3.0 I.D. Agilent Zorbax HILIC Plus silica column with 3.5 μm average particle size. The final conditions for HPLC analysis were an isocratic flow rate of 0.800 mL $min^{-1}$ with 10 mM ammonium formate buffer (pH 3.7) in 90:10 acetonitrile:water. The column temperature was maintained at 30°C, and the injection volume of 20 μL, and detection at 210 nm. Nitrate concentrations in the IL phase were determined using a Dionex ICS-1000 ion chromatograph equipped with a 25 μL fixed-loop manual injection port, a conductivity detector, Dionex AS18/AG18 analytical and guard columns (4 X 250 and 4 X 50 mm), a Dionex ASRS 300 (4 mm) conductivity suppressor, and 37 mM NaOH eluent. The instrument was operated using Chromeleon software version 6.80. Strontium concentrations in water (before and after extraction) were measured using the same ion chromatograph equipped with Dionex CS12A analytical and CG12A guard columns (4 x 250 and 4 x 50 mm), and 30 mM

methanesulfonic acid eluent. IC eluent flow rates were 1.00 mL/min, and the column temperature was maintained at 30°C.

### 7.2.3 Methods

Distribution ratios ($D_M$) were determined as a ratio of the count rate in the organic phase to that of the aqueous phase using commercial radiotracers, assayed *via* gamma spectroscopy or liquid scintillation counting using standard procedures. In each metal distribution experiment, the organic phase consisted of DCH18C6 dissolved in the designated ionic liquid, and the aqueous phase nitric acid concentration was systematically adjusted either by conducting separate experiments for each condition, or adding acid after each condition had been sampled. Unless otherwise noted, acid dependencies for metal extraction were performed at 0.1 M DCH18C6 in the organic phase. All organic phases were pre-equilibrated with aqueous phase prior to the introduction of the metal ions or radiotracer. Each equilibrated phase was sampled for analysis in at least duplicate with resulting uncertainties based on counting statistics that were generally within 10%, although the uncertainty interval was considerably wider for the highest distribution ratios values ($D_M \geq 1000$). Additionally, for radiometric measurements, the sum of the count rates in each phase yielded recoveries within 10% of the radiotracer stock solution used, indicating that equilibrium was established with only two phases involved. Nitric acid concentrations were determined by titration with a standard sodium hydroxide solution (Ricca Chemical Company, Arlington, TX).

The concentration of anions in organic solvents was determined by the standard addition method to avoid variability in elution and response due to matrix effects [7.6].

However, if the samples are sufficiently diluted in the same solvent as the standards, then matrix effects will be minimal and direct external standardization may be employed. Thus, the development of a method for the determination of the nitrate ion concentration in the IL phase began by evaluating two different diluents for the IL phase: 30% methanol or 50% acetonitrile in water. A 30% methanol diluent resulted in poor chromatography and a lower response than desired. The lower limit of quantification (LLOQ, calculated from the standard error of the estimate) using this composition was 2 ppm. By injecting blank 30% methanol it was determined that the large baseline disturbance in Fig. 7.1 panel A was due to the interference band from elution of the sample plug as it passed through the eluent suppressor. That is, the alcohol was being electrolytically reduced in the suppressor. Acetonitrile was therefore explored as an aprotic, less reactive alternative. Though an interference band was associated with acetonitrile as well (Fig. 7.1 panel B), the baseline was significantly improved, leading to a LLOQ of 0.2 ppm nitrate, ten-fold less than obtained with 30% methanol. In addition to the favorable LLOQ, an RSD (n=4) of 3%, 101% recovery at 1.0 ppm for a sample of IL diluted with 50% acetonitrile, and a calibration curve (0.1 ppm to 10 ppm) providing good linearity ($R^2 > 0.999$), all demonstrate that the method using 50% acetonitrile diluent was sufficient to determine nitrate in the IL phase post-extraction.

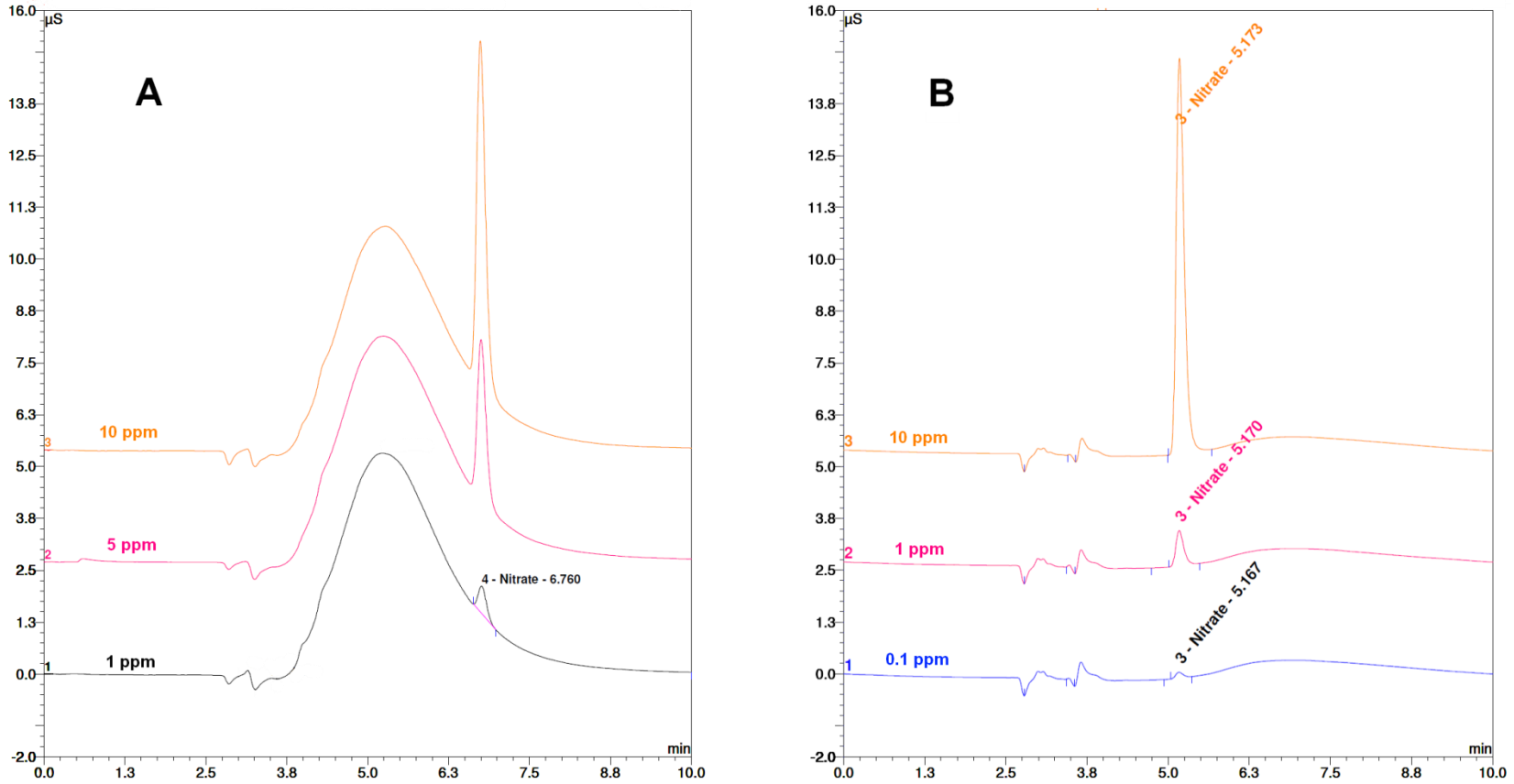


**Figure 7.1: Overlay of chromatograms from the injection of nitrate ion standards in (A) 30% methanol diluent and (B) 50% acetonitrile diluent.**

Samples were prepared by the following procedure. A solutions of 0.10 M DCH18C6 in $C_5C_1imTf_2N$ or neat $C_5C_1imTf_2N$ was preconditioned by vortex mixing with twice the volume of water, disengaging the phases by centrifugation at 3000 rcf, and discarding the aqueous phase to obtain the conditioned IL phase. Extraction was performed by vortex mixing the conditioned IL phase with an equal volume of the appropriate aqueous strontium nitrate solution, disengaging the phases by centrifugation at 3000 rcf, and separating the phases for further sample processing. Nitrate determination in the IL phase was performed by weighing 136.7 mg of the IL in a 10.00 mL volumetric flask (grade A) and dissolving in acetonitrile. The IL sample was further diluted by 20-fold with 50% acetonitrile in water before injection on the IC. The density of the IL phase post-extraction was determined by averaging the weight of of four 0.100 mL aliquots taken from the IL phase. The IC standard calibrators (0.1 ppm to 10 ppm nitrate) were prepared by dilution of an standard nitrate solution (Fluka Analytical, TraceCERT®) in the 50% acetonitrile diluent used for the sample. The aqueous phase was analyzed for $C_5C_1im^+$ by the HPLC-UV method provided in section 7.2.2, using a standard prepared from the dried (80°C in vacuo ≥ 12 hours) IL synthesized in-house. Aqueous samples from the extraction were diluted 10-fold in acetonitrile prior to injection on the HPLC. Extractions without crown ether present were used to determine the innate solubility of the IL in the aqueous phase, which was subtracted from the amount with crown ether present to determine the increase in dissolution.

## 7.3 Measuring the contributions of two prominent pathways

### 7.3.1 Extraction of strontium from water by DCH18C6 in $C_5C_1imTf_2N$

Using the HPLC-UV method (Chapter 5) and the ion chromatographic approach described in section 7.2.3, the pathways contributing to the extraction of strontium nitrate from water into $C_5C_1imTf_2N$ have been evaluated. Prior studies [7.7] on this system have demonstrated that the aqueous solubility of the $C_5C_1im^+$ ion increases with the extraction of $Sr^{2+}$ at a ratio consistent with the 2:1 stoichiometry in Eqn 7-1.

$$Sr\bullet DCH18C6^{2+} + 2\ IL^+_{\ IL} \leftrightharpoons Sr\bullet DCH18C6^{2+}_{\ IL} + 2\ IL^+ \qquad (7\text{-}1)$$

However, studies [7.2] of the co-extraction of nitrate under similar conditions have shown that an amount of nitrate corresponding to approximately 10% of the amount of strontium extracted is also transferred into the IL phase. Because the aqueous phase in this case is a neutral solution of $Sr(NO_3)_2$, the electroneutrality requirement in this system means that those nitrate ions must be accompanied by an equivalent of cations or that an equivalent of anions from the IL phase must be transferred to the aqueous phase. In light of the hydrophobicity of $Tf_2N$ and a lack of precedence for anion exchange or ion-pair extraction *via* $Tf_2N$ in these systems [7.7], the explanation for the co-extraction of nitrate from water into the IL phase must be that it is accompanied by an equivalent of $Sr^{2+}$ *via* the ion-pair partitioning pathway depicted in Eqn. 7-2.

$$Sr^{2+} + 2\ NO_3^- + DCH18C6_{IL} \leftrightharpoons Sr(NO_3)_2\bullet DCH18C6_{IL} \qquad (7\text{-}2)$$

The plots in Fig. 7.2 depict the relationship between the aqueous phase concentration of the IL cation following extraction of $Sr^{2+}$ by DCH18C6 in $C_5C_1imTf_2N$ and the initial aqueous phase concentration of $Sr(NO_3)_2$.

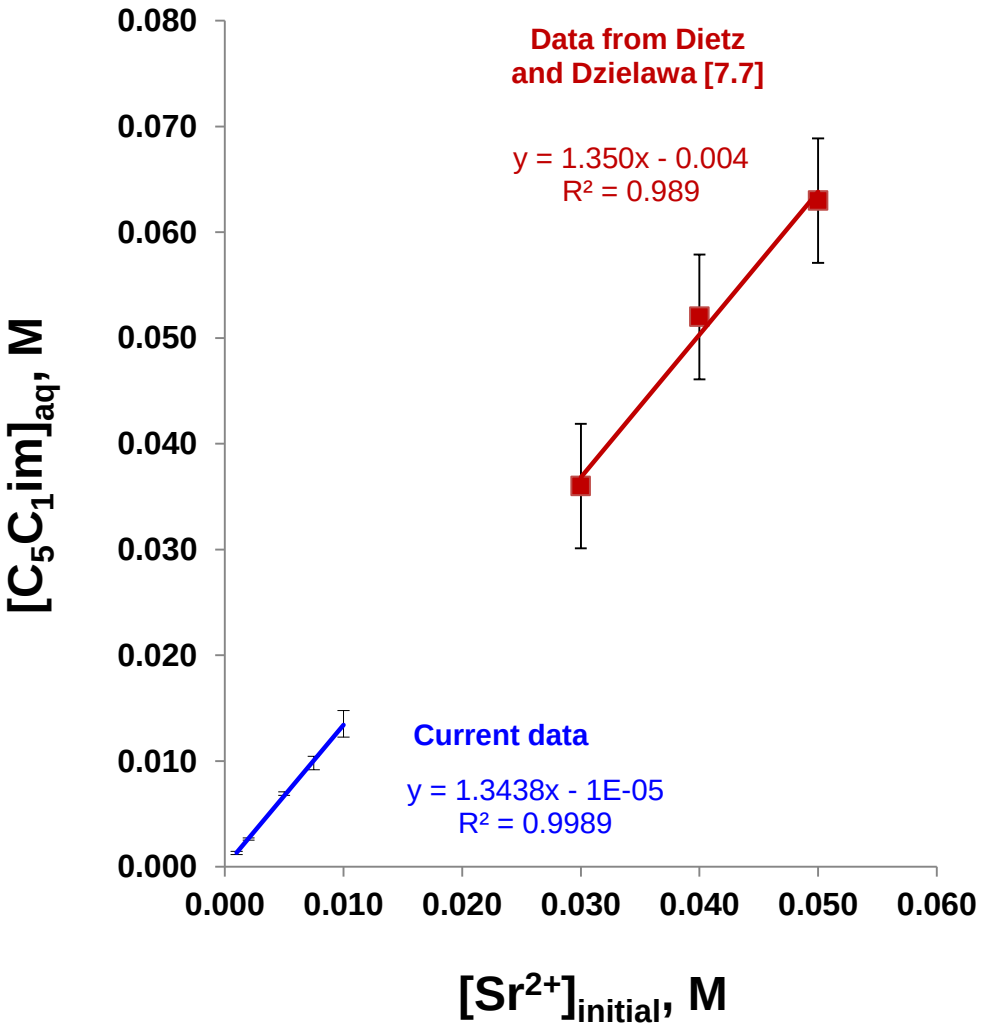


**Figure 7.2: Effect of the initial concentration of $Sr(NO_3)_2$ (1-10 mM and 30-50 mM) on the dissolution of $C_5C_1im^+$ in water in the extraction of strontium by DCH18C6 (0.10 M) in $C_5C_1imTf_2N$.** Curves are linear least-squares fits. Error bars are the standard error of the estimate for previous data [7.7] and based-on standard deviations (n=3) at the 95% confidence interval for the current data.

Upon examination, it is immediately apparent that although the plots agree well with one another, the observed slopes deviate from the value of 2 expected if the only partitioning mode were that defined by Eqn. 7-1. In fact, they are approximately 33% lower than anticipated – a difference that can *only* be attributed to the contribution from the neutral complex/ion-pair partitioning mode (Eqn.7-2). The occurrence of both partitioning modes in this system would not be unexpected given that the solubility of $C_5C_1imTf_2N$ in water is 0.03 M [7.7] and the solubility of water in $C_5C_1imTf_2N$ is nearly 1 M (Chapter 4 Table 4.2), providing favorable conditions for ion exchange and ion pair extraction, respectively.

### 7.3.2 Results for the determination of two contributions by subtraction

Emerging from these insightful results is a question: How much of each pathway is involved? To resolve this question, one must examine, if possible, the equilibrium concentrations of the species associated with each process, or determine the amount of one process that is measureable and subtract that contribution from the total metal ion extraction to attain the other. Therefore, the values to be measured in the system at hand are the overall $Sr^{2+}$ extraction (total by gamma spectroscopy), the IL cation solubilization in the aqueous phase (ion exchange, by HPLC-UV), and nitrate co-extraction (ion-pair, by IC). Note that they must be considered over a range of $Sr(NO_3)_2$ concentrations that do not approach the capacity of the available DCH18C6 ligands in the IL phase. By comparing the amount of ion exchange of the IL cation or the amount of nitrate extracted into the IL to the total $Sr^{2+}$ extracted, their relative contributions can be determined. In the present experiment, the contribution from ion-pair extraction based on the equilibrium

nitrate concentration in the IL phase was subtracted from the total $Sr^{2+}$ extracted to estimate the contribution from ion exchange. The system of $Sr^{2+}$ extraction from water was chosen for this study because one should be able to arrive at a similar result by the subtraction of the ion exchange component from the total extraction, yielding an estimate of the contribution from ion-pair extraction.

Table 7.1 provides the results for the determination of the total $Sr^{2+}$ extraction from 7.90 mM $Sr(NO_3)_2$ into 0.10 M DCH18C6 in $C_5C_1imTf_2N$, the theoretical metal-nitrato complex extraction contribution, and the contribution of ion exchange predicted from difference of ion pair from the total. Included for comparison, is the contribution from ion exchange determined by the excess dissolution of the IL cation in the aqueous phase upon extraction.

**Table 7.1**
**Relative contributions from ion exchange and ion pair partitioning to the extraction of strontium ions from water into 0.10 M DCH18C6 in $C_5C_1imTf_2N$**

| **Total $Sr^{2+}$ Extraction** [a] | | |
|---|---|---|
| **$D_{Sr\text{-}85}$ with 7.9 mM $Sr(NO_3)_2$** | **$\%E_{Sr}$** | **Total $Sr^{2+}_{(IL)}$, mM** |
| 125 ± 6 | 99.2% | 7.86 ± 0.4 |
| **Contribution from Ion Pair Extraction** [a] | | |
| **$[NO_3^-]$IL, mM** | **Theoretical $Sr^{2+}$ Extracted** | **$\%E_{Sr}$ by ion pair** |
| 6.18 ± 0.2 | 3.1 ± 0.09 | 40 ± 4% |
| **Percent Contribution from Ion Exchange** [a] | | |
| **$\%E_{Sr}$ by difference from ion-pair** | **Based on $[C_5C_1im^+]_{aq}$ (HPLC-UV)** | |
| 60 ± 5% | 67 ± 5% | |

[a] Uncertainties reported are for the sum of error from instrumental analysis and standard deviations of four replicates for each measurement at the 95% confidence interval

The estimation of the influence of ion exchange based on the determination of the nitrate co-extracted into the IL is in reasonable agreement with the value determined directly by the measurement of the excess dissolution of $C_5C_1im^+$ in the aqueous phase. That the measurements of the percent contributions to $Sr^{2+}$ extraction resulted in uncertainties on the order of that expected (± 10%) for these techniques, is encouraging. Still, how the 40% of extraction from the ion pair pathway is the missing fraction which led to the lower slopes of the plots in Fig. 7.2 is not initially evident. To make this assessment, the plots in Fig. 7.3 are the best fit curves for the dissolution of $C_5C_1im^+$ and that which has been adjusted by 40% extraction, both with respect to all amounts of strontium extracted into the IL phase. The adjusted values of $[C_5C_1im^+]_{aq}$ result in a slope (1.93) that is within 3% of that expected for the second order reaction in Eqn. 7-1. This result verifies the accuracy of the method for the determination of the contributions by subtraction of one partitioning mode from the other.

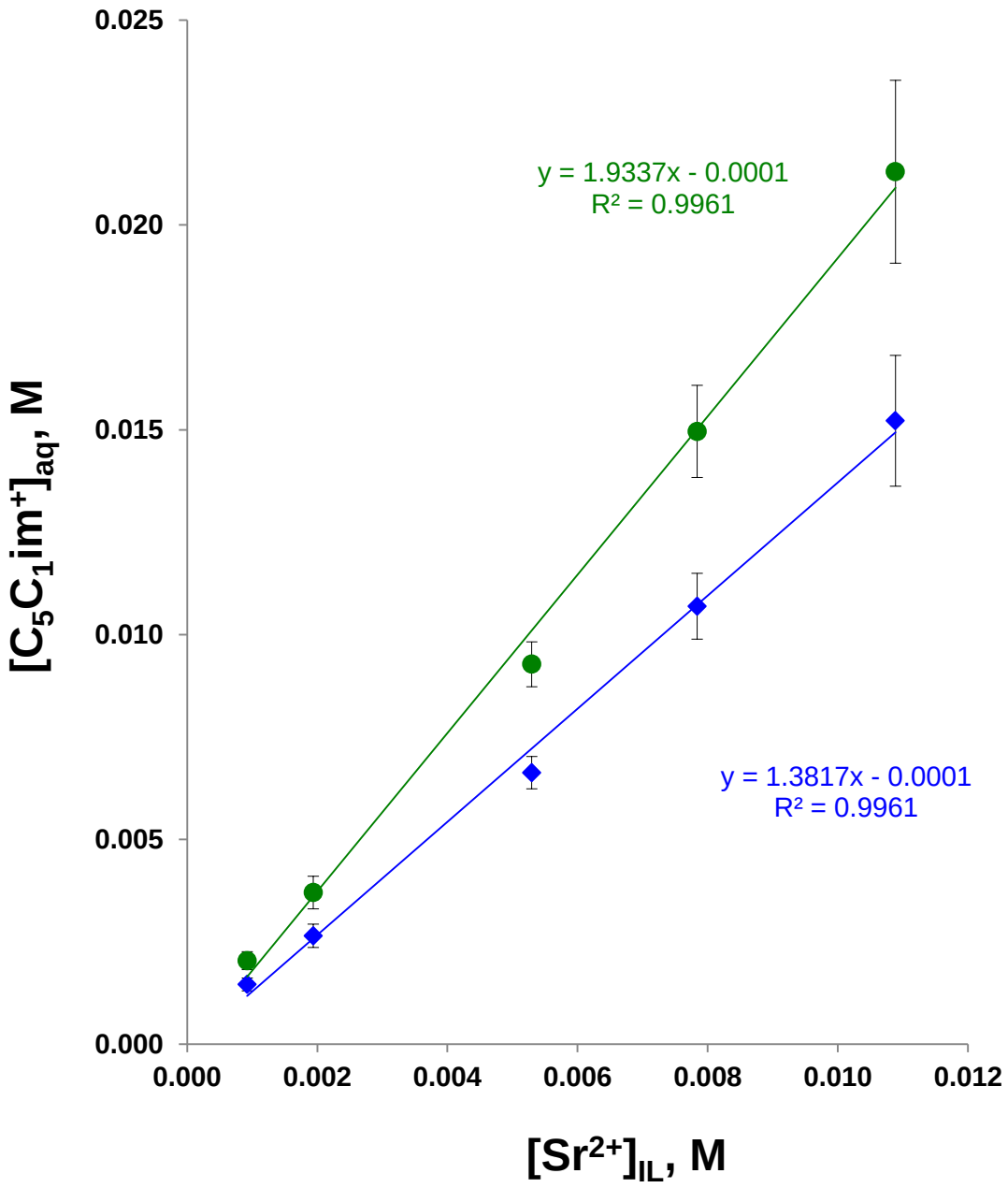


**Figure 7.3: The effect of strontium extraction by DCH18C6 (0.10 M) in $C_5C_1imTf_2N$ on the dissolution of $C_5C_1im^+$ in the water.** Plot symbols represent (◆) for the $[C_5C_1im^+]_{aq}$ from ion exchange only and (●) for the $[C_5C_1im^+]_{aq}$ + the contribution from ion pair extraction. Curves are linear least-squares fits. Error bars based-on standard deviations (n=3) at the 95% confidence interval for the current data.

## 7.4 Conclusions

The methodologies introduced in this study represent the first efforts to establish the relative contributions of the various metal ion extraction pathways involving IL solvents. A new method for the direct determination of nitrate co-extraction into the IL phase has been developed and shows promise to provide a means to measure the contribution from ion pair extraction. The conditions chosen for this experiment were such that either ion exchange or ion pair extraction could be determined independently. However, that the results are comparable from each approach by difference from the total $\%E_{Sr}$, indicates that similar techniques may be used for analysis of highly acidic conditions, for which the amount of nitrate extraction from conditioning must be accounted. The HPLC-UV method for IL cation quantification has again proven to be quite useful, and is expected to perform very well with samples from highly acidic media, because nitrate is not appreciably retained on the column. By subtracting the contributions to total $Sr^{2+}$ extraction from the ion pair and ion exchange pathways shown here, it is anticipated that the influence from the pathway of crown ether-mediated ion exchange may be elucidated. Studies to determine if this approach will work in actual practice are currently underway.

## 7.5 References

[7.1] E.P. Horwitz, M.L. Dietz, D.E. Fisher, *Solv.Ext. Ion Exch*. **1990**, 8, 199-208.

[7.2] M.L. Dietz, J.A. Dzielawa, I. Laszak, B.A. Young, M.P. Jensen, *Green Chem*. **2003**, 5, 682-685.

[7.3] C.A. Hawkins, S.L. Garvey, M.L. Dietz, *Sep. Purif. Technol*., **2012**, 89, 31-38.

[7.4] E.M. Burke, F. X. Suarez, D.C. Hillman, E. M. Heithmar, Water Res. 1989, 23,519-521.

[7.5] G.M Sergeev, M.S Blinova, J. Chrom. A. 1999, 847, 345-349.

[7.6] *Determination of Trace Anions in Organic Solvents*, DIONEX Application Note 85, http://www.dionex.com/en-us/webdocs/4173-AN85_LPN0482-03.pdf, accessed on 07 November 2012.

[7.7] M.L. Dietz, J.A. Dzielawa, *Chem. Commun*., **2001**, 2124-2125.

# CHAPTER 8:

# EFFORTS TOWARD IMPROVED METAL ION EXTRACTION SYSTEMS BASED ON IONIC LIQUIDS

## 8.1 Introduction

This research program has its origins in the belief that new metal ion separation systems based on RTILs could succeed in providing significantly greater extraction efficiency and selectivity for elements of interest (*i.e.*, strontium) than conventional solvents. This is, in fact, what has generally been found to hold true under various conditions in the extraction of $Sr^{2+}$ from aqueous acidic nitrate media by crown ethers in sufficiently hydrophobic ILs [8.1]. For example, employing 0.10 M DCH18C6 in $C_{10}C_1imTf_2N$ at 2 M to 3 M nitric acid, the $Sr^{2+}$ extraction efficiencies and the selectivities for $Sr^{2+}$ versus $Na^+$ are approximately 5-fold greater than those in 1-octanol (8.1, Chapter 3]. Similar, but more gainful conditions are provided by $C_{12}OHC_4imTf_2N$, in which the extraction efficiencies are 5- to 15-fold those of 1-octanol and selectivities of $Sr^{2+}$ versus $Na^+$ are close to 5-fold those in 1-octanol, all other conditions being the same [8.2, Chapter 4]. Such improvements in solvent extraction behavior using ILs have the potential to substantially increase the capacity and throughput of practical Sr-selective extraction systems. Moreover, the advantages of using ILs over paraffinic alcohols include their non-volatility, non-flammability, and the structural flexibility allowing facile modification of certain of their physicochemical properties. On the basis of what we now know about the behavior of ILs as extraction solvents for metal ions, the current studies attempts have been made to assess the feasibility of employing ILs as the basis for practical extraction media.

## 8.2 Experimental

### 8.2.1 Materials

All chemicals were reagent grade and used without additional purification, unless noted otherwise. All aqueous solutions were prepared using deionized water with a specific resistance of at least 18 $M\Omega \cdot cm^{-1}$. Dicyclohexano-18-crown-6 ether (DCH18C6) was purchased from Parish Chemical (Orem, UT) as a mixture of the *cis-syn-cis* and *cis-anti-cis* isomers. 4,4',(5')-di(*tert*-butyl-cyclohexano)-18-crown-6 (DtBuCH18C6) was obtained from EiChroM Technologies, Inc. (Lisle, IL). The 4z,5'z-*cis-syn-cis*-DtBu18C6 isomer has been isolated by A. Pawlak *via* precipitation with perchloric acid. Strontium nitrate solutions were prepared from the dried (110°C for at least 4 hours) salt (Aldrich, Milwaukee, WI). The strontium-85 and sodium-22 radiotracers wre purchased as nominal solutions from Eckert and Ziegler Isotope Products, Inc. (Valencia, CA). Ion chromatographic eluent was prepared from methanesulfonic acid (puriss., Fluka, Milwaukee, WI). A strontium standard solution (J.T. Baker, Instra-Analyzed®) was used to determine (by IC) the concentration of strontium nitrate solutions. Solutions of DtBuCH18C6 in ILs were prepared by weighing the material into a 2 mL volumetric flask, adding a portion of the IL, and heating in an oven to 110 °C to dissolve the crown ether. The heated solution was then centrifuged in the flask to bring the liquid level below the mark and cooled to room temperature. The solution was then brought to the mark, heated if necessary, and mixed thoroughly. Ionic liquids were synthesized as $Tf_2N$ salts according to the procedures reported in Chapter 4. Magnetic ILs were prepared from the chloride salts according to procedures previously reported [8.4, 8.5].

### 8.2.2 Instruments

Gamma spectroscopy was performed using a PerkinElmer model 2480 automatic gamma counter equipped with WIZARD2 software. Strontium concentrations for the determination of strontium nitrate stocks and extraction chromatographic column capacity were measured using a Dionex ICS-1000 ion chromatograph equipped with a 25 μL fixed-loop manual injection port, a CSRS 300 cation self-regenerating eluent suppressor, a conductivity detector, Dionex CS12A analytical and CG12A guard columns (4 X 250 and 4 X 50 mm), using a 30 mM methanesulfonic acid eluent. IC eluent flow rates were 1.50 mL/min, and the column temperature was maintained at 30°C. The instrument was operated using Chromeleon software version 6.80.

### 8.2.3 Methods

Distribution ratios ($D_M$ ) were determined as the ratio of the count rate in the organic phase to that of the aqueous phase using commercial radiotracers. Assays were carried out *via* gamma spectroscopy using standard procedures. In each metal ion distribution experiment, the organic phase consisted of crown ether dissolved in the designated ionic liquid, and the aqueous phase nitric acid concentration was systematically adjusted either by conducting separate experiments for each condition, or adding the appropriate amount of acid after each sampling. All organic phases were pre-equilibrated with aqueous phase prior to the introduction of the metal radiotracer. Additionally, the sum of the count rates in each phase yielded recoveries within 10% (most often < 10%) that of the radiotracer stock solution used, indicating that equilibrium was established with only two phases involved. Room temperature was maintained at 23 ± 2°C. Each equilibrated phase was

sampled for analysis in at least duplicate, with resulting uncertainties based on counting statistics that were generally within 10%, although the uncertainty interval was considerably wider for the highest $D_M$ values ($D_M \geq 1000$). Nitric acid concentrations were determined by titration with a standard sodium hydroxide solution (Ricca Chemical Company, Arlington, TX).

Preparation of crown ether loaded Amberchrom CG-7lm (hereafter referred to as resin), began with the treatment of the crude resin (Rohm & Haas, Philadelphia, PA) to remove all traces of preservatives and unreacted monomer. From the ethanol slurry received, a portion was decanted and the polymeric beads were soaked for 12 hours in distilled water. The material was then washed several times with water through a vacuum filter assembly, followed by methanol washes until the filtrate was no longer turbid. The washed material was transferred to a round-bottom flask using methanol and the solvent removed by rotary evaporation. Once purified, the resin (1.20 g) was slurried in methanol, and 0.800 g of a 1 M solution of DtBuCH18C6 in 1-octanol, $C_{10}C1imTf_2N$, or $C_{12}OHC_1imTf_2N$ was added. The resulting mixture was gently stirred for several minutes. The methanol was then removed under vacuum at 40 °C to yield *ca*. 2 g of the crown ether loaded resin. If the material showed signs of bead aggregation (*i.e.*, clumping), then methanol was added to create a slurry and the process was repeated until a free-flowing dry powder was obtained. All resins were prepared using the same lot (EIChroM, EXP 336) of DtBuCH18C6.

Weight distribution ratios ($D_w$) were determined radiometrically using commercial radiotracers. $D_w$ is defined by Equation 2-1. Each $D_w$ value is the average of at least three replicates with resulting uncertainties based on counting statistics that were generally

within 10%. Weight distribution experiments of resins were performed as batch tests by contacting known weights of the dry resin (20-25 mg accurately weighed to ± 0.1 mg) with 1.00 mL of a radiotracer spiked acid solution in glass culture tubes. The resin beads were suspended in the solution by gently plucking the tubes periodically and allowing them to soak for at least 30 minutes. Resin beads that remained suspended after standing were settled by centrifugation. A portion of the supernatant was filtered through 0.45 $\mu$m polypropylene filters to remove microparticles. Aliquots of the 100 µL were transferred to gamma counting tubes and assayed *via* gamma spectroscopy using standard procedures.

Measurements of resin capacities were made using resins prepared from 1.0 M DtBuCH18C6 in 1-octanol and 0.60 M DtBuCH18C6 in $C_{10}C_1imTf_2N$. The former was loaded, as the commercial resin, at 40% (w/w) in the beads, and the latter was loaded at 47.3% (w/w) so as to compensate for the difference in solution densities (*i.e.*, 0.882 g/mL and 1.187 g/mL, respectively), and apply the same volume into the resin pores. The resin beds were prepared in Invitrogen Quick Gel Extraction Columns (Grand Island, NY, lot 0348). The empty columns were weighed and resin filled to a mark at 0.40 mL. Then they were weighed to determine the amount of dry resin in the bed, which was used to calculate the theoretical capacities. The resulting dry column bed densities were 0.30 g/mL and 0.37 g/mL for the 1-octanol resin and the $C_{10}C_1imTf_2N$ resin, respectively. These values compare well with the value of 0.35 g/mL noted by the manufacturer of the commercial resin. A stock of 0.5 M strontium nitrate in 3.0 M $HNO_3$ was prepared for metal loading the columns. The columns were conditioned with 3 column volumes of 3.0 M $HNO_3$. Loading of the strontium nitrate solution was set to ½ of the bed volume (0.20 mL).

Washes with 3 column volumes of 3.0 M $HNO_3$ were collected for analysis to ensure that the removal of unbound $Sr^{2+}$ was complete. Elution was performed with 3 column volumes of water. These eluate samples were evaporated and reconstituted in water to prepare for analysis by ion chromatography. The stock solution, rinsate, and eluate samples were sufficiently diluted with water prior to analysis in triplicate. Figure 8.1 is a detailed flow chart of this procedure.

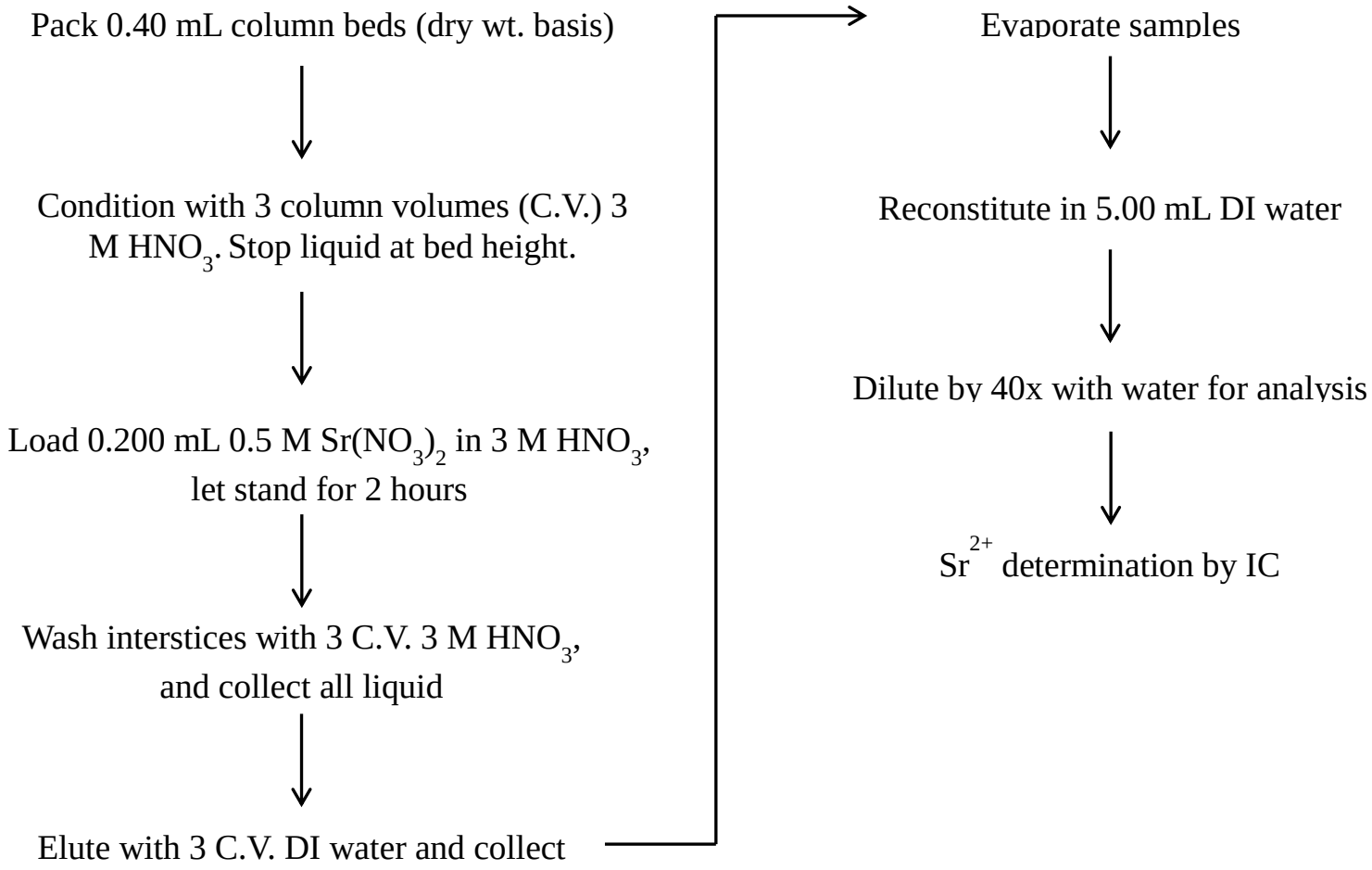


**Figure 8.1: Flow chart of the procedure used to determine extraction chromatographic resin capacity.**

## 8.2 Solvent Extraction

### 8.2.1 Conventional ionic liquid solvents

To explore the possibility of combining conventional extractants with the enhanced extraction found utilizing IL solvents, a set of experiments was performed comparing solvent extraction results using DCH18C6 with those obtained for DtBuCH18C6 (4,4',(5')-di(*tert*-butyl-cyclohexano)-18-crown-6), whose increased hydrophobicity reduces loss of the ligand to the aqueous phase [8.6]. Of particular interest is the question of whether the enhanced extraction efficiency and selectivity (versus 1-octanol) of divalent $Sr^{2+}$ over monovalent metal ions (e.g., $Na^{+}$) would be preserved in the DtBuCH18C6 system. Figure 8.2 compares the nitric acid dependency of $D_{Sr}$ and $D_{Na}$ in a solvent extraction system comprising the 4z,5'z-*cis*-*syn*-*cis*-isomer of DtBuCH18C6 (structure shown in Fig. 8.2) in 1-octanol or $C_{10}C_1imTf_2N$ to that obtained using DCH18C6. As shown in Fig. 8.3, the general trend of increasing $D_{Sr}$ with nitrate concentration for $Sr^{2+}$ extraction is observed in both solvents, consistent (as expected) with neutralcomplex/ion-pair extraction. Also apparent is that the $D_{Sr}$ values are 10-fold greater in the extraction by 4z,5'z-*cis*-*syn*-*cis*-DtBuCH18C6.

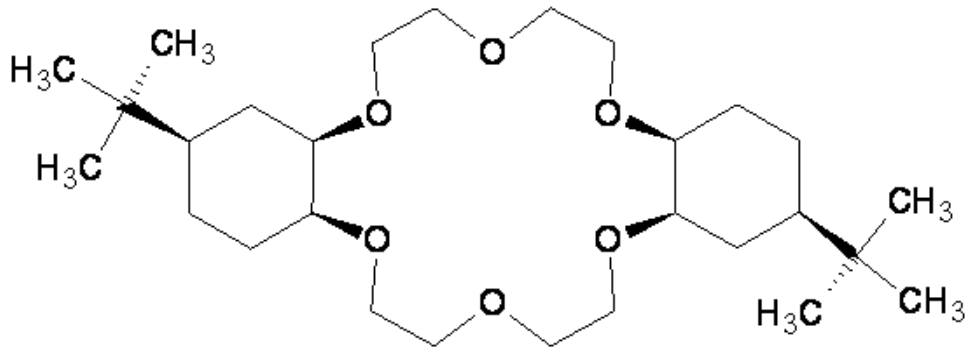


**Figure 8.2: Structure of 4z,5'z-*cis*-*syn*-*cis*-di(*tert*-butyl-cyclohexano)-18-crown-6.**

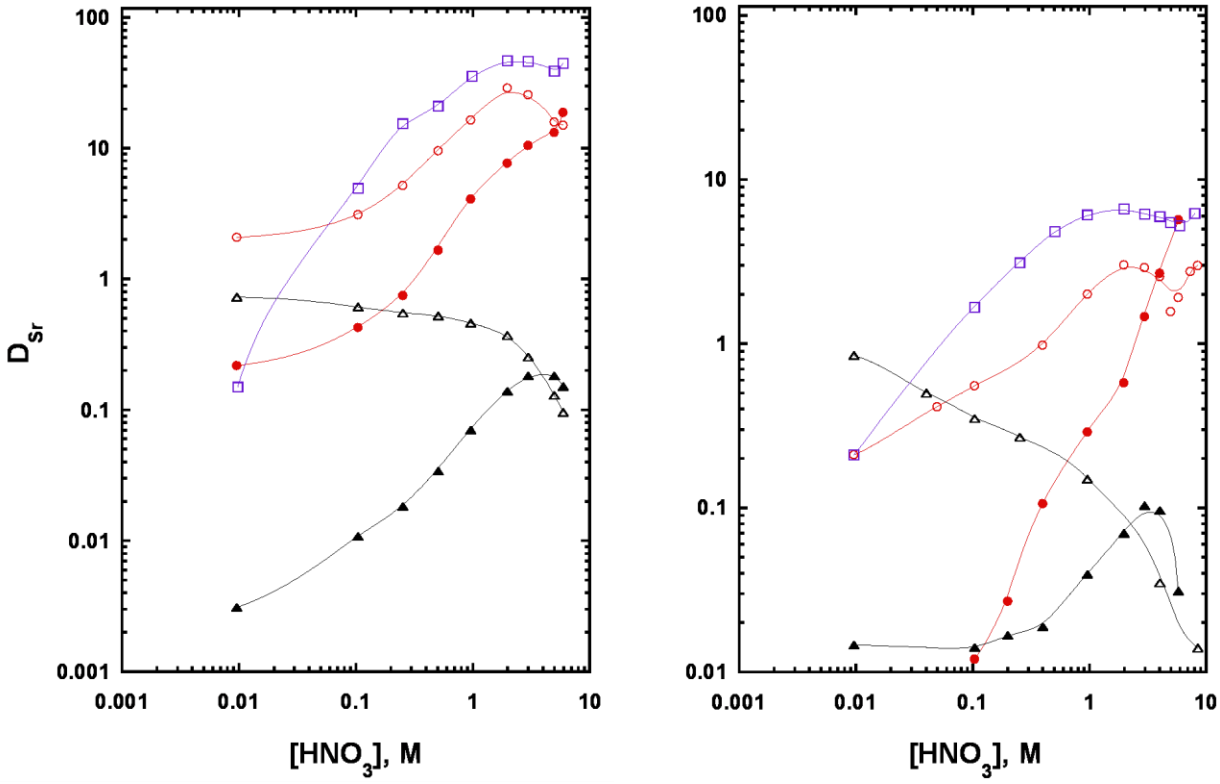


**Figure 8.3: Effect of nitric acid concentration on the extraction of $Sr^{2+}$ into (●) 1-octanol, (○) $C_{10}C_1imTf_2N$, and (□) $C_{12}OHC_4imTf_2N$ and $Na^+$ into (▲) 1-octanol and (△) $C_{10}C_1imTf_2N$ by 0.10 M 4z,5'z-*cis-syn-cis*-DtBu18C6 (left panel) and 0.10 M DCH18C6 (right panel).** The smooth curves are intended only as a guide to the eye.

Though the $D_{Sr}$ for this isomer in 1-octanol has been predicted to be comparable to that of *cis-syn-cis*-DCH18C6, based on calculations from binding reorganization energies [8.7], the greater hydrophobicity of this ligand compared to that of DCH18C6 apparently leads to higher distribution ratios. The $D_{Sr}$ at 2 M to 3 M acid for $C_{12}OH_4imTf_2N$ is 1.5 to 2-fold higher than that for $C_{10}C_1imTf_2N$, which is 2.5 to 4-fold higher than that for 1-octanol, while the Sr/Na separation factors are only 1.5 to 2 times those in 1-octanol. Both of these parameters are somewhat less than the gains observed using the DCH18C6

extractant. Extraction of $Sr^{2+}$ into $C_{12}OHC_4imTf_2N$ by DtBuCH18C6 appears to respond more to changes in acidity than it does when extracted by DCH18C6, which may provide more efficient extraction (at high acid) and stripping (with dilute acid). Although the shapes of the acid dependencies for $Sr^{2+}$ extraction into $C_{10}C_1imTf_2N$ are the same with both extractants, the same cannot be said for $Na^+$ extraction. For the extraction of sodium in the DCH18C6/IL system, a dependency exhibiting a significant downward slope is observed, which has been attributed to the effect of the crown ether-mediated ion exchange pathway with increasing acid [8.8]. In contrast, the acid dependency of $Na^+$ extraction by 4z,5'z-*cis*-*syn*-*cis*-DtBu18C6 in $C_{10}C_1imTf_2N$ is relatively flat until *ca*. 2 M $HNO_3$, suggesting that this pathway is less prominent in the DtBuCH18C6/IL system. Because the curve does not show dependence on nitrate concentrations, is likely that the dominant partitioning pathway associated with the extraction of $Na^+$ by DtBuCH18C6 in $C_{10}C_1imTf_2N$ involves the exchange of the IL cation for the cationic complex. Also noted is that the sodium acid dependency in DCH18C6/1-octanol rolls over at high acidity to a greater extent than in the DtBuCH18C6 system, suggesting that competition from the acid for ligand binding is much more marked in the DCH18C6 system. In fact, all of these general differences in trends are consistent with a lesser propensity to extract acid by DtBuCH18C6 than by DCH18C6. In any event, solvent extraction employing DtBuCH18C6 in the $C_{10}C_1imTf_2N$ solvent under these conditions displays significant improvements over 1-octanol.

### 8.3.2 Feasibility of magnetic ionic liquids as solvents

Another class of ionic liquids that has sparked interest in various applications is that based on tetrahedral transition metal anionic complexes (e.g., tetrahaloferrate(III)) [8.4, 8.5, 8.9-8.12]. Owing to the presence of high-spin $d^5$ metal ions in these compounds, they tend to display observable ferromagnetism [8.9, 8.11], and therefore, can be manipulated using strong magnets. Combining the demonstrable gains in metal ion extraction efficiency and selectivity using IL solvents with the ability to control them by applying a magnetic field is an attractive prospect. Although it has been reported that tetrahaloferrate(III) anions, for instance, are stable in aprotic solvents, in amphiprotic solvents they undergo dissociation due to the formation of stronger hydrogen bonds with the solvent [8.10, 8.13]. To explore whether or not this would preclude their use in metal ion extraction systems, a series of magnetic ILs were synthesized and tested for their ability to withstand contact with aqueous solutions.

The first such compound to be examined was $[P_{666,14}][FeCl_4]$, because of the availability of large quantities of the $[P_{666,14}][Cl]$ precursor. The neat $[P_{666,14}][FeCl_4]$ IL was contacted with aqueous solutions of nitric acid, hydrochloric acid, and aluminum nitrate over a range of ionic strength, the results of which are shown in Fig. 8.3. It was anticipated that nitric acid would probably lead to decomposition of the IL anion, but that by using hydrochloric acid, the dissociation would be mitigated by the common-ion effect. This turned-out not to be the case, however, as the IL showed signs of decomposition at an acid or salt concentration on the order of 0.1 M.

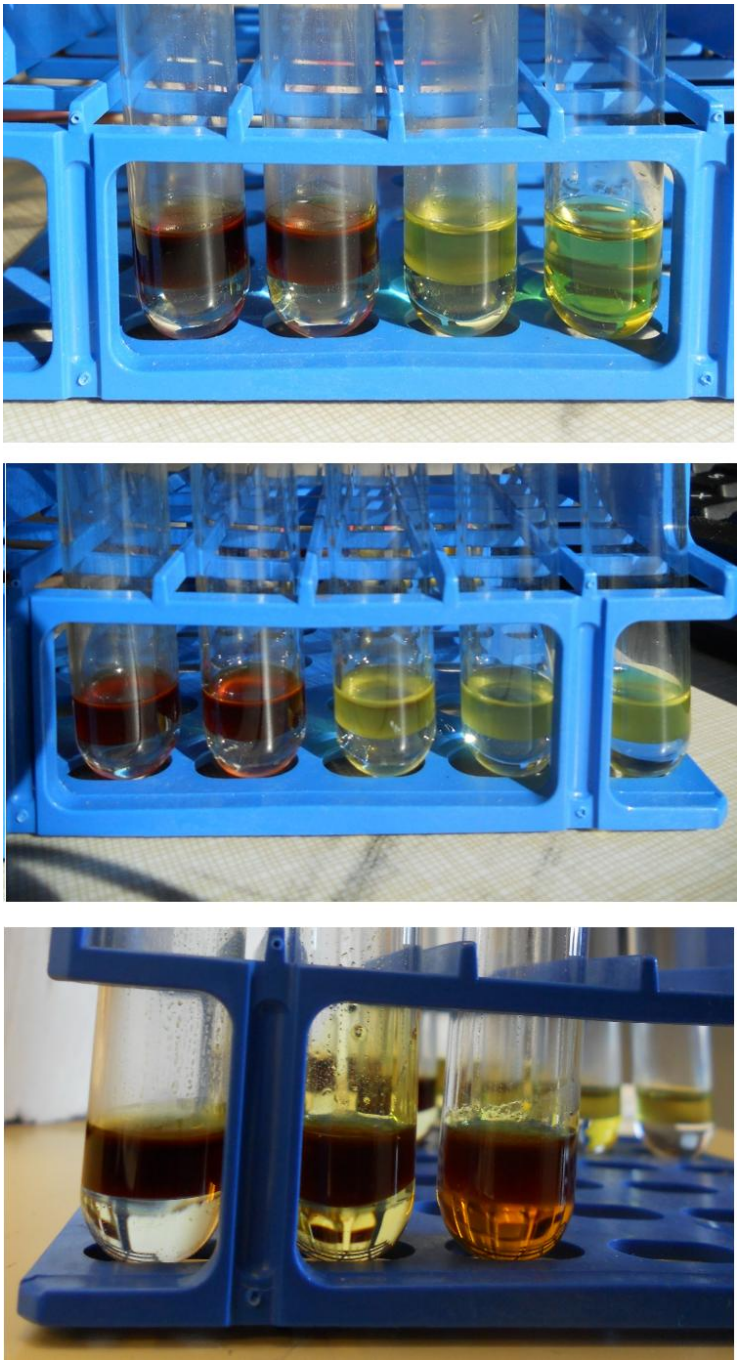

**Figure 8.4: Photos of the results from contacting $[P_{666,14}][FeCl_4]$ with various aqueous solutions.** The conditions are from left to right: water, 0.01 M, 1 M, and 6 M nitric acid (top panel), water 0.08 M, 0.8 M, 3 M, and 6 M HCl (middle panel), and water, 0.25 M, and 1 M $Al(NO_3)_3$ (bottom panel).

As an alternative, 1,3-dialkylimidazolium salts were examined, because hydrogen-bond interactions with organic cations have been reported to stabilize the anion [8.13, 8.14]. Similar results were obtained by contacting $[C_{10}C_1im][FeCl_4]$ (not shown) and $[C_{10}C_1im]_2[Co(NCS)_4]$ (Fig. 8.5). The latter, tetraisothiocyanatocobaltate(II) salt, is an ink-like liquid [8.5] that could provide enhanced extraction kinetics, were it to prove stable under the conditions of the extractions. Nevertheless, these compounds turned-out to be similarly labile, indicating that the tetrahedral high-spin transition metal complex class of magnetic ILs will not support the conditions necessary to perform metal ion extraction. It may be possible that more stable cage-like complexes with larger ligands could protect the labile ion. However, there were ample opportunities to perform interesting, fundamental studies on non-magnetic ILs. Therefore, this line of research was abandoned.

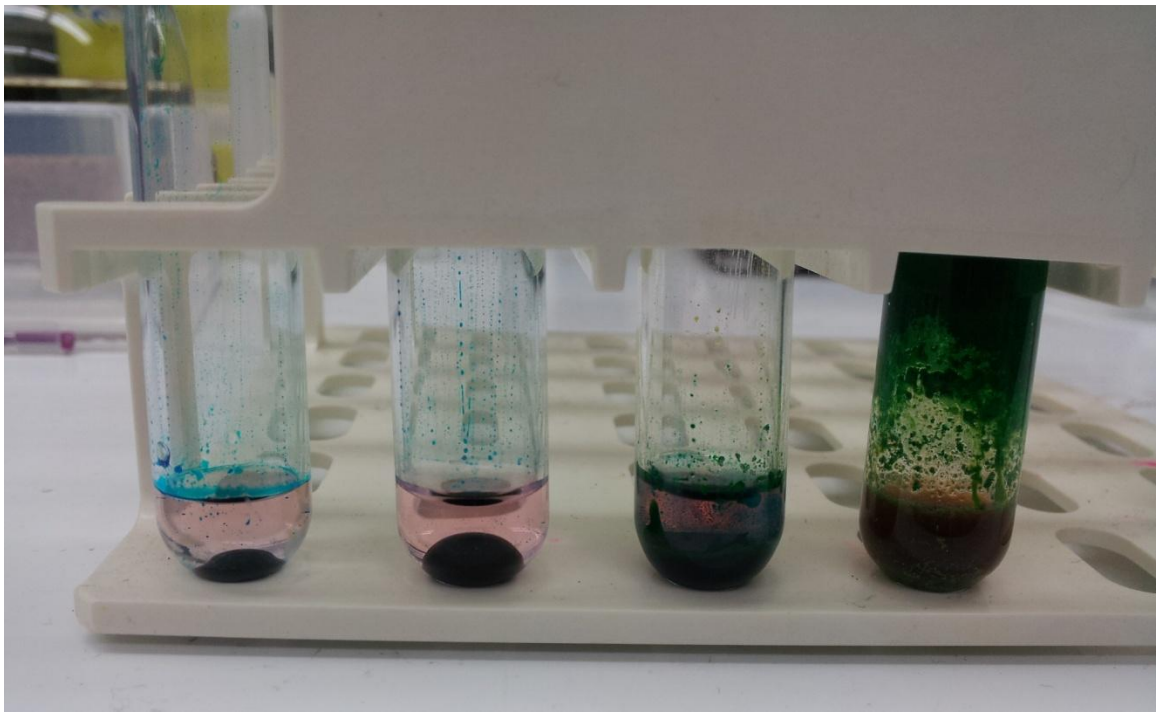

**Figure 8.5: Photo of the results from contacting $[C_{10}C_1im]_2[Co(NCS)_4]$ with (from left to right) water, 0.1 M $HNO_3$, 1 M $HNO_3$, 4 M $HNO_3$.**

## 8.4 Extraction Chromatographic Materials

### 8.4.1 Ionic Liquid-based Sr-selective resin

The results of studies utilizing DtBuCH18C6 in $C_{10}C_1imTf_2N$ for the solvent extraction of $Sr^{2+}$ and $Na^+$ (representative alkaline earth and alkali metal ions, respectively) demonstrated that significant improvements to the commercial resin (Sr resin) might possibly be achieved simply by replacing the solvent (1-octanol) with an IL. To investigate this prospect, resins incorporating 40% (w/w) of a 1.0 M solution of DtBuCH18C6 in 1-octanol, $C_{10}C_1imTf_2N$, or $C_{12}OHC_4imTf_2N$ were prepared and evaluated for metal ion uptake. Figure 8.6 is a plot of the nitric acid dependencies of the weight distribution of $Sr^{2+}$ on these resins. Immediately apparent in these plots is the reduced extraction provided at high acidity by the resins comprising IL versus the conventional material. It is also important to note how the acid dependencies of extraction into the IL, is less steep than that for 1-octanol, which is also observed in liquid-liquid extraction and is consistent with variations in the composition of the extracted complexes [8.15]. Additionally, there is essentially no difference between the $D_w$ values of the dialkyl IL and the hydroxylated IL, whereas in the solvent extraction systems, the extraction of $Sr^{2+}$ was at least 1.5-times greater with the hydroxylated analog.

Theoretically, as long as the extraction mechanisms of the two systems are the same, then the translation of solvent extraction media to the solid support of a resin should be straightforward [8.15]. However, several possible issues could give rise to the difference in results from those obtained from solvent extraction, barring any noticeable change in partitioning pathway. First, solvent extraction does not always correlate with extraction

chromatographic materials due to differences observed in the availability of the ligand in the solid support. For perspective on this matter, the Stokes-Einstein equation [8.16] relates diffusion coefficients of solutes to the viscosity of the medium by an inverse proportionality. Consequently, the diffusion of solutes into the pores of the beads can be diminished by higher viscosity of the solution impregnated therein. The viscosities of the neat solvents can provide reasonable estimates of the differences in viscosity observed by the metal ions or complexes, once they have transferred to the IL side of the interface. At standard temperature and pressure, the viscosity of 1-octanol is 7.2 cP [8.17], whereas that of a typical IL can be on the order of 300-1000 cP [8.18]. This relation of solute diffusion and viscosity may also provide insight into how the ligand can be sequestered by the less mobile IL. Indeed, the provision of a transport path for solutes to interact with the ligand may be quite difficult, requiring that the large IL ions translate or rotate when in fact they are in a highly ordered state dictated largely by coulombic attractions.

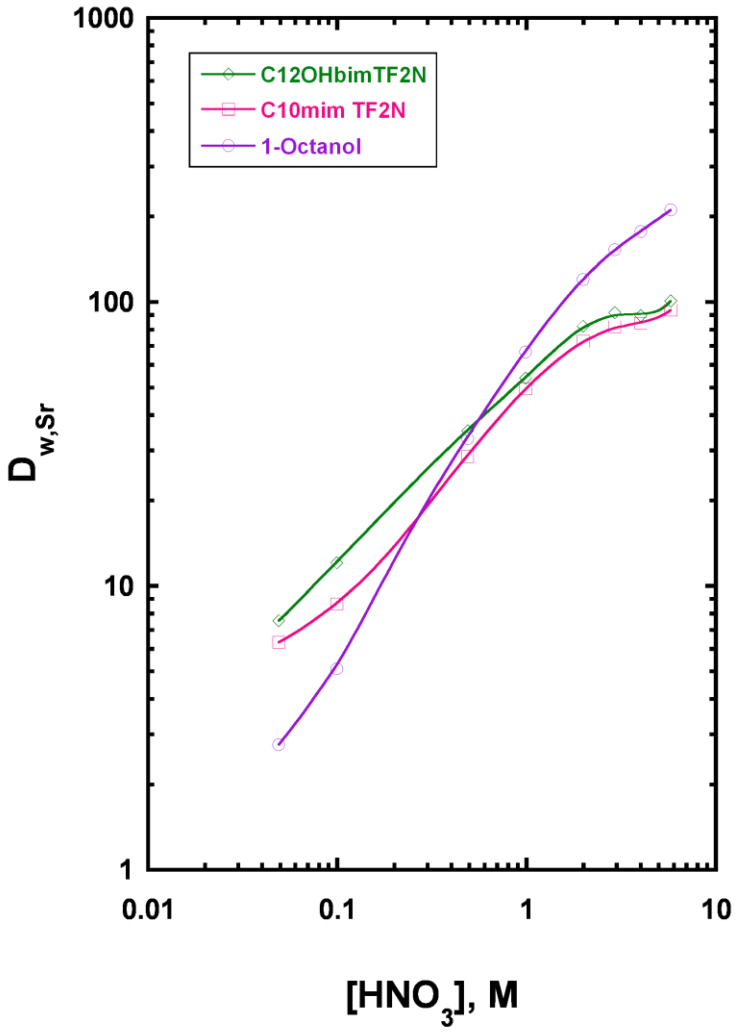


**Figure 8.6: Effect of nitric acid concentration on the batch test uptake of strontium by resins prepared with 1.0 M DtBuCH18C6 in 1-octanol, $C_{10}C_1imTf_2N$ or $C_{12}OH_4imTf_2N$.**

**Table 8.1**
**Effect of DtBuCH18C6 concentration in $C_{10}C_1imTf_2N$ and 1-octanol on the solvent extraction of $Sr^{2+}$ from 1.0 M $HNO_3$**

| [DtBuCH18C6], M | Mole Ratio (IL:crown ether) | IL Phase Observations | $D_{Sr}$ |
|---|---|---|---|
| 0.25 | 8.0 | cloudy, but phase disengaged | 25.1 |
| 0.40 | | cloudy, but phase disengaged | 34.5 |
| 0.50 | 3.5 | cloudy, but phase disengaged | 43.2 |
| 0.60 | | cloudy, but phase disengaged | 47.9 |
| 0.75 | | cloudy, but phase disengaged | 33.1 |
| 1.0 | 1.2 | crown ppt'd resulting in phase ambiguity | not measured |

| [DtBuCH18C6], M | Mole Ratio (octanol:crown ether) | Organic Phase Observations | $D_{Sr}$ |
|---|---|---|---|
| 0.25 | 22 | clear after 1st contacts | 8.7 |
| 0.50 | 9.4 | clear after 1st contacts | 15.1 |
| 0.75 | 5.4 | clear after 1st contacts | 19.4 |
| 1.0 | 3.1 | clear post-equilibrium | 26.5 |

Of course, the solvent extraction experiments were performed using solutions of *0.1 M* DtBuCH18C6, which is ten-fold less than was applied to the resin. It is possible that the solubility of the crown ether in ILs diminishes or the nature of the complex extracted changes when exposed as a thin layer within the pores of the beads. Solubility represents another possible source of the low $D_w$ values obtained with ILs. In a follow-up investigation, it was determined that the mole ratios of the 1-octanol:crown ether and IL:crown ether differ significantly, due to the different molar volumes of the respective solvents. Table 8.1 provides an assortment of data from extractant dependency experiments performed from 0.25 M to 1.0 M DtBuCH18C6. When the crown ether concentration reaches 1 M, the mole ratio of IL to crown ether approaches 1:1, while for 1-octanol it is 3:1. A combination of the extractant and the ionic liquid is therefore more likely to behave like the crown ether itself than a 1-octanol solution at the same concentration. When combined with a significant drop in $D_{Sr}$ with increasing [DtBuCH18C6], and the observation that the crown ether precipitates from the 1.0 M solution in $C_{10}C_1imTf_2N$ upon mixing with acid, these results point to a distinctive composition issue for high molar mass solvents like ionic liquids. A graphical representation (Fig. 8.7) of the extractant dependencies in Table 8.1 clearly shows how the IL significantly outperforms 1-octanol in solvent extraction near the point (0.6 M DtBuCH18C6) that the acid contacted IL phase becomes unstable, as indicated by the observations of the crown ether precipitation (Table 8.1).

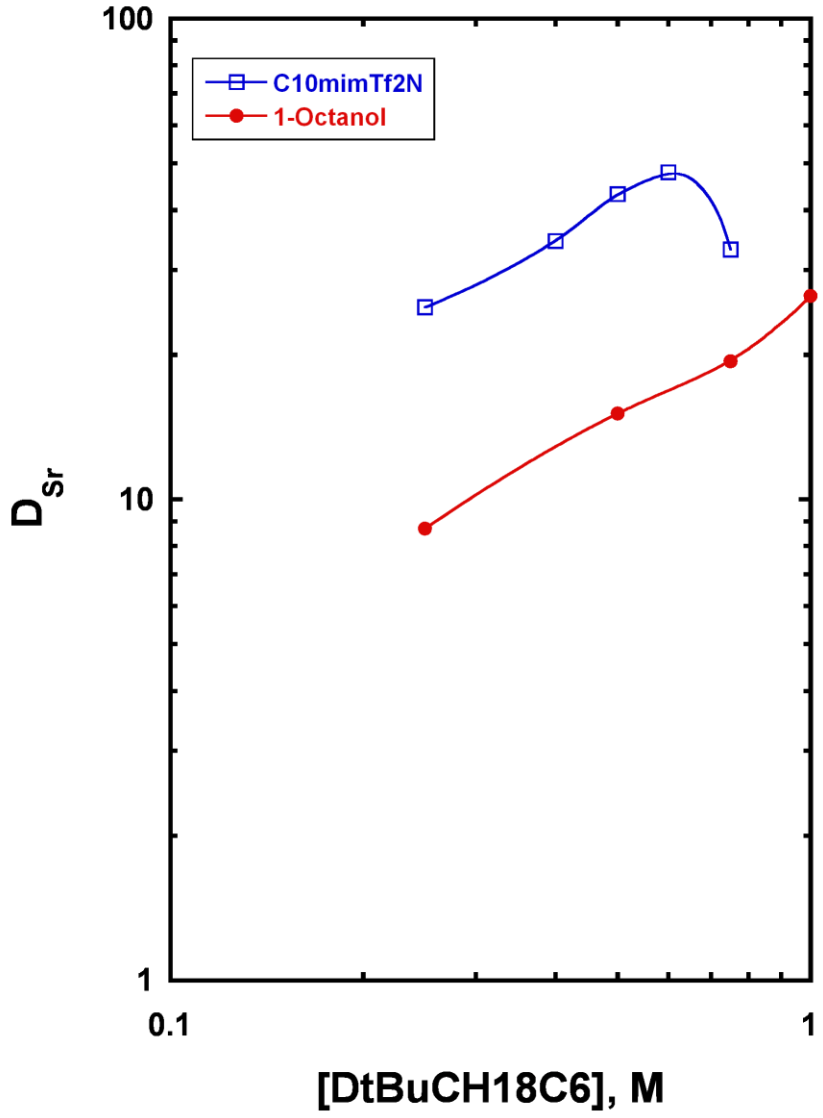


**Figure 8.7: Effect of DtBuCH18C6 concentration on extraction of strontium from 1 M $HNO_3$ into 1-octanol and $C_{10}C_1imTf_2N$.**

This crown ether concentration (0.60 M) is interpolated to yield a mole ratio with the IL of *ca*. 3:1 (IL:ligand), which coincides with that for the 1-octanol solution at 1.0 M crown ether.

Further investigation has revealed that, while 1 M $HNO_3$ will precipitate the 1.0 M crown ether from $C_{10}C_1imTf_2N$, water will lead to a precipitate only after contact has been sustained overnight. Taken together, these observations suggest that, upon contact with acid, it is the crown ether-acid adduct (most likely with hydronium ion) that is most insoluble in the IL in the presence of acid. This is not entirely unexpected; in fact, this same process is used to isolate individual isomers from commercial preparations of DtBuCH18C6, by selectively precipitating the acid adducts from with various concentrations of strong acid in contact with *n*-hexane [8.19]. As a possibly related matter, ionic liquids comprising long alkyl groups have been studied spectroscopically, revealing that the hydrophobic side chains and the polar head groups tend to pack in nanostructural domains, providing pockets with vastly different degrees of polarity [8.20-8.22]. Therefore, the hydrophobic domains would likely resemble a long aliphatic alkane, not unlike hexane. Interestingly, precipitation from contacting the 1.0 M DtBuCH18C6 in $C_{12}OHC_4imTf_2N$ mixture with 1 M $HNO_3$ is much more subtle at first, and then proceeds to the extent observed for $C_{10}C_1imTf_2N$ after standing overnight. This might suggest that slower shifts in reorganization of the ions in the hydroxyl functionalized ILs provides, temporarily, a better solvation environment for the acid adduct. Considering that dyes dissolved in $C_2OHC_1$imTf2N have been explored by time-resolved fluorescence demonstrating slower rotation and solvation dynamics associated with hydrogen bond interactions with the IL cation [8.23], it is plausible that this slower change in $C_{12}OHC_4imTf_2N$ can be viewed from this same perspective. Although ILs composed of dicyanamide [8.24] and tetraisothiocyanatometalate [8.5] anions have proven to be much more mobile than their $Tf_2N^-$ and $PF_6^-$ counterparts, as of yet, there are no chemically

stable ILs possessing both the substantial hydrophobicities and low viscosities that may be required. Likewise, there have been no reports of the use of co-solvents or modifiers that could reduce the viscosity substantially without adversely impacting the solvation effects of the IL.

### 8.4.2 Application to column chromatography

As an essential parameter of effective extraction chromatographic media, capacity is directly related to the availability of the active ligand and the formation of the extracted complex. Based on the batch tests of the resins prepared from ILs, they evidently have a significantly lower capacity than those prepared with the same formal concentration of crown ether in 1-octanol. But, by how much do the two resins differ in this respect? While the evidence is circumstantial, the crown ether solution stability would be expected to have an impact on the behavior of an IL-based Sr-selective resin. One likely scenario is that the aqueous solution contacts the stationary phase at the entrance of pores, and upon precipitation the solid ligand prevents the diffusion of solutes past that threshold, effectively reducing capacity. Then, there is the matter of the crown/IL solution viscosity. Upon dissolution the material that once was a pure ionic liquid, mobile enough to dispense by pouring, becomes a rigid liquid, requiring elevated temperatures to facilitate mixing and transfer. Both of these behaviors will significantly limit the accessibility of the larger pore volume. In all likelihood, both of these behaviors are at the heart of the matter with lower-than-expected $D_w$ values. Measurements of capacity can be made by applying the resins to a column configuration and performing the extraction on a bed of known density and composition. The procedure employed for the determination of resin capacity is provided with a flow chart (Fig. 8.1) in the Methods (section 8.2.3). With the

knowledge that the resins prepared using 1 M DtBuCH18C6 in IL will more likely result in crown ether precipitation, the latest version of the resin contained a 0.6 M solution in $C_{10}C_1imTf_2N$ (see Table 8.1), so as to isolate the effect that solution viscosity may have.

Table 8.2 presents the results of the capacity measurements. The recoveries were quantitative, based on the sum of the rinsates and eluates compared to the stock solution. The capacity of the octanol resin was in agreement with the literature value (75%) [8.25] for Sr resin. Given that the IL-based resin capacity was 17% less than that of the commercial resin, and that crown ether precipitation was not expected at this concentration, lower accessibility of the pore volume due to the viscosity of the IL solution is proposed as a likely source of the disparity between the resins. However, this figure may not account for all of the differences observed in the batch tests.

**Table 8.2**
**Results of the column capacity measurements of resins**

| Sample | $Sr^{2+}$ Amount | Theoretical Capacity | %Capacity / %Recovery | Uncertainty |
|---|---|---|---|---|
| Octanol Eluate | 3.51 mg | 4.74 mg | 74.2% capacity | 1.6% |
| Octanol Rinsate | 5.05 mg | | 98.8% recovery | 3.5% |
| IL Eluate | 1.78 mg | 3.74 mg | 57.3% capacity | 1.4% |
| IL Rinsate | 6.88 mg | | 99.9% recovery | 3.1% |
| 0.5 M $Sr(NO_3)_2$ Stock | 0.4948 M | | | 0.008 M |

## 8.5 Conclusions

The studies reported here have provided an improved understanding of the advantages and limitations of metal ion extraction systems based on ILs. Increases observed in the divalent metal ion (*i.e.*, $Sr^{2+}$) extraction efficiency and selectivity over monovalent metal ions (i.e., $Na^{+}$), versus that of conventional solvents may offer distinct advantages in current processes. As the basis of liquid-liquid extraction media, ILs may find a niche, particularly in processes that involves elevated temperatures, which decrease the viscosity of the IL solutions without the risk of volatilization of the solvent. One such process where the volatility or flammability of a solvent may pose an extreme hazard would be in the reprocessing of spent nuclear fuel (e.g., SREX) [8.26]. Moreover, if the enhanced extraction behavior can be exploited at half the typical ligand concentrations, then there may be some cost benefit to employing ILs (provided, of course, that these solvents can eventually be prepared cheaply and on a large scale. Despite the improvements observed in liquid-liquid extraction, the outlook for analytical-scale radiochemical separations is not as promising. When impregnated on a porous solid support, IL-extractant mixtures behave quite differently. The physicochemical basis for disparity between the results for solvent extraction and extraction chromatographic resins based on ILs appears to be the result of several factors (*i.e.*, viscosity, solution stability). Results of studies investigating the possible causes suggest that both crown ether/IL solution stability and viscosity play a critical role in limiting the diffusion of solutes into the pore volume essential for retention and column capacity. Ultimately, the outcome of the resin studies suggest that it is unlikely that strontium-selective extraction

chromatographic materials comprising crown ethers dissolved ILs will be a viable alternative to those already on the market.

## 8.6 References

[8.1] C.A. Hawkins, S.L. Garvey, M.L. Dietz, *Sep. Purif. Technol*., **2012**, 89, 31-38.

[8.2] C.A. Hawkins, A. Rud, S.L. Garvey, M.L. Dietz, *Sep. Sci. and Technol.* 10.1080/01496395.2012.697527, 27 June 2012.

[8.3] E.P. Horwitz, M.L. Dietz, D.E. Fisher, *Solv.Ext. Ion Exch*. **1990**, 8, 199-208.

[8.4] R.E. Del Sesto, T.M. McCleskey, A.K. Burrell, G.A. Baker, J.D. Thompson, B.L. Scott, J.S. Wilkes, P. Williams, *Chem. Commun*., **2008**, 447–449.

[8.5] T. Peppel, M. Köckerling, M. Geppert-Rybczyńska, R.V. Ralys, J.K. Lehmann, S.P. Verevkin, A. Heintz, *Angew. Chem. Int. Ed*. **2010**, 49, 7116 –7119.

[8.6] E.P. Horwitz, M.L. Dietz, D.E. Fisher, *Anal. Chem*. **1991**, 63, 522-525.

[8.7] Communication from Benjamin P. Hay, Oak Ridge National Laboratory, **2006**.

[8.8] M.L. Dietz, D.C. Stepinski, *Green Chem*. **2005**, 7, 747–750.

[8.9] S. Hayashi, H. Hamaguchi, *Chem. Soc. Jap. Chem. Let.*, 2004, 33, 1590-1591.

[8.10] D. Wyrzykowski, A. Pattek-Janczyk, T. Maniecki, K. Zaremba, Z. Warnke, Thermochimica Acta, **2006**, 443, 72–77.

[8.11] S.H. Lee, S.H. Ha, S-S. Ha, H-B. Jin, C-Y You, Y-M. Koo, *J. Appl. Phys*., 2007, 101, 09J102.

[8.12] J. Wang, H. Yao, Y. Nie, L. Bai, X. Zhang, J. Li, *Ind. Eng. Chem. Res*. **2012**, 51, 3776−3782.

[8.13] U. Bentrupa, M. Feistb, E. Kemnitz, Prog. *Solid State Chem*. **1999**, 27, 75-129.

[8.14] P.B. Hitchcock, K.R. Seddon, T. Welton, *J. Chem. Soc. Dalton Trans*. **1993**, 2639-2643.

[8.15] T.Braun and G. Ghersini, *Extraction Chromatography, Journal of Chromatography Library Vol. 2*, Elsevier, New York, **1975**.

[8.16] C. C. Miller, *Proceedings of the Royal Society of London. Series A, Containing Papers of a Mathematical and Physical Character*, **1924**, 106, pp. 724-749.

[8.17] S. Matsuo and T. Makita, *Int. J. Thermophys*. **1989**, 10, 833-843.

[8.18] J.G. Huddleston, A.E. Visser, W.M. Reichert, H.D. Willauer, G.A. Broker, R.D. Rogers, *Green Chem*. **2001**, 3, 156-164.

[8.19] M.L. Dietz, C. Felinto, S. Rhoads, M. Clapper, J.W. Finch, B.P. Hay, *Sep. Sci. Technol.* **1999**, 34, 2943-2956.

[8.20] A. Triolo, O. Russina, H-J. Bleif, E. Di Cola, *J. Phys. Chem. B*, **2007**, 111, 4641-4644.

[8.21] D. Xiao, J.R. Rajian, A. Cady, S. Li, R.A. Bartsch, E.L. Quitevis, *J. Phys. Chem. B*, **2007**, 111, 4669-4677.

[8.22] O. Russina, A. Triolo, L. Gontrani, R. Caminiti, D. Xiao, L.G Hines Jr, R.A Bartsch, E.L. Quitevis, N. Plechkova, K.R Seddon, *J. Phys.: Condens. Matter*, **2009**, 21, 424121.

[8.23] A. Paul, A. Samanta, *J. Phys. Chem. B*, **2007**, 111, 4724-4731.

[8.24] D.R. MacFarlane, J. Golding, S. Forsyth, M. Forsyth, G.B. Deacon, Chem. Commun. **2001**, 1430–1431.

[8.25] E.P. Horwitz, R. Chiarizia, M.L. Dietz, *Sol. Extr. Ion Exch*. **1992**, 10, 313-342.

[8.26] E.P. Horwitz, M.L. Dietz, D.E. Fisher, *Sol. Extr. Ion Exch*. **1990**, 8, 557-572.

# CHAPTER 9:
# CONCLUSIONS AND RECOMMENDATIONS

## 9.1 Conclusions

Because of their remarkable ability to extract a variety of substances while providing non-volatile, nonflammable, thermally-stable liquid phases with flexible chemistry, ionic liquids (ILs) have been widely investigated as replacements for conventional (molecular) solvents for an enormous range of purposes. Comparisons with their conventional counterparts (*i.e.*, *n*-alcohols) have provided a foundation for understanding extraction into ILs and a benchmark by which to measure improvements, based on several criteria. These include increases in extraction efficiency and separation factors versus those observed in conventional solvent systems, and behavior that allows not just facile extraction, but also recovery of the solvent and the solute(s) and reuse of the solvent. Extraction systems based on ILs comprising 1,3-dialkylimidazolium ($C_nC_m$im) cations and the hydrophobic *bis*[(trifluoromethyl)sulfonyl]imide ($Tf_2N$) anion have, under certain conditions, displayed all these characteristics.

The extraction of metal ions into ILs has proven, in many instances, to be far more complex than in conventional solvents. However, understanding the IL systems and choosing appropriate conditions to design efficient and selective extractions is possible, given a more fundamental appreciation of IL systems in general. Therefore, the objective of these studies was to provide an improved basis for understanding metal ion extraction from aqueous solutions into room-temperature ionic liquids by investigating the variety of possible extraction pathways and some of the major factors (*i.e.*, IL hydrophobicity, nature of the extracted metal ion, aqueous acidity, and the water content of the organic phase) determining their balance. As a test system, the extraction of alkali and alkaline

earth metal ions from acidic nitrate media *via* neutral crown ethers into hydrophobic $C_nC_m$im$Tf_2$N ILs was examined. Considering that the unfavorable metal ion complex extraction by way of ion exchange pathways has a tendency to predominate in many of these systems, the design of the components for practical extraction media has been centered on their prevention. A three-path model was demonstrated to be a generic representation of the pathways observed in the extraction of metal ions by neutral crown ethers in ILs by studying the effect of systematic variation in the alkyl substituents of the imidazolium cation on the observed trends in extraction data for various metal ions. The effect of water content of ILs was explored by synthesizing a homologous series of $C_nC_m$im$Tf_2$N ILs and their 1-(*ω*-hydroxyalkyl) analogs. For the first time, a meaningful correlation has been demonstrated between the extraction of strontium and the water content of ILs, as has been observed previously for oxygenated aliphatic solvents. That a single correlation described both systems suggests that a specific quantity of water is necessary for the co-extraction of the aqueous anion in the predominantly neutral complex/ion-pair extraction involved.

In the pursuit of the key factors relating IL structure to solvation behavior, IL hydrophobicity has been a recurrent theme. Octanol-water distribution ratios ($D_{ow}$) were measured as an indicator of IL hydrophobicity and demonstrated to provide the basis of a quantitative scale relating extraction behavior to IL structural features. Specifically, it has been shown that the behavior of $C_nC_m$im-based ILs as extraction solvents is related to the $D_{ow}$, thus providing a means to predict the performance of other families of ILs. As a result of this study, a benchmark log $D_{ow}$ value of *ca*. 2 (based on $C_{10}C_1$im$Tf_2$N) has been established as the minimum value required for ILs exhibiting the ability to efficiently and

selectively extract strontium and acid dependence similar to conventional solvents. These techniques are expected to provide a foundation for guidelines to select an appropriate IL solvent for the extraction of metal ions.

To more rapidly determine the concentration of ILs in various sample types, a new HPLC-UV method was developed for their quantification. The method represents a significant improvement over previously developed chromatographic methods for the separation of ILs in that it provides greater efficiencies, lower detection limits, and higher throughput. Additionally the method offers the ability to analyze a variety of sample types, which has proven beneficial in this research, and is expected to support many other efforts. Rigorous evaluation of the normal-phase separation to determine the underlying solute retention mechanisms resulted in the conclusion that that non-adsorptive ion exchange is the predominant mode of retention. The method also provided the means to measure the contribution of ion exchange of the IL cation in the extraction of metal ions. Paired with a newly engineered IC technique to determine the nitrate content of the IL phase post-extraction, the possibility of determining the relative contributions of competing extraction pathways was explored. Through these techniques the quantification of the relative contributions from two competing extraction modes (*i.e.*, ion exchange via the IL cation, and neutral complex/ion-pair extraction) has been demonstrated in the well-characterized extraction of strontium from water, indicating that similar methods may be used across a range of conditions.

Finally, in a set of experiments examining various means for the practical application of ILs in metal ion extraction, the solvent extraction behavior of a substantially hydrophobic IL was compared with that of the traditional 1-octanol system. Five-fold

improvements to extraction efficiency and modest gains in separation factor for strontium over sodium were observed for the IL systems. Particularly good behavior was observed for the 0.1 M DtBuCH18C6 in $C_{12}OHC_4imTf_2N$ system, suggesting that applications employing solvent extraction of strontium may benefit from similar solvents. However, when these same materials were studied in an extraction chromatographic (EXC) medium, the improvements in solvent extraction were shown not to directly translate to EXC. An investigation into the causes of such non-ideal behavior indicated that at three factors may limit the extraction efficiency on the solid support: the IL viscosity (which leads to poor transport of the solute), crown ether insolubility in the IL phase, and a constraint is placed on the mole fraction-based composition of that solution by the high molecular weight ILs employed.

While the studies reported in this work have provided a better understanding of how IL-based metal ion extraction systems behave, it is important to note that this field remains far from settled. The structure-property relationships available in the design of ILs are limited by imagination. Considering the selection of appropriate solvents and complexants, it is hoped that the knowledge and techniques provided in this work will facilitate the continued development of this understanding and assist in the generation of improved technologies for a variety of extraction media.

## 9.2 Recommendations

In light of the efforts to expand the knowledge base of IL-based extraction systems, several recommendations are made in the following sections. Alhough these do not represent a comprehensive list of interests, they include both the forthcoming studies in this laboratory and as possible endeavors that may revolutionize the field.

### 9.2.1 Expanding the knowledge base to other ionic liquid families

Although the objective of this work was to study 1,3-dialkylimidazolium ionic liquids (particularly the hydrophobic $Tf_2N$ salts), other common IL cations (*e.g.*, *N*-alkylpyridimium, *N*-alkylquinolinium, *N*-dialkylpyrrolidinium) are amenable to the same approaches employed here. Any ILs incorporating an appropriate chromophore (*e.g.*, an aromatic anion) will, in fact, be suitable for the analytical methods applied. Perhaps, a somewhat less common IL ion such as amino acids, which due to their dual functionalities can provide either cations or anions, may yield "greener" alternatives to the heterocyclic moieties used here.

### 9.2.2 Determining the effect of self-aggregation of ionic liquids on behavior as solvents

On many occasions, the surface activity of the most hydrophobic ILs was reflected in their behavior as solvents and solutes. For instance, in the differences observed among the $C_{10}C_nTf_2N$ series for both water content (Chapter 4) and the correlation of their $D_{ow}$ to the carbon number (Chapter 6), the two-tail amphiphilic characteristics of the ILs led to deviations from trends that were established with near homologues. The measurement of

surface tension should therefore become a regular part of the assessment of ILs of this type. In some cases, interfacial surface tension measurements, along with light scattering techniques, may provide a means to understand their aggregation behavior.

### 9.2.3 Developing a useful chromatographic resin from ionic liquids

While these and other studies have demonstrated how difficult it may be to produce practical radioanalytical separations media by simply replacing a conventional solvent with an IL that behaves well in solvent extraction, there are some directions that might be worth pursuing. Along the lines of rendering the physical properties of the ILs more amenable, there are some indications that viscosities may be lowered by the use of particular anions that disrupt short-range coulombic interactions with the cation (*e.g.*, dicyanamide and amino acids) [9.1, 9.2]. Although these anions tend to be too hydrophilic for the biphasic extraction of metal ions, the same principles may be explored for a more hydrophobic anion. Studies [9.3] have also suggested that mixtures of ionic liquids may provide the flexibility to modify the physicochemical properties of IL systems. It is possible that a combination and an appropriate composition of a mixture of ILs may provide the lowered viscosities desired. Furthermore, it is common in conventional solvent systems to add modifiers that impart properties allowing easier handling of those materials. For instance, 5% lauryl nitrile is added to the diluent in the SREX process to lower its viscosity and make it easier to handle in the strontium extraction from spent nuclear fuel (SREX process) [9.4, 9.5].

Another aspect of the extraction of strontium, in particular, that could use some innovation is in the ligands employed. Some of the issues observed with the crown ethers

in previous and present studies were that they also extract acid and have considerable affinity for other cations like potassium and lead(II). A more selective, possibly pre-organized, extractant might mitigate the competition observed and increase the capacity of extraction media significantly. Of course, these endeavors would require advanced synthetic and molecular modeling techniques, as well as the facilities and spectroscopic equipment to elucidate metal coordination environments.

### 9.3 References

[9.1] D.R. MacFarlane, J. Golding, S. Forsythe, G.B. Deacon, *Chem. Commun*., 2001, 1430-1431.

[9.2] H. Yu, Y. Ting Wu, Y. Jiang, Z. Zhou, Z. Zhang, *New J. Chem*., **2009**, 33, 2385-2390.

[9.3] H. Niedermeyer, J.P. Hallett I.J. Villar-Garcia, P. A. Hunt, T. Welton , *Chem. Soc. Rev*., **2012**, 41, 7780-7802.

[9.4] [1.3] E.P. Horwitz, M.L. Dietz, D.E. Fisher, *Sol. Extr. Ion Exch*. **1991**, 9, 1-25.

[9.5] E.P. Horwitz, M.L. Dietz, M.P. Jensen, International solvent extraction conference, Melbourne (Australia), **1996**.

# CURRICULUM VITAE

**Cory A. Hawkins**

## Education

Ph.D. in Chemistry, University of Wisconsin-Milwaukee Dec 2012

Dissertation: "Fundamental and Applied Studies of Metal Ion Extraction by Crown Ethers into Imidazolium-based Room Temperature Ionic Liquids", Advisor: Mark. L. Dietz, Ph.D.

B.S. in Chemistry, Southern Oregon University 2000

## Experience

*Research Assistant,* University of Wisconsin - Milwaukee, Milwaukee, WI 2008-2011

- Led a research program aimed at elucidating the principles of Group 1 and 2 metal ion transfer from aqueous acidic solutions into room temperature ionic liquids. Developed techniques to quantify pathways of ion transport under a wide range of conditions.
- Synthesized new ionic liquids.
- Supervised undergraduate researchers and training junior graduate research assistants.

*Teaching Assistant,* University of Wisconsin - Milwaukee, Milwaukee, WI 2007-2011

- Taught laboratories and discussions for Analytical and General Chemistry.

*Graduate Research Assistant,* Argonne National Laboratory - Argonne, IL 2010

- Performed radiochemical and chromatographic analysis for a project to develop an improved radiostrontium bioassay, sponsored by the Centers for Disease Control. Patent application submitted for device designed from these studies.

*Analyst II,* Bioanalytical Systems Inc., McMinnville, OR 2006-2007

- Served as lead analyst on tissue methods development and analysis projects. Managed team members in the development and validation of HPLC-UV and HPLC-MS/MS methods for small molecule pharmaceuticals. Performed sample analysis in a GLP environment.

*Analyst I,* Bioanalytical Systems Inc., McMinnville, OR 2002-2006

- Developed and validated HPLC-UV and HPLC-MS/MS methods for small molecule drug products, substances, and biological matrices. Performed sample analysis in a GLP environment.

*Analyst I,* LC Resources, Inc., McMinnville, OR 2000-2002

- Developed and validated HPLC-UV and HPLC-MS/MS methods for small molecule drug products, substances, and biological matrices. performed sample analysis in a GLP environment; operated and maintained instruments and equipment.

**Publications**

C.A. Hawkins, A. Rud, S.L. Garvey, M.L. Dietz, Evaluation of hydroxyalkyl-functionalized imidazolium-based ionic liquids as solvents for the extraction of metal ions, *Sep. Sci. and Technol.*, 10.1080/01496395.2012.697527, **27 June 2012**.

C.A. Hawkins, I.A. Shkrob, C.J. Mertz, M.L. Dietz, M.D. Kaminski, Novel Tandem Column Method for the Rapid Isolation of Radiostrontium from Human Urine, *Anal. Chim. Acta*, **2012**, 746, 114-122.

S.L. Garvey, C.A. Hawkins, M.L. Dietz, Effect of Aqueous Phase Anion on the Mode of Facilitated Ion Transfer into Room-Temperature Ionic Liquids, *Talanta*, **2012**, 95, 25-30.

C.A. Hawkins, S.L. Garvey, M.L. Dietz, Structural Variations in Room-Temperature Ionic Liquids: Influence on Metal Ion Partitioning Modes and Extraction Selectivity, Separation and Purification Technology, **2012**, 89 31-38.

M.L. Dietz, S.L. Garvey, C.A. Hawkins, Mechanisms of metal ion transfer into RTILs - implications for their use as extraction solvents,19th International Solvent Extraction Conference, Salesianos Impresores, Santiago, Chile, Chapter 8, **2011**.

C.A. Hawkins and J.W. Dolan, Understanding Split Peaks, *LC/GC*, **2003**, 21, pages 1134-1138.

**Patents and Patent Applications**

ANL-IN-10-037, Non-Provisional Application for: Method for Rapid Separation and Counting of Radioactive Strontium From Urine, Inventors: M.D. Kaminski, C.J. Mertz, I.A. Shkrob, M.L. Dietz, C.A. Hawkins, filed July 2011.

**Honors and Awards**

| | |
|---|---|
| 3rd Prize Paper ACS I&EC Division Graduate Student Symposium | Aug. 2012 |
| 3rd Prize Poster Milwaukee ACS YCC Poster Symposium | Nov. 2011 |
| 1st Prize, Graduate Research, UW-Milwaukee Chemistry | May 2011 |
| 3rd Prize, Graduate Research, UW-Milwaukee Chemistry | May 2010 |
| Outstanding Service to the SOU Chemistry Department | 2000 |

**Presentations**

C.A. Hawkins, A. Rud, S.L. Garvey, M.L. Dietz, *Room-temperature ionic liquid-based solvent extraction systems for improved fission product separations*, 244th ACS Meeting and Exposition, I&EC Division Graduate Student Awards Symposium, Philadelphia, PA, 21 August 2012.

C.A. Hawkins, A. Rud, S.L. Garvey, M.L. Dietz, Poster: *Three Pathway Model for Metal Ion Partitioning into Room Temperature Ionic Liquids: Interrogating the Factors Contributing to Extraction*, UW-Milwaukee Chemistry & Biochemistry Department, 27 April 2012.

C.A. Hawkins, A. Rud, M.L. Dietz, Poster: *Evaluation of hydroxyalkyl-functionalized imidazolium-based ionic liquids as solvents for the extraction of metal ions*, Milwaukee Section ACS Younger Chemists Committee Poster Symposium, Milwaukee, WI, 4 November 2011.

C.A. Hawkins, A. Rud, S.L. Garvey, M.L. Dietz, *Evaluation of hydroxyalkyl-functionalized imidazolium-based ionic liquids as solvents for the extraction of metal ions*, 17th Symposium on Separation Science and Technology for Energy Applications, Gatlinburg, TN, 23-27 October 2011.

Dietz, M.L. Garvey, S.L. C.A. Hawkins, *Mechanisms of metal ion transfer into RTILs - implications for their use as extraction solvents*, 19th International Solvent Extraction Conference, Santiago, Chile, 3-7 October 2011.

C.A. Hawkins, M.L. Dietz, Poster: "Fundamental aspects of group 1 and 2 metal ion transfer into imidazolium-based room temperature ionic liquids", UW-Milwaukee Chemistry & Biochemistry Department, 6 May 2011.

C.A. Hawkins, S.L. Garvey, A.J. Pawlak, M.L. Dietz, Poster: "Fundamental aspects of metal ion transfer into room temperature ionic liquids", 241st ACS Meeting and Exposition, Anaheim, CA, 28 March 2011.

C.A. Hawkins, M.L. Dietz, Poster: "Fundamental Aspects of Metal Ion Transfer into Room-Temperature Ionic Liquids: Toward Improved Methods for Rapid Determination of Strontium-90 in Bioassay Samples", UW-Milwaukee Chemistry & Biochemistry Department, 7 May 2010

C.A. Hawkins, M. Kiser, T. Fleischmann, Poster: "Does Column Switching Reduce Phospholipid Ion Suppression in the Analysis of Rapamycin Using LC-ESI-MS/MS?", 54th ASMS Conference on Mass Spectrometry, Seattle, WA, 2006.

**Professional Affiliations**

American Chemical Society 1999-present

Chairperson, Milwaukee ACS Younger Chemists Committee 2009-2010

- Organizer of 1st Annual Chemistry in Southeastern Wisconsin Symposium

American Society for Mass Spectrometry 2006-2007

President of SOU Chemistry Student Affiliates of the ACS 1999-2000